

Mechanisms of resistance in relapsed/refractory diffuse large B cell lymphoma

Ryan N. Rys

Department of Physiology, Faculty of Medicine, McGill University, Montreal

February 2024

A thesis submitted to McGill University in partial fulfillment of the requirements
of the degree of Doctorate in Physiology

© Ryan N. Rys 2024

Table of Contents

I.	Abstract.....	6
II.	Résumé	9
III.	Acknowledgements.....	12
IV.	Contribution to Original Knowledge	14
V.	Contribution of Authors.....	15
VI.	List of Figures and Tables	17
VII.	List of Abbreviations	19
	Chapter 1: Introduction	24
	1.1: General Introduction	24
	1.2: Rationale, Hypothesis, and Aims	27
	Chapter 2: Literature Review.....	28
	2.1: B Cell Development and Function.....	29
	2.2: Diffuse Large B Cell Lymphoma.....	32
	2.2.1: Epidemiology & Prognostic Features.....	32
	2.2.2: Molecular and Pathological Features	33
	2.2.3: Recurrent Mutations in DLBCL.....	35
	2.2.4: New Genetic Classification of DLBCL.....	39
	2.2.5: Features of Relapsed DLBCL	43
	2.2.6: Current Advances in DLBCL Treatment	45
	2.3: Apoptotic Pathways	48
	2.3.1: Intrinsic and Extrinsic Apoptosis	48
	2.3.2: Inhibition of Intrinsic Apoptosis in DLBCL	51
	2.4: BH3 Profiling.....	52
	2.5: Circulating Tumor DNA Sequencing.....	53

Chapter 3: Apoptotic Blocks in Primary Non-Hodgkin B Cell Lymphomas Identified by BH3

Profiling	58
3.1: Preface.....	58
3.2: Simple Summary	61
3.3: Abstract	61
3.4: Introduction	62
3.5: Results	66
3.5.1: BH3 Profiling Is Reproducible in Primary Cells.....	67
3.5.2: Normal B Lymphocytes Are Partially Dependent on BCL2.....	69
3.5.3: Defects in Pro-Apoptotic Signaling Are a Feature of High-Grade Lymphomas and Poor Responses to Venetoclax	69
3.5.4: Lack of BCL2 Expression and MCL1 Dependency Result in a Poor Venetoclax Response in Class C B-NHLs.....	74
3.5.5: Dynamic BH3 Profiling (DBP) Reveals Drugs That Can Synergize with Venetoclax	80
3.6: Discussion	82
3.7: Materials and Methods.....	87
3.7.1: Sample Acquisition and Preparation	87
3.7.2: BH3 Profiling	88
3.7.3: Dynamic BH3 Profiling (DBP)	88
3.7.4: Immunofluorescence	89
3.8: Conclusions	90
3.9: Supplemental Methods.....	91
3.9.1: Patient Sample Preparation.....	91
3.9.2: BH3 Profiling- Additional Information.....	91
3.9.3: Cell Culture	92
3.9.4: MTT Assay Protocol	92
3.9.5: Western blotting	93
3.9.6: Statistics.....	93
3.10: Supplemental Figures.....	95
3.11: Author Contributions	104
3.12: Funding	105
3.13: Institutional Review Board Statement	105

3.14: Informed Consent Statement.....	105
3.15: Data Availability Statement	105
3.16: Acknowledgements	105
3.17: Conflicts of Interest.....	106
3.18: References	106
Chapter 4: Predicting Relapsed/Refractory Diffuse Large B Cell Lymphoma Using Serial ctDNA Analysis	117
4.1: Preface.....	117
4.2: Abstract	120
4.3: Introduction	121
4.4: Materials and Methods.....	122
4.4.1: Patient Selection and Sample Collection.....	122
4.4.2: Targeted Panel Hybridization.....	123
4.4.3: Targeted Sequencing and Variant Calling.....	124
4.4.4: ctDNA Detection and Quantification	124
4.5: Results	125
4.5.1: Cohort Statistics and Panel Performance	125
4.5.2: Early Treatment ctDNA Dynamics Predict Refractory DLBCL.....	125
4.5.3: Tracking Measurable Residual Disease.....	126
4.5.4: Mutational Analysis of Diagnosis vs. Relapse ctDNA	127
4.5.5: Genetic Landscape of Refractory, Early, and Late Relapse Groups	129
4.5.6: Evolution of DLBCL in Response to Immunotherapy	130
4.6: Discussion	132
4.7: Acknowledgements	136
4.8: Funding	136
4.9: Authorship Contributions.....	136
4.10: Disclosure of Conflicts of Interest	136
4.11: References	137
4.11: Tables	148
4.12: Figure Legends.....	152
4.13: Figures.....	156

4.14: Supplemental Figures.....	160
4.15: Supplemental Methods.....	163
4.15.1: cfDNA Extraction and Library Construction	163
4.15.2: UMI Processing and Single Nucleotide Variant Calling.....	164
4.15.3: Measurable Disease Tracking.....	165
4.15.4: Statistics and Visualization.....	165
Chapter 5: Discussion & Conclusion.....	166
5.1: DLBCL Therapeutic Resistance and Apoptosis	166
5.2: Early Detection of rrDLBCL using ctDNA	168
5.3: Mutational Profile of REFR DLBCL.....	169
5.4: Mutational Profiles of ER and LR DLBCL	171
5.5: Technical Advantages of rrDLBCL Panel Sequencing	173
5.6: ctDNA Analysis of BH3 Profiles.....	174
5.7: Future Directions in rrDLBCL Clinical Management	177
5.8: Conclusion & Summary	178
Chapter 6: References.....	181

I. Abstract

Diffuse large B-cell lymphoma (DLBCL) is the most common non-Hodgkin lymphoma (NHL) and is a particularly aggressive disease with poor outcomes in the relapse setting. Patients are treated with chemotherapy and rituximab, an antibody targeting CD20 (R-CHOP). Approximately 50% of patients will experience disease progression and unfortunately, the majority of patients with relapsed/refractory disease (rrDLBCL) will die from their lymphoma. The standard of care for fit patients in the relapse setting is salvage chemotherapy as a bridge to autologous stem cell transplant (ASCT). More recently, chimeric antigen receptor (CAR) T cell therapy has provided improved survival to rrDLBCL over ASCT as a second line therapy. However, the majority of rrDLBCL will still progress following therapy and improving the outcomes for these patients is an unmet clinical need. We need to better understand the biological mechanisms responsible for relapsed disease and the ways by which malignant cells resist specific therapies. The benefit of therapies such as CART is improved when tumor burden is low at the time of infusion, and many patients are ineligible for treatment due to toxicity concerns. Therefore, there is a growing need to identify patients who are refractory to treatment as early as possible so there may be an earlier therapeutic intervention and possibly improved survival.

Newer genetic classification of DLBCL, e.g. the LymphGen algorithm, has identified as many as seven genetic subtypes of DLBCL with potential therapeutic targets. However, additional mutations are acquired via selective pressure of therapy that may also contribute to rrDLBCL. While these mutations can be detected from peripheral blood via targeted sequencing of plasma circulating tumor DNA (ctDNA), the enrichment of certain mutations at relapse has

not fully explained the chemo-resistant nature of DLBCL. We hypothesized that there may be functional defects in apoptotic activation in primary lymphoma that is not explained by genomic events. Using a technique called BH3 profiling, we aimed to expand on our understanding of apoptosis in DLBCL and compare it to other lymphomas. In addition, we also hypothesized that early treatment failure can be identified by serial profiling of ctDNA during therapy. Therefore, we applied a custom panel of 194 genes specific to rrDLBCL to 547 samples from 237 patients to determine if ctDNA can be used to identify patients that require early intervention and/or a change of therapy.

BH3 profiling of 124 primary NHL tumor samples led to the identification of a subset of DLBCL that has remarkable reductions in apoptotic response and an apparent defect in pro-apoptotic proteins (BAX/BAK) needed for cell death. We also show that the majority of NHL depend on anti-apoptotic proteins MCL1 and BCL2 for survival, indicating a potential rationale for their targeting in certain NHL. Secondly, we used a novel method of disease monitoring involving the analysis of ctDNA to assess the mutational status of patients as they progress through therapy. We identified that ctDNA levels both pretreatment and mid-therapy are higher in patients who will be refractory to treatment. Moreover, mutations in *TNFAIP3* and *BTG2* were associated with improved survival, while rrDLBCL had a large number of mutations involved in cell survival and immune evasion (*BCL2*, *MYC*, *B2M*, *CD83*). Monitoring ctDNA in advance of relapse, we were able to detect ctDNA as early as 7 months before clinical presentation of relapsed disease, showing the use of ctDNA monitoring in detecting relapse even in patients with response to therapy.

Taken together, we have identified both functional and genetic defects in DLBCL that contribute to disease progression. The resulting work supports to the potential utilization of

apoptotic analysis and ctDNA monitoring in future patient care to aid in treatment management and subsequently, optimization of patient response.

II. Résumé

Le lymphome diffus à grandes cellules B (LDGCB) est le lymphome non hodgkinien (LNH) le plus courant et est une maladie particulièrement agressive avec des mauvais résultats dans le contexte de la rechute. Les patients sont traités par chimiothérapie et rituximab, un anticorps ciblant CD20 (R-CHOP). Environ 50% des patients connaîtront une progression de la maladie et malheureusement, la majorité des patients atteints de maladie réfractaire ou récidivante (rrLDGCB) mourront de leur lymphome. Le traitement standard en rechute pour les patients en forme est la chimiothérapie de sauvetage suivie d'une greffe de cellules souches autologues (GSCA). Plus récemment, la thérapie par cellules T à récepteur d'antigène chimérique (CART) a permis d'améliorer la survie des rrLDGCB par rapport à la GSCA en deuxième ligne de traitement. Cependant, la majorité des rrLDGCB progressera toujours après la thérapie et améliorer les résultats pour ces patients est un besoin non comblé. Nous devons mieux comprendre les mécanismes biologiques responsables de la maladie récidivante et les moyens par lesquels les cellules malignes résistent à des thérapies spécifiques. La thérapie cellulaire est plus efficace et moins toxique lorsque la charge tumorale est minimale au moment de l'infusion. Par conséquent, il y a un besoin croissant d'identifier les patients qui sont réfractaires au traitement le plus tôt que possible afin qu'il puisse y avoir une intervention thérapeutique plus précoce qui pourrait donner une survie améliorée.

Les nouvelles classifications génétiques du LDGCB, par exemple l'algorithme LymphGen, ont identifié jusqu'à sept sous-types génétiques du LDGCB avec des cibles thérapeutiques potentielles. Cependant, des mutations supplémentaires sont acquises via la pression sélective de la thérapie qui peuvent également contribuer au rrLDGCB. Bien que ces mutations puissent être détectées dans le sang périphérique via le séquençage ciblé de l'ADN

tumoral circulant (ctDNA), l'enrichissement de certaines mutations lors de la rechute n'a pas pleinement expliqué la nature chimio-résistante du LDGCB. Nous avons émis l'hypothèse qu'il pourrait y avoir des défauts fonctionnels dans l'activation apoptotique dans le lymphome primaire qui ne sont pas expliqués par des événements génomiques. En utilisant une technique appelée profilage BH3, nous avons cherché à approfondir notre compréhension de l'apoptose dans le LDGCB et à la comparer à d'autres lymphomes. De plus, nous avons également émis l'hypothèse que l'échec du traitement précoce peut être identifié par un profilage sériel de l'ADN tumorale circulante (ctDNA) dans le plasma pendant la thérapie. Par conséquent, nous avons appliqué un panel personnalisé de 194 gènes spécifiques au rrLDGCB à 547 échantillons provenant de 237 patients pour déterminer si le ctDNA peut être utilisé pour identifier les patients nécessitant une intervention précoce et/ou un changement de thérapie.

Le profilage BH3 de 124 échantillons de tumeurs LNH primaires a permis d'identifier un sous-ensemble de LDGCB qui présente des réductions remarquables de la réponse apoptotique et un défaut apparent dans les protéines pro-apoptotiques (BAX/BAK) nécessaires à la mort cellulaire. Nous montrons également que la majorité des LNH dépendent des protéines anti-apoptotiques MCL1 et BCL2 pour leur survie, indiquant une justification potentielle pour leur ciblage dans certains LNH. Deuxièmement, nous avons utilisé une nouvelle méthode de surveillance de la maladie impliquant l'analyse du ctDNA pour évaluer le statut mutationnel des patients alors qu'ils progressent dans la thérapie. Nous avons identifié que les niveaux de ctDNA à la fois avant le traitement et en milieu de traitement sont plus élevés chez les patients qui seront réfractaires au traitement. De plus, les mutations dans *TNFAIP3* et *BTG2* étaient associées à une survie améliorée, tandis que rrLDGCB avait un grand nombre de mutations impliquées dans la survie cellulaire et l'évasion immunitaire (*BCL2*, *MYC*, *B2M*, *CD83*). En surveillant le ctDNA

avant la rechute, nous avons pu détecter le ctDNA dès 7 mois avant la présentation clinique de la maladie récidivante, montrant l'utilisation du suivi du ctDNA dans la détection de la rechute même chez les patients ayant une réponse à la thérapie.

Pris ensemble, nous avons identifié des défauts fonctionnels et génétiques dans le LDGCB qui contribuent à la progression de la maladie. Le travail résultant soutient l'utilisation potentielle de l'analyse apoptotique et du suivi du ctDNA dans les soins futurs aux patients pour aider à la gestion du traitement et, par conséquent, à l'optimisation de la réponse des patients.

III. Acknowledgements

I would like to sincerely thank everyone who has helped and supported me throughout my degree. Pursuing a PhD is a long and difficult road, with many ups and downs. This journey was made infinitely easier due to the support of numerous family members, friends, colleagues, and mentors. You all have my deepest gratitude and I will never be able to thank you enough.

First, I would like to thank my supervisors Dr. Mark Blostein and Dr. Nathalie Johnson. They have both had profound impacts not only on my career, but on my growth as a scientist and a person. From them I learned the fundamentals of research, the value of collaboration, and how we can use research to improve lives. Both my supervisors have always supported me and for that I will be forever grateful. I would also like to thank my committee members, Dr. Volker Blank, Dr. Koren Mann, Dr. Stephanie Lehoux, and Dr. Prem Ponka, for their mentorship and insightful contributions to my project planning and development.

I would also like to acknowledge all the help provided by the core staff at the Lady Davis Institute. Particularly, Christian Young for his immense expertise in both imaging and flow cytometry which helped to facilitate this research.

An important thank you is necessary for the many friends and colleagues at the Lady Davis Institute and Department of Physiology who have given me so much help over the past years. I could not have done this without any of you. There are too many of you to name, so I will just simply say thank you to everyone.

I would also like to thank my family for their support. To my parents, Joyce and Nick, it is only on the back of your love and support that I am able to accomplish anything. Everything I do is a testament to the encouragement and belief you have given me. To my siblings, Eric, Joey,

and Lauren, I owe you all for the rest of my life for the unwavering support you have shown me. I love you all more than you will ever know.

Lastly, I would like to thank my partner, Maria Vittoria. You have made me a better person since I met you and I would have never been able to accomplish this without you. I love you and thank you from the bottom of my heart.

IV. Contribution to Original Knowledge

Chapter 3: Apoptotic Blocks in Primary Non-Hodgkin B Cell Lymphomas Identified by BH3 Profiling

This manuscript contributes to the understanding of apoptotic dysfunction in non-Hodgkin lymphoma. It identifies a subset of diffuse large B cell lymphoma patients who have severe pro-apoptotic dysfunction and are extremely resistant to cell death. At the time, this was the largest study of primary tumor samples in NHL using the BH3 profiling technique. NHL cell survival was found to depend on both MCL1 and BCL2 proteins. Finally, we show the potential synergistic effect of BCL2 inhibition with chemotherapy, in particular in combination with microtubule inhibitors.

Chapter 4: Predicting Relapsed/Refractory Diffuse Large B Cell Lymphoma Using Serial ctDNA Analysis

Using ctDNA monitoring, we validated the use of a novel panel in detecting rrDLBCL during therapy. This work identifies refractory DLBCL as early as cycle two of therapy and also shows the utility of ctDNA sequencing in routine clinical follow-up. We show that ctDNA detection at end of therapy is predictive of inferior progression free survival and that disease can be detected 2-7 months prior to normal clinical presentation of relapse. Mutational profiles of refractory and early relapse DLBCL show impairment in apoptosis, cell survival pathways, and immune evasion, while patients with complete remission had common mutations in *TNFAIP3* and *BTG2*. Use of ctDNA in response to immunotherapies also validated ctDNA monitoring in the relapsed setting and highlighted potential novel mutations in therapeutic resistance.

V. Contribution of Authors

Chapter 1: Introduction

RNR wrote the introduction with editing and guidance from NAJ.

Chapter 2: Literature Review

RNR wrote the literature review with editing and guidance from NAJ.

Chapter 3: Apoptotic Blocks in Primary Non-Hodgkin B Cell Lymphomas Identified by BH3 Profiling

This chapter contains work published as an original research article in *Cancers* (Basel). The contributions of the authors are detailed as follows: Conceptualization, C.M.W., P.S., J.R., A.L. and N.A.J.; Formal Analysis, R.N.R., C.M.W., D.G., C.G., A.G., E.B., L.S., T.P.-H., S.D., S.d.R. and K.K.M.; Resources, J.H., S.F., A.S., G.O., C.S., D.W.S., and N.A.J.; Investigation, R.N.R., C.M.W., D.G., A.G., E.B., L.S., T.P.-H., and S.D.; Methodology, C.G.; Visualization, R.N.R.; Supervision, K.K.M., S.d.R., N.A.J.; Writing—Original Draft Preparation, Review & Editing, C.M.W., R.N.R., and N.A.J.; Funding Acquisition, N.A.J. All authors have read and agreed to the published version of the manuscript.

Chapter 4: Predicting Relapsed/Refractory Diffuse Large B Cell Lymphoma Using Serial ctDNA Analysis

This chapter contains work under preparation for publication as an original research article. The contributions of the authors are detailed as follows: NAJ and RDM conceptualized the study; RNR and AA performed the experiments; RNR, CKR, and ER analyzed the data; EB provided clinical data; NAJ, RDM, DWS, and CS supervised the study and contributed to

experimental design; RNR and NAJ wrote the original manuscript; all authors reviewed, edited, and approved the final manuscript.

Chapter 5: Discussion

RNR wrote the discussion with editing and guidance from NAJ.

Chapter 6: Conclusion and Summary

RNR wrote the conclusion with editing and guidance from NAJ.

VI. List of Figures and Tables

Table 2.1: DLBCL Subtypes According to Gene Expression and Genetic Classifiers.....	40
Figure 2.1: Apoptotic Pathways in Cancer	49
Figure 2.2: Analysis Pipeline of Circulating Tumor DNA by CAPP-Seq Using Error Correction	55
Figure 3.1: BH3 profiling assay: rationale and methodology.....	65
Figure 3.2: BH3 profiling of peripheral blood (PB) and tonsil B cells.....	68
Figure 3.3: Competency and priming of the mitochondrial pathway according to lymphoma subtype	70
Figure 3.4: Sensitivities to BCL2 and MCL1 inhibition according to lymphoma subtype	72
Figure 3.5: Expression of MCL1 in DLBCL by immunofluorescence.....	76
Figure 3.6: BCLXL and other anti-apoptotic protein dependency	79
Figure 3.7: Dynamic BH3 profiling performed in Toledo and OCI-Ly8 cell lines	81
Figure 3.S1: BH3 profiling	95
Figure 3.S2: Normal B Cell Response.....	96
Figure 3.S3: Full BH3 profiling results for all non-malignant cell types tested.....	97
Figure 3.S4: Full BH3 profiling results for all NHL samples tested	99
Figure 3.S5: Expression of BAK, BID, and BCL2 in DLBCL BH3 profiles.....	99
Figure 3.S6: Immunofluorescence of BAK, BID, and BCL2.....	100
Figure 3.S7: Combination of WEHI-539 and Venetoclax in FL and DLBCL.....	101

Figure 3.S8: Expression of BIM in vincristine treated NHL cell lines.....	102
Table 3.S1: Characteristics of all 124 lymphoma samples used for BH3 profiling.....	103
Table 3.S2: Mean intensity values for immunofluorescence staining of PAX5+ cells.....	104
Table 4.1: Clinical Characteristics of Cohorts	148
Table 4.2: Sample Collection Characteristics	150
Table 4.3: CAPP-Seq Panel for rrDLBCL	151
Figure 4.1: Overview of Sample Collection and Cohort Development.....	152
Figure 4.2: ctDNA Quantification During R-CHOP	152
Figure 4.3: Log Fold Changes in ctDNA in Paired Diagnostic and Post Cycle 2 Samples.....	152
Figure 4.4: Tracking Measurable Residual Disease in REFR and ER DLBCL.....	153
Figure 4.5: Mutational Overview of SNVs in Diagnostic and Relapse Cohorts	153
Figure 4.6: Genetic Landscape of Relapse Groups.....	153
Figure 4.7: Mechanisms of Resistance in rrDLBCL Treated with Immunotherapy	154
Figure 4.S1: Survival based on ctDNA level at diagnosis	154
Figure 4.S2: ctDNA Quantification at Relapse.....	154
Figure 4.S3: Variant Calling Based on Cell of Origin	155
Figure 4.S4: Variant Calling of Relapse Groups at Diagnosis.....	155
Figure 4.S5: Variant Calling of Relapse Groups after R-CHOP.....	155
Figure 4.S6: Pathway Enrichment Analysis of Relapse Groups at Diagnosis.....	156
Figure 5.1: Comparison of Diagnostic ctDNA Mutations and BH3 Profiles	177

VII. List of Abbreviations

Abbreviation	Definition
ABC	activated B cell-like
AID	activation-induced cytidine deaminase
ASCT	autologous stem cell transplant
B2M	beta 2 microglobulin
BAD	BCL2 associated agonist of cell death
BAK	BCL2 antagonist/killer 1
BAX	BCL2 associated X protein
BCL2	B cell lymphoma 2
BCL6	B cell lymphoma 6
BCLW	B-cell lymphoma W
BCLXL	B-cell lymphoma extra large
BCR	B cell receptor
BH3	BCL2 homology 3
BID	BH3 interacting-domain death agonist
BIM	BCL2 interacting mediator of cell death
BIRC6	Baculoviral IAP repeat-containing protein 6
BiTE	bispecific T cell engager
BR	bendamustine and rituximab
BTG1	B-cell translocation gene 1
BTG2	B-cell translocation gene 2
BTK	Bruton's tyrosine kinase
C2	cycle 2 of therapy
CAPP-Seq	cancer personalized profiling by deep sequencing
CARD11	caspase recruitment domain-containing protein 11
CART	chimeric antigen receptor T cell

CCND3	cyclin D3
cfDNA	cell free DNA
CLL	chronic lymphocytic leukemia
CNS	central nervous system
COO	cell of origin
CR	complete remission
CREBBP	CREB binding protein
CRS	cytokine release syndrome
CSR	class switch recombination
CT	computed tomography
ctDNA	circulating tumor DNA
CTLA-4	cytotoxic T-lymphocyte associated protein 4
DA-R-EPOCH	dose adjusted rituximab, etoposide, cyclophosphamide, vincristine, and doxorubicin
DBP	dynamic BH3 profiling
DEL	double expressor lymphoma
DHITsig	double-hit signature
DISC	death inducing signaling complex
DLBCL	diffuse large B cell lymphoma
DNMT3A	DNA methyltransferase 3 alpha
DR4/5	Death Receptor 4/5
DTX1	deltex E3 ubiquitin ligase 1
DZsig	dark zone signature
ECOG	eastern cooperative oncology group
EOT	end of treatment
EP300	E1A-associated protein p300
ER	early relapse
EZH2	enhancer of zeste homolog 2
FADD	FAS-associated death domain

FDC	follicular dendritic cell
FISH	fluorescence in situ hybridization
FL	follicular lymphoma
FOXO1	forkhead box protein O1
GC	germinal center
GCB	germinal center B cell-like
GDP	gemcitabine, cisplatin, dexamethasone
HDACi	histone deacetylase inhibitor
HGBCL-DH	high-grade b cell lymphoma with rearrangements in <i>BCL2</i> and <i>MYC</i>
HGBCL-TH	high-grade b cell lymphoma with rearrangements in <i>BCL2</i> , <i>BCL6</i> , and <i>MYC</i>
hGE	haploid genome equivalent
HIV	human immunodeficiency virus
HRK	activator of apoptosis hara-kiri
IAP	inhibitor of apoptosis protein
ICANS	immune effector cell-associated neurotoxicity
IF	immunofluorescence
Ig	immunoglobulin
IGH	immunoglobulin heavy locus
IHC	immunohistochemistry
IPI	international prognostic index
JAK	Janus kinase
KMT2D	histone-lysine N-methyltransferase 2D
LAG-3	lymphocyte activation gene 3
LN	lymph node
LR	late relapse
LSH	loop sheet helix
MAP2K1	mitogen-activated protein kinase kinase 1
MCL	mantle cell lymphoma

MCL1	myeloid cell leukemia sequence 1
MHC	major histocompatibility complex
MHG	molecular high-grade signature
MOMP	mitochondrial outer membrane permeabilization
MRD	measurable residual disease
MS4A1	membrane-spanning 4A 1
mTOR	mammalian target of rapamycin
MYD88	myeloid differentiation primary response 88
MZL	marginal zone lymphoma
NCCN	US national comprehensive cancer network
NF- κ B	nuclear factor kappa light chain enhancer of activated B cells
NHL	non-Hodgkin lymphoma
NMF	non-negative matrix factorization
NOTCH1	neurogenic locus notch homolog protein 1
NOTCH2	neurogenic locus notch homolog protein 2
OS	overall survival
PAX5	paired box 5
PB	peripheral blood
PD-1	programmed cell death protein 1
PD-L1	programmed death ligand 1
PET	positron emission tomography
PFS	progression free survival
PI3K	phosphoinositide 3-kinase
PMBCL	primary mediastinal b cell lymphoma
PUMA	p53 upregulated modulator of apoptosis
R-CHOP	rituximab, cyclophosphamide, doxorubicin, vincristine and prednisone
REFR	refractory
rrDLBCL	relapsed/refractory diffuse large B cell lymphoma

SCNA	somatic copy number alteration
SLL	small lymphocytic leukemia
SNV	single nucleotide variant
STAT3	signal transducer and activator of transcription proteins 3
STAT6	signal transducer and activator of transcription proteins 6
SV	structural variant
SYK	spleen tyrosine kinase
T _{FH}	T follicular helper cell
TIM-3	T-cell immunoglobulin and mucin-domain containing-3
TNFAIP3	tumor necrosis factor alpha-induced protein 3
TNFR1	tumor necrosis factor receptor 1
TNFRSF14	tumor necrosis factor receptor superfamily member 14
TP53	tumor protein p53
TRAIL	TNF-related apoptosis-inducing ligand
UMI	unique molecular identifier
VAF	variant allele fraction
WES	whole exome sequencing
WGS	whole genome sequencing

Chapter 1: Introduction

1.1: General Introduction

Diffuse large B-cell lymphoma (DLBCL) is the most common non-Hodgkin lymphoma (NHL) and is an aggressive disease that is treated with cyclophosphamide, doxorubicin, vincristine, prednisone, and rituximab (R-CHOP)[1]. While this approach is curative in many cases, 30-40% of cases will not respond to treatment and ultimately develop disease progression[1]. Clinical response rates have remained relatively stagnant and non-responding DLBCL will progress, often termed relapsed/refractory disease (rrDLBCL). The vast majority of rrDLBCL cases will prove fatal and improved clinical treatment for this group represents an unmet need.

Over the past decade, major advancements have been made in the understanding of tumor biology at diagnosis and relapse via gene expression and sequencing of tumor biopsies. Historically, gene expression profiling stratified DLBCL into sub-populations based on similar cell of origin (COO) gene expression signatures. These are called germinal center B cell-like (GCB) and activated B cell-like (ABC)[2], as their expression profiles closely resembled B-cells in different stages of development. However, it became increasingly evident that GCB and ABC DLBCL had diverse genetic events occurring within these groups themselves. For example, while GCB gene expression usually has a good prognosis compared to ABC, some GCB patients also have poor prognosis such as “double-hit” cases with translocations in both *MYC* and *BCL2* (termed high-grade B cell lymphoma with *MYC* and *BCL2* rearrangement, HGBCL-DH)[3,4]. DLBCL molecular classifiers based on the underlying genetic profiles have improved our understanding of different DLBCL subtypes. Chapuy et al. clustered DLBCL into 5 main

subtypes, of which 2 displayed inferior outcomes (clusters 3 and 5)[5]. Notably, cluster 3 was of GCB origin, more likely to have *MYC* and *BCL2* rearrangements, and showed a subset of these patients have poor prognosis. A second genetic classifier, LymphGen, has demonstrated novel genetic subtypes in DLBCL, some of which correlate with inferior outcomes (N1 and MCD subtypes)[6]. This also resulted in separate classification of certain aggressive subtypes, for example those with a double-hit genetic signature (EZB subtype with *MYC* translocations), similar to cluster 3 previously mentioned. The identification of genetic signatures reminiscent of HGBCL-DH was further expanded upon by a newly identified 104 gene expression profile, known as the dark zone signature (DZsig)[7,8]. This validated a subset of GCB DLBCL with inferior outcomes while resembling HGCBCL-DH, regardless of rearrangement status of *BCL2* and *MYC*. Additionally, these cases were found to resemble lymphomas originating from the dark-zone of germinal centers (e.g. Burkitt lymphoma), hence the name.

Genetic analysis of relapsed DLBCL has shown that in comparison to diagnosis, specific genes have been enriched and are implicated in disease progression. Exome sequencing of rrDLBCL biopsies revealed evidence for clonal selection of mutations in *TP53*, *FOXO1*, *KMT2C*, *CCND3*, *NFKBIZ*, and *STAT6*[9]. *TP53* is commonly mutated at diagnosis, but is also enriched at relapse and supporting *TP53* mutations as a primary driver of rrDLBCL. Sequencing of a large cohort of plasma circulating tumor DNA at relapse also identified additional mutations that are more common at relapse. These included *TP53*, *FOXO1*, *KMT2D*, *CREBBP*, *NFKBIE*, and *MS4A1*[10]. Some of these mutations were sub-clonal and then expanded after therapy. For example, *MS4A1* is the gene encoding for CD20, the target of rituximab, and these mutations arose in response to R-CHOP. This highlights some DLBCL that have innate resistance to therapy (e.g. *TP53* mutated DLBCL) and those that have acquired treatment resistance in

response to therapeutic pressure (*MS4A1*). This is supported by inferior survival with reduced CD20 expression and the loss of CD20 antigen in up to 20% of rrDLBCL[11–14]. While genetic studies have identified drivers of rrDLBCL and mechanisms of disease resistance, they cannot fully explain phenotypes seen at relapse. This is evident in the case of CD20 loss, where the majority of cases experience reduction in CD20 without any mutations in *MS4A1*.

With improved knowledge of lymphoma biology, new targeted and immune-based therapies have been tested in rrDLBCL. Ibrutinib is a BTK inhibitor that has shown effectiveness in ABC rrDLBCL[15], and this later translated to improved survival in MCD and N1 subtypes when combined with RCHOP[16]. CD79b is a subunit of the B cell receptor and is the target of polatuzamab vedotin, which is an antibody drug conjugate. It has shown moderate responses in rrDLBCL[17], and was also investigated in frontline therapy[18]. Additional drugs targeting BCL2 (venetoclax) or PI3K have been explored in DLBCL, but with limited effectiveness[19–21]. While some therapies were promising, the responses in rrDLBCL are short-lived and they have not provided significant benefits over standard R-CHOP in the frontline. An alternative strategy to treat rrDLBCL is to use immunotherapy that will target an antigen present on all lymphoma, for instance the B cell markers CD20 and CD19. Bispecific T cell engagers (BiTE) are novel immunotherapies that target CD20 on malignant B cells and direct them to CD3 expressing T cells for cell-mediated killing[22,23]. As a monotherapy in rrDLBCL, complete response rates to BiTE therapy have been around 40%[24–26]. These are also being explored in combination with R-CHOP with favorable safety results[27]. In recent years, therapy in the relapse setting has been revolutionized by the introduction of chimeric antigen receptor T (CART) cell therapy. Patient T cells are isolated and genetically modified to express a CAR that is designed to target malignant specific antigens. In the context of rrDLBCL, this is normally

CD19 expressed on malignant B-cells. After the modification of these cells, they are expanded and then re-infused into the patient to assist in targeted T-cell mediated killing of DLBCL cells[28]. Responses to CART cell therapy have been impressive, with efficacy in 40% of DLBCL at relapse[29–31]. rrDLBCL with low disease burden and good performance status at the time of CART treatment is associated with favorable responses[32–35]. This will lead to CART therapy as the new standard of care in second line settings of DLBCL in Canada, with improved survival compared to previous standard of salvage chemotherapy followed by autologous stem cell transplant[36,37]. Unfortunately, there is still a need to optimize CART therapy treatments, which are very expensive and require specialized care. Improved detection of rrDLBCL would allow for more timely administration of CART therapy.

Taken together, there is a need to understand the mechanisms of relapsed disease to develop novel strategies to overcome them. There is also a need to improve our detection of emergent resistance to therapy, so that clinical intervention can be applied earlier. Therefore, the main aim of my thesis is to identify functional mechanisms of DLBCL therapeutic resistance and correlate these results to relapsed/refractory detection and clinical outcomes.

1.2: Rationale, Hypothesis, and Aims

Given the resistant nature of DLBCL, we wanted to elaborate on the functional changes in malignant B cells that allows them to survive after chemotherapy, and develop improved detection of refractory DLBCL before and during treatment. There is a need to further understand rrDLBCL biology especially in the context of chemotherapy resistance. The BCL2 inhibitor venetoclax shows different response rates across NHL, despite the consistent expression of the target. Therefore, additional mechanisms are contributing to cell survival, particularly in DLBCL. While functional defects may contribute to refractory disease, there is also a need to

identify rrDLBCL early during treatment. As the effectiveness of CART cell therapy has been associated with performance status and reduced tumor burden, determining rrDLBCL quickly will allow for potential novel therapeutic interventions and optimized treatments.

Our hypothesis is that DLBCL will have a reduced intrinsic apoptotic response in comparison to other NHL. Moreover, additional anti-apoptotic proteins may contribute to enhanced resistance in DLBCL. We will also identify mutations that, under pressure from treatment course, are either stable or clonally develop in surviving malignant cells. These mutations will help detect rrDLBCL and may also be implicated in resistance to specific therapies. The first study of this thesis will elaborate on the ability of DLBCL to undergo apoptosis and identify functional defects associated with cell survival and venetoclax resistance. The second study of my thesis will analyze the mutational landscape of rrDLBCL using serial patient samples as they progress through treatment and use ctDNA to predict rrDLBCL. In addition, the kinetics of ctDNA dynamics will be studied as patients progress through R-CHOP, and measurable residual disease will be analyzed to use ctDNA to predict relapse prior to clinical presentation. In summary, the aims of my work are to determine apoptotic dysfunction in primary DLBCL tissue, then identify mutations that are implicated in rrDLBCL, characterize the genetics of relapse, use ctDNA to predict rrDLBCL and finally, correlate our genetic findings to phenotypic observations of therapeutic resistance previously identified.

Chapter 2: Literature Review

The following is a review of the current literature surrounding DLBCL: subtypes, epidemiology, pathology, and genetics, as well as relevant biological processes involved in

disease progression. Additionally, techniques including BH3 profiling and next generation sequencing are discussed in detail.

2.1: B Cell Development and Function

B cell development is important for understanding DLBCL, as malignant B cells “inherit” the B cell program from their cell of origin, and thus some features of DLBCL are acquired from different stages of development. B cells act as antigen presenting cells of the adaptive immune system and secrete highly specific antibodies. The key events in their development are the combinatorial rearrangement of V, D, and J gene segments in the Heavy (H) chain locus and of V and J genes in the Light (L) chain loci[38–40] of immunoglobulin (Ig) anchored to the cell membrane.

Ig is expressed in 2 forms: a soluble form secreted by B cells into the bloodstream to bind pathogens and a membrane bound form that is the main structural unit of the B cell receptor (BCR)[41]. The BCR is transmembrane protein complex responsible for the activation of B cells via the binding of antigens and the cooperation of other cells of the immune system (e.g. T helper cells)[42]. It is necessary for proper B cell function and survival and is expressed in mature B cells[43]. BCR activation is primarily mediated by antigen encounters, as immature pre-B cells exit the bone marrow. Conformational changes induce the activation of CD79a and CD79b, which complex with the BCR and promote intracellular signaling. These are phosphorylated by SRC tyrosine kinase family members, which promotes the recruitment and activation of spleen tyrosine kinase (SYK)[44]. SYK then promotes multiple intracellular signaling cascades important for B cell survival and differentiation including ATK/mTOR, which is mediated by PI3K, and activation of BTK, which leads to increased NF- κ B signaling. Chronic BCR signaling

is commonly seen in DLBCL and as such proteins in this cascade (SYK, BTK, and PI3K) are under investigation as potential therapeutic targets[44–46].

B cells express several additional markers as they develop, many of which are shared with DLBCL. These include CD45, a leukocyte marker, and more B cell specific markers (CD19 and CD79a)[47,48]. CD19 is a common B cell marker expressed in most lineages and, in cooperation with CD21, aids in BCR related signaling transduction responses in B cells and is necessary for B cell development[38,49]. CD20 is widely expressed on B cells prior to differentiation into antibody secreting plasma cells. This was the first B cell specific marker discovered[50] and it plays a role in proper BCR function and B cell development. Although there is no known ligand for CD20, it has proved to be the single most important therapeutic target in B cell malignancies[51,52] due to the effectiveness of rituximab.

In the follicles of lymphoid organs, B cells mature at sites called germinal centers (GC) where cells will undergo the development of a BCR that has a high affinity for the specific antigen encountered after its release from adult bone marrow. Here, Ig class switching recombination (CSR) at the H chain locus and somatic hypermutation of its V genes allow the development of Ig proteins specific to the antigen encountered by the naïve B cell[53,54]. This maturation is assisted mainly by an enzyme called activation-induced cytidine deaminase (AID), with AID expression in GCs using an RNA editing method to assist in Ig diversification[55]. The B cell is impressive for its ability to perform CSR, with hypermutation allowing for many diverse BCRs and class switching leading to diverse effector functions. This allows an extremely diverse number of antigen specific Ig, but this may come at a cost. Owing to the constant changes in BCR maturation, this process is very error prone, and subsequent deregulation of the system is implicated in numerous hematological malignancies. For example, AID helps with

class-switching but has also been implicated in tumorigenesis and the translocation of certain genes in DLBCL[56]. This AID induced somatic hypermutation is a driving cause in many of the mutations found in DLBCL[57].

Germinal centers are dynamic environments and naïve B cells migrate through different compartments of the GC as they undergo progressive rounds of selection [58,59]. The regions of the germinal center are firstly the dark zone, which is where B cells that have been activated by antigen exposure begin to clonally expand and then experience previously mentioned hypermutation. Cells then migrate to the light zone, during which positive selection of high-affinity BCRs is done following interaction with both T follicular helper cells (T_{FH}) and follicular dendritic cells (FDC)[60]. Following selection, B cells may then migrate out of the GC to become plasma or memory cells, or they may migrate back to the dark zone for additional rounds of hypermutation. The organization of the germinal center is of great importance due to the progressive migration of B cells and the rounds of potential hypermutation. Defects in specific regions of the GC or steps in this reaction can result in malignancies associated with the different stages of B cell maturation. Therefore, the mutations present in many lymphomas are reflective of the time during which they exit the GC reaction as malignant cells.

Several transcription factors play a role in regulating B cell development, differentiation, and activation. *BCL6* is the master regulator of the GC reaction and necessary for proper differentiation of GC B cells[59]. *MYC* is an important oncogene that encodes for a transcription factor that is a key regulator of the cell cycle and cell proliferation[61]. The expression of *MYC* is low in the GC and is restricted to a small subset of light zone B cells, but it is necessary for GC maintenance[62,63]. Dysregulation of *MYC* and subsequent overexpression is commonly associated with lymphomagenesis and increased cellular proliferation in aggressive lymphomas.

Additionally, the antiapoptotic protein BCL2 is normally not expressed in germinal centers, but is worth mentioning due to its contrary overexpression in several malignancies, including DLBCL.

2.2: Diffuse Large B Cell Lymphoma

2.2.1: Epidemiology & Prognostic Features

Lymphoma is a broad spectrum of hematological malignancies arising from tissues in the lymphatic system. There are over 70 subtypes of B cell lymphoid proliferations and lymphomas, with large B cell lymphomas alone having 18 different characterizations according to the most recent World Health Organization Classification of Haematolymphoid Tumours[4]. The majority of lymphomas are NHL with roughly 74,000 new cases diagnosed each year in the United States and 10,000 each year in Canada[64], with the incidence increasing with age[65]. Amongst the risk factors associated with NHL, some of the most prominent are age (median age at DLBCL diagnosis is mid-60s), viral exposure and immunosuppression. HIV and Epstein-Barr Virus are two viruses that increase the risk of certain NHL[66,67]. Also, as much as 90% of NHL are B cell malignancies which include mantle cell lymphoma (MCL), follicular lymphoma (FL), marginal zone lymphoma (MZL), DLBCL, high grade B cell lymphoma with translocations in *MYC* and *BCL2* or *BCL6* (HGBCL-DH or HGBCL-TH), and Burkitt lymphoma (BL)[68,69]. DLBCL is the largest subtype of NHL, comprising over 30% of total cases[64,68,70]. Other NHL will be mentioned due to their biological overlap with DLBCL, which can arise *de novo* in patients and be difficult to distinguish from other NHL such as HGBCL-DH or BL. DLBCL can also arise from indolent lymphomas (e.g. FL), known as transformed DLBCL[71,72]. This thesis will analyze both cases of *de novo* and transformed DLBCL, and highlight differences, if any, that occur between these subtypes.

The use of the international prognostic index (IPI) is used to assess the risk for DLBCL patients and help determine the risk of associated chemoimmunotherapy regimens[73,74]. IPI takes into account patient age, Ann Arbor staging, serum lactate dehydrogenase levels, Eastern Cooperative Oncology Group (ECOG) performance status, and the presence of extra-nodal sites in order to assign patients to a scale from 0-5, with scores of 3-5 having inferior prognosis[75]. Newer interpretations of these variables have led to the inclusion of updated scoring systems such as the US National Comprehensive Cancer Network (NCCN)-IPI that may better improve risk stratification in this patients based on routine clinical variables[74,76]. Many additional prognostic features based on disease biology and genetics have yet to be incorporated into a validated clinical prognostic tool, but will be mentioned in subsequent sections.

2.2.2: Molecular and Pathological Features

DLBCL displays abnormally large B cells that have lost normal lymphoid organization. These cells have now committed to an aggressively proliferating phenotype. DLBCL is normally diagnosed via core-needle or excisional biopsies analyzed by a hematopathologist, as well as immunophenotyping by immunohistochemistry (IHC), flow cytometry, fluorescence in situ hybridization (FISH) and additional molecular testing[77]. These tumor cells have large nucleoli and cytoplasm leading to a disruption of the overall lymph node structure[78]. Gene expression profiling has defined two subgroups of DLBCL named germinal center B-cell-like (GCB) and activated B-cell-like (ABC), with the ABC subgroup having an inferior progressive free survival (3-year 40-50% in ABC, 75% in GCB) [77,79–81]. They are so named because their gene expression profiles closely resemble B cells at different stages of differentiation. Therefore, this classification is termed “cell of origin” (COO) and is currently used as an additional method of risk stratification in most clinical settings. ABC cases are characterized by chronic BCR

signaling and continued activation of NF- κ B. GCB DLBCL is associated with mutations in genes in the germinal center such as *BCL6*, as well as translocations in *BCL2*. Clinically, IHC algorithms such as Han's algorithm, are often used to separate in cases into GCB and non-GCB, an approximation of gene expression signatures[82]. Specific cytogenetic alterations are associated with a poor outcome in DLBCL, namely alterations in *MYC*, *BCL2* and *TP53*. FISH is used to determine the chromosomal alterations present in *BCL2* and *MYC*. Common translocations are seen in *BCL2* (14;18) with *IGH* partner (q32;q21), and a *MYC* translocation at 8q24, with these events occurring in around 10-20% of DLBCL cases[83–86]. *IGH* is the most common partner for *BCL2* and *MYC* rearrangements but these genes also have a variety of other potential gene partners. Rearrangements in *BCL2* are exclusive to GCB cases[86], and when they co-occur with *MYC* they are classified as high grade B cell lymphoma with translocations in *MYC* and *BCL2* and/or *BCL6* (HGBCL-DH or HBCL-TH)[4]. These particular cases of lymphoma are characterized by poor outcomes after R-CHOP, even though they are usually confined to GCB subtypes[87]. The overexpression of *BCL2* by IHC, primarily responsible for cell survival by inhibiting intrinsic apoptosis, occurs in 50-60% DLBCL, while overexpression of *MYC* is seen in 45% of cases. Co-expression of these is seen in 30% of cases and is related to particularly poor prognosis (commonly referred to as double-expressor lymphomas, DEL)[88–90]. It is important to note that DEL is considered a different entity than HGBCL-DH, in which the translocations of *BCL2*, *MYC* and/or *BCL6* are required for -DH classification. DEL is indicative of a poor prognosis, but while HGBCL-DH is rare, it is estimated that up 30% of DLBCL may be DEL[88,91]. This highlights that not all mutations in these genes may have equivalent impacts on protein expression or survival, as HGBCL-DH normally has inferior survival compared to DEL. A significant number of patients without translocations still have

overexpression of BCL2 or MYC[88], and therefore single nucleotide variant mutations in these genes may also contribute significantly to their expression, as discussed later in this thesis.

2.2.3: Recurrent Mutations in DLBCL

Recurrent mutations in DLBCL contribute to disease progression and therapeutic resistance, making them potential targets for novel therapy. They occur most often in aberrant BCR signaling, epigenetic regulation, cell cycle and differentiation, apoptosis, and immune evasion[92,93]. Several mutations seen in DLBCL are preferential to ABC subtype, most importantly alterations to BCR signaling, labeled chronic activation of the BCR[94]. Mutations in the BCR subunit *CD79b* are seen more commonly in ABC DLBCL and additional mutations in *CARD11*, which assists in BCR signal transduction, have led to gain of function increases in BCR activation[95]. This activation is linked to NF- κ B and PI3K signaling (critical for cell survival in malignant populations) by Burton's tyrosine kinase (BTK)[15]. In fact, the use of a BTK inhibitor, Ibrutinib, has shown some efficacy in clinical trials of patients with ABC gene expression and is also being tested in combination with other drugs in multiple B cell malignancies[96–99]. Polatuzumab vedotin is an antibody-drug conjugate for CD79b that has shown activity in DLBCL either with BR or when paired with RCHOP[17,18,100–102], highlighting the targeting of CD79b for therapy. *MYD88* mutations have been noted in ABC groups as well and are usually tied to increases in NF- κ B and JAK/STAT pathway activation[103,104]. JAK/STAT pathway mutations have become relevant to DLBCL progression as well, as mutations in *STAT6* and *STAT3* have been noted to contribute to signaling dysfunction in DLBCL[105,106].

Epigenetic dysregulation via methyl- or acetyltransferases is a commonly seen in GCB DLBCL and is a major factor in DLBCL biology. *KMT2D* mutations have been reported in

DLBCL and FL, which encodes a histone methyltransferase and is implicated in the regulation of genes involved in B cell signaling and migration[107–109]. Other epigenetic-related mutations are seen in DLBCL[110], such as another methyltransferase gene called *EZH2*. This gene is mutated in almost 30% of GCB cases and is necessary for proper germinal center formation[111,112]. Clinical trials exploring the efficacy of *EZH2* inhibitors in patients harboring these mutations are ongoing[113,114]. *CREBBP* encodes an acetyltransferase and inactivation of it in DLBCL has been linked to the deregulation of toll-like receptor signaling, apoptosis, and NF- κ B[115,116]. *EP300* encodes another acetyltransferase that works with *CREBBP* to influence gene expression and is frequently mutated in DLBCL[93]. Due to the epigenetic dysregulation seen in DLBCL, the use of histone deacetylase (HDAC) inhibitors as a potential therapeutic target has increased in recent years, although large scale success in therapy has yet to be seen[117–120].

Deleterious, recurrent mutations are seen in major transcription factors (*MYC* and *TP53*) helping to regulate the cell cycle, survival, and proliferation. *MYC* codes for human MYC protein which is a transcription factor that controls a large number of genes involved in a multitude of physiological processes including cell growth and proliferation, and many studies have shown its alteration in DLBCL to result in aggressive and proliferating disease, with inferior overall and progression free survival [121–124]. Classified as a proto-oncogene, mutations in *MYC* contribute to malignant transformation due to increased expression and ultimately uncontrolled cellular replication[125]. Additionally, *MYC* amplification has been seen in some cases with a potential negative impact as well on outcomes[126]. Burkitt lymphoma is well known for alterations in *MYC* and the aforementioned t(8;14)(q24;q32) being a hallmark of BL pathogenesis[127]. In DLBCL and other lymphomas, *MYC* dysregulation is not the primary

event, but nonetheless contributes to aggressive disease course[128]. Along with translocation of this gene in 5-15% of DLBCL cases, overexpression of MYC protein has also been correlated with inferior prognosis[127,129]. Additional mutations affecting *MYC* are rarer, but do occur in DLBCL. These include single nucleotide variants, usually missense mutations, as well as structural variants that are generally an amplification of *MYC*[130,131]. However, these additional mutations are not associated with inferior outcomes to the extent of *MYC* translocations. Gene expression profiling has recently identified a double-hit signature (DHITsig, since renamed to DZsig) that is reminiscent of HGBCL-DH[7,8,132,133]. DZsig interestingly was assigned to roughly 25% of GCB DLBCL, but only half of those harbor rearrangements in *MYC* and *BCL2*. This identifies a subset of GCB DLBCL that have inferior outcomes, outside of HGBCL-DH, and highlights additional dysfunction in *MYC* activity that corresponds to poor outcomes. An additional gene expression signature, named the molecular high-grade signature (MHG), also identified a subset of GCB DLBCL with expression patterns consistent with HGBCL-DH, immune evasion, and proliferation[134]. These two signatures (MHG and DZsig) displayed significant overlap and concordance, supporting the identification of GCB DLBCL subsets with poor prognosis in addition to cases of *MYC* and *BCL2* translocations[132].

TP53 is a tumor suppressor gene located in the 17p13.1 chromosome and encodes p53 protein. This transcription factor is often considered the “guardian of the genome”, as it has a hand in many physiological roles such as cell cycle regulation, DNA repair, and apoptosis. It plays a key role in responding to cellular stress signals and suppressing malignancy. As such, mutations in *TP53* are frequent in most cancers as mutant TP53 protein is no longer able to intervene and halt tumorigenic proliferation[135]. Mutations in *TP53* are often described in NHL (around 20% of DLBCL cases)[136], with inactivation of the gene being common in GCB

DLBCL, but also mutated in ABC DLBCL and cases with unclassifiable gene expression signatures[107,137–139]. As a tumor suppressor gene, inactivating or loss-of-function mutations are described as being deleterious to p53 function. However there is also evidence that some gain-of-function mutations can equally have oncogenic effects[140]. *TP53* is generally considered to be prognostic in DLBCL, with patients with mutated DLBCL showing inferior outcomes[141]. However, *TP53* as a single prognostic factor has shown variable results across malignancies and cohorts. Location and types of mutation are heterogenous in DLBCL, with some mutations being linked to worse prognosis. Mutations in DNA binding domains of *TP53* are very common and are associated with worse survival when compared to non-DNA binding mutations[137]. Even so, this same study showed no correlation with mutations in the L2 DNA binding region of *TP53* and prognosis. Also in this study, the prognostic capability of *TP53* was also restricted to GCB DLBCL. Mutations in the L2 region and ABC DLBCL proved to be prognostic in another study by Xu-Monette et al. highlighting the heterogenic nature of *TP53* mutations in DLBCL[141]. The role of *TP53* in DLBCL pathogenesis is undeniable, however its use as a prognostic factor remains somewhat controversial[142]. It appears that *TP53* likely conveys a poor prognosis but as a single factor there are more robust measurements at diagnosis such as IPI, *BCL2* expression and *MYC* protein expression[143]. Given the heterogenous presentation of *TP53* mutational status in DLBCL, it is probable that the location of the mutation, and its specific effect on either protein expression or function, is important for oncogenic potential.

Additionally, a substantial number of mutations in DLBCL may contribute to apoptotic dysfunction and as well as immune-evasion. *BCL2* mutations are common in FL and GCB DLBCL, but less common in ABC patients or other NHL[144]. Individual *BCL2* mutations have

not been as prognostic as *BCL2* overexpression or the particular combination of *BCL2* and *MYC* translocation events (HGBCL-DH)[86,88]. Venetoclax is a *BCL2* inhibitor that has shown remarkable responses in chronic lymphocytic leukemia, but its effect has not been as robust in DLBCL[145–147]. The loss of MHC class II gene expression has been noted in NHL and it is theorized to contribute to loss of immunosurveillance in DLBCL[148,149]. Additionally, *B2M* which is the gene that encodes the beta-2 microglobulin subunit of MHC class I molecules, has been mutated in DLBCL and contributes to reduced antigen presentation and immune escape[150]. *FOXO1* is a transcription factor that plays roles in cell cycle regulation and promotes extrinsic apoptosis/cell death. Its dysregulation via inactivating mutations, as well as increased PI3K signaling, contributes to DLBCL pathogenesis in some patients[151,152]. *TNFRSF14* modulates immune cell interaction and is frequently mutated in FL but also in DLBCL[153,154]. Across many cancers, programmed death ligands have been mutated and are key targets for immunotherapy. These constitute some of the most researched aspects of immune dysfunction, in which therapy targeting immune checkpoints (often in regulatory T cells) attempt to rescue T cell exhaustion experienced by the immune system[155]. However, DLBCL has a “cold” tumor microenvironment that is dominated by malignant cells and mutations in PD-1/PD-L1 axis are present in only 5-10% of cases[156–158]. Therefore, immune checkpoint inhibitors have not yet translated into clinical benefit, as PD-1 inhibitors have proven ineffective thus far in DLBCL[159–162]. Other genes related to immune regulation and being explored in immunotherapy include *CTLA-4*, *TIM-3*, and *LAG-3*[163–165].

2.2.4: New Genetic Classification of DLBCL

Moving beyond COO, two new molecular classifications have been described that classify DLBCL into subtypes that share similar genomic alterations. Since the early 2000s,

many attempts have been made to appropriately classify different groups of DLBCL patients. Early identification of such groups could inform the use of personalized medicine for patients who may benefit from alternative forms of treatment. These classifiers have revealed the complexities of DLBCL genetics goes far beyond the initial stratifications of GCB vs. ABC. Key features of these genetic classifiers, as well as gene expression profiles, are summarized below in Table 2.1.

Table 2.1. DLBCL Subtypes According to Gene Expression and Genetic Classifiers.

DLBCL Subtype	Genetic Classifier	Associated Mutations	Prognosis (R-CHOP)
EZB	Lymphgen (Wright et al. 2020)	BCL2 Fusion, EZH2, TNFRSF14, KMT2D, CREBBP, EP300, FAS	Based on MYC+/-
EZB MYC+	Lymphgen (Wright et al. 2020)	MYC Amp/Fusion, TP53, GNA13, DDX3X, FOXO1	Poor
EZB MYC-	Lymphgen (Wright et al. 2020)	TNFAIP3, CARD11, TP73 loss	Favorable
MCD	Lymphgen (Wright et al. 2020)	MYD88 (L265P), CD79b, PIM1, CDKN2A loss, BTG1	Poor
N1	Lymphgen (Wright et al. 2020)	NOTCH1, ID3, BCOR, IKBKB	Poor
ST2	Lymphgen (Wright et al. 2020)	SGK1, TET2, SOCS1, STAT3	Favorable
BN2	Lymphgen (Wright et al. 2020)	BCL6 Fusion, NOTCH2, TNFAIP3, DTX1, TMEM30A	Favorable
A53	Lymphgen (Wright et al. 2020)	TP53 loss, B2M	Poor (ABC)
C0	Chapuy et al. 2018	No Genetic Drivers	Favorable
C1	Chapuy et al. 2018	BCL6 Fusion, NOTCH2, SPEN, FAS, B2M	Favorable
C2	Chapuy et al. 2018	TP53 loss, CDKN2A loss	Poor
C3	Chapuy et al. 2018	BCL2 Fusion, KMT2D, CREBBP, EZH2, TNFSF14	Poor
C4	Chapuy et al. 2018	Histone Genes, CD83, SGK1, CARD11, STAT3	Favorable
C5	Chapuy et al. 2018	MYD88 (L265P), CD79b, 18q gain	Poor
DLBCL Subtype	Gene Expression Classifier	Associated Characteristics	Prognosis
ABC	Cell of Origin (Alizadeh et al. 2000)	Chronic BCR Signaling, NF-κB Activation, MYD88 (L265P)	Poor
GCB	Cell of Origin (Alizadeh et al. 2000)	BCL2/MYC Translocations, Double-Hit Signatures, Epigenetic Dysfunction	Favorable
MHG	Molecular High-Grade (Sha et al. 2019)	BCL2/MYC mutations and translocations, Immune Evasion, Proliferation	Poor
DZSig	Dark Zone Signature (Ennishi et al. 2019)	BCL2/MYC mutations and translocations, Immune Evasion, Proliferation	Poor

Table 2.1: Recent classification of DLBCL is described based on both gene expression (MHG, DZsig, COO) [7,79,134] or mutational profiles [5,139]. Association with prognosis after R-CHOP therapy is also displayed.

Two attempts at genetic classification have come out that aimed to incorporate gene expression signatures with the underlying genetic aberrations common to patient populations[5,139,166]. The first by Chapuy et al. identified 5 new genetic subtypes of DLBCL with varying prognostic value. They utilized whole exome sequencing on many DLBCL tumors at diagnosis to identify genetic aberrations via single nucleotide variants (SNVs), somatic copy number alterations (SCNAs), and structural variants (SVs). Non-negative matrix factorization (NMF) consensus clustering[167] was implemented to identify five genetic signatures in their cohort, labeled C1-C5. C1 tumors were typically represented by activating mutations in *NOTCH2* and conversely inactivating mutations in *SPEN*, the regulator of *NOTCH2*. C2 DLBCL were mostly affected by inactivation of *TP53* via SNVs and as well copy loss of 17p arm where this gene is located. This included both ABC and GCB DLBCL, which both typically contain dysfunctional *TP53*. C3 was defined by mutations affecting genes with epigenetic activity, *KMT2D*, *CREBBP*, and *EZH2* which primarily exhibit their epigenetic effects by modifying chromatin. The C4 signature was similar to C3, in that mutations in epigenetic modifiers were common, but in this instance, it was restricted to histone modification and 4 core histone genes. Finally, C5 was defined by gains in 18q, likely leading to increased *BCL2* expression as well as mutations in *MYD88* (L265P hotspot) and *CD79b*. These in contrast to other signatures, were almost always ABC DLBCL and had similar mutational landscapes to those described in CNS lymphoma. Also, the similarities shown between certain subtypes and associated lymphomas (FL, MZL) show how DLBCL can develop at multiple stages of B cell development, or progress from indolent lymphoma, and thus contribute to specific genetic signatures and different evolution patterns.

The most recent attempt at disease wide genetic classification utilizes a clustering algorithm, while also introducing a Bayesian model for assigning probabilities of a tumors likelihood of belonging to a certain subtype[6]. This classifier is termed LymphGen and assigned seven subtypes to DLBCL: EZB (MYC+ or MYC-), ST2, MCD, N1, BN2, and A53. EZB is assigned to samples that are associated with mutations in epigenetic regulators, most notably *EZH2*, *KMT2D*, *CREBBP*, and *EP300* amongst others. Further subclassification of EZB tumors revealed that this subtype includes the HGBCL-DH or DZsig pattern commonly seen in aggressive DLBCL. This resulted in the division of EZB into 2 classes: MYC+ or MYC-, with MYC+ EZB being more consistent with the HGBCL-DH lymphoma, and displayed worse prognosis than MYC- EZB. ST2 was a newer subtype introduced by the LymphGen classifier and is named for recurrent mutations in *SGKI* and *TET2*, these tumors are associated with dysfunctional PI3K and JAK/STAT signaling. Meanwhile, MCD and N1 classification are specific to ABC DLBCL. MCD tumors are characterized by mutations in *CD79b* and *MYD88* (L265P hotspot). N1 subtype is named due to the mutations in *NOTCH1* which a predominant in these tumors. Both MCD and N1 were significantly associated with worse overall survival than other subtypes such as ST2 and EZB. BN2 is perhaps the most under-appreciated subtype via gene expression analysis, as most cases that are BN2 tumors were from various COO. BN2 is defined in *NOTCH2*, and confers an improved overall survival when compared to N1 and MCD subgroups. Lastly, LymphGen also defines A53 as a group of DLBCL that are characterized by *TP53* dysfunction and mutations in *B2M*.

While many cases remained unclassified or genetically composite, these classifiers continue to improve and serve as impressive tools for analyzing both gene expression and mutational landscapes of DLBCL. Many gene signatures overlap across these classifiers,

indicating some clear mechanisms of disease progression in certain DLBCLs. However, the differences between the results from these, due to changes in the sequencing techniques, and importantly the data processing and bioinformatics implemented by each classifier, shows that DLBCL remains incredibly complex with no clear agreement in the field with regards to subtyping. It is possible that current subtypes will continue to evolve and new sub-groups of patients will be identified.

2.2.5: Features of Relapsed DLBCL

Analysis of relapsed DLBCL samples has identified recurrent mutations that contribute to disease progression. Relapsed sample studies are fewer than diagnostic DLBCL, given the lack of available tissue since patients are not routinely re-biopsied outside of clinical trials. However, several studies have identified genes important for progression and that may be particularly enriched in rrDLBCL[10,105,168]. Morin et al. used whole exome sequencing of rrDLBCL biopsies to discover increased mutational burden in *TP53*, *FOXO1*, *KMT2C*, *CCND3*, *NFKBIZ*, and *STAT6* at relapsed compared to diagnosis[169]. This provided evidence for the clonal expansion of these genes, as malignant clones resistant to therapy survive into relapse. The transcription factor *STAT6* had not been described in *de novo* DLBCL before, and this implicated D419 mutations as a potential hotspot for GCB rrDLBCL. Aberrant JAK/STAT signaling was further expanded upon in rrDLBCL, as D419 mutations contributed to increased STAT6 phosphorylation, increased transcription of STAT6 target genes, and increases in CD4+ tumor infiltrating T cells[170].

In addition to JAK/STAT signaling malfunction, selective pressure from R-CHOP or other CD-20 targeting therapies has been implicated in the loss of the target antigen, CD20. The sequencing of a large cohort of rrDLBCL plasmas identified the clonal evolution of genes

implicated in R-CHOP resistance: *TP53*, *KMT2D*, *CREBBP*, *FOXO1*, *NFKBIE*, and *MS4A1*[10]. Some of the genes overlap with those previously identified, but the addition of *MS4A1* (encoding CD20), shows CD20 loss in response to therapy. Mutations in *MS4A1* at relapse were predominantly frameshift insertions/deletions that result in a truncated form of the protein that is lacking the rituximab binding epitope. Additional missense mutations (Y86C, Y86H, G98R) were also demonstrated to reduced binding to rituximab, suggesting that multiple genetic mechanisms support CD20 loss after therapy. These results were supported by the reduced expression of CD20 by IHC and the identification of sub-clonal *MS4A1* malignant cells before therapy that become clonal after therapy[10]. This also suggested that clonal evolution can occur early on during frontline therapy, which is supported by up to 20% of rrDLBCL experiencing loss of CD20[14,171]. While enriched at relapse, *MS4A1* mutations alone do not explain the amount of antigen loss seen in rrDLBCL, implicating other mechanisms of reduced CD20 expression. These results are also supported in second or third line therapies, which demonstrated reduced transcription of CD20, and mutations resulting in epitope disruption or a truncated form of the protein[172].

These studies also provided additional evidence for altered NF- κ B signaling (*NFKBIZ*, *NFKBIE*) and altered epigenetic signaling (*KMT2C*, *KMT2D*) at relapse. Additional copy number variants (CNV) have been shown in rrDLBCL, with recurrent deletions in tumor suppressors *TP53* and *PTEN*, with gains in *STAT6* and *BCL2*, amongst others[173]. These contribute to a complex genetic landscape of variants in rrDLBCL, but with common themes emerging in dysfunctional cell survival, JAK/STAT, and NF- κ B pathways. However, there is no clear genetic profile underlining refractory cases and resistance to R-CHOP, considering the

number of relapses (~50%), different pathways implicated in rrDLBCL, and the lack of mutations seen in certain subsets, e.g. CD20 loss.

2.2.6: Current Advances in DLBCL Treatment

Frontline treatment of DLBCL normally consists of chemo-immunotherapy in the form of R-CHOP[174–176]. R-CHOP is an anthracycline based regimen that focuses on DNA damaging agents combined with rituximab to induce cell death in malignant cells. The binding of rituximab to its target CD20, results antibody dependent cellular cytotoxicity, complement pathway activation, and apoptosis of B cells[51,177]. These effects are mediated primarily by natural killer cells, but additional cell death is also achieved through antibody dependent cellular phagocytosis via macrophages. This led to improvements in patient survival in DLBCL, with roughly 60% of patients being cured after initial treatment[1,178,179]. However, 45-50% of DLBCL treated with R-CHOP will experience relapse or refractory disease, even in some cases when initial responses to therapy are very good. rrDLBCL has extremely poor outcomes and represents an unmet clinical need. Patients presenting with aggressive disease such as those with HGBCL-DH lymphoma, are often selected for more potent therapy regimens at frontline, e.g., DA-R-EPOCH[180]. Patients with measurable disease after frontline therapy, may also be candidates for radiation therapy[181], in attempts to achieve clinical remission.

Recently, clinical trials have explored the use of additional therapies in a frontline setting in DLBCL. This includes the addition of the BCL2 inhibitor venetoclax in combination with R-CHOP in a frontline setting, which displayed good responses, tolerable safety profiles and increased efficacy in BCL2 IHC positive patients[182]. The most significant improvement on R-CHOP therapy has come with the POLARIX study, which reported a 6.5% progression free survival (PFS) advantage (2 year PFS 76.7% versus 70.2%, p=0.2) when polatuzumab vedotin

was substituted for vincristine in R-CHOP in the frontline setting[18]. This modest PFS benefit did not translate to an overall survival advantage and has not been widely adopted as the new standard of care in DLBCL.

For many years, the standard of rrDLBCL is salvage chemotherapy followed by consolidation with autologous stem cell transplant (ASCT) in eligible patients[183]. Salvage chemotherapies have similar efficacy but different toxicities[184,185]. The goal is to establish chemo-sensitivity, i.e. achieve a partial or complete response after 2 or 3 cycles, given that the therapeutic effect of ASCT is the high-dose chemotherapy conditioning regimen given before the infusion of stem cells. The most commonly used salvage therapy in Canada is gemcitabine, cisplatin, and dexamethasone (GDP)[186]. Gemcitabine works as a DNA damaging agent in conjunction with cisplatin (which is a platinum complex, these salvage therapies are often referred to as platinum-based salvage).

More recently the introduction of CART therapy has dramatically transformed the treatment of relapsed DLBCL. CART is an immunotherapy in which a patient's T cells are extracted and genetically engineered with an antigen receptor targeted to malignant cells of interest. They are termed chimeric because they are designed with receptors that both identify the antigen and activate the T cell, as opposed to activation by other immune cells[28]. It has shown very promising results in rrDLBCL with complete response rates above 40% in clinical trials[29–31]. Treatment was particularly effective in patients with reduced tumor burden at the time of CART infusion[32–35,187]. Moreover, real-world studies of CART use in rrDLBCL demonstrated similar response rates to those seen in clinical trials, supporting the potential use of CART in rrDLBCL in normal clinical practice[188–190]. The ZUMA-7 and TRANSFORM trials confirmed superior progression free survival and response rates in rrDLBCL receiving

CART in 2L therapy to those receiving ASCT [36,37]. This is likely to lead to a shift in treatment strategies for rrDLBCL patients in the near future following the demonstration of CART efficacy and response in 2L settings. Unfortunately, many patients are not eligible for CART therapy due to frailty and toxicity concerns, as common adverse effects are immune effector cell-associated neurotoxicity (ICANS) and cytokine release syndrome (CRS). CART is also being investigated in frontline treatment with effective response rates, but the associated toxicities may result in overtreatment of patients who may already be cured by R-CHOP[191,192]. Additional issues in CART treatment include extreme costs associated with therapy and the production of CARTs, as well as specialized care to manage toxicities. These challenges outline the need for optimization of CART treatment strategies to harness the curative potential of this breakthrough therapy.

Additional immunotherapies have been investigated in clinical trials, with the most successful responses seen in bispecific T cell engagers (BiTE) therapy, antibody-drug conjugates combined with chemo-immunotherapy (polatuzamab vedotin and bendamustine-rituximab), and anti-CD19 therapy with an immunomodulatory agent (tafasitamab and lenalidomide). These therapies have subsequently all been approved by Health Canada for rrDLBCL and are treatment options for patients who are ineligible for ASCT. BiTE therapies aim to modulate the immune system's ability to kill tumor cells by binding CD3 on T cells and directing them to CD20 expressed on the malignant B cells[22,23]. As a monotherapy in rrDLBCL, they have shown some effectiveness[24,25] and are a viable treatment option for patients after 2 lines of therapy, although disease progression is still likely. Complete response rates to many BiTEs are between 40-60% in most cases, which is very promising given their use as a monotherapy and in a heavily pre-treated and resistant DLBCL population[26]. More recently, the BiTE therapy glofitimab

(CD3xCD20) is also being explored in the frontline setting with R-CHOP[27]. Polatuzamab vedotin is antibody-drug conjugate that delivers a microtubule inhibitor to malignant cells by targeting CD79b. Use as a monotherapy[193], and in combination with rituximab[100], showed some effectiveness in DLBCL and prompted additional exploration in combination with chemotherapy (BR). BR and polatuzamab showed an improved survival in patients ineligible for ASCT when compared to BR alone (median survival 12.4 months vs. 4.7 months)[17,102]. Finally, tafasitamab is antibody treatment targeting CD19 on DLBCL cells and is used in combination with lenalidomide, an immunomodulatory drug with antineoplastic activity[194]. This combination showed an objective response above 40%, although less than 15% achieved a complete response[195,196]. These therapies hold potential promise in rrDLBCL that cannot receive ASCT or CART but are not as effective as those preferred treatment strategies. Newer targeted therapies are continually being explored, and this is partly due to our expanding understanding of the genetics of DLBCL, which has helped to identify novel targets for therapy.

2.3: Apoptotic Pathways

2.3.1: Intrinsic and Extrinsic Apoptosis

Apoptosis or programmed cell death, is an important mechanism for destroying cells that are non-functional or may possibly become malignant. To better understand the BH3 technique discussed later, it is important to outline the functional pathways of apoptosis. It is primarily split between the intrinsic and extrinsic pathway. These pathways are activated differently, but they include significant overlap and both end with the destruction of the cell. A general figure (adapted from Carneiro et al. *Nature Reviews Clinical Oncology*. 2020.) describing apoptotic pathways in the context of cancer is provided below[197].

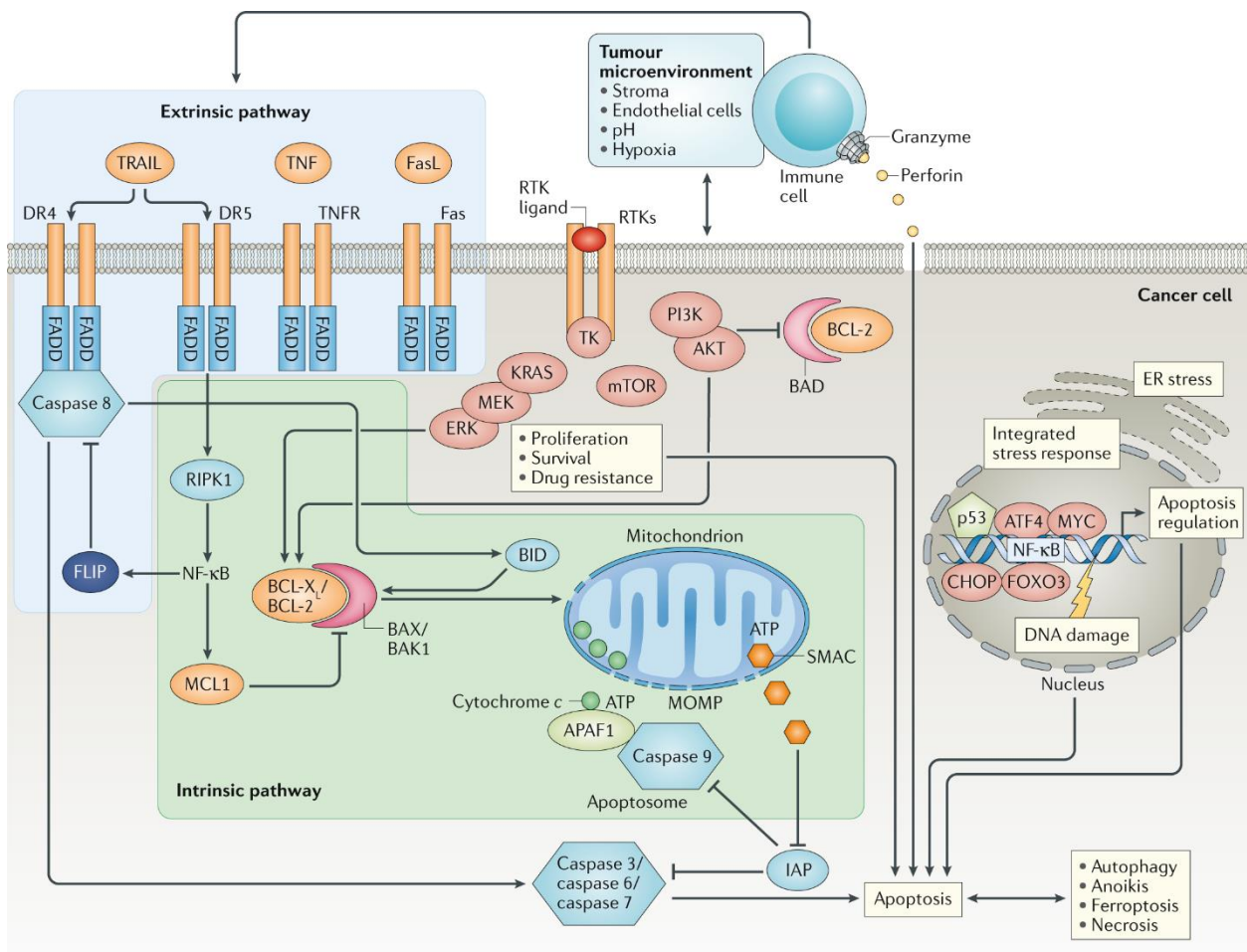


Figure 2.1: Apoptotic Pathways in Cancer. (Adapted from Carneiro et al.[197]). This figure describes general pathways of both intrinsic and extrinsic apoptosis. Activation of death receptors (e.g. DR4/5, TNFR, and FAS) by cytokines and ligands expressed on immune cells results in the subsequent recruitment of FADD and Caspase 8 to form the death-inducing signaling complex (DISC). Meanwhile, in response to cellular stress or DNA damage, activation of intrinsic apoptosis is achieved by the cleavage of BID followed by activation of BAX/BAK to form pores on the mitochondrial membrane. This leads to mitochondrial outer membrane permeabilization (MOMP), the release of cytochrome c, and subsequent recruitment of the apoptosome (APAF1 and Caspase 9). Importantly, intrinsic apoptosis can be inhibited by anti-apoptotic proteins such as BCL2, MCL1, and BCLXL, which bind pro-apoptotic proteins and prevent them from initiating MOMP. Significant overlap exists between these pathways, as seen by the ability of Caspase 8 to activate BID, inhibitors of apoptosis (IAP) proteins effects on Caspase activation, and the influence of both pathways to perturbations in RTK activation and downstream NF-κB signaling.

The intrinsic pathway is sometimes called the mitochondrial pathway, as the pathway revolves around mitochondrial membrane proteins and the permeabilization of said membrane. The proteins responsible for this are the *BCL2* family of proteins, which contains both pro-apoptotic and pro-survival proteins. These proteins share various *BCL2* homology (BH) regions, labeled BH1-4. BH3 regions are the primary activators of apoptosis and the proteins that only have BH3 domains are highly apoptotic[198]. In response to an apoptotic stimulus, such as DNA damage, cells upregulate the signaling of the BH3-only activators BIM/BID. They bind to effector proteins, BAX/BAK, which are pore-forming proteins. This binding activates the effectors and allows the formation of pores in the mitochondrial membrane. Cytochrome c is released as a consequence of this mitochondrial outer membrane permeabilization (MOMP), which leads to the formation of the apoptosome. Subsequent steps involve caspase activation, DNA fragmentation, externalization of phosphatidylserine, and finally the phagocytosis of the cell. This process is inhibited by pro-survival *BCL2* proteins, which contain all 4 BH domains. These proteins include BCL2, MCL1, BCLXL, and BCLW. Their primary function is to bind pro-apoptotic proteins and prevent them from activating the apoptotic cascade and MOMP. However, there exists another BH3-only class of proteins called sensitizers (BAD, NOXA, PUMA, HRK) that function to sequester the pro-survival proteins and free BIM/BID[199].

The extrinsic pathway is named so because it involves the activation of apoptosis through stimuli from outside the cell. Tumor necrosis factor (TNF) receptors are a group of membrane bound proteins that function primarily in inflammation and apoptosis. Several TNF receptors are implicated in extrinsic apoptosis, most notably FAS and TNFR1[200,201]. For example, the binding of FAS by FAS-ligand, expressed on cytotoxic T cells, initiates the formation of death-inducing signaling complex (DISC). After activation of death receptors, the death effector

protein FADD is recruited and binds to caspases 8 and 10, thus forming the DISC. This then leads to additional caspase activation and cell death. The TNF family has other receptors such as TNFR1, that may influence apoptosis as well by recruiting a protein called TRADD to initiate caspase activation. Extrinsic apoptosis overlaps with the intrinsic pathway, as activated caspase 8 through the DISC has been shown to cleave BID into tBID (the truncated, activated form of BID), and increase the activation of effector proteins leading to MOMP. Additional death receptors such as DR4/5 can activate extrinsic apoptosis after binding of TRAIL, highlighting multiple receptors that can be activated by either cytokines, or direct cell-cell interactions by immune cells.

Outside of these pathways, cell death can also be achieved by a multitude of other processes, which include direct cell-mediated death by granzymes and perforin (cytotoxic T cells and natural killer cells), autophagy, and necrosis (Figure 2.1). These pathways are important to note for potential therapeutic avenues in cells that are resistant to multiple forms of apoptotic activation, but will not be discussed in depth in this thesis.

2.3.2: Inhibition of Intrinsic Apoptosis in DLBCL

While there are genomic alterations contributing to apoptotic inhibition, such as those resulting in overexpression of BCL2, there are additional mechanisms involved in the dysfunction to the apoptotic pathway in DLBCL[197,202]. This is made apparent by the relatively poor response to venetoclax in DLBCL, as well as the general lack of mutations seen in additional apoptotic proteins (e.g. MCL1). Intrinsic or mitochondrial apoptosis is an important pathway that engages cell death after exposure to chemotherapy, but is often dysfunctional in DLBCL and contributes to the survival of malignant cells. This process is inhibited by pro-survival *BCL2* proteins, which include BCL2, MCL1, BCLXL, and BCLW[203]. Their primary

function is to bind pro-apoptotic proteins (BIM/BAX) and prevent their initiation of the apoptotic cascade. MCL1 is normally necessary for germinal center formation and B cell development[204,205], but has shown prominent anti-apoptotic activity in DLBCL cell lines and mouse models[206–208]. In addition to BCL2, MCL1 has been shown to contribute to apoptotic resistance primarily in BCL2 negative and/or MCL1 positive DLBCL cell lines, as inhibiting MCL1 led to increased apoptosis in these cases[209,210]. Targeting both MCL1 and BCL2 with polatuzamab vedotin and venetoclax has been proposed as a method for overcoming MCL1 and BCL2 dependent inhibition in DLBCL[211]. Additional contributions towards intrinsic apoptotic resistance have been assessed in BCLXL and BCLW. BCLXL is a known survival factor in platelets, but has shown reduced contribution to apoptotic inhibition in DLBCL when compared to MCL1[210]. As well, it is not a promising target due potential thrombocytopenia concerns in addition to low apoptotic inhibition in most DLBCL[212]. BCLW has been shown to be overexpressed in NHL gene expression studies[213] but further studies showed it may not be required for malignant cell growth in DLBCL[214]. Overall, *in vitro* studies have shown MCL1 and BCL2 to be the primary contributors of intrinsic apoptotic dysfunction in DLBCL and have contributed to our understanding of therapeutic resistance on a functional level.

2.4: BH3 Profiling

BH3 profiling has emerged as a relatively easy, but powerful tool for predicting the apoptotic competency of both normal and malignant cells [203,215,216]. It uses BH3 mimetics and various BCL2 protein inhibitors to identify the balance between pro-apoptotic proteins and pro-survival proteins in the intrinsic apoptotic pathway. It was previously used to identify three classes of apoptotic block[217], two of which indicate defects in pro-apoptotic proteins (class A/B). The analysis of cytochrome c release in response to BH3 peptides BIM and PUMA are key

for determining the type of apoptotic block present in each sample. These are possibly the two most crucial BH3-only proteins involved in the activation BAX/BAK. While BIM is a direct activator of the apoptotic effector proteins, PUMA mainly acts as pan-sensitizer, as it broadly sequesters all types of anti-apoptotic proteins. PUMA can also directly activate BAX/BAK, but this effect is less dramatic when compared to BIM, especially when using BH3 domain peptides instead of full proteins, as is done in the BH3 profiling technique[218,219]. Class A blocks do not respond to PUMA as they have ineffective activators BIM/BID, while class B blocks do not respond to BIM or PUMA, as they have ineffective effectors BAX/BAK. Class C blocks respond to both, as the primary proteins responsible for their block are pro-survival BCL2 family proteins. BH3 profiling was chosen as our method for determining apoptotic dependencies in NHL samples due to its ease of use via flow cytometry and having been a reliable indicator of response to BCL2 related therapy in associated hematological malignancies[220–223]. In that context, BH3 profiling has predicted the response of venetoclax in CLL, which is dependent on BCL2 for survival[220]. Profiling of tissue samples in myeloma and acute myeloid leukemia has also aided in predicting responses to chemotherapy[221–223]. While apoptotic block was demonstrated in DLBCL cell lines[217], it had not yet been explored in multiple primary NHL, including DLBCL. That led to the use of BH3 profiling in this thesis to investigate causes of apoptotic block and venetoclax resistance in DLBCL.

2.5: Circulating Tumor DNA Sequencing

Advancements in sequencing technology and methodology have resulted in circulating tumor DNA (ctDNA) becoming a powerful tool for monitoring disease and measuring measurable residual disease (MRD). The monitoring of patient responses and tumor changes as disease progresses are made difficult by the invasive nature of taking repeat tumor biopsies.

However, blood collection is a routine, non-invasive procedure that may hold value in patient prognostics. Human plasma contains cell-free DNA (cfDNA), which is DNA that has been shed from various cells into the bloodstream or lymphatic system. The process by which cells do this outside of apoptosis or necrosis, is still poorly understood. However, cfDNA has potential prognostic value in cancers as well as other disease[224–228]. Part of cfDNA consists of ctDNA, which is similar to cfDNA, as it is DNA shed from cells, but this is specifically the DNA shed from tumor cells. ctDNA has been identified in most cancers, and as such offers a potentially non-invasive way to monitor a patient’s disease[229–231]. ctDNA assays hold great value in DLBCL as potential novel predictive tools for relapse, and may contribute to improved detection of rrDLBCL as patients are under surveillance. This would translate into more effective and timely administration of therapeutic interventions in high-risk patients, particularly in the case of CARTs in 2L therapy.

The preferred technique for analyzing and detecting ctDNA in solid and hematological malignancy has been targeted, high-depth sequencing. Particularly, the use of Cancer Personalized Profiling by deep Sequencing (CAPP-Seq) has been used by many research groups to analyze specific mutational patterns in known genes of cancer progression[232,233]. CAPP-Seq leverages specific panels for the cancer of choice, in which the genes most associated with said cancer are targeted at an ultra-high depth (~1500X). Custom panels are altered by different research groups to include additional genes of interest. While whole genome and whole exome sequencing (WGS and WES, respectively) allows wider coverage of the genome that may be lacking in CAPP-Seq, this technique has benefit of not only being able to profile the mutational landscape of known drivers of disease, but also ultra-low detection of ctDNA. This makes

CAPP-Seq the methodology of choice for ctDNA monitoring and analyzing changes in ctDNA dynamics as patients progress through therapies.

CAPP-Seq analysis of fragmented ctDNA is usually performed as follows. ctDNA extracted from plasma is built into DNA libraries incorporating indexes for multiplexing samples together, but also using unique molecular identifiers (UMIs). UMIs allow for the tagging of individual strands of DNA prior to PCR duplication. During downstream bioinformatic analysis, these UMIs can be used to collapse reads originating from the same molecule, and thus reduce the number of errors in variant calling and increase the confidence of our true somatic mutations[233]. After libraries are built, they are then hybridized with biotinylated probes corresponding to the genes of interest in the custom panel designed for the specific research question or malignancy. Finally, after hybridization capture, the final DNA molecules are sequenced at high-depth to detect low variant allele fraction mutations using a bioinformatic pipeline with a matched normal that underwent the same processing (Figure 2.2).

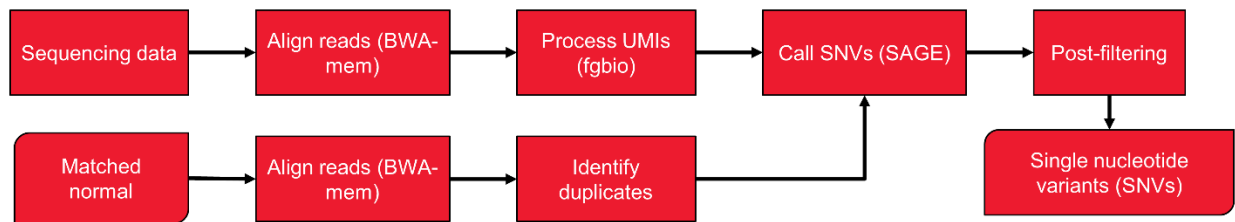


Figure 2.2: Analysis Pipeline of Circulating Tumor DNA by CAPP-Seq Using Error Correction. A general description of ctDNA analysis proposed by our group is provided here, where targeted sequencing data from ctDNA is aligned and processed with a matched normal to identify duplicates and filter germline variants. Then unique molecular identifiers (UMIs) are used in error suppression as described by Newman et al. [233]. We then applied SAGE variant caller (<https://github.com/hartwigmedical/hmftools/tree/master/sage>) and custom post-filtering to identify candidate single nucleotide variants.

Utilizing CAPP-Seq in DLBCL, the concentration of ctDNA pre-therapy and the rate of decline in ctDNA on treatment, are prognostic for response to therapy in both frontline and relapse settings. Pretreatment levels of ctDNA correlated with DLBCL staging, IPI scores, tumor burden as measured by PET scan, and progression free survival[234]. Diagnostic levels of ctDNA also correlated with time to treatment, which reflected advanced disease, i.e. patients with short diagnosis to treatment interval had higher levels of ctDNA[235]. The prognostic effect of ctDNA detection appears to be enhanced at later timepoints. Log fold decreases in ctDNA concentration after the first or second cycle of R-CHOP also correlated with R-CHOP responses by end of treatment[234]. Monitoring ctDNA changes during therapy, particularly increases in ctDNA may hold significant value for predicting rrDLBCL. Following treatment, analyzing ctDNA at the end of R-CHOP allowed for improved detection of MRD than traditional methods such as PET/CT. This correlated to an improved progression free and overall survival in patients that were ctDNA negative and helped to identify false-negatives produced by imaging analysis[236,237]. End of treatment ctDNA detection was made more powerful by the recent advancement in phased variant sequencing (Phased-Seq). This method utilizes phased variants occurring closely together on the same DNA molecule to improve limits of detection and sensitivity of ctDNA assays[238]. This requires a separate panel construction, specifically dedicated to phased variant detection, which is specific to certain regions of recurrent mutations in DLBCL and related malignancies. These tools are being explored in the context of clinical trials, that may help validate their use as a clinical assay in identifying therapeutic resistance and patient prognosis[239–242]. There is still a need for ctDNA monitoring to be tested in an appropriate prospective manner before it can be fully integrated into clinical settings and inform on patient treatment decisions[243].

In addition to studying ctDNA dynamics, a variety of additional sequencing analyses have been used to inform on cancer genetics and biology. WGS has been used in a variety of ctDNA sequencing to emphasize novel mutational patterns in different cancers, as well as potentially relevant non-coding mutations. WGS of ctDNA was used to predict treatment response and identify likelihood of disease progression in solid cancers[244]. ctDNA analysis in prostate cancer has also involved deep WGS (187x median depth) that helped to identify clonal structures and potential genetic mechanisms of resistance that are potentially missed in sequencing that utilizes a narrower approach[245]. In the context of DLBCL, ctDNA matched with patient biopsies revealed the ability of ctDNA to capture the entire disease heterogeneity that was not accurately reflected in biopsies[246]. Fragmentomics is the analysis of fragmentation patterns in cfDNA, and was recently used to accurately infer gene expression and ctDNA levels from plasma in DLBCL and other malignancies[246,247]. These highlight the potential versatility of ctDNA samples via multiple methods of detection, gene expression profiling and mutational investigation.

Due to the relatively young nature of the field, there is not a standardized method of quality control, data interpretation, or data reporting when it comes to ctDNA mutational analysis. This has created a large barrier to the implementation of ctDNA monitoring in a clinical setting, however many groups are working on developing platforms using ctDNA analysis for clinical use (e.g. Foresight Diagnostics, Roche Avenio Platform)[238,248]. The associated costs and feasibility of these platforms in routine clinical setting remains to be seen. However, current ctDNA sequencing technology is an encouraging assessment tool that may one day be used clinically to predict rrDLBCL.

Chapter 3: Apoptotic Blocks in Primary Non-Hodgkin B Cell Lymphomas Identified by BH3 Profiling

3.1: Preface

DLBCL is an aggressively proliferating disease, often leading to treatment resistance and relapse. The goal of most treatment regimens is to trigger the apoptotic cascade in malignant cells, either through direct targeting or DNA damaging agents, and ultimately lead to cell death. Therefore, it seems reasonable to hypothesize that DLBCL resistant to therapy has developed the ability to circumvent this apoptotic activation. This is a known phenomenon in DLBCL, given the high mutational prevalence in genes directly involved in the apoptotic pathway such as *BCL2*. However, the targeting of *BCL2* protein in DLBCL has proven less effective than associated NHLs which all express *BCL2*[146,249]. Therefore, we were interested in the intrinsic competency of apoptosis in DLBCL and other NHL. It seems likely that there are multiple factors contributing to apoptotic block in DLBCL and may include some intrinsic differences in the function of pro-apoptotic proteins. The aim of this study was to explore the differences in apoptotic activation between NHL using a technique called BH3 profiling[215]. By exposing patient tumor single cell suspensions to various peptides and inhibitors in different parts of the apoptotic cascade, we can determine how readily cells undergo apoptosis when given appropriate stimuli. If they are resistant to apoptotic activation, we can also determine at which step of the pathway they are unable to continue with apoptosis. This is of particular interest to pro-apoptotic dysfunction, which has not been readily described in most NHL. Apoptotic dysfunction in NHL usually refers to an increase in expression or function of pro-survival proteins such as *MYC* or *BCL2*. Therefore, this study explores additional mechanisms of

apoptotic resistance, and subsequently therapeutic resistance, in DLBCL using primary patient samples, a rare sample collection.

Apoptotic Blocks in Primary Non-Hodgkin B Cell Lymphomas Identified by BH3 Profiling

Ryan N. Rys^{1,2,†}, Claudia M. Wever^{2,3,†}, Dominique Geoffrion^{2,3,4}, Christophe Goncalves², Artin Ghassemian^{2,3}, Eugene Brailovski³, Jeremy Ryan⁵, Liliana Stoica², José Hébert^{6,7}, Tina Petrogiannis-Haliothis⁸, Svetlana Dmitrienko⁸, Saul Frenkiel⁹, Annette Staiger^{10,11}, German Ott¹⁰, Christian Steidl¹², David W. Scott¹², Pierre Sesques², Sonia del Rincon^{2,3}, Koren K. Mann^{2,3}, Anthony Letai⁵ and Nathalie A. Johnson^{2,3,13,*}

1. Department of Physiology, McGill University, Montreal, QC H3G 1Y6, Canada
2. Lady Davis Institute for Medical Research, Jewish General Hospital, Montreal, QC H3T 1E2, Canada
3. Department of Medicine, McGill University, Montreal, QC H4A 3J1, Canada
4. Department of Experimental Surgery, McGill University, Montreal, QC H3G 1A4, Canada
5. Department of Medical Oncology, Dana-Farber Cancer Institute, Boston, MA 02115, USA
6. Department of Medicine, Université de Montréal, Montreal, QC H3T 1J4, Canada
7. Division of Hematology-Oncology and Quebec Leukemia Cell Bank, Maisonneuve Rosemont Hospital, Montreal, QC H1T 2M4, Canada
8. Division of Pathology, Jewish General Hospital, Montréal, QC H3T 1E2, Canada
9. Department of Otolaryngology-Head and Neck Surgery, Jewish General Hospital, Montreal, QC H3T 1E2, Canada
10. Department of Pathology, Robert-Bosch Hospital, 70184 Stuttgart, Germany
11. Dr. Margarete-Fischer-Bosch-Institute of Clinical Pharmacology, University of Tübingen, 70376 Stuttgart, Germany
12. Center for Lymphoid Cancer, BC Cancer, Vancouver, BC V5Z 1L3, Canada
13. Departments of Medicine and Oncology, Jewish General Hospital, Montreal, QC H3T 1E2, Canada

* Author to whom correspondence should be addressed.

† These authors contributed equally to this work.

Cancers 2021, 13(5), 1002; <https://doi.org/10.3390/cancers13051002>

Received: 2 February 2021 / Revised: 17 February 2021 / Accepted: 23 February 2021 /
Published: 28 February 2021

(This article belongs to the Special Issue B Cell Lymphoma)

3.2: Simple Summary

The BCL2 protein is expressed in many non-Hodgkin lymphomas (NHLs) as well as associated leukemias, e.g., chronic lymphocytic leukemia (CLL). It functions as a cell survival protein that reduces that ability of a cell to undergo mitochondrial apoptosis. However, the BCL2 inhibitor venetoclax is mainly effective in CLL, despite the expression of its protein target in NHL. We hypothesized that other mechanisms are inhibiting apoptosis in NHL: defects in pro-apoptotic signaling and/or the expression of anti-apoptotic proteins other than BCL2. Our study makes use of a technique known as BH3 profiling, which is a functional assay that determines the apoptotic competency of cells on primary NHL samples. By determining how cells in NHL avoid apoptosis upon exposure to venetoclax, we can identify patients who may benefit from additional therapies and potentially improve the response of drugs currently undergoing clinical trials for NHL.

3.3: Abstract

To determine causes of apoptotic resistance, we analyzed 124 primary B cell NHL samples using BH3 profiling, a technique that measures the mitochondrial permeabilization upon exposure to synthetic BH3 peptides. Our cohort included samples from chronic lymphocytic leukemia (CLL), follicular lymphoma (FL), diffuse large B-cell lymphoma (DLBCL), high-grade B cell lymphoma with translocations in MYC and BCL2 (HGBL-DH), mantle cell lymphoma (MCL) and marginal zone lymphoma (MZL). While a large number of our samples displayed appropriate responses to apoptosis-inducing peptides, pro-apoptotic functional defects, implicating BAX, BAK, BIM or BID, were seen in 32.4% of high-grade NHLs (12/37) and in 3.4% of low-grade NHLs (3/87, $p < 0.0001$). The inhibition of single anti-apoptotic proteins

induced apoptosis in only a few samples, however, the dual inhibition of BCL2 and MCL1 was effective in 83% of samples, indicating MCL1 was the most common cause of lack of response to the BCL2 inhibitor, venetoclax. We then profiled Toledo and OCI-Ly8 high-grade lymphoma cell lines to determine which drugs could reduce MCL1 expression and potentiate venetoclax responses. Doxorubicin and vincristine decreased levels of MCL1 and increased venetoclax-induced apoptosis (all $p < 0.05$). Overall, in primary NHLs expressing BCL2 that have no defects in pro-apoptotic signaling, a poor response to venetoclax is primarily due to the presence of MCL1, which may be overcome by combining venetoclax with doxorubicin and vincristine-based chemotherapy or with other anti-microtubule inhibitors.

Keywords: NHL, BCL2, MCL1, apoptosis, DLBCL, BH3 profiling, venetoclax

3.4: Introduction

BCL2 is an oncogene that inhibits apoptosis [1,2]. It is expressed in many non-Hodgkin lymphomas (NHLs), including chronic lymphocytic leukemia/small lymphocytic leukemia (CLL/SLL), mantle cell lymphoma (MCL), marginal zone lymphoma (MZL), ~60% of diffuse large B-cell lymphomas (DLBCLs), and 85% of follicular lymphomas (FLs) [3]. BCL2 expression is associated with inferior survival when there is concurrent expression of MYC, an oncogene that can stimulate cellular proliferation [4,5]. This is the case in double-expressor (DE) DLBCLs and high-grade B cell lymphomas with translocations in MYC and BCL2, also known as “double-hit lymphomas” (HGBL-DH) [6]. Higher levels of BCL2 expression are associated with the presence of a BCL2 translocation and possibly an inferior outcome in DLBCLs [7]. Venetoclax is a BCL2 homology 3 (BH3) mimetic that selectively inhibits BCL2 [8]. While effective in CLLs [9,10], venetoclax is less successful in other NHLs despite them expressing the

BCL2 target [11,12]. Understanding why certain NHL cells survive after exposure to venetoclax may lead to more effective treatment regimens for these patients.

Mitochondrial apoptosis is the primary mechanism of cell death following exposure to chemotherapy and cell fate lies in the balance between the pro- and anti-apoptotic BCL2 family of proteins [13]. This family of proteins share 1–4 BH domains, with BH3-only proteins being the most potent initiators of apoptosis. Upon cellular stress, “activator” BH3 proteins BIM and BID activate “effector” proteins BAX and BAK, leading to mitochondrial outer membrane permeabilization (MOMP) and subsequent cytochrome c release, an irreversible step committing the cell to undergo apoptosis. This process is inhibited by anti-apoptotic proteins (e.g., BCL2, MCL1, BCLXL, BCLW, BCLB, and BFL1), which bind to the pro-apoptotic BH3 proteins in order to prevent activation of BAX/BAK. Pro-apoptotic “sensitizer” proteins (e.g., PUMA, NOXA, BAD, and HRK), indirectly promote apoptosis by binding to anti-apoptotic proteins, thus releasing BIM/BID to activate BAX/BAK (Figure 1A). BH3 profiling assesses the functional dynamics between pro- and anti-apoptotic proteins to predict what is inhibiting mitochondrial apoptosis in live cells [14]. It uses cytochrome c release as a measure of commitment to apoptosis after exposing cells to different synthetic peptides or inhibitors, which have differing affinities for the anti-apoptotic proteins [15] (Figure 1B). BH3 profiling of DLBCL cell lines revealed three classes of apoptotic blocks, as described by Deng et al., demonstrating defects in pro-apoptotic signaling (classes A and B) or increased expression of anti-apoptotic proteins (class C) [16]. The analysis of cytochrome c release in response to BH3 peptides BIM and PUMA are key for determining the type of apoptotic block present in each sample. While BIM is a direct activator of the apoptotic effector proteins, PUMA mainly acts as a pan-sensitizer, as it broadly sequesters all types of anti-apoptotic proteins. PUMA can also

directly activate BAX/BAK, but this effect has been less pronounced than BIM, especially when using BH3 domain peptides instead of full-length proteins [17,18]. Therefore, the subsequent release of cytochrome c in response to these peptides can identify whether apoptotic defects are present due to pro- or anti-apoptotic dysfunction (Figure 1, Figure S1). Class A blocks have strong responses to BIM but weak responses to PUMA, indicating the insufficient function of activator proteins to bind to BAX/BAK. Class B blocks do not respond to BIM or PUMA, have weak responses to all peptides, and indicate dysfunctional effector proteins. Class C blocks are the most common and show strong responses to several peptides, particularly to anti-apoptotic inhibition, indicating an excess of anti-apoptotic proteins as a mechanism of cell survival (Figure 1C, see supplemental methods in supplementary materials). A sample with a class C block is considered “primed” if removing the anti-apoptotic BCL2 proteins, for example with PUMA, would initiate MOMP, implying the presence of functional BIM/BID and BAX/BAK. BH3 profiling has been valuable in predicting the response to chemotherapy and BH3 mimetics in CLL [19], acute leukemias and multiple myeloma [20,21,22]. It has also predicted the response to BH3 mimetics in DLBCL cell lines [16] but has not yet been reported in primary NHLs due to the lack of archived cells frozen as viable cell suspensions.

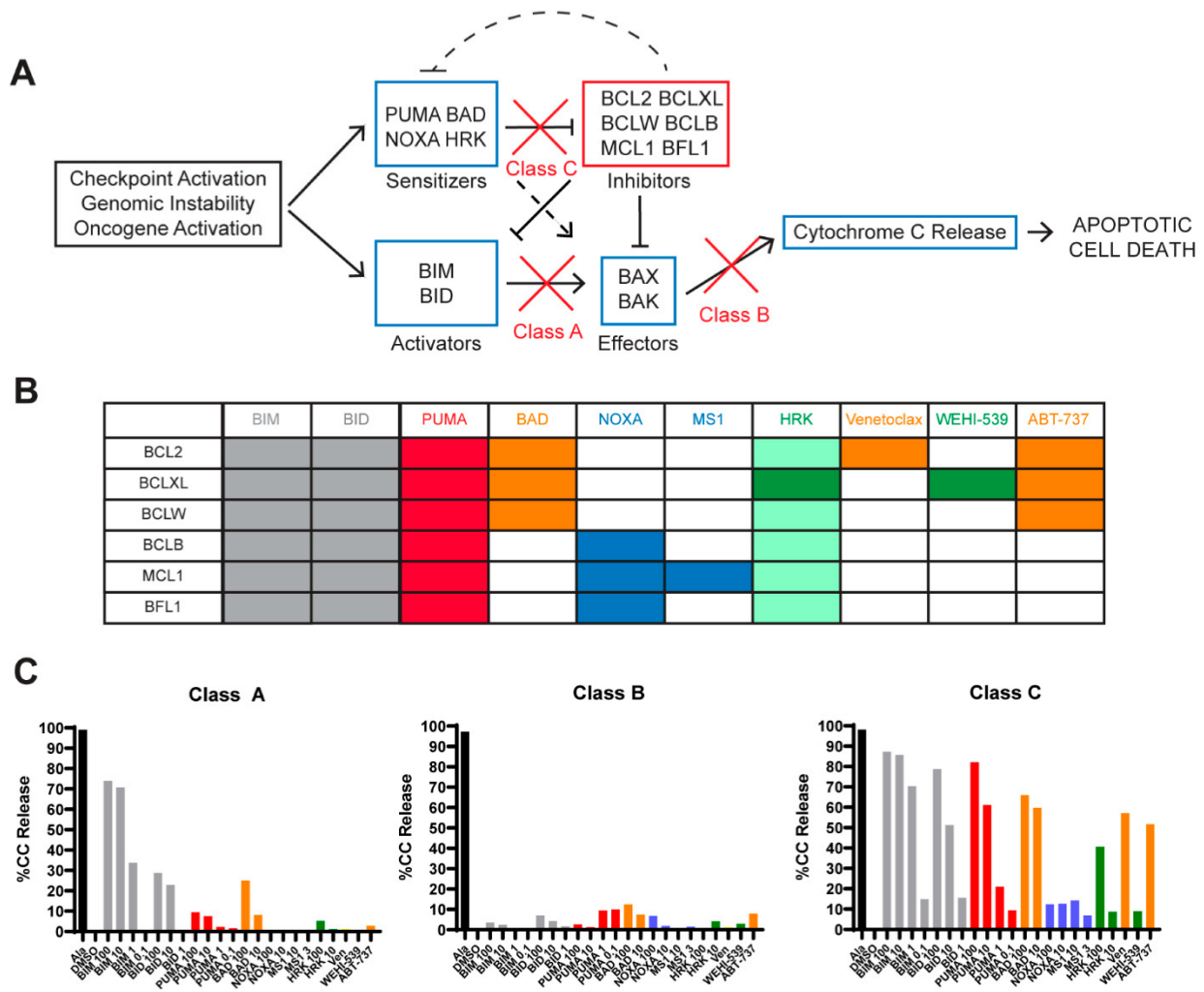


Figure 3.1. BH3 profiling assay: rationale and methodology. (Adapted from Deng et al. [16]). (A) Anti-apoptotic BCL2 family members inhibit the mitochondrial apoptotic pathway. Upon oncogene activation or cellular damage, activator and/or sensitizer proteins are upregulated, which allows BAX and BAK to oligomerize, leading to cytochrome c release, which results in apoptotic cell death. Anti-apoptotic BCL2 family members inhibit pro-apoptotic and sensitizer proteins, preventing BAX and BAK from inducing mitochondrial outer membrane polarization (MOMP), the commitment to apoptosis. (B) Pattern of interaction between the anti-apoptotic proteins (rows) present in cells and the pro-apoptotic synthetic peptides or drugs (columns) used in the BH3 profiling assay. PUMA (illustrated by red columns) inhibits all the inhibitors and is a pan-sensitizer, as well as contributing to BAX and BAK activation. Orange colors indicate peptides that inhibit the BCL2 protein with venetoclax inhibiting only BCL2 whereas BAD and ABT-737 inhibit BCL2, BCLXL, and BCLW. Blue columns are used to highlight mantle cell lymphoma (MCL)1-dependence where MS1 specifically inhibits MCL1, whereas NOXA inhibits BCLB, MCL1

and BFL1. Green columns indicate BCL-XL-dependence where WEHI-539 only inhibits BCLXL and HRK is mainly a BCL-XL inhibitor but can also inhibit other anti-apoptotic proteins with lower affinities, including BCL2. (C) BH3 profiles are illustrated in graphical form with % of the cells undergoing cytochrome c release on the Y axis after exposure to each drug/peptide on the X axis. Alamethicin (ALA) is a control that induces cytochrome c release in all cells independent of BAX or BAK. DMSO is the negative vehicle control because it does not induce cytochrome c release. Representative samples from our cohort were used to demonstrate different classes of apoptotic block. This high-grade B cell lymphoma with translocations in MYC and BCL2 (HGBL-DH) sample shows a class A block, where cells were competent to undergo apoptosis (i.e., functional BAX/BAK) because exogenous activators BIM and BID could induce MOMP (grey bars). Two diffuse large B-cell lymphoma (DLBCL) samples shown here represent a class B and C BH3 profile. In class B blocks, cells fail to undergo MOMP upon exposure to BIM or BID BH3 synthetic peptides, indicating that there is no functional BAX or BAK, and are incompetent for undergoing apoptosis through the mitochondrial pathway. In class C blocks, cells are competent to undergo apoptosis (grey BIM/BID), primed (red PUMA) and depend mainly on BCL2 (orange bars).

We hypothesized that BCL2+ NHLs that do not respond to venetoclax have defects in pro-apoptotic signaling or express other anti-apoptotic proteins not targeted by venetoclax. Our aims were to use BH3 profiling to determine the apoptotic blocks present in primary NHLs and to determine whether exposure to chemotherapy agents could identify drugs that could synergize with venetoclax and maximize cell death. We found that NHLs have mostly class C blocks, depending mainly on BCL2 and MCL1 for survival, but we also discovered a subset of samples displaying clear pro-apoptotic protein defects. Finally, we found that pre-treatment with doxorubicin and vincristine sensitizes DLBCL cell lines to venetoclax.

3.5: Results

3.5.1: BH3 Profiling Is Reproducible in Primary Cells

We first established the reproducibility of BH3 profiling and physiologic responses to apoptotic stimuli using peripheral blood (PB) and tonsillar B cells from 24 different healthy individuals. Normal B cells had high cytochrome c responses to BIM and PUMA (>60%), with PB B cells having a much lower coefficient of variation (CV) (5.1% for BIM, 8.4% for PUMA) than tonsillar B cells (13.6% for BIM, 17.2% PUMA). The increased variability in tonsils may reflect a differing biology and the increased manipulation of these cells when generating a cell suspension. Considering that the majority of our samples are derived from patient lymph nodes, we cannot rule out these contributions to any variability in responses. For those reasons, tonsillar B cells were used to establish thresholds to define class A/B blocks, as it reflects the largest part of our cohort. Low cytochrome c responses (0–30%) were defined as being greater than 2.5 standard deviations away from the lowest mean response in tonsillar B cells, with no normal B cell (PB or tonsil) falling into this range (Figure 2A, Figure S2). We also measured cytochrome c release in DLBCL cell lines and demonstrated that cytochrome c release by BH3 profiling correlates with cell viability at 17 h (Figure S1B). Cell viability studies in primary cells proved to be ineffective, as there were insufficient cells to run subsequent experiments and/or poor viability for these cells under standard culture conditions. However, the results from our cell lines support that cytochrome c release after MOMP is an early commitment to apoptosis. The summary of all BH3 profiles is provided in Figures S3 and S4.

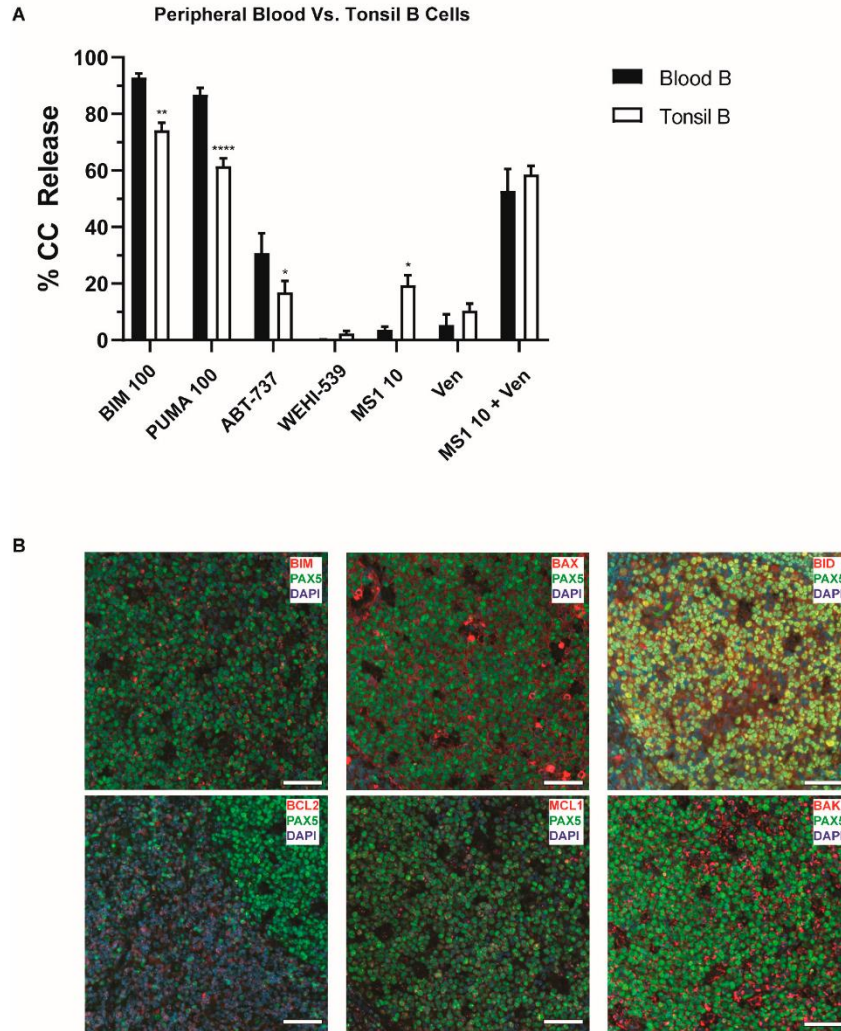


Figure 3.2. BH3 profiling of peripheral blood (PB) and tonsil B cells. (A) The percentage of cells undergoing cytochrome c release is displayed on the y-axis according to different cell subsets identified on the x-axis. Shown is the comparison of frozen B lymphocytes from tonsils and peripheral blood. Tonsillar B cells have lower responses to BIM and PUMA, while showing increased responses to MS1. Bars represent the mean \pm standard error of the mean (SEM). Analysis was carried out using a 2-way ANOVA comparing peptide exposure or subtype with cytochrome c release. * $p < 0.05$, ** $p < 0.01$, **** $p < 0.0001$. (B) Representative merged immunofluorescence (IF) images of normal tonsil. Images were taken on a 20 \times objective highlighting staining of DAPI (blue), PAX5 (green, AF594) and the protein of interest (red, AF647). Scale bars represent 50 μ m. Pro-apoptotic proteins are expressed in normal germinal center (GC) cells, along with MCL1. BCL2 expression is confined to the edges of the GC follicle and PAX5 negative cells.

3.5.2: Normal B Lymphocytes Are Partially Dependent on BCL2

We then compared the BH3 profiles of PB and tonsillar B cells to determine if there were any differences in “priming” or dependence on anti-apoptotic proteins. Tonsillar B cells had lower responses to PUMA and BIM (all $p < 0.001$), suggesting they were more resistant to apoptosis and less “primed” for cell death than PB B cells. Both groups had relatively low responses to individual anti-apoptotic protein inhibition, except that tonsillar B cells had higher responses to MS1 ($p < 0.05$), suggesting they were more MCL1-dependent (Figure 2A). Much higher cytochrome c responses were achieved when combining inhibitors to both BCL2 and MCL1. Immunofluorescence staining for PAX5, a B cell transcription factor used for identification [23], and intrinsic apoptotic proteins was carried out on tonsil tissue to establish the expression of these proteins, as previously reported [24,25,26]. Germinal center (GC) cells expressed BAX, BIM, BID, and BAK, while MCL1 was expressed in multiple punctae and BCL2 was preferentially expressed outside the GC (Figure 2B). Taken together, normal B lymphocytes had typical class C profiles, were primed, and dependent on BCL2 and MCL1 for survival.

3.5.3: Defects in Pro-Apoptotic Signaling Are a Feature of High-Grade Lymphomas and Poor Responses to Venetoclax

Low grade NHLs (FL, CLL, MZL and MCL) had class C blocks, as determined by responses to BIM and PUMA, with similar profiles to normal B cells (Figure 2 and Figure 3). Although we were limited to 12 samples, we showed that MCL had significantly lower PUMA responses compared to PB B cells ($p = 0.0320$). CLL and SLL are generally considered to be different representations of the same disease, their main difference being that the malignant cells arise from either the blood/bone marrow (CLL) or the lymph nodes (SLL). Comparing CLL/SLL

cells obtained from different compartments, PB versus lymph node (LN), SLL cells had similar responses to BIM and PUMA but higher responses to MS1, indicating a more prominent MCL1 dependence in the LN, similar to our tonsillar controls (Figure 4C). Overall, low-grade NHLs are primed and would undergo apoptosis except for the presence of anti-apoptotic proteins.

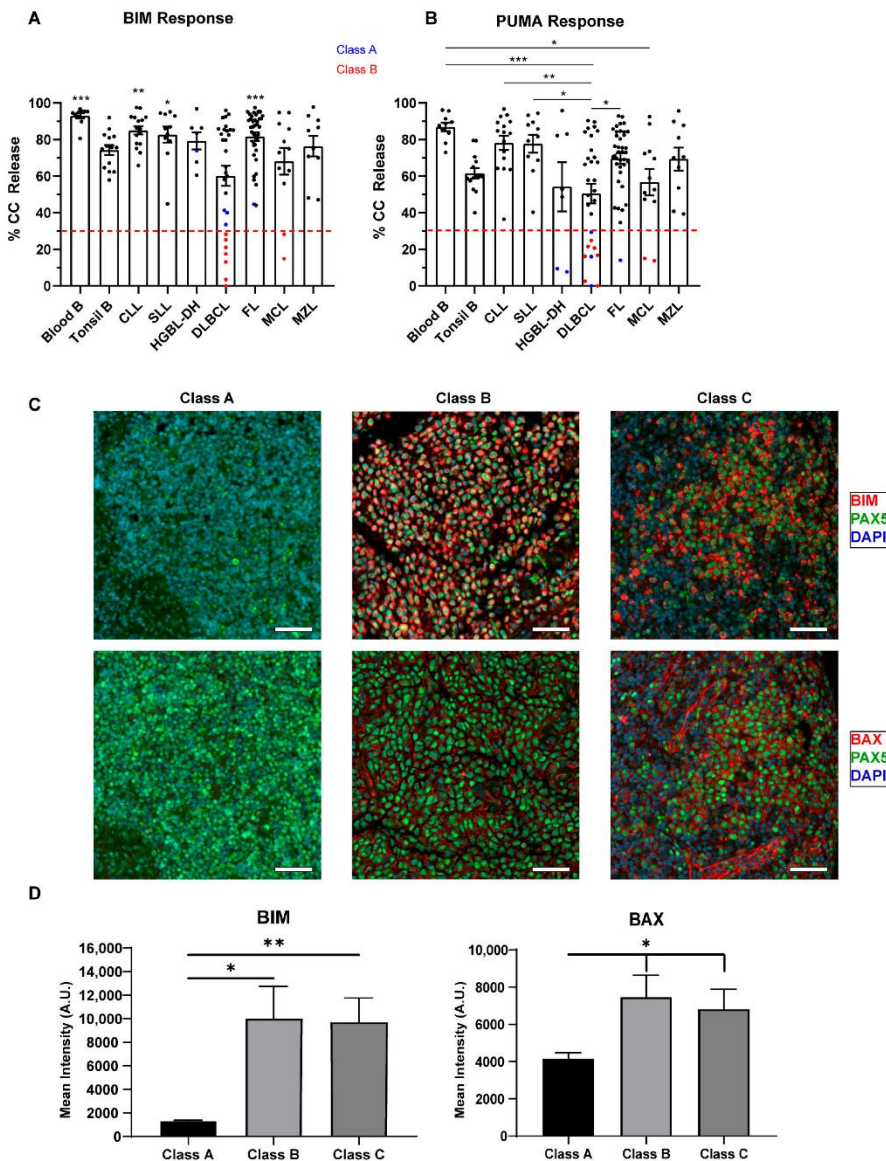


Figure 3.3. Competency and priming of the mitochondrial pathway according to lymphoma subtype. We measured cytochrome c release, displayed on the y-axis, after exposure to 100 μM of BIM (A) and 100 μM of PUMA (B) peptides in different untreated lymphoma subsets (10 frozen blood B, 14 tonsil B, 16 chronic

lymphocytic leukemia (CLL), 11 small lymphocytic leukemia (SLL), 7 high-grade B cell lymphomas with translocations in MYC and BCL2 (HGBL-DH), 30 DLBCL, 38 follicular lymphomas (FL), 12 mantle cell lymphoma (MCL), 10 marginal zone lymphoma (MZL)). For BIM, we defined a threshold of <30% as having a class B block, i.e., having dysfunctional BAX or BAK. For PUMA, we defined a threshold of <30% as being unprimed. Red dashed lines highlight the 30% cut-off, with samples below this threshold being class A/B apoptotic blocks. Class A block samples are in blue and class B block samples are in red. Dots represent individual samples, bars represent the mean \pm standard error of the mean (SEM). A one-way ANOVA with Tukey multiple comparison was used to determine statistical significance between non-Hodgkin lymphoma (NHL) subtypes. Only comparison to DLBCL was determined to be significantly different in BIM response. DLBCL samples are less primed than other NHL and high-grade lymphomas have a higher percentage of class A/B blocks. * $p < 0.05$, ** $p < 0.01$, *** $p < 0.001$. (C) Representative merged IF stains at 20 \times for DAPI (blue), PAX5 (green, AF594) and BIM/BAX (red, AF647) in class A, B, and C DLBCL samples. Scale bars represent 50 μm . (D) Quantification of the mean pixel intensity across all classes of apoptotic block in DLBCL. Samples were analyzed using Qupath software and t-test with Welch's correction was used to compare columns, bars represent the mean \pm standard error of the mean (SEM). * $p < 0.05$, ** $p < 0.01$. Class A samples may have decreased expression of BIM and possibly BAX compared to Class B and C samples.

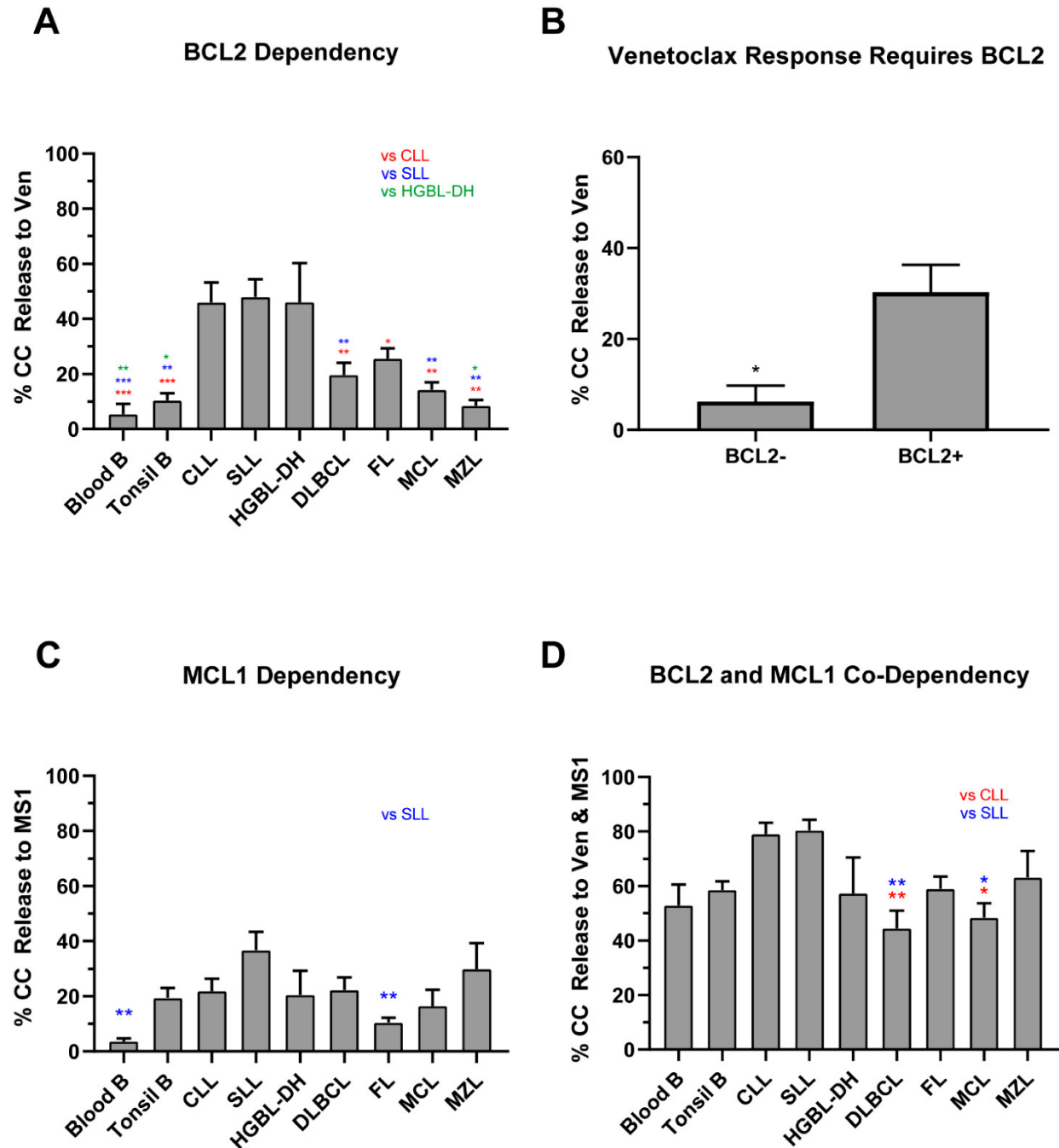


Figure 3.4. Sensitivities to BCL2 and MCL1 inhibition according to lymphoma subtype. We measured cytochrome c release, displayed on the y-axis, after exposure to 1 μ M of venetoclax and 10 μ M of MS1 in different lymphoma subsets (x-axis). A one-way ANOVA with Tukey multiple comparison was used to determine statistical significance between NHL subtypes. Bars represent the mean \pm standard error of mean (SEM). (A) Comparison of lymphoma subtypes based on venetoclax response. CLL, SLL, and HGBL-DH showed notable responses to BCL2

inhibition. (B) Venetoclax responses in DLBCL and HGBL-DH samples according to BCL2 protein expression (present in >50% of cells). Venetoclax responses were not seen in high-grade NHL in the absence of BCL2. T-test with Welch's correction was applied to assess significance. (C) MS1 responses in lymphoma subtypes. SLL displays the greatest response to single MCL1 inhibition. (D) NHL response to dual inhibition of BCL2 and MCL1 by venetoclax and MS1. All subtypes display increased responses when compared to singular inhibition. * $p < 0.05$, ** $p < 0.01$, *** $p < 0.001$. Abbreviations: CLL, chronic lymphocytic leukemia; FL, follicular lymphoma; DLBCL, diffuse large B cell lymphoma; HGBL-DH, high grade B cell lymphoma with translocations in MYC and BCL2; MCL, mantle cell lymphoma; MZL, marginal zone lymphoma.

DLBCL had significantly lower responses to both BIM and PUMA ($p = 0.0002$ for both, Figure 3A) compared to normal lymphocytes, suggesting that high-grade NHLs tend to have dysfunctional pro-apoptotic signaling. DLBCL displayed a wider range of responses to both peptides when compared to controls and other subtypes (BIM CV: 50.3%, PUMA CV: 58.3%), reflecting the heterogeneous nature of this disease. Class B blocks were observed in nine samples: seven DLBCL and two MCL and class A blocks in six samples: three DLBCL, two HGBL-DH, and one FL. Class A and B blocks were detected in 32.4% of cases with high-grade histology (12/37) compared to 3.4% of low-grade lymphomas (3/87, $p < 0.0001$). Data on clinical outcome were available in 24/37 of the high-grade cases, with 67% (16/24) of cases experiencing a relapse, suggesting that class A/B blocks may be associated with chemoresistance. We hypothesized that the functional defects in these cases as shown by BH3 profiling is a result of reduced expression or the absence of pro-apoptotic proteins. Additionally, formalin-fixed paraffin embedded (FFPE) tumor tissue was available for 15 DLBCL patients that underwent BH3 profiling (two class A, five class B, eight class C). The expression of BIM and BAX was assessed by immunofluorescence dual staining in all three classes of apoptotic block

(Figure 3B, C, Table S2). The mean intensity values for BIM and BAX showed a reduced expression in the two class A samples, indicating that the reduction of these proteins may be a contributing factor to their apoptotic defects and reduced response to BH3 mimetics. These observations would need to be validated on a larger sample set. Interestingly, class B samples had a similar expression of BAX compared to apoptotic competent class C samples. We did see a reduction in the expression of BIM in class B samples, but not to the extent seen in class A ($p = 0.1554$). Additional staining for BAK, BID, and BCL2 revealed similar expression levels across all classes of apoptotic blocks (Figures S5 and S6). Overall, our data suggest that class B samples have the pro-apoptotic proteins necessary to initiate cell death, but there is an additional mechanism at play which inhibits these cells from releasing cytochrome c.

3.5.4: Lack of BCL2 Expression and MCL1 Dependency Result in a Poor Venetoclax Response in Class C B-NHLs

Since 88% (109/124) of B-NHLs had class C blocks, we first determined how many samples were primarily BCL2-dependent. As expected, CLL and SLL had the greatest responses to venetoclax, significantly higher than all other subtypes except for HGCL-DH (all $p < 0.05$, Figure 4A). In fact, 70% of CLL/SLL and 57% HGCL-DH (19/27 and 4/7, respectively) displayed BCL2-dependency, versus only 21% (19/90) for all other NHLs ($p < 0.0001$ and $p = 0.0310$, respectively, response defined as $\geq 30\%$ cytochrome c release). We then assessed the venetoclax response in DLBCL stratified by BCL2 protein expression via clinical immunohistochemistry at diagnosis (see supplemental methods in supplementary materials). A lack of BCL2 protein expression in primary high-grade lymphomas, i.e., BCL2- negative defined as being present in $< 50\%$ of cells, was associated with a very low venetoclax response (the mean response was 30.3% for BCL2+ and 6.3% for BCL2-negative, $p = 0.0371$, Figure 4B). The cell

of origin subtype or presence of BCL2 translocations were not associated with venetoclax response (Table S1). These data support previous findings that venetoclax is ineffective in the absence of its target, BCL2 protein [27].

MCL1 was the second most common dependency in NHLs. The mean responses to the MCL1 specific inhibitor MS1 were lower than venetoclax with the highest responses (30%–40%) observed in SLL and MZL (Figure 4C). Low responses (15–30%) were detected in CLL, DLBCL, MCL and HGBL-DH and the lowest responses were in seen in FL (10%). Interestingly, 6/30 of the DLBCL samples and 3/10 of the MZL samples profiled showed an MCL1-dominant response, with no response to BCL2 inhibition. Dual-IF of MCL1 in our FFPE DLBCL (Figure 5A, B) samples showed that the responders to MS1 had relatively high expression of the protein and that overall increased expression trended with increased cytochrome c release by BH3 profiling (Figure 5C). Similar to the on-target engagement of venetoclax with BCL2, our data support the necessary expression of the target MCL1 for a successful response to targeted inhibition.

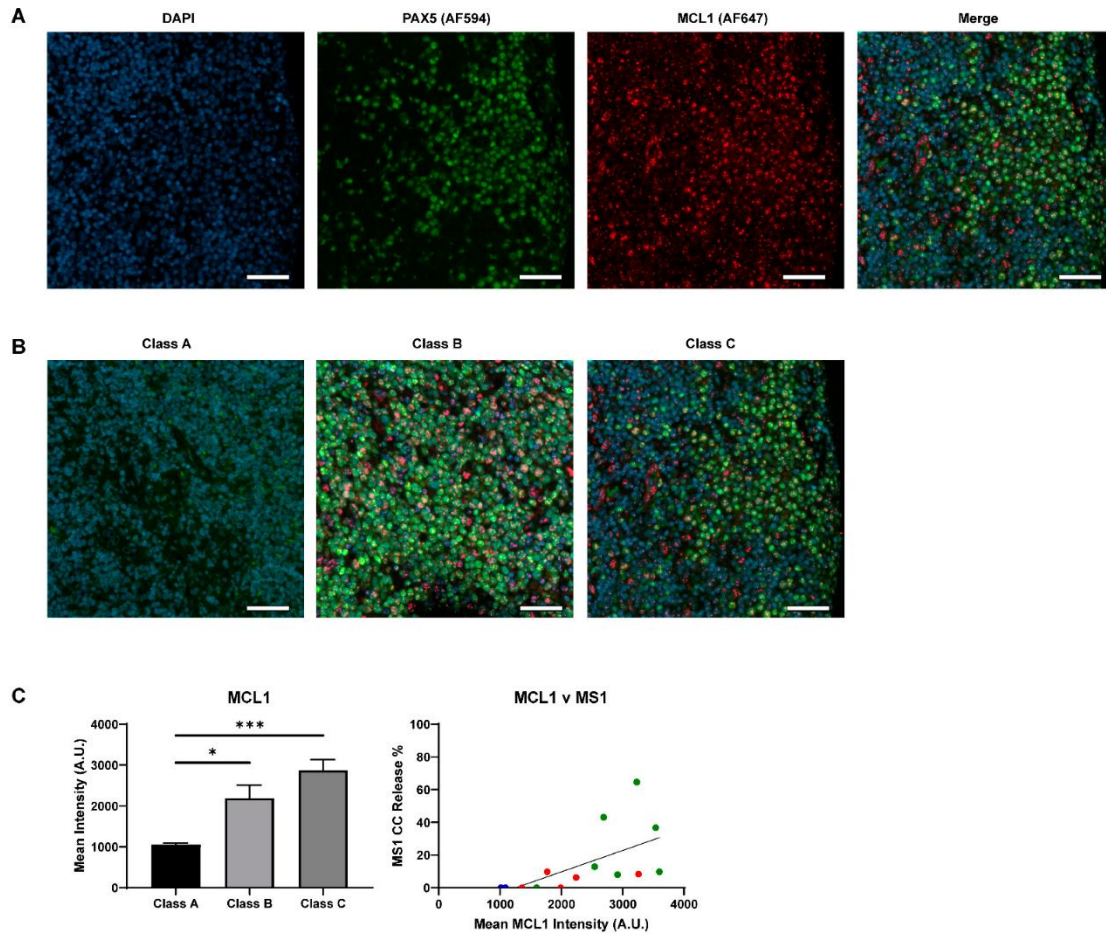


Figure 3.5. Expression of MCL1 in DLBCL by immunofluorescence. (A) Representative 20× single channel images of DAPI (blue), PAX5 (green, AF594), and MCL1 (red, AF647), as well as a merged image, in a class C sample. Scale bars represent 50 μ m. (B) Qualitative comparison of MCL1 expression in class A, B, and C samples. The same sample from panel A is used in this panel. PAX5 staining was weak in class A when co-stained with MCL1, but this tissue was confirmed to be PAX5 positive in previous stains. Scale bars represent 50 μ m. (C) The mean pixel intensity of all samples in each class, as calculated by Qupath. T-test with Welch's correction was used to compare columns, bars represent the mean \pm standard error of the mean (SEM). Spearman linear regression analysis was applied to analyze the correlation between cytochrome c release to MS1 (10 μ M) and mean MCL1 intensity ($R^2 = 0.3525$). Dot colors represent class of sample: A (blue), B (red), C (green). Response was only seen in class C samples with high MCL1 expression and mean MCL1 expression was lower in Class A/B samples * $p < 0.05$, *** $p < 0.001$.

Given the modest responses to single peptides, we speculated that more than one anti-apoptotic protein was involved in inhibiting apoptosis in class C NHLs. The individual responses to MCL1 in our own samples, and the published data supporting that MCL1 inhibits apoptosis in DLBCL [27,28] and AML/NHL cell lines [29,30], prompted us to test the co-dependency of BCL2 and MCL1 in a subset of our NHLs. MCL, CLL, FL, and DLBCL samples all showed significant increases in cytochrome c release when using both venetoclax and MS1 together in the BH3 profiling assay, compared to single agents venetoclax or MS1 (all $p < 0.05$, Figure 4A, C, D). CLL and SLL displayed the greatest response to combination therapy, with the levels of cytochrome c release significantly greater when compared to DLBCL ($p = 0.0014$ and 0.0011 , Figure 4D). In fact, the levels of cytochrome c release were similar to those seen with PUMA, which inhibits all anti-apoptotic proteins, suggesting the contribution of a third anti-apoptotic protein beyond BCL2 and MCL1 is minimal. HGBL-DH had similar responses to dual inhibition as with venetoclax alone ($p = 0.84$) but most of the HGBL-DH in our dataset were obtained from PB and marrow, so we cannot exclude that HGBL-DH obtained from LN compartments would have more MCL1 co-dependence, as was the case with tonsils and nodal SLL. Overall, we note that the dual inhibition of MCL1 and BCL2 was effective in 83% of NHLs.

The evaluation of additional anti-apoptotic proteins was carried out to verify our hypothesis that BCL2 and MCL1 were the primary causes of apoptotic block in primary NHL. NOXA, an MCL1, BCLB and BFL1 inhibitor, had low responses in all subtypes except for SLL (Figure 6A). However, the NOXA responses were similar to the MS1 responses, indicating the low contribution of BCLB and BFL1 to cell survival. BCLXL dependency was low across all subtypes, with the mean WEHI-539 responses being $<10\%$ and very few samples showing a response (Figure 6B). HRK, another BCLXL inhibitor, displayed more modest responses in

NHL but this is likely due to the fact that it also has low affinity binding for other anti-apoptotic proteins (Figure 6C). Responses to ABT-737 and venetoclax were similar, suggesting the effect of ABT-737 was mainly through BCL2 inhibition, not BCL-XL. Similar to MS1, we tested the combination of WEHI-539 and venetoclax in a subset of FL and DLBCL profiles (Figure S7). There was no significant increase in the release of cytochrome c with the additional targeting of BCLXL by WEHI-539 compared to venetoclax alone. Thus, our data argue against BCLW or BCLXL being significant contributors to poor venetoclax responses in primary NHLs (Figure 6D).

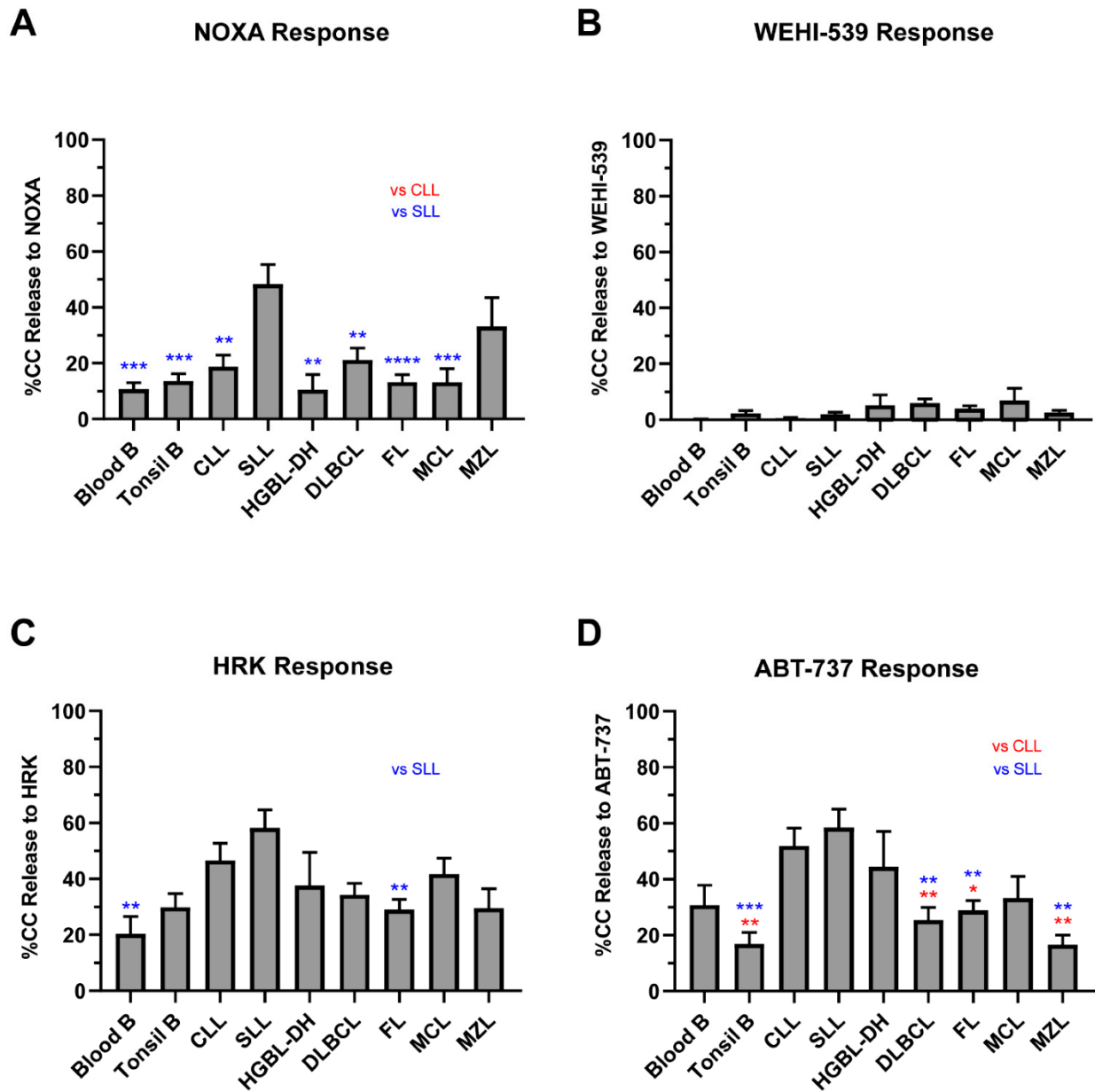


Figure 3.6. BCLXL and other anti-apoptotic protein dependency. Graphs show cytochrome c release after 90-min exposure to 100 μ M of NOXA (A), 1 μ M of ABT-737 (B), 1 μ M of WEHI-539 (C), and 100 μ M of HRK (D) in all NHL subtypes. Bars measure the mean of all samples; error bars indicate standard error of the mean (SEM). A one-way ANOVA with Tukey multiple comparison was used to determine statistical significance between subtypes. NHLs respond poorly to the singular inhibition of anti-apoptotic proteins but respond better when multiple proteins are targeted. BCLXL contributes only modestly to cell survival in our cohort. * $p < 0.05$, ** $p < 0.01$, *** $p < 0.001$, **** $p < 0.0001$.

In summary, the BH3 profiling of primary NHLs shown here supports at least three causes of poor venetoclax responses: pro-apoptotic signaling defects, a lack of BCL2 protein expression in high-grade lymphomas, as well as co-dependence on MCL1, observed in all NHL subtypes.

3.5.5: Dynamic BH3 Profiling (DBP) Reveals Drugs That Can Synergize with Venetoclax

Given that venetoclax is being tested in combination with other chemotherapies, such as rituximab, cyclophosphamide, doxorubicin, and vincristine (components of RCHOP) in DLBCL [31] and bendamustine-rituximab in FL [32], we determined whether exposure to frontline chemotherapy drugs could bring cells closer to the apoptotic threshold and synergize with venetoclax to initiate apoptosis. Since the supply of primary lymphoma cells is limited, and their growth and viability are poor *ex vivo* over long periods of culture, we performed BH3 profiling on HGBL-DH cell lines after exposure to different chemotherapies *in vitro*. The change in priming (Δ priming %) was calculated by subtracting the untreated response from the treated response as determined by BH3 profiling. (Figure 7A). Mafosphamine (cyclophosphamide), dexamethasone, and bendamustine did not prime the cells or sensitize them to venetoclax. Within components of RCHOP, doxorubicin and vincristine significantly increased cellular responses to venetoclax (Figure 7B), a feature that was shared with other microtubule-targeting drugs, such as vinblastine and monomethyl auristatin E (MMAE). Vincristine and vinblastine increased the cells' priming, as measured by increased responses to 1 μ M of PUMA peptide, suggesting these may be effective in correcting class A blocks (Figure 7C).

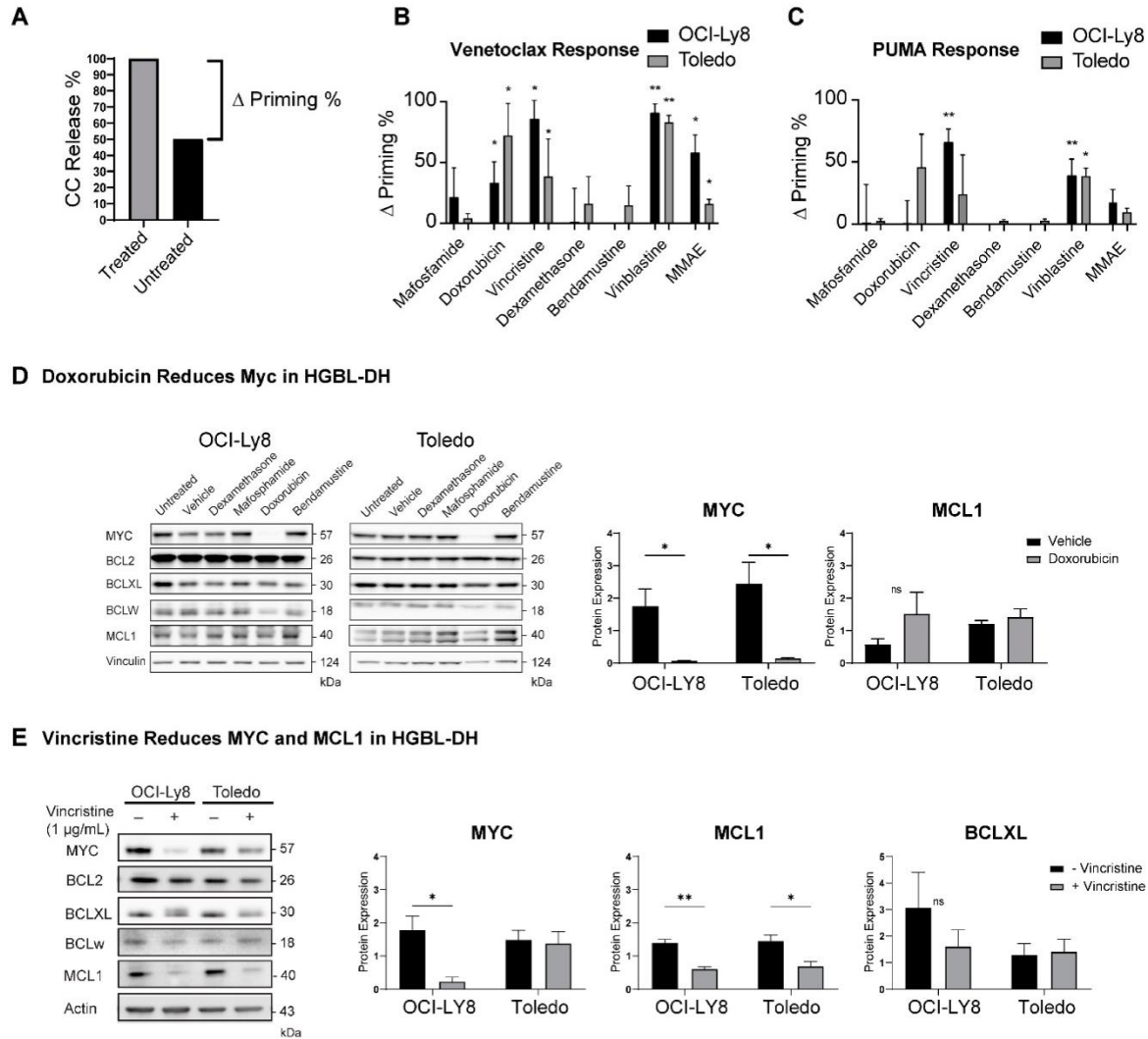


Figure 3.7. Dynamic BH3 profiling performed in Toledo and OCI-Ly8 cell lines. The % of untreated cells undergoing cytochrome c release was subtracted from the % of cells undergoing cytochrome c release in treated samples to determine an increase in release named “ Δ Priming” (example shown in panel (A)). Cytochrome c release was measured in cells upon exposure to 1 μ M of venetoclax (B) and 1 μ M PUMA (C) after a 17 h incubation with dimethyl sulfoxide (control) and different drugs. Welch’s t tests were used to compare individual treatments to the individual control groups. Microtubule targeting components of RCHOP such as doxorubicin and vincristine increased cells priming and sensitivity to venetoclax. * $p < 0.05$, ** $p < 0.01$. (D) Western blot measuring anti-apoptotic protein and MYC levels in OCI-Ly8 and Toledo cell lines after 17 h treatment with dexamethasone, mafosfamide, doxorubicin, and bendamustine. Doxorubicin significantly decreases the expression of MYC in both cell lines after treatment. (E) Western blot measuring anti-apoptotic protein and MYC levels in OCI-Ly8 and Toledo

cell lines after 17 h treatment with vincristine. Bars measure the mean of all samples; error bars indicate SEM. Vincristine significantly reduces MCL1 expression in both cell lines while also reducing MYC expression in OCI-LY8. BCLXL was not significantly reduced after treatment with vincristine. * $p < 0.05$, ** $p < 0.01$. ns, non-significant.

We then evaluated whether chemotherapy could change the levels of anti-apoptotic proteins or MYC in DLBCL. We hypothesized that the concentration of proteins with the shortest half-lives, such as MYC [33] and MCL1 [34], may decrease after exposure to drugs that cause cell cycle arrest and/or inhibit transcription [35]. Maphosphamide, dexamethasone, or bendamustine did not change the levels of anti-apoptotic proteins or MYC in these DLBCL cell lines. Doxorubicin exposure decreased MYC but had no effect on the levels of anti-apoptotic proteins (Figure 7D). Vincristine had the most dramatic effect on cells by decreasing MYC in OCI-Ly8, and MCL1 levels in both cell lines, without significantly changing the levels of other proteins (Figure 7E). Levels of BIM remained constant in treated samples, indicating that vincristine increases priming by reducing the availability of MCL1, as opposed to activating BIM (Figure S8). Therefore, doxorubicin and microtubule-targeting drugs might synergize with venetoclax in NHL that overexpress MYC, BCL2 and MCL1. Overall, this suggests that combining RCHOP or other microtubule inhibitors with venetoclax could be effective in BCL2+ NHLs. This strategy may also help in correcting class A blocks, as shown by increases in overall priming, but would not be effective in overcoming class B blocks.

3.6: Discussion

The overexpression of BCL2 protein is a common mechanism of inhibiting apoptosis in NHL. We used BH3 profiling to study the mitochondrial apoptotic pathway in viable primary

NHL cells and determine which BH3 proteins are keeping the cells alive. Our three main findings are that a lack of a venetoclax response is primarily a consequence of pro-apoptotic protein dysfunction, the absence of BCL2 protein and the presence of MCL1, the initial finding being a novel feature of lymphomas with high-grade morphology. This study provides original insights into apoptotic resistance in rare primary NHL samples that could not be extrapolated from immortalized cell lines. Based on our dynamic BH3 profiling results, venetoclax would have synergistic effects with microtubule inhibitors and doxorubicin. Overall, this new knowledge may help tailor treatment regimens for patients with B-NHLs and subsets of CLL patients, such as those presenting with Richter's transformation or those receiving ibrutinib, which may synergize with venetoclax by reducing expression of MCL1 and BCLXL [36,37].

This study improves our understanding of the apoptotic dependencies of normal B cells in both PB and tonsils. While normal PB B lymphocytes express BCL2, their dependency on MCL1 relatively protects them from venetoclax-induced apoptosis. This work may also provide some insight into why venetoclax may be more active in clearing lymphoma cells from the PB compared to nodal compartments [38]. Compared to tonsillar B cells, PB B cells were significantly more primed, closer to the apoptotic threshold and less dependent on MCL1. This may in part be attributed to B cells that are at different stages of differentiation, since BCL2+ naïve and memory B cells are found predominantly in the PB compartment, whereas tonsils contain germinal center B cells, which are known to be BCL2-negative and MCL1-dependent [26,39,40,41]. It is also possible, however, that factors within the tissue microenvironment affect priming or dependency on other anti-apoptotic proteins, notably MCL1 [42]. Thus, the higher MCL1 dependency in LN compartments may be a source of early relapse in CLL patients treated with single agent venetoclax.

The profound pro-apoptotic defects observed in a subset of DLBCLs indicates a mechanism of resistance to venetoclax, and possibly chemotherapy, that is under-appreciated. This feature was especially prevalent in HGBL-DH and DLBCL, suggesting an association between pro-apoptotic defects, high-grade lymphomas, and clinical resistance to conventional RCHOP chemotherapy or drugs targeting apoptosis. Low responses to BIM and PUMA imply that the effector proteins BAX/BAK are not functioning correctly. Anti-apoptotic proteins can bind directly to BAX/BAK but low responses to drugs targeting these proteins suggests that the problem lies with dysfunctional pro-apoptotic proteins or the subsequent steps prior to cytochrome c release. Our protein expression data imply that these proteins are expressed, except for class A samples, but more samples are needed for verification. The nature of this dysfunction warrants further exploration, as some studies have indicated that apoptosis can proceed in some cancer cell lines treated with BH3 mimetics without functional BH3-only proteins such as BIM and PUMA [43]. Therefore, methods independent of BH3-mediated apoptosis may also be involved and contribute to class A/B dysfunction. This also suggests that finding alternative means of triggering cell death that are outside of mitochondrial apoptosis may be beneficial to patients with low responses to any combination of BH3 mimetics. Studying additional samples of high-grade morphology would be important to further understand the relationship between the functional defects in apoptosis (phenotype) and their underlying genomic alterations (genotype). We recently reported a class B block in a patient with relapsed Burkitt lymphoma, where a mutation in BAX resulted in no production of BAX protein [44]. Mutations in BAX or BAK, however, are not a typical feature of de novo or relapsed DLBCL [45]; therefore, it is more likely that the class B phenotype seen in our samples arose by a different mechanism. Overall, these data suggest that BH3 profiling may be a useful technique to identify patients that could benefit

from therapies that kill lymphoma cells independent of the mitochondrial pathway. Such therapies include immunotherapies that initiate death via cell-mediated or complement-mediated cytotoxicity. Examples include chimeric antigen receptor T (CAR-T) cell regimens, bi-specific T cell engagers (BiTEs), immune check-point inhibitors or other immunomodulating agents [46,47,48,49].

The main cause of a lack of venetoclax response in B-NHLs in our study is the presence of MCL1. Due to the rarity of primary viable NHL samples, the number of samples studied is limited. That said, we provide the largest analysis of primary NHL samples by BH3 profiling to date, highlighting the relative contribution of each potential cause of poor venetoclax responses according to the NHL subtype. Dependency on BCL2, MCL1 and BCLXL has recently been reported in NHL cell lines [50,51], but we did not find a significant contribution for BCLXL in our primary NHL samples. Given that NHL, specifically DLBCL, is such a heterogenous disease, we cannot rule out that other anti-apoptotic proteins contribute to tumor cell survival in minor subsets of patients if a larger number of samples were analyzed. There is some evidence that primary treatment with RCHOP may influence anti-apoptotic protein dependency [51]. Our samples are all from untreated patients, therefore it may be that anti-apoptotic protein dependencies other than BCL2 and MCL1 will exist in this population after treatment or at relapse. Co-expression of BCL2 and MCL1 has been reported in NHLs [12,52,53,54] and MCL1 dependency is also seen in acute myelogenous leukemia and multiple myeloma [55,56]. In lymphomas, MCL1 dependence is likely inherited from the normal B cell counterpart and by being within the microenvironment of the lymph node compartment [57,58]. In DLBCL cell lines, NOXA amplification or MCL1 inhibition has sensitized DLBCL to venetoclax, but only when BIM is present [27]. Treatment with venetoclax and MS1 greatly increased the apoptotic

response of primary patient samples and appeared synergistic in some cases. Our data confirm prior reports that MCL1 protein levels decrease following exposure to vincristine [59,60]. In fact, three different microtubule inhibitors sensitized cells to venetoclax, suggesting that this is a class effect. RCHOP and venetoclax should be effective in high-grade lymphomas that express BCL2 protein, are not class B, and co-depend on BCL2 and MCL1 (53% of our diagnostic DLBCL samples). This combination appeared to translate into a clinical benefit in patients with BCL2+ DLBCL in the phase II CAVALLI study [31]. Thus, BH3 profiling could be used to predict patients' responses to venetoclax and select drugs that could be synergistic. Recently, a high-throughput BH3 profiling methodology was developed to screen the efficacy of numerous drugs on inducing apoptosis in malignant cells [61].

Placed into a clinical context, the BH3 profiling of primary lymphoma samples has allowed us to gain insight into why there is such great variability in clinical responses to venetoclax in NHLs. Our results mirror those obtained in clinical trials, where CLL is the most venetoclax-responsive NHL, while FL, MCL, and DLBCL have more modest responses. While the BH3 profiling assay in our study is relatively easy to apply, its main limitation is the requirement of a large number of live malignant cells (5–10 million) in a cell suspension. In cases where enough cells are available, BH3 profiling could be applied clinically to identify patients who would benefit from conventional chemotherapy (class C), targeted therapies such as venetoclax, or are candidates for alternative immunotherapies (class B). Based on our dynamic BH3 profiling results, combinations using venetoclax and microtubule agents with or without anthracyclines would be effective in NHLs having class A or C blocks. Thus, adding venetoclax to RCHOP-like regimens or to the MMAE-conjugated anti-CD79b antibody polatuzumab [62,63] may be strategies to overcome the chemo-resistance associated in a subset of patients

with BCL2+ high-grade lymphomas. The lack of venetoclax responses in BCL2-negative DLBCL supports the notion that the presence of BCL2 protein is required to obtain a response to venetoclax, and that patients who have BCL2-negative lymphomas may not benefit from venetoclax-based regimens. Our report of pro-apoptotic defects in DLBCL and HGBL-DH, as seen by the increased frequency of class A/B samples, indicates a mechanism of resistance to venetoclax and possibly chemotherapy that has yet to be sufficiently explored and warrants future studies into the possible rescue of these defective proteins.

3.7: Materials and Methods

3.7.1: Sample Acquisition and Preparation

For this project, we profiled 148 samples: 111 samples were obtained at the Jewish General Hospital in Montreal, 12 from the Banque de cellules leucémiques du Québec (BCLQ), 13 from the British Columbia Cancer agency, and 23 from Robert-Bosch Hospital, Stuttgart, Germany. This project was approved by the Research Ethics Board protocols [11-047 and 12-052]. Of these 148 samples, 124 were NHL: 16 CLL, 11 SLL, 38 FL, 29 DLBCL, 7 HGBL-DH, 12 MCL, 10 MZL and 1 HGBL without translocations in MYC and BCL2, which was included within the DLBCL category in Table S1. All samples were taken prior to chemotherapy (n = 124). Normal controls included B cells from 14 tonsils and 10 PB samples. All cells were obtained from disaggregated tissue cell suspensions, blood, or fluids and viably cryopreserved using protocols outlined in the supplemental methods in supplementary materials. We also used HGBL-DH and DLBCL cell lines SUDHL10, Toledo, and OCI-Ly8; generous gifts from Dr. Letai and Dr. Dalla Favera. These were verified by short tandem repeat (STR) profiling and cultured in standard conditions described in the supplemental methods in supplementary materials.

3.7.2: BH3 Profiling

We used the iBH3 profiling method described previously [44]; originally by Ryan et al. [64]. We thawed 5–10 million cells and stained them with antibodies to the following cell surface markers: CD3, CD19, CD5 (for CLL/SLL only) and CD4, CD8, CD14 (for peripheral blood mononuclear cells only). We exposed cells to digitonin followed by synthetic BH3 peptides that selectively bind specific anti-apoptotic proteins (Figure 1B) and measured cytochrome c release as a read out for mitochondrial apoptosis. We also used the drugs MS1 (MCL1 inhibitor), WEHI-539 (BCLXL inhibitor), ABT-737 (BCL2, BCLXL, and BCLW inhibitor) and venetoclax (BCL2 inhibitor) to further characterize the presence of anti-apoptotic proteins present in cells. Selected drug/peptide concentrations are based upon previously established protocols and applied in various doses where appropriate. We acquired the data on an LSR Fortessa cytometer (BD Biosciences, San Jose, CA, USA) using DIVA (BD Biosciences) software. Our gating strategy is illustrated in Figure S1A. We normalized the data to the DMSO, positive control for cytochrome c retention (i.e., intact mitochondria) and used alamethicin as our positive control for cytochrome c release (MOMP). See supplemental methods in supplementary materials for further description of BH3 profiling and determination of apoptotic block thresholds.

3.7.3: Dynamic BH3 Profiling (DBP)

Cells were incubated for 17 h (h) with 1% PBS, 1% DMSO, or one of the following drug concentrations: 1.2 μM of vincristine, 2 μM of mafosphamide, 50 μM of bendamustine, 10 μM of doxorubicin, 0.5 μM of dexamethasone, 1 $\mu\text{g/mL}$ of vinblastine, 10 ng/mL of monomethyl auristatin E (MMAE). To assess the effect of the drugs on the priming of the cells, and the cells' sensitivities to venetoclax, we measured the responses to both 1 μM of PUMA peptide and 1 μM

of venetoclax in vehicle-treated and drug-treated cells. We then subtracted the untreated response from the treated response to obtain a measure of the change in responses. We performed dynamic BH3 profiling after a 17 h exposure to drugs and measured the levels of anti-apoptotic proteins and MYC by Western blot (see supplemental methods in supplementary materials).

3.7.4: Immunofluorescence

Patient tissue was preserved in formalin-fixed paraffin-embedded blocks that were cut at 4 μ M, placed on SuperFrost/Plus slides (VWR, Radnor, PA, USA), and dried overnight at 37 °C. The slides underwent a double immunofluorescence stain for PAX5 and either BIM, BID, BAX, BAK, MCL1, or BCL2. After deparaffinization and hydration, antigen retrieval was carried out in a TRIS/EDTA pH 9.0 buffer for 20 min in a pressure cooker. The slides were blocked with 10% donkey serum for 30 min and then incubated overnight with primary antibody for PAX5 (1:100, Abcam, Cambridge, UK, ab211293) and for the protein of interest at the following dilutions: BIM (1:25, Abcam, ab32158), BID (1:100, Santa Cruz Biotechnology, Dallas, TX, USA, sc-373939), BAX (1:100, Abcam, ab32503), BAK (1:50, Abcam, ab32371), MCL1 (1:50, Abcam, ab32087), or BCL2 (1:50, Abcam, ab32124). After the removal of the primary antibodies, the slides underwent a 1-h secondary antibody incubation with rat AF594 (Invitrogen, Carlsbad, CA, USA, A21209, 1:250) and mouse/rabbit AF647 (Invitrogen, A21235/A21245, 1:500). Finally, the slides were incubated for 15 min with DAPI (Invitrogen, D1306) and mounted with coverslips using prolong gold antifade mountant (Invitrogen, P10144). Imaging was carried out using a Zeiss (Oberkochen, Germany) Axio scan Z1 fluorescence slide scanner at 20 \times magnification. Image analysis was carried out using Qupath software for quantitative pathology and bioimage analysis [65]. DAPI was used to identify all cells and then cell intensity

for the protein of interest was gated on Pax5+ cells, which were determined as the highest 50% of AF594 expressing cells.

3.8: Conclusions

BCL2 is an attractive target for NHL patients given its role in cell survival and patient prognosis. While clinical trials for venetoclax have shown promising results, there is a wide range of responses to single-agent therapy. Our study helps to highlight potential mechanisms by which malignant cells survive, even after the inhibition of BCL2. Notably, MCL1 has been implicated in previous studies of NHL cell lines as an additional pro-survival protein, important for avoiding apoptosis. This is supported by our analysis of primary patient samples, where the dual inhibition of MCL1 and BCL2 was effective in the majority. While targeting both directly may currently prove to be difficult therapies that affect MCL1 levels outside of direct inhibition may provide an avenue to increase venetoclax effectiveness in NHL. Our cohort also highlights a previously underreported group in NHL that has severe pro-apoptotic defects. While these samples were few, they all displayed resistance to peptides and inhibitors targeting anti-apoptotic proteins. Patients displaying this BH3 profile are unlikely to respond to therapies involved in activating mitochondrial apoptosis. The mechanism of this defect remains to be seen, as it is unlikely to be a result of reduced protein expression (potentially the case in class A) or genetic aberrations to the genes responsible for their production. In summary, the BH3 profiling of patient samples is a fast and effective technique that could identify patients who may benefit from a specific targeted therapy. The continued expansion of our cohort via BH3 profiling and the discovery of the source of class B, pro-apoptotic defects can help inform future clinical trial and patient management decisions for certain subclasses of NHL patients.

3.9: Supplemental Methods

3.9.1: Patient Sample Preparation

Patient samples that were collected in liquid form (blood or other fluid) were diluted in phosphate buffered saline (PBS) (total of 3–6 mL) and were gently layered onto 3 mL of ficoll medium, spun with no brake at 800 G for 20 mins, and the opaque interface layer containing the peripheral blood mononuclear cells (PBMCs) was isolated. Tissue-derived patient samples were disaggregated using the GentleMACS C tube system according the manufacture's procedures (Miltenyi Biotec, Bergisch Gladbach, Germany). Isolated cells of interest were transferred to freezing medium (10% dimethyl sulfoxide (DMSO) and 90% fetal bovine serum (FBS)) and frozen in cryovials at -80°C overnight before being transferred to liquid nitrogen for long-term storage.

3.9.2: BH3 Profiling- Additional Information

We used the LIVE/DEAD™ Fixable Aqua Dead Cell Stain Kit (Thermo Fisher Scientific, Waltham, MA, USA, L34957) to assess viability, and used only live cells in our analysis. After viability staining, we stained with the following antibodies for flow cytometry, all obtained from BD biosciences (San Jose, CA, USA): CD3 BV786 (clone SK7, catalog number 563800), CD19 (clone H1B19, catalog number 561295), CD5 (clone UCHT2, catalog number 555353, used only for CLL/SLL), CD14 (clone M ϕ P9, catalog number 563744, used only for PBMCs), CD4 (clone RPA-T4, catalog number 560345, used only for PBMCs), CD8 (clone SK1, catalog number 641400, used only for PBMCs). Antibodies were incubated with the samples for 30mins at 4°C , in PBS + 2% FBS. Fc block (BD biosciences, catalog number 564220) was used prior to staining PBMCs. We defined a class B block as having a response of $<30\%$ to $100\ \mu\text{M}$ BIM peptide, a threshold that was selected because it was more than 2.5

standard deviations below the normal distribution of cytochrome c release in normal B cells in response to BIM or PUMA (Figure S2 and Figure 2). A class A block was defined as having response of $\geq 30\%$ to 100 μM BIM but $< 30\%$ to 100 μM PUMA peptide, a promiscuous sensitizer peptide that binds to all the anti-apoptotic proteins. Class C blocks were identified as having responses of $>30\%$ to both BIM and PUMA.

3.9.3: Cell Culture

Suspension cells were incubated in culture flasks at 37 °C. SU-DHL-4, SU-DHL-6, SU-DHL-8, and SU-DHL-10 cell lines were cultured in 10% FBS in RPMI-1640; OCI-Ly1 and OCI-Ly8 cells were cultured in 0.1% β -mercaptoethanol added to 10% FBS in RPMI-1640 medium; TOLEDO were cultured in 20% FBS in RPMI 1640 medium. 2.5 mL of 10,000 IU penicillin/10,000 $\mu\text{g}/\text{mL}$ streptomycin solution was added to every 500 mL stock bottle of cell medium to inhibit bacterial growth. All cell lines tested negative in the past 6 months for mycoplasma using a PCR detection from ABM (Richmond, BC, Canada, Cat. G238). Cell lines were verified using short tandem repeat analysis (TCAG, SickKids, Toronto, ON, Canada).

3.9.4: MTT Assay Protocol

The TACS® MTT Cell Proliferation Assay kit was purchased from Trevigen® (Gaithersburg, MD, USA). Cells were plated into 96-well plates at 100,000 cells/ well for 17 hours. Cells were counted using a hemocytometer, harvested, centrifuged at 300 G for 5 minutes, and resuspended in fresh medium immediately prior to plating at a cell concentration of 1 million cells/mL. 20 \times drug solutions were prepared by diluting a 1000 \times drug stock solution in DMSO by 50-fold in the appropriate cell medium. After incubation, 10 μL of MTT solution was added to each well and plates were incubated again for between 2–4 hours or until visible appearance of violet formazan precipitate. The precipitate was then solubilized by addition of 100 μL of

detergent solution and left at 37 °C overnight. Absorbance was measured at 570 nm with a reference wavelength at 700 nm. Absorbance measurements were blank-corrected and % viability was normalized to the average of untreated cells for constructing viability curves and to DMSO for correlating to BH3 profiles. Percentages of viable cells after 17-hour treatment with venetoclax were calculated by normalizing to DMSO vehicle representing 100% viability. Spearman's correlation analysis was performed using GraphPad Prism to determine the correlations between MTT vs. % cytochrome C release. Statistical significance was calculated as $p < 0.05$ according to Student's t-test (two-tailed).

3.9.5: Western blotting

Western blots were performed according to standard procedures as described previously (42), with the added usage of the primary antibody against BIM (catalog number ab32158, abcam, Cambridge, UK), Vinculin (catalog number 4650S, Cell Signaling Technology, Danvers, MA, USA), or actin (clone I-19, catalog number SC1616, Santa Cruz Biotechnology, Dallas, TX, USA). Western blots were imaged using an Azure (Dublin, CA, USA) c600 gel imaging system. Protein levels were calculated the following way: Protein level = Optical density for the Protein/Optical density for the loading control.

3.9.6: Statistics

We determined if there were any significant differences between lymphoma subtypes and normal cells by comparing the percentage of cells releasing cytochrome c upon exposure to each peptide using a one-way ANOVA with Tukey multiple comparison. Two-way ANOVA was used to compare peptide exposure/subtype to cytochrome c release in normal B cells. The differences between the levels of protein expression by immunofluorescence, western blot and the changes in priming upon exposure to chemotherapy were determined using Welch's t test.

Spearman's correlation analysis was performed to determine correlations where appropriate. A p value of < 0.05 was considered significant. Statistical analysis was performed in Prism7/8 (GraphPad Software, Inc., San Diego, CA, USA) and SPSS (version 23, IBM, Armonk, NY, USA).

3.10: Supplemental Figures

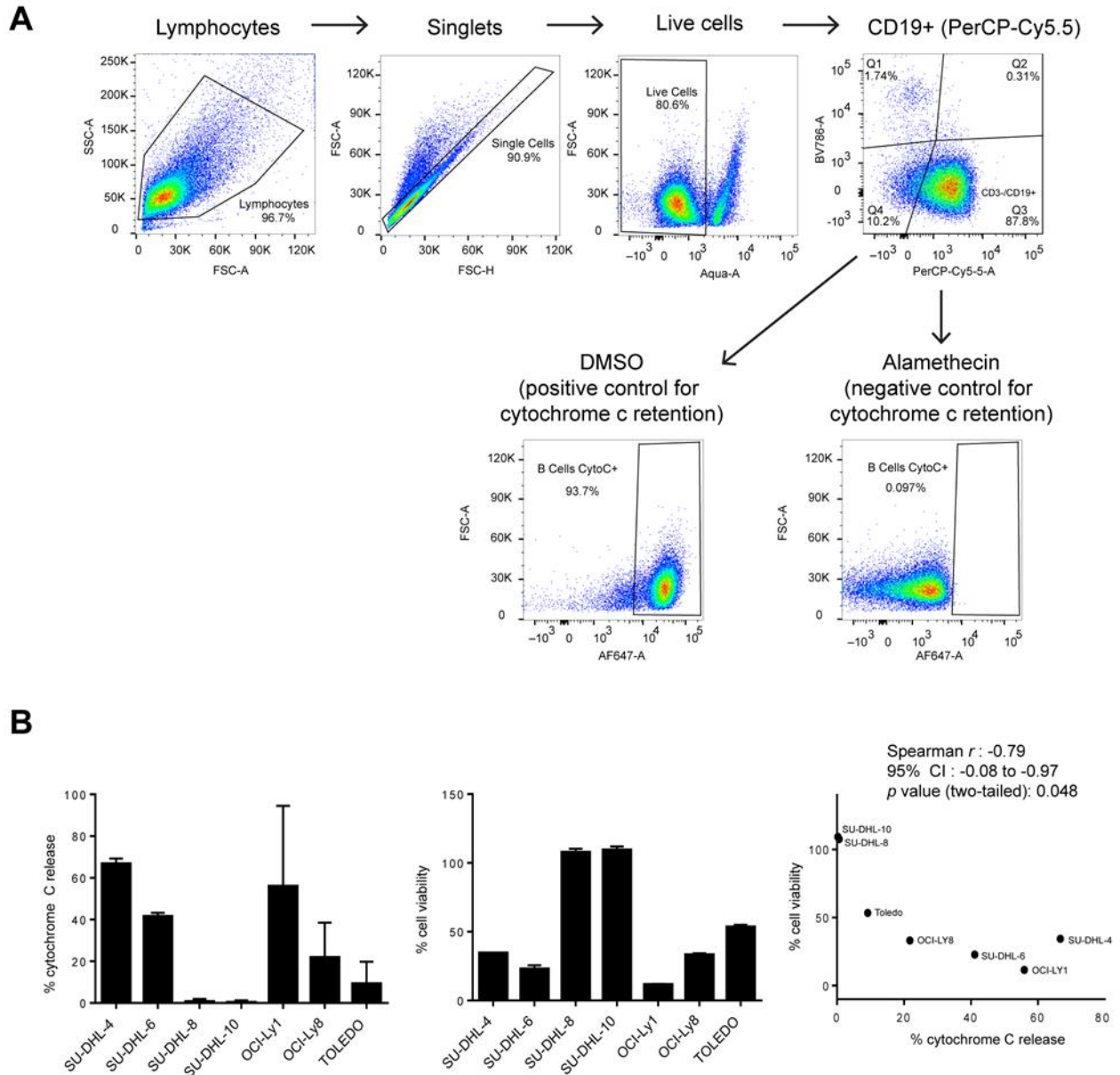


Figure 3.S1. BH3 profiling. (A) Gating strategy used to identify population of interest for BH3 profiling analysis.

Cytochrome c stains positively when retained in the cell. Therefore, Alamethicin is a negative control for

cytochrome c retention and a positive control for cytochrome c release. DMSO acts as the inverse control: positive for retention and negative for release. (B) Left panel: cytochrome C release of seven DLBCL cell lines in response to venetoclax as measured by BH3 profiling. Center panel: Cell viability after 17-hour treatment with 2.4 μM venetoclax. Viability was normalized to DMSO vehicle as 100% viability and cell medium blanks as 0%. Right panel: Correlation of cell viability after treatment with venetoclax for 17 hours and cytochrome C release by BH3 profiling. There is a significant negative correlation between the two variables, indicating that increasing cytochrome C release in response to venetoclax during BH3 profiling correlates significantly to decreasing cell viability in response to venetoclax treatment.

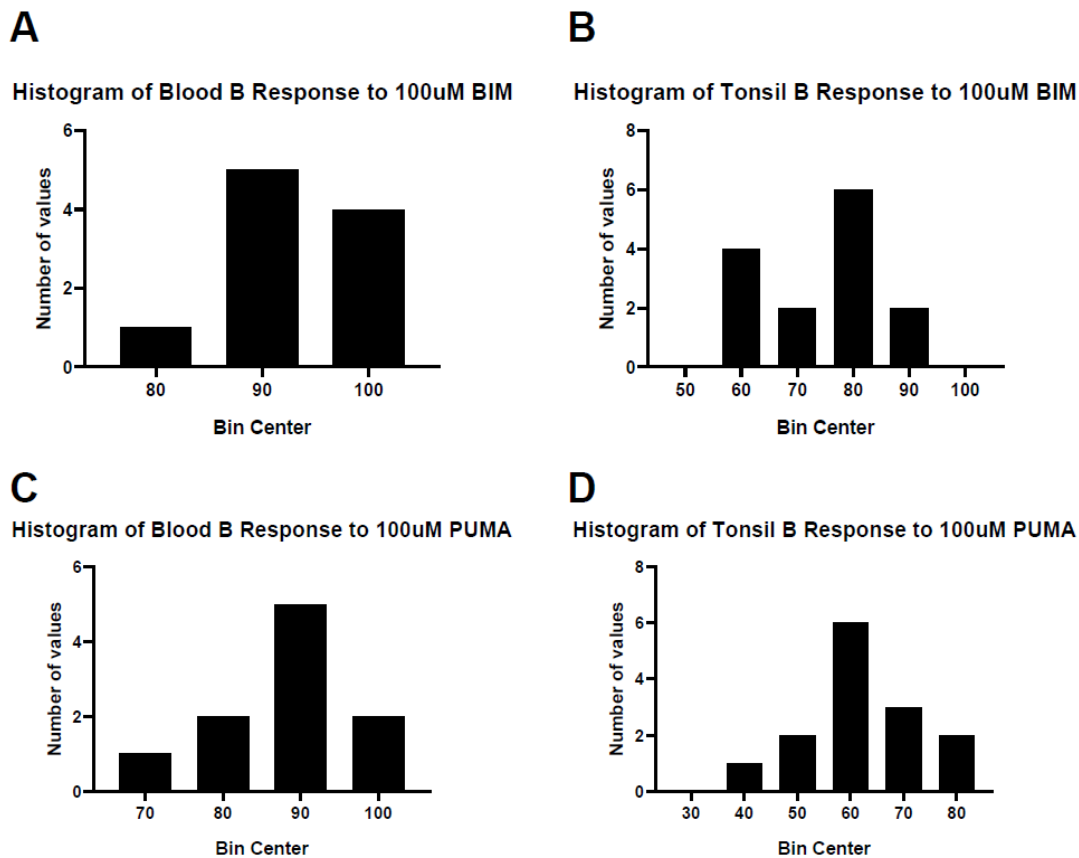


Figure 3.S2. Normal B Cell Response. Histograms showing the range of responses for normal B cells to 100 μM BIM (A, B) and 100 μM PUMA (C, D) in PB and LN. These responses were used to determine the threshold for class A/B samples outlined in the methods. PB shows less variation and higher overall responses.

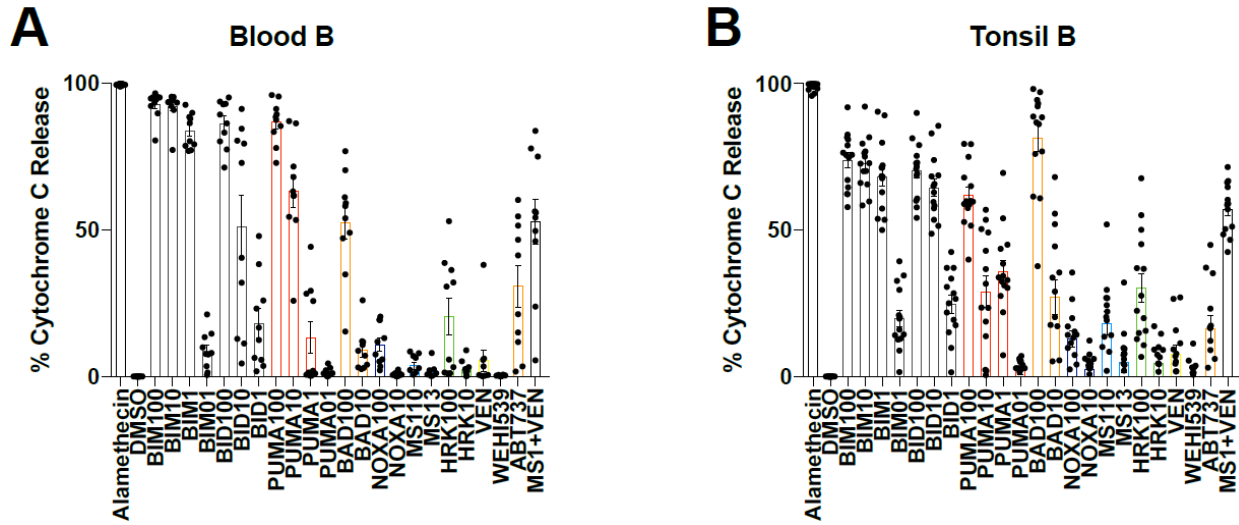


Figure 3.S3. Full BH3 profiling results for all non-malignant cell types tested. (A) BH3 profiling of peripheral blood (PB) B cell controls (n = 10) showing % of the cells undergoing cytochrome c release on the Y axis after exposure to each drug/peptide on the X axis. Cells exhibit a Class C response with multiple anti-apoptotic protein dependencies. (B) BH3 profiling of tonsil B cell (n = 14). Tonsillar samples are similar to PB controls but are slightly less primed and more dependent on MCL1.

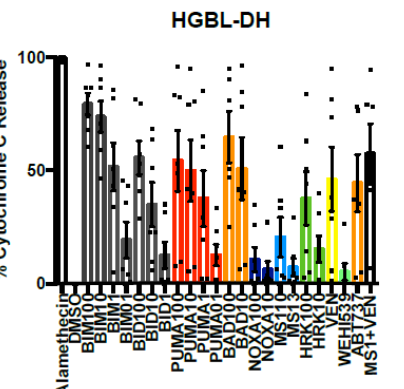
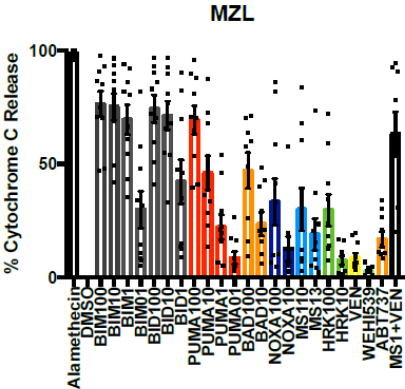
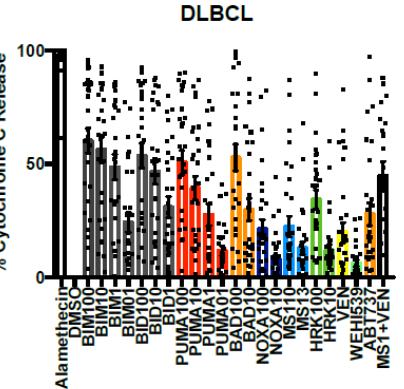
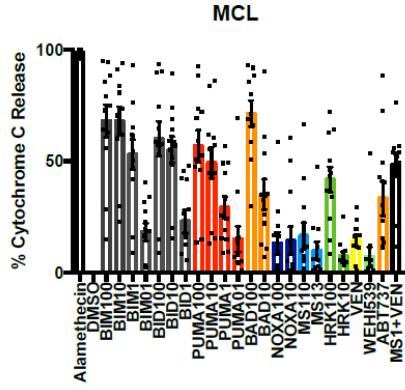
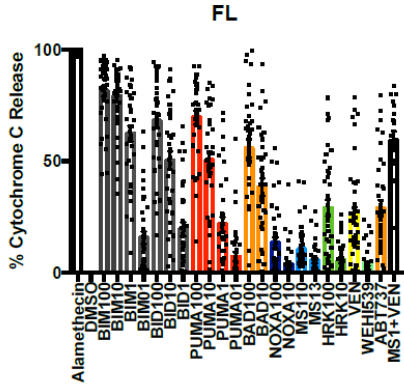
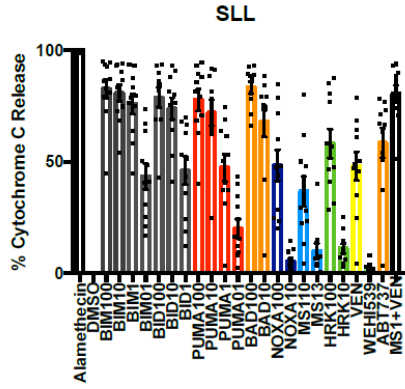
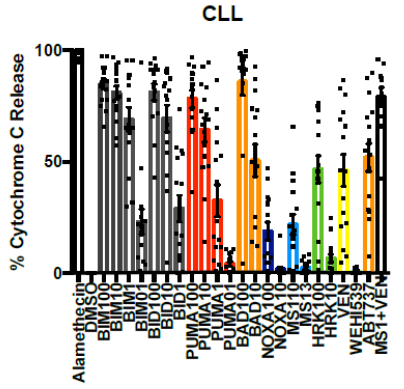


Figure 3.S4. Full BH3 profiling results for all NHL samples tested. Full BH3 profiles for all NHL subtypes tested. See supplemental table 1 for full summary of samples used for analysis.

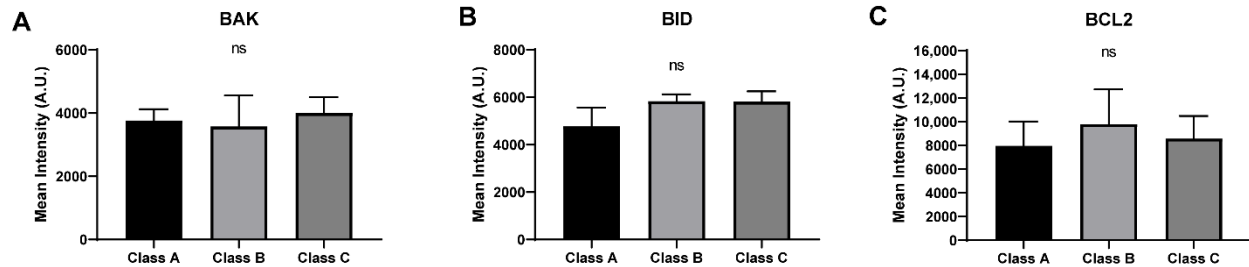


Figure 3.S5. Expression of BAK, BID, and BCL2 in DLBCL BH3 profiles. Quantification of mean pixel intensity across all classes of apoptotic block in BAK (A), BID (B), and BCL1 (C). Samples were analyzed using Qupath software (see methods) and t-test with Welch's correction was used to compare columns, bars represent the mean \pm standard error of the mean (SEM). No significant differences in expression intensity were seen in these proteins across all classes. ns, non-significant.

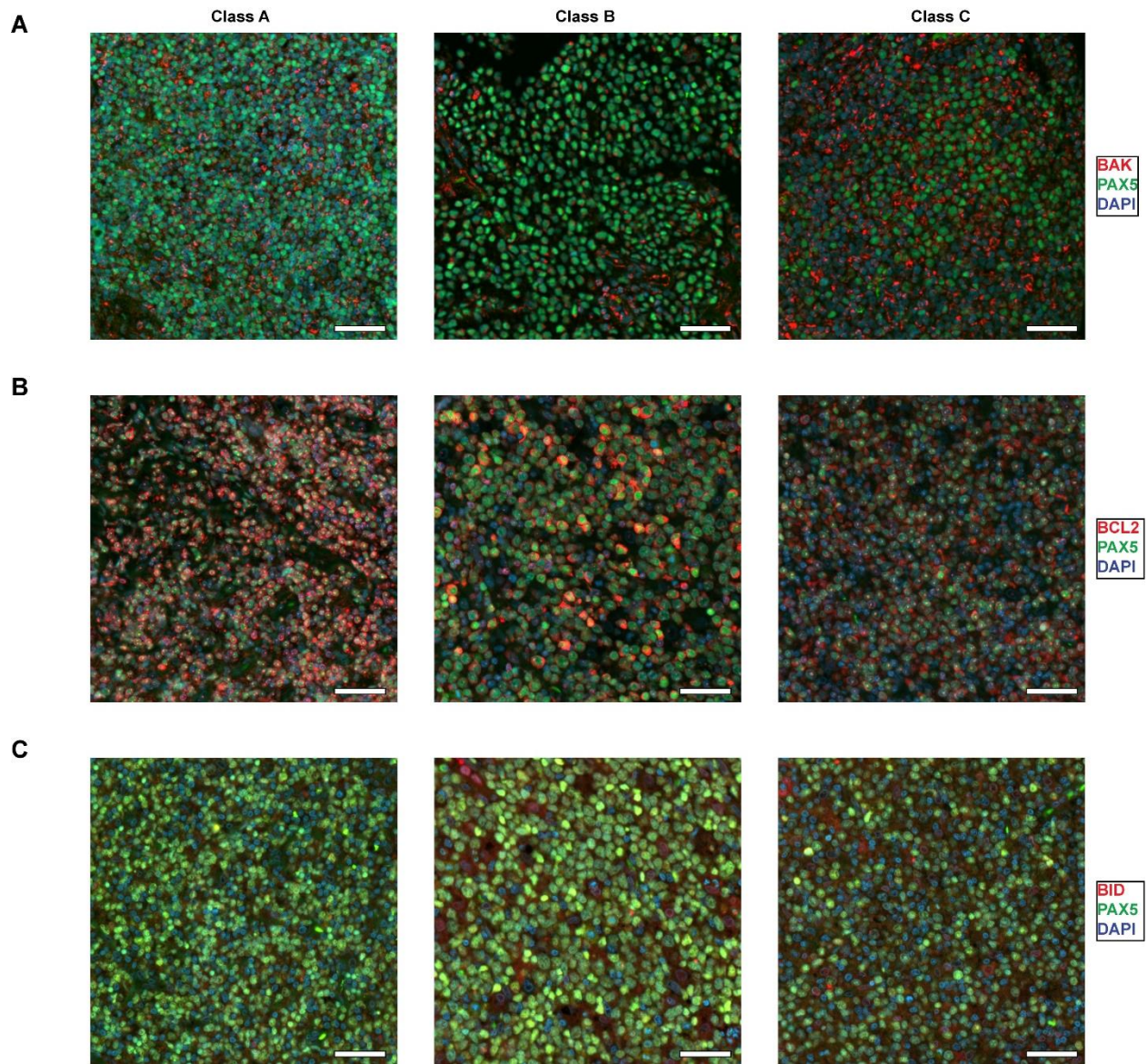


Figure 3.S6. Immunofluorescence of BAK, BID, and BCL2. Representative merged IF stains at 20 \times for DAPI (blue), PAX5 (green, AF594) and BAK/BID/BCL2 (red, AF647) in class (A), (B), and (C) samples. Scale bars represent 50 μ m.

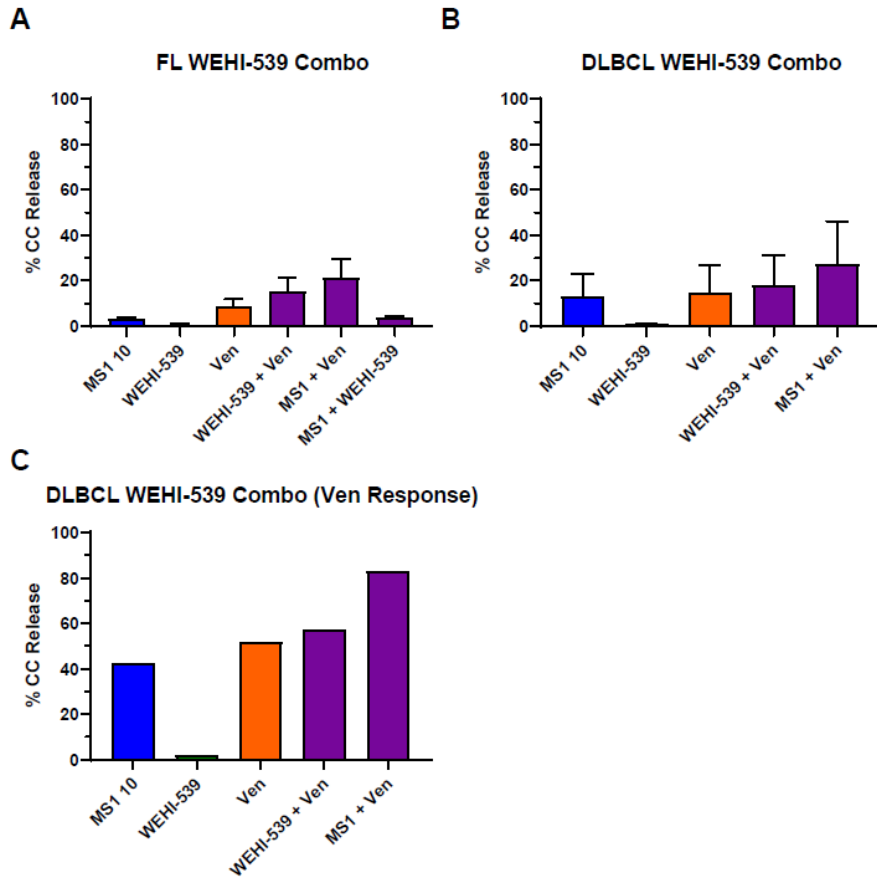


Figure 3.S7. Combination of WEHI-539 and Venetoclax in FL and DLBCL. A subset of FL (n = 7) and DLBCL (n = 4) samples also included combination of either 10 μ M MS1 or 1 μ M WEHI-539 and 1 μ M Venetoclax during BH3 profiling. Error bars represent standard error of mean (SEM) (A) Summary BH3 profiles of FL samples also incubated with combination targeting of BCLXL and BCL2. Only marginal increases in cytochrome c release are seen with the additional targeting of BCLXL by WEHI-539. Additional samples in this group (n = 3) were also treated with combination MCL1 and BCLXL targeted inhibitors (MS1 and WEHI-539, respectively). These samples showed no response and implicated BCL2 as the primary protein responsible for cell survival. (B) Summary BH3 profiles of DLBCL samples also incubated with combination targeting of BCLXL and BCL2. Only marginal increases in cytochrome c release are seen with the additional targeting of BCLXL by WEHI-539. (C) Specific DLBCL sample with a strong response to venetoclax. Here the targeting of BCLXL provides little benefit to cytochrome c release and is substantially less than combination treatment with MS1.

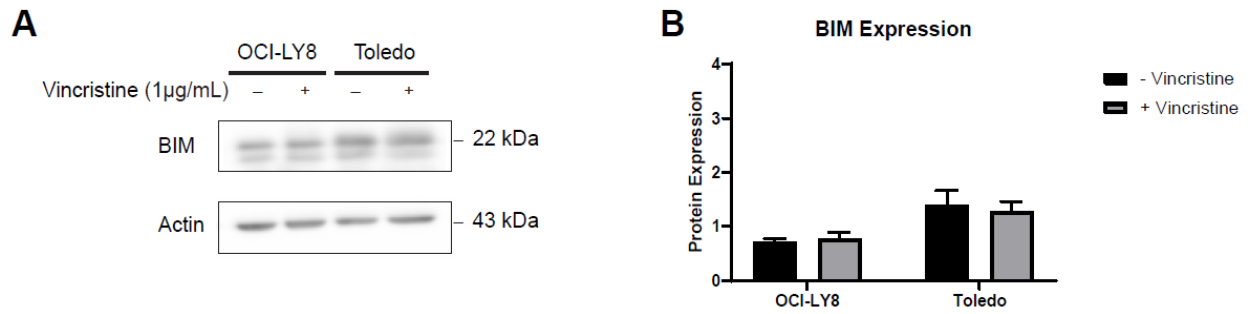


Figure 3.S8. Expression of BIM in vincristine treated NHL cell lines. (A) Representative western blot of BIM expression after 17 h treatment with 1 µg/mL vincristine. (B) Quantification of BIM expression via western blot (n = 3). No difference in expression was seen between treated and untreated samples, as analyzed by multiple paired t-tests. Error bars represent standard error of mean (SEM).

Characteristics	Number of cases
CLL/SLL	27 (16 blood, 11 LN)
Follicular lymphoma (FL)	38 (LN)
Marginal zone lymphoma (MZL)	10 (LN)
Mantle cell lymphoma (MCL)	12 (LN)
HGBL-DH	7 (1 LN, 6 fluid)
DLBCL*	30 (26 LN, 4 fluid)
BCL2 protein > 50% cells	
Positive	19
Negative	8
Not available	3
BCL2 translocation	
Present	3
Absent	19
Not available	8
Cell of origin	
GCB	11
Non-GCB	16
Not available	3

Table 3.S1: Characteristics of all 124 lymphoma samples used for BH3 profiling. Lymphoma cells were obtained from lymph nodes (LN) that were disaggregated into a cell suspension or cells were already in single cell suspension derived from fluid samples that included peripheral blood, cerebrospinal fluid, pleural fluid, ascites and bone marrow. Cell of origin was determined by immunohistochemistry using Han’s criteria except for 4 DLBCL samples from the British Columbia Cancer Agency where nanostring was used. The one unclassifiable sample was assigned to the non-GCB group. *One patient with high-grade B cell lymphoma without concurrent *MYC* and *BCL2* translocations was included in the DLBCL cohort, sample taken at the time of diagnosis (LN). Abbreviations: LN, lymph node; HGBL-DH, high grade B cell lymphoma double hit, with translocations in *MYC* and *BCL2*; DLBCL, diffuse large B cell

lymphoma; CLL, chronic lymphocytic leukemia; SLL, small lymphocytic lymphoma; GCB, germinal center B cell lymphoma.

Class	BAX Mean Intensity (A.U.)	BIM Mean Intensity (A.U.)	MCL1 Mean Intensity (A.U.)	BCL2 Mean Intensity (A.U.)	BAK Mean Intensity (A.U.)	BID Mean Intensity (A.U.)
A	3853.288417	1374.648764	1091.10804	5903.325116	3398.310483	5573.286071
A	4472.266827	1258.928672	1015.728332	10023.18012	4124.485058	3978.781223
B	7098.61491	9941.187506	2240.660679	14709.78703	2019.337381	6476.903207
B	5663.862758	10344.48309	1770.131158	14601.15274	2436.199947	5347.320627
B	10129.45186	5841.492441	3258.356392	7003.465439	5521.539065	6601.324827
B	6285.105063	5258.880078	1989.559763	N/A	6339.458534	5469.620352
B	4417.091844	4276.640875	1360.384019	2839.007864	1579.364029	5278.815957
C	10121.14511	19828.45307	2326.923568	17134.13658	3957.462731	4675.663653
C	1796.305482	3839.670857	1599.298839	4141.41242	1875.73769	6049.616008
C	5556.709505	18974.15932	2543.152245	5029.490361	3289.689541	5781.86078
C	7413.787418	5760.20464	3538.071734	8811.855963	5670.484968	4504.526667
C	10668.02037	10522.29172	2690.25151	9510.976622	5689.042839	5305.112272
C	6117.23331	11526.97544	3597.869027	N/A	3654.310946	7910.982896
C	8247.859508	12880.31174	3229.2039	N/A	N/A	N/A
C	8084.438601	4547.557853	2916.041703	6871.081087	3846.662773	6457.956317

Table 3.S2: Mean intensity values for immunofluorescence staining of PAX5+ cells. Mean intensity was calculated by Qupath image analysis software. Cell intensity for protein of interest was gated on Pax5+ cells, which were determined as the highest 50% of AF594 expressing cells. Values shown are the mean intensity of all Pax5+ cells in a sample analyzed and samples labeled “N/A” indicate either a staining failure and/or lack of sufficient tissue to characterize the expression of stained protein.

3.11: Author Contributions

Conceptualization, C.M.W., P.S., J.R., A.L. and N.A.J.; Formal Analysis, R.N.R., C.M.W., D.G., C.G., A.G., E.B., L.S., T.P.-H., S.D., S.d.R. and K.K.M.; Resources, J.H., S.F., A.S., G.O., C.S., D.W.S., and N.A.J.; Investigation, R.N.R., C.M.W., D.G., A.G., E.B., L.S., T.P.-H., and S.D.; Methodology, C.G.; Visualization, R.N.R.; Supervision, K.K.M., S.d.R., N.A.J.; Writing—Original Draft Preparation, Review & Editing, C.M.W., R.N.R., and N.A.J.;

Funding Acquisition, N.A.J. All authors have read and agreed to the published version of the manuscript.

3.12: Funding

This research was supported by Abbvie and the Canadian Institute for Health Research (CIHR) (operating 299607 awarded to NAJ). C.M.W. and R.N.R. received salary awards from the Cole Foundation. D.G. received a salary award from CIHR. S.D. is supported through a Cole Foundation award.

3.13: Institutional Review Board Statement

The study was conducted according to the guidelines of the Declaration of Helsinki, and approved by the Research Ethics Board of the Lady Davis Institute protocols [11–047 and 12–052].

3.14: Informed Consent Statement

Informed consent was obtained from all subjects involved in this study.

3.15: Data Availability Statement

The data presented in this study are available on request from the corresponding author. The data are not publicly available due to privacy restrictions.

3.16: Acknowledgements

We acknowledge the support of the patients and their families who have consented to participate in lymphoma tissue banking within the Banque de cellules leucémiques du Québec (BCLQ). We thank the Jewish General Hospital Foundation and the Cole Foundation for supporting the lymphoma cell bank at the JGH and the Cancer Research Network of the Fonds de Recherche du Québec en Santé for financially supporting the BCLQ.

3.17: Conflicts of Interest

N.A.J. has received research funding from Roche Canada and consulting fees/honoraria from Roche, Abbvie, Lundbeck, Seattle Genetics, Janssen, and Gilead. At the time of submission, C.M.W. is employed by Astrazeneca plc. A.L. discloses consulting and laboratory research support from AbbVie, Novartis, and Astrazeneca. He is an equity-holding co-founder of Flash Therapeutics and Vivid Biosciences.

3.18: References

1. Reed J.C., Cuddy M., Slabiak T., Croce C.M., Nowell P.C. Oncogenic potential of bcl-2 demonstrated by gene transfer. *Nature*. 1988;336:259–261. doi: 10.1038/336259a0.
2. Vaux D.L., Cory S., Adams J.M. Bcl-2 gene promotes haemopoietic cell survival and cooperates with c-myc to immortalize pre-B cells. *Nature*. 1988;335:440–442. doi: 10.1038/335440a0.
3. Swerdlow S.H., Campo E., Pileri S.A., Harris N.L., Stein H., Siebert R., Advani R., Ghielmini M., Salles G.A., Zelenetz A.D., et al. The 2016 revision of the World Health Organization classification of lymphoid neoplasms. *Blood*. 2016;127:2375–2390. doi: 10.1182/blood-2016-01-643569.
4. Johnson N.A., Slack G.W., Savage K.J., Connors J.M., Ben-Neriah S., Rogic S., Scott D.W., Tan K.L., Steidl C., Sehn L.H., et al. Concurrent expression of MYC and BCL2 in diffuse large B-cell lymphoma treated with rituximab plus cyclophosphamide, doxorubicin, vincristine, and prednisone. *J. Clin. Oncol*. 2012;30:3452–3459. doi: 10.1200/JCO.2011.41.0985.
5. Green T.M., Young K.H., Visco C., Xu-Monette Z.Y., Orazi A., Go R.S., Nielsen O., Gadeberg O.V., Mourits-Andersen T., Frederiksen M., et al. Immunohistochemical double-

- hit score is a strong predictor of outcome in patients with diffuse large B-cell lymphoma treated with rituximab plus cyclophosphamide, doxorubicin, vincristine, and prednisone. *J. Clin. Oncol.* 2012;30:3460–3467. doi: 10.1200/JCO.2011.41.4342.
6. Herrera A.F., Mei M., Low L., Kim H.T., Griffin G.K., Song J.Y., Merryman R.W., Bedell V., Pak C., Sun H., et al. Relapsed or Refractory Double-Expressor and Double-Hit Lymphomas Have Inferior Progression-Free Survival After Autologous Stem-Cell Transplantation. *J. Clin. Oncol.* 2017;35:24–31. doi: 10.1200/JCO.2016.68.2740.
 7. Tsuyama N., Sakata S., Baba S., Mishima Y., Nishimura N., Ueda K., Yokoyama M., Terui Y., Hatake K., Kitagawa M., et al. BCL2 expression in DLBCL: Reappraisal of immunohistochemistry with new criteria for therapeutic biomarker evaluation. *Blood.* 2017;130:489–500. doi: 10.1182/blood-2016-12-759621.
 8. Souers A.J., Levenson J.D., Boghaert E.R., Ackler S.L., Catron N.D., Chen J., Dayton B.D., Ding H., Enschede S.H., Fairbrother W.J., et al. ABT-199, a potent and selective BCL-2 inhibitor, achieves antitumor activity while sparing platelets. *Nat. Med.* 2013;19:202–208. doi: 10.1038/nm.3048.
 9. Stilgenbauer S., Eichhorst B., Schetelig J., Coutre S., Seymour J.F., Munir T., Puvvada S.D., Wendtner C.-M., Roberts A.W., Jurczak W., et al. Venetoclax in relapsed or refractory chronic lymphocytic leukaemia with 17p deletion: A multicentre, open-label, phase 2 study. *Lancet Oncol.* 2016;17:768–778. doi: 10.1016/S1470-2045(16)30019-5.
 10. Roberts A.W., Davids M.S., Pagel J.M., Kahl B.S., Puvvada S.D., Gerecitano J.F., Kipps T.J., Anderson M.A., Brown J.R., Gressick L., et al. Targeting BCL2 with Venetoclax in Relapsed Chronic Lymphocytic Leukemia. *N. Engl. J. Med.* 2016;374 doi: 10.1056/NEJMoa1513257.

11. Davids M.S., Roberts A.W., Seymour J.F., Pagel J.M., Kahl B.S., Wierda W.G., Puvvada S., Kipps T.J., Anderson M.A., Salem A.H., et al. Phase I First-in-Human Study of Venetoclax in Patients With Relapsed or Refractory Non-Hodgkin Lymphoma. *J. Clin. Oncol.* 2017;35:826–833. doi: 10.1200/JCO.2016.70.4320.
12. Klanova M., Klener P. BCL-2 proteins in pathogenesis and therapy of B-Cell non-hodgkin lymphomas. *Cancers (Basel)* 2020;12:938. doi: 10.3390/cancers12040938.
13. Fulda S., Debatin K.-M. Extrinsic versus intrinsic apoptosis pathways in anticancer chemotherapy. *Oncogene.* 2006;25:4798–4811. doi: 10.1038/sj.onc.1209608.
14. Certo M., Del Gaizo Moore V., Nishino M., Wei G., Korsmeyer S., Armstrong S.A., Letai A. Mitochondria primed by death signals determine cellular addiction to antiapoptotic BCL-2 family members. *Cancer Cell.* 2006;9:351–365. doi: 10.1016/j.ccr.2006.03.027.
15. Del Gaizo Moore V., Letai A. BH3 profiling--measuring integrated function of the mitochondrial apoptotic pathway to predict cell fate decisions. *Cancer Lett.* 2013;332:202–205. doi: 10.1016/j.canlet.2011.12.021.
16. Deng J., Carlson N., Takeyama K., Dal Cin P., Shipp M., Letai A. BH3 profiling identifies three distinct classes of apoptotic blocks to predict response to ABT-737 and conventional chemotherapeutic agents. *Cancer Cell.* 2007;12:171–185. doi: 10.1016/j.ccr.2007.07.001.
17. Kim H., Rafiuddin-Shah M., Tu H.C., Jeffers J.R., Zambetti G.P., Hsieh J.J.D., Cheng E.H.Y. Hierarchical regulation of mitochondrion-dependent apoptosis by BCL-2 subfamilies. *Nat. Cell Biol.* 2006;8:1348–1358. doi: 10.1038/ncb1499.
18. Kuwana T., Bouchier-Hayes L., Chipuk J.E., Bonzon C., Sullivan B.A., Green D.R., Newmeyer D.D. BH3 domains of BH3-only proteins differentially regulate Bax-mediated

mitochondrial membrane permeabilization both directly and indirectly. *Mol. Cell.* 2005;17:525–535. doi: 10.1016/j.molcel.2005.02.003.

19. Del Gaizo Moore V., Brown J.R., Certo M., Love T.M., Novina C.D., Letai A. Chronic lymphocytic leukemia requires BCL2 to sequester prodeath BIM, explaining sensitivity to BCL2 antagonist ABT-737. *J. Clin. Investig.* 2007;117:112–121. doi: 10.1172/JCI28281.
20. Touzeau C., Ryan J., Guerriero J., Moreau P., Chonghaile T.N., Le Gouill S., Richardson P., Anderson K., Amiot M., Letai A. BH3 profiling identifies heterogeneous dependency on Bcl-2 family members in multiple myeloma and predicts sensitivity to BH3 mimetics. *Leukemia.* 2016;30:761–764. doi: 10.1038/leu.2015.184.
21. Pan R., Hogdal L.J., Benito J.M., Bucci D., Han L., Borthakur G., Cortes J., Deangelo D.J., Debose L., Mu H., et al. Selective BCL-2 inhibition by ABT-199 causes on-target cell death in acute myeloid Leukemia. *Cancer Discov.* 2014 doi: 10.1158/2159-8290.CD-13-0609.
22. Ni Chonghaile T., Roderick J.E., Glenfield C., Ryan J., Sallan S.E., Silverman L.B., Loh M.L., Hunger S.P., Wood B., DeAngelo D.J., et al. Maturation stage of T-cell acute lymphoblastic leukemia determines BCL-2 versus BCL-XL dependence and sensitivity to ABT-199. *Cancer Discov.* 2014;4:1074–1087. doi: 10.1158/2159-8290.CD-14-0353.
23. Cobaleda C., Schebesta A., Delogu A., Busslinger M. Pax5: The guardian of B cell identity and function. *Nat. Immunol.* 2007;8:463–470. doi: 10.1038/ni1454.
24. Bai M., Skyrilas A., Agnantis N.J., Kamina S., Tsanou E., Grepis C., Galani V., Kanavaros P. Diffuse large B-cell lymphomas with germinal center B-cell-like differentiation immunophenotypic profile are associated with high apoptotic index, high expression of the proapoptotic proteins bax, bak and bid and low expression of the antiapoptotic proteins. *Mod. Pathol.* 2004;17:847–856. doi: 10.1038/modpathol.3800130.

25. Krajewski S., Bodrug S., Krajewska M., Shabaik A., Gascoyne R., Berean K., Reed J.C.
Immunohistochemical analysis of Mcl-1 protein in human tissues: Differential regulation of Mcl-1 and Bcl-2 protein production suggests a unique role for Mcl-1 in control of programmed cell death in vivo. *Am. J. Pathol.* 1995;146:1309–1319.
26. Vikstrom I., Carotta S., Luthje K., Peperzak V., Jost P.J., Glaser S., Busslinger M., Bouillet P., Strasser A., Nutt S.L., et al. Mcl-1 Is Essential for Germinal Center Formation and B Cell Memory. *Science.* 2010;330:1095–1099. doi: 10.1126/science.1191793.
27. Wendel H.-G., Mondello P., Liu Y., Nanjangud G., de Stanchina E., Seshan V.E., Younes A., Tannan N.B., Erazo T., Asgari Z., et al. NOXA genetic amplification or pharmacologic induction primes lymphoma cells to BCL2 inhibitor-induced cell death. *Proc. Natl. Acad. Sci. USA.* 2018;115:12034–12039. doi: 10.1073/pnas.1806928115.
28. Wenzel S.S., Grau M., Mavis C., Hailfinger S., Wolf A., Madle H., Deeb G., Dörken B., Thome M., Lenz P., et al. MCL1 is deregulated in subgroups of diffuse large B-cell lymphoma. *Leukemia.* 2013;27:1381–1390. doi: 10.1038/leu.2012.367.
29. Teh T.-C., Nguyen N.-Y., Moujalled D.M., Segal D., Pomilio G., Rijal S., Jabbour A., Cummins K., Lackovic K., Blombery P., et al. Enhancing venetoclax activity in acute myeloid leukemia by co-targeting MCL1. *Leukemia.* 2017 doi: 10.1038/leu.2017.243.
30. Phillips D.C., Xiao Y., Lam L.T., Litvinovich E., Roberts-Rapp L., Souers A.J., Levenson J.D. Loss in MCL-1 function sensitizes non-Hodgkin's lymphoma cell lines to the BCL-2-selective inhibitor venetoclax (ABT-199) *Blood Cancer J.* 2015;5:e368. doi: 10.1038/bcj.2015.88.
31. Morschhauser F., Feugier P., Flinn I.W., Gasiorowski R., Greil R., Illes A., Johnson N.A., Larouche J.-F., Lugtenburg P.J., Patti C., et al. A phase II study of venetoclax plus R-CHOP

- as first-line treatment for patients with diffuse large B-cell lymphoma. *Blood*. 2020 doi: 10.1182/blood.2020006578.
32. Zinzani P.L., Topp M.S., Yuen S.L.S., Rusconi C., Fleury I., Pro B., Gritti G., Crump M., Hsu W., Punnoose E.A., et al. Phase 2 Study of Venetoclax Plus Rituximab or Randomized Ven Plus Bendamustine+Rituximab (BR) Versus BR in Patients with Relapsed/Refractory Follicular Lymphoma: Interim Data. *Blood*. 2016;128:617. doi: 10.1182/blood.V128.22.617.617.
33. Herrick D.J., Ross J. The half-life of c-myc mRNA in growing and serum-stimulated cells: Influence of the coding and 3' untranslated regions and role of ribosome translocation. *Mol. Cell. Biol.* 1994;14:2119–2128. doi: 10.1128/MCB.14.3.2119.
34. Nijhawan D., Fang M., Traer E., Zhong Q., Gao W., Du F., Wang X. Elimination of Mcl-1 is required for the initiation of apoptosis following ultraviolet irradiation. *Genes Dev.* 2003;17:1475–1486. doi: 10.1101/gad.1093903.
35. Inoue-Yamauchi A., Jeng P.S., Kim K., Chen H.-C., Han S., Ganesan Y.T., Ishizawa K., Jebiwott S., Dong Y., Pietanza M.C., et al. Targeting the differential addiction to anti-apoptotic BCL-2 family for cancer therapy. *Nat. Commun.* 2017;8:16078. doi: 10.1038/ncomms16078.
36. Ben-Dali Y., Hleuhel M.H., da Cunha-Bang C., Brieghel C., Poulsen C.B., Clasen-Linde E., Bentzen H.H.N., Frederiksen H., Christiansen I., Nielsen L.H., et al. Richter's transformation in patients with chronic lymphocytic leukaemia: A Nationwide Epidemiological Study. *Leuk. Lymphoma*. 2020;61:1435–1444. doi: 10.1080/10428194.2020.1719092.
37. Haselager M.V., Kielbassa K., ter Burg J., Bax D.J.C., Fernandes S.M., Borst J., Tam C., Forconi F., Chiodin G., Brown J.R., et al. Changes in Bcl-2 members after ibrutinib or

- venetoclax uncover functional hierarchy in determining resistance to venetoclax in CLL. *Blood*. 2020;136:2918–2926. doi: 10.1182/blood.2019004326.
38. Roberts A.W., Ma S., Kipps T.J., Coutre S.E., Davids M.S., Eichhorst B., Hallek M., Byrd J.C., Humphrey K., Zhou L., et al. Efficacy of venetoclax in relapsed chronic lymphocytic leukemia is influenced by disease and response variables. *Blood*. 2019;134:111–122. doi: 10.1182/blood.2018882555.
39. Lømo J., Smeland E.B., Krajewski S., Reed J.C., Blomhoff H.K. Expression of the Bcl-2 homologue Mcl-1 correlates with survival of peripheral blood B lymphocytes. *Cancer Res*. 1996;56:40–43.
40. Opferman J.T., Letai A., Beard C., Sorcinelli M.D., Ong C.C., Korsmeyer S.J. Development and maintenance of B and T lymphocytes requires antiapoptotic MCL-1. *Nature*. 2003;426:671–676. doi: 10.1038/nature02067.
41. Dai J., Luftig M.A. Intracellular BH3 Profiling Reveals Shifts in Antiapoptotic Dependency in Human B Cell Maturation and Mitogen-Stimulated Proliferation. *J. Immunol*. 2018;ji1701473. doi: 10.4049/jimmunol.1701473.
42. ten Hacken E., Burger J.A. Molecular pathways: Targeting the microenvironment in chronic lymphocytic leukemia--focus on the B-cell receptor. *Clin. Cancer Res*. 2014;20:548–556. doi: 10.1158/1078-0432.CCR-13-0226.
43. Greaves G., Milani M., Butterworth M., Carter R.J., Byrne D.P., Eyers P.A., Luo X., Cohen G.M., Varadarajan S. BH3-only proteins are dispensable for apoptosis induced by pharmacological inhibition of both MCL-1 and BCL-XL. *Cell Death Differ*. 2019;26:1037–1047. doi: 10.1038/s41418-018-0183-7.

44. Wever C.M., Geoffrion D., Grande B.M., Yu S., Alcaide M., Lemaire M., Riazalhosseini Y., Hébert J., Gavino C., Vinh D.C., et al. The genomic landscape of two Burkitt lymphoma cases and derived cell lines: Comparison between primary and relapse samples. *Leuk. Lymphoma*. 2018;1–16. doi: 10.1080/10428194.2017.1413186.
45. Morin R.D., Assouline S., Alcaide M., Mohajeri A., Johnston R.L., Chong L., Grewal J., Yu S., Fornika D., Bushell K., et al. Genetic Landscapes of Relapsed and Refractory Diffuse Large B-Cell Lymphomas. *Clin. Cancer Res*. 2016;22:2290–2300. doi: 10.1158/1078-0432.CCR-15-2123.
46. Zhang J., Medeiros L.J., Young K.H. Cancer immunotherapy in diffuse large B-cell lymphoma. *Front. Oncol*. 2018;8:1–12. doi: 10.3389/fonc.2018.00351.
47. Neelapu S.S., Locke F.L., Bartlett N.L., Lekakis L.J., Miklos D.B., Jacobson C.A., Braunschweig I., Oluwole O.O., Siddiqi T., Lin Y., et al. Axicabtagene Ciloleucel CAR T-Cell Therapy in Refractory Large B-Cell Lymphoma. *N. Engl. J. Med*. 2017;377:2531–2544. doi: 10.1056/NEJMoa1707447.
48. Locke F.L., Ghobadi A., Jacobson C.A., Miklos D.B., Lekakis L.J., Oluwole O.O., Lin Y., Braunschweig I., Hill B.T., Timmerman J.M., et al. Long-term safety and activity of axicabtagene ciloleucel in refractory large B-cell lymphoma (ZUMA-1): A single-arm, multicentre, phase 1–2 trial. *Lancet Oncol*. 2019;20:31–42. doi: 10.1016/S1470-2045(18)30864-7.
49. Lejeune M., Köse M.C., Duray E., Einsele H., Beguin Y., Caers J. Bispecific, T-Cell-Recruiting Antibodies in B-Cell Malignancies. *Front. Immunol*. 2020;11 doi: 10.3389/fimmu.2020.00762.

50. Smith V.M., Dietz A., Henz K., Bruecher D., Jackson R., Kowald L., Van Wijk S.J.L., Jayne S., Macip S., Fulda S., et al. Specific interactions of BCL-2 family proteins mediate sensitivity to BH3-mimetics in diffuse large B-cell lymphoma. *Haematologica*. 2019 doi: 10.3324/haematol.2019.220525.
51. de Jong M.R.W., Langendonk M., Reitsma B., Nijland M., van den Berg A., Ammatuna E., Visser L., van Meerten T. Heterogeneous Pattern of Dependence on Anti-Apoptotic BCL-2 Family Proteins upon CHOP Treatment in Diffuse Large B-Cell Lymphoma. *Int. J. Mol. Sci.* 2019;20:6036. doi: 10.3390/ijms20236036.
52. Tahir S.K., Smith M.L., Hessler P., Rapp L.R., Idler K.B., Park C.H., Levenson J.D., Lam L.T. Potential mechanisms of resistance to venetoclax and strategies to circumvent it. *BMC Cancer*. 2017;17:1–10. doi: 10.1186/s12885-017-3383-5.
53. Herling C.D., Abedpour N., Weiss J., Schmitt A., Jachimowicz R.D., Merkel O., Cartolano M., Oberbeck S., Mayer P., Berg V., et al. Clonal dynamics towards the development of venetoclax resistance in chronic lymphocytic leukemia. *Nat. Commun.* 2018;9:727. doi: 10.1038/s41467-018-03170-7.
54. Klanova M., Andera L., Brazina J., Svadlenka J., Benesova S., Soukup J., Prukova D., Vejmelkova D., Jakska R., Helman K., et al. Targeting of BCL2 Family Proteins with ABT-199 and Homoharringtonine Reveals BCL2- and MCL1-Dependent Subgroups of Diffuse Large B-Cell Lymphoma. *Clin. Cancer Res.* 2016;22:1138–1149. doi: 10.1158/1078-0432.CCR-15-1191.
55. Touzeau C., Maciag P., Amiot M., Moreau P. Targeting Bcl-2 for the treatment of multiple myeloma. *Leukemia*. 2018;32:1899–1907. doi: 10.1038/s41375-018-0223-9.

56. Olejniczak E.T., Fischer M.A., Fesik S.W., Lee T., Gorska A.E., Ramsey H.E., Ayers G.D., Arrate M.P., Strickland S.A., Savona M.R., et al. A Novel MCL1 Inhibitor Combined with Venetoclax Rescues Venetoclax-Resistant Acute Myelogenous Leukemia. *Cancer Discov.* 2018;8:1566–1581. doi: 10.1158/2159-8290.cd-18-0140.
57. Vikström I.B., Slomp A., Carrington E.M., Moesbergen L.M., Chang C., Kelly G.L., Glaser S.P., Jansen J.H.M., Leusen J.H.W., Strasser A., et al. MCL-1 is required throughout B-cell development and its loss sensitizes specific B-cell subsets to inhibition of BCL-2 or BCL-XL. *Cell Death Dis.* 2016;7:e2345. doi: 10.1038/cddis.2016.237.
58. Smit L.A., Hallaert D.Y.H., Spijker R., de Goeij B., Jaspers A., Kater A.P., van Oers M.H.J., van Noesel C.J.M., Eldering E. Differential Noxa/Mcl-1 balance in peripheral versus lymph node chronic lymphocytic leukemia cells correlates with survival capacity. *Blood.* 2007;109:1660–1668. doi: 10.1182/blood-2006-05-021683.
59. Wertz I.E., Kusam S., Lam C., Okamoto T., Sandoval W., Anderson D.J., Helgason E., Ernst J.A., Eby M., Liu J., et al. Sensitivity to antitubulin chemotherapeutics is regulated by MCL1 and FBW7. *Nature.* 2011;471:110–114. doi: 10.1038/nature09779.
60. Brunelle J.K., Ryan J., Yecies D., Opferman J.T., Letai A. MCL-1-dependent leukemia cells are more sensitive to chemotherapy than BCL-2-dependent counterparts. *J. Cell Biol.* 2009;187:429–442. doi: 10.1083/jcb.200904049.
61. Bhola P.D., Ahmed E., Guerriero J.L., Sicinska E., Su E., Lavrova E., Ni J., Chipashvili O., Hagan T., Pioso M.S., et al. High-throughput dynamic BH3 profiling may quickly and accurately predict effective therapies in solid tumors. *Sci. Signal.* 2020;13:1–12. doi: 10.1126/scisignal.aay1451.

62. Morschhauser F., Flinn I.W., Advani R., Sehn L.H., Diefenbach C., Kolibaba K., Press O.W., Salles G., Tilly H., Chen A.I., et al. Polatuzumab vedotin or pinatuzumab vedotin plus rituximab in patients with relapsed or refractory non-Hodgkin lymphoma: Final results from a phase 2 randomised study (ROMULUS) *Lancet Haematol.* 2019;6:e254–e265. doi: 10.1016/S2352-3026(19)30026-2.
63. Sehn L.H., Herrera A.F., Flowers C.R., Kamdar M.K., McMillan A., Hertzberg M., Assouline S., Kim T.M., Kim W.S., Ozcan M., et al. Polatuzumab Vedotin in Relapsed or Refractory Diffuse Large B-Cell Lymphoma. *J. Clin. Oncol. Off. J. Am. Soc. Clin. Oncol.* 2020;38:155–165. doi: 10.1200/JCO.19.00172.
64. Ryan J., Montero J., Rocco J., Letai A. iBH3: Simple, fixable BH3 profiling to determine apoptotic priming in primary tissue by flow cytometry. *Biol. Chem.* 2016;397:671–678. doi: 10.1515/hsz-2016-0107.
65. Bankhead P., Loughrey M.B., Fernández J.A., Dombrowski Y., McArt D.G., Dunne P.D., McQuaid S., Gray R.T., Murray L.J., Coleman H.G., et al. QuPath: Open source software for digital pathology image analysis. *Sci. Rep.* 2017;7:1–7. doi: 10.1038/s41598-017-17204-5.

Chapter 4: Predicting Relapsed/Refractory Diffuse Large B Cell Lymphoma Using Serial ctDNA Analysis

4.1: Preface

Our study of apoptotic dysfunction revealed that DLBCL is less sensitive to apoptotic activation than other NHL. This work highlights a population of high-risk patients having a DLBCL with profound apoptotic dysfunction that could not be predicted based on the underlying COO or alterations in genes coding for BH3 proteins. With funding from the Marathon of Hope, we have submitted our samples with class A, B and C apoptotic blocks, for whole genome and whole RNA sequencing to identify the genomic alterations that may explain the functional defects. However, the delays with this project precluded these results from being included in this thesis. While the BH3 profiling assay can be performed at diagnosis and relapse, it requires live cells in suspension and thus is not practical to do in routine clinical practice. A dynamic biomarker that predicts the emergence of rrDLBCL over the course of therapy and using a non-invasive method would be desirable. We focused our attention on serial analysis of plasma ctDNA as this could easily be sampled at several time points. Based on our previous published data, we designed a panel to capture genes that are most altered at relapse and diagnosis. Early identification of resistant disease to frontline treatment with R-CHOP is needed, as these patients are candidates for immediate clinical intervention with additional therapy and/or potential early selection for CART. Recently, ctDNA detection has become an extremely interesting tool for studying malignancies non-invasively, as well as longitudinally. Therefore, we sought to use serial ctDNA monitoring with our custom panel of rrDLBCL genes to confirm ctDNA prognostic capabilities, but also to study how mutational profiles and ctDNA changes differed between refractory, early relapse, late relapse and patients with complete remission. Detecting

refractory or early relapse DLBCL is paramount for improved treatment regimens in patients with pro-apoptotic defects or additional mechanisms of disease progression.

Early Identification of Relapsed/Refractory Diffuse Large B Cell Lymphoma Using Serial ctDNA Sampling

Ryan N. Rys^{1,2}, Christopher K. Rushton³, Elie Ritch³, Abdelrahman Ahmed², Eugène Brailovski^{2,4}, Christian Steidl⁵, David W. Scott⁵, Ryan D. Morin^{3,†}, and Nathalie A. Johnson^{2,4,6,†}

1. Department of Physiology, McGill University, Montreal, QC H3G 1Y6, Canada
2. Lady Davis Institute for Medical Research, Jewish General Hospital, Montreal, QC H3T 1E2, Canada
3. Department of Molecular Biology & Biochemistry, Simon Fraser University, Burnaby, BC V5A 1S6, Canada
4. Department of Medicine, McGill University, Montreal, QC H4A 3J1, Canada
5. Center for Lymphoid Cancer, BC Cancer, Vancouver, BC V5Z 1L3, Canada
6. Departments of Medicine and Oncology, Jewish General Hospital, Montreal, QC H3T 1E2, Canada

† These authors contributed equally to this work.

(Manuscript in Preparation)

4.2: Abstract

Diffuse Large B Cell Lymphoma (DLBCL) is the most common non-Hodgkin lymphoma and 40% of patients treated with frontline chemo-immunotherapy (R-CHOP) will experience relapsed or refractory DLBCL (rrDLBCL), which is associated with a very poor outcome. A subset of patients could be eligible for chimeric antigen receptor T cell (CART) therapy in second line (2L). Low disease burden and good performance status is associated improved outcomes, thus identifying early treatment failure or minimal residual rrDLBCL may improve outcomes to CART. Circulating tumor DNA (ctDNA) has been validated as a non-invasive method to analyze disease genetics in DLBCL. We tested the prognostic significance of ctDNA profiling using a novel CAPP-Seq panel of 194 genes on a retrospective cohort of 543 plasma samples obtained from 237 patients during therapy and surveillance follow up, 170 treated in 1L and 107 with > 2L treatment (40 across both cohorts). Median follow-up for diagnostic and relapse cohorts were both 2.9 years. All cases were processed with unique molecular identifiers and sequenced to a deduplicated read depth of ~500x in parallel with matched germline DNA. In 1L, we detected ctDNA in 94/99 samples at pre-therapy, 42/106 at mid therapy, 9/29 at end of therapy (EOT). Pretreatment ctDNA levels correlated both with the international prognostic index (IPI) ($p=0.0148$) and response to 1L ($p=0.0139$). Mid- and EOT levels were higher in patients with refractory disease, defined as relapse <9 months after diagnosis. High levels of ctDNA at relapse correlated with IPI ($p=0.0156$), PFS ($p=0.0379$) and OS ($p=0.0205$) in 2L therapy. Finally, in 37 samples during post R-CHOP surveillance, we also showed the utility of ctDNA in serial sampling and relapse detection, as we were able to detect relapsed disease in 18/24 (75%) of patients with a future relapse, ranging from 2-7 months prior to standard clinical methods. In summary, we have demonstrated the implementation of a novel gene panel focused

on recurrent mutations implicated in rrDLBCL. This panel not only has prognostic utility but can also increase detection of refractory disease in response to treatment, and thus provide actionable information for potential changes in clinical intervention, particularly after cycle 2 and/or completion of 1L therapy.

4.3: Introduction

Diffuse large B cell lymphoma (DLBCL) is the most common non-Hodgkin lymphoma (NHL), accounting for 20-30% percent of newly diagnosed B cell lymphoma every year [1–3]. DLBCL is treated with R-CHOP chemoimmunotherapy (rituximab, cyclophosphamide, doxorubicin, vincristine and prednisone), where rituximab targets CD20 on malignant B cells [4,5]. The substitution of vincristine with the anti-CD79b antibody drug conjugate polatuzumab vedotin can improve progression free survival over standard R-CHOP but it is still expected at least 40-45% of DLBCL will experience relapsed/refractory disease (rrDLBCL) [6]. rrDLBCL has dismal outcomes [7], with median progression free and overall survival (PFS/OS) rates below 1 year in most cases. Autologous stem cell transplant (ASCT) is a standard second-line treatment (2L) [8], however these responses are limited in patients with refractory disease, as long-term remission is achieved in less than 20% of patients achieving no response on R-CHOP [9,10]. Responses to chimeric antigen receptor T cell (CAR) therapies are extremely promising, as commercial CAR cells induce complete response rates in over 50% of patients and has led to improved PFS over ASCT in 2L [11–15]. Advances in the genetic classification of DLBCL has identified numerous subtypes of DLBCL beyond the traditional cell of origin split between germinal center B cell-like (GCB) and activated B cell-like (ABC) [16–18]. While this has provided new insights into the pathogenesis of DLBCL and potential novel therapeutic targets, patient care in a frontline setting has remained relatively stable. Most patients currently receive

the same clinical treatment course regardless of genetic subtype. Early identification of rrDLBCL may potentially improve outcomes by introducing alternative 2L or 3L treatments before patients become symptomatic from a high tumor burden, both risk factors for poor responses to cellular therapies [19–22].

Circulating tumor DNA (ctDNA) has become an important tool for assessing genomic alterations as patients progress through therapy [23,24]. In DLBCL, it has been shown to be prognostic at pretreatment levels as well as in response to R-CHOP as early as cycle 2 of therapy [25,26]. Analyzing ctDNA is particularly enticing due to the non-invasive method of sample collection (plasma) and the potential to capture the entire disease heterogeneity regardless of tumor site [27]. We designed our panel of DLBCL to confirm the use of ctDNA assessment in the frontline setting of DLBCL and to detect early rrDLBCL. We aimed to validate the prognostic value of ctDNA profiling in plasma samples taken over the course of therapy in 237 patients and to explore the mutational landscapes of rrDLBCL presented by refractory, early relapse, late relapse and patients in remission.

4.4: Materials and Methods

4.4.1: Patient Selection and Sample Collection

Patients diagnosed with high-grade B cell lymphoma morphology and provided informed consent were included in this analysis (n =237). This included *de novo* DLBCL (n=175), as well as DLBCL transformed from indolent lymphoma (n=47), high grade B cell lymphoma with concurrent MYC and BCL2 translocations (HGBL-DH) (n=8), T cell rich B cell lymphoma (n=2), primary mediastinal B cell lymphoma (PMBCL) (n=4), and plasmablastic lymphoma (PBL) (n=1). Patients were divided into different relapse groups based on the time from diagnosis to disease progression following 1L treatment as previously described by Hilton et al

[28]. This resulted in 4 groups based on response to 1L, regardless of sample timepoint: refractory (REFR, <9 months from diagnosis), early relapse (ER, 9-24 months), late relapse (LR, >24 months), and clinical responders (CR, >24 months with no relapse). Patient characteristics, pathology and treatment details are provided in Table 1. This project was approved by the research ethics board at the Jewish General Hospital in Montreal for acquisition of samples within our lymphoma bank (protocol #11-047) and for sequencing ctDNA samples (protocol #18-030).

Plasma (~2 ml) was collected as part of routine clinical care in EDTA coated tubes and frozen for subsequent use, within 4-8 hours of collection use between 2011 and 2022. Collection times were pre therapy, post cycle 1-2 of R-CHOP, end of R-CHOP treatment, and any subsequent relapses or treatments at relapse (Figure 1). Due to the heterogenous nature of our sample collection, samples were collected in 2 timeframes: a diagnostic cohort, consisting of samples taken from pre-treatment until post R-CHOP surveillance, and a relapse cohort, consisting of samples taken at relapse and through subsequent therapies. A total of 543 samples were collected and a total summary of the samples extracted for this study is provided in Table 2. 40 cases had sample spanning both cohorts and these cases were used to analyze the detection of ctDNA prior to clinical relapse. cell-free DNA (cfDNA) extraction and library preparation is described in the supplemental methods.

4.4.2: Targeted Panel Hybridization

cfDNA libraries underwent hybridization with a custom panel designed with Twist Biosciences following similar protocols to those done in the CAPP-Seq assay [23,24]. Our panel includes 194 genes (Table 3) that were selected due to their involvement in DLBCL as known drivers of disease, as well as genes used for subtyping and classification. Target enrichment

using Twist hybridization and wash kit (#105561) was done by pooling 8 samples at a time at 187.5 ng of library per sample. Samples were then dried using a vacuum concentrator with low heat. Hybrid capture was done with the pooled libraries and our custom panel for 16 hours, after which captured targets were isolated and enriched by PCR.

4.4.3: Targeted Sequencing and Variant Calling

Final hybridized samples were pooled at between 70 and 100 samples with unique indexes for sequencing on the NovaSeq6000 platform (Illumina) using 150bp paired-end (PE) reads. Reads were allocated to achieve a theoretical raw read depth of 1500X. Raw sequencing data was aligned against the human reference genome GRCh38 using BWA-MEM [29], after which unique molecular identifiers (UMIs) were processed using the fgbio toolkit (<https://github.com/fulcrum-genomics/fgbio>). Single nucleotide variants were called in matched tumor-normal mode using SAGE (<https://github.com/hartwigmedical/hmftools/tree/master/sage>) and custom post-filtering was applied to remove artifacts and low-quality variants (supplemental methods).

4.4.4: ctDNA Detection and Quantification

Detection of one or more somatic mutations after variant calling and filtering was the criteria for ctDNA positivity. ctDNA quantification was assessed following previously described methods by Kurtz et al [25]. To quantify the level of total ctDNA in samples, we used haploid genome equivalents per milliliter of plasma (hGE/mL). The average allele fraction of all somatic mutations in a sample was multiplied by the total cfDNA concentration of that sample. This number was represented as a log 10 value for our final measurement of Log hGE/mL. ctDNA levels were measured in our diagnostic cohort at diagnosis, after cycle 2 of R-CHOP, and end of R-CHOP treatment. In our relapse cohort, ctDNA was quantified at relapse after 1L treatment.

Log fold change between paired diagnosis and cycle 2 was used to measure changes in ctDNA in response to treatment. Samples with undetectable ctDNA after cycle 2 were assigned a log fold change of -6, a value outside the range producible in this assay.

4.5: Results

4.5.1: Cohort Statistics and Panel Performance

Clinical details of both cohorts are in Table 1 and the median follow up time for the diagnostic cohort and the relapse cohort were both 2.9 years. In the diagnostic cohort, median age of diagnosis was 69 years and the average IPI score was 2.9. 52% of cases were GCB subtype by Han's algorithm, 33% non-GCB, and 41% experienced relapse at some point during follow up. The relapse cohort had similar average IPI (2.9) and number of GCB cases (53%), but a lower median age of diagnosis of 63 years and an increase in non-GCB cases (38%). Our panel was successful in detecting ctDNA in 94/99 (95%) samples pretreatment and 34/46 (74%) of samples at relapse after 1L. Detection of ctDNA in pretreatment samples was achieved in 13/14 (93%) of REFR, 14/14 (100%) of ER, 5/5 (100%) of LR, and 60/63 (95%) of CR. Three additional samples pretreatment had detectable ctDNA but could not be assigned a relapse group due to deaths unrelated to DLBCL. At relapse, detection of ctDNA was 14/16 (88%) in REFR, 13/17 (76%) in ER, and 7/13 (54%) in LR. In patients with isolated CNS relapse, plasma ctDNA was detected in 2/6 (33%) cases.

4.5.2: Early Treatment ctDNA Dynamics Predict Refractory DLBCL

We first evaluated the prognostic value of our panel in the diagnostic cohort for whom pretreatment ctDNA was detectable (94 samples) by correlating ctDNA levels to IPI, clinical outcome, and response category. Levels of ctDNA correlated with IPI score, as IPI 4 (2.211 log hGE/mL) and 5 (2.805 log hGE/mL) had the highest average ctDNA levels (Figure 2A,

p=0.0148). There was a trend for ctDNA high samples to have a reduced disease specific progression free survival (p=0.0915, median PFS: 5.044) and overall survival (p=0.2188) when compared to ctDNA low cases (Figure S1A and B). However, the average ctDNA levels at diagnosis were significantly higher in patients with REFR disease (REFR=2.507 vs CR=1.953, p=0.0369). ctDNA level also correlated with progression in response to 1L as measured by PET/CT (Figure 2B, PD=2.536, PR=1.678, CR=1.966; p=0.0133).

Analyzing levels of ctDNA at cycle 2 and EOT, a decrease from pretreatment values and levels at EOT were significantly different across different outcome groups. The average levels of ctDNA were higher in the REFR/ER patients after C2 when compared to patients who achieved a CR with no subsequent relapse event (Figure 2C, p=0.0395). Most notably, detection of ctDNA at the end of treatment (EOT) was exclusive to patients with REFR or ER disease (Figure 2D, p=0.0010). This translated to inferior progression free survival (PFS) in patients with ctDNA positive samples after 1L therapy (Figure 2E, p=<0.0001, HR:19.25). The average log fold decrease in ctDNA from pretreatment to C2 was significantly lower in REFR/ER compared to CR patients (Figure 3A, p=0.0443) but this did not translate to a statistically significant difference in PFS (Figure 3B, p=0.0798). Overall, ctDNA dynamics before, during, and after treatment can predict REFR and ER patients in 1L settings.

4.5.3: Tracking Measurable Residual Disease

We next analyzed 24 cases with serial ctDNA sampling starting from diagnosis to relapse to identify ctDNA dynamics over time in REFR or ER DLBCL. Primary REFR patients display detectable disease while undergoing therapy, that stabilizes through relapse. Case 970 (Figure 4A), shows a REFR DLBCL that has detectable disease at cycle 2 of R-CHOP with a similar mutational profile as at diagnosis. The allele frequency of these mutations is maintained into

relapse and, while the patient had a reduction in the variant allele fraction (VAF) of these mutations after methotrexate for CNS relapse, the disease remained detectable until progression. Serial MRD tracking allows for the detection of disease in patients that initially respond to therapy, but later develop relapse, which could include both ER and LR cases. In case 2288 (Figure 4B), the patient achieved a CR to R-CHOP therapy, but we detected very low VAF mutations (1%) at the EOT. These were clearly detectable at 6 months and significantly expanded 3 months prior to relapse. Analysis of all surveillance cases revealed detection of ctDNA in 18/23 (78%) patients with a future relapse, ranging from 2-7 months prior to relapse. These cases outline the potential for ctDNA MRD surveillance in patients after R-CHOP therapy, which can detect disease as early as 7 months prior to clinical relapse, a significant time window where early clinical intervention could be taken to possibly improve the response to 2L or 3L therapy.

4.5.4: Mutational Analysis of Diagnosis vs. Relapse ctDNA

We applied a similar approach to study ctDNA dynamics at relapse timepoints. We observe a similar phenomenon where the levels of ctDNA were not different amongst relapse groups (i.e. REFR, ER, LR) but did correlate with IPI ($p=0.0156$), PFS ($p=0.0379$, median survival=1.536), and OS ($p=0.0205$, median survival=2.099) after 2L therapy (Figure S2). We next analyzed the mutation profiles detected at different time points and outcome groups to determine if these could add an additional layer of information that can enhance the prognostic value of ctDNA profiling, focusing on non-synonymous variants as these likely have a higher impact on disease biology. Top variant calls for all sample groups are available in Figure S4 (diagnosis). Overall, our cohort at diagnosis revealed a typical DLBCL mutational landscape with high mutational rates in known DLBCL drivers such as *TP53* (36%), *KMT2D* (32%) and

CREBBP (23%) (Figure 5A). Epigenetic regulators are highly represented at diagnosis in our cohort, including *EZH2*, *CREBBP* and *KMT2D*. Our diagnosis cohort is GCB rich, with 52% of cases being GCB vs non-GCB (33%) via Han's algorithm. This is reflected in our mutations as epigenetic dysfunction tends to be more prevalent in GCB DLBCL. GCB samples had increased mutational rates in *BCL2*, *MYC*, *KMT2D*, and *EZH2* (Figure S3A). Non-GCB cases followed a differential mutational pattern, with high prevalence of genes *B2M*, *NOTCH2*, *TNFAIP3* and *PIMI* (Figure S3B). *TP53* mutations were highly selective for GCB DLBCL ($p=0.0029$), with 51% of GCB DLBCL having these variants.

There were significant differences in the mutation pattern of *TP53* in patients achieving CR versus those who experience relapse. *TP53* mutations were mainly confined to DNA binding regions (Figure 5B). But on further inspection, mutations in the CR group were enriched in hotspots of the L2 and L3 loop of *TP53* (47.6%; p.G245S, p.R248W), whereas mutations in the relapse groups were enriched in loop sheet helix (LSH) motifs (codons 272-287) (44% vs 5% in CR, $p=0.0171$). This was consistent in mutated *TP53* at relapse, as LSH mutations remained but L2 mutations are no longer present. These results suggest that not all *TP53* mutations are associated with a negative outcome in DLBCL.

The mutations detected at the time of relapse reflect the patterns observed in prior rrDLBCL cohorts (Figure S5) [30,31]. *KMT2D*, *TP53*, and *CREBBP* were the most commonly mutated genes (Figure 5C). Other mutations of interest at relapse include genes affecting apoptosis and cell survival (*FAS*, *BCL2*). Statistical comparison of samples taken at diagnosis and relapse reveals several genes are enriched between these cohorts. Diagnostic DLBCL had prominent mutations in *ZNF608*, *DTX1*, *NOTCH2*, and *BCL7A*, with none of these genes being

detected at relapse (Figure 5D). rrDLBCL had near significant increases in the mutational prevalence of *DNMT3A* and *EP300* (Figure 5D, $p < 0.1$).

4.5.5: Genetic Landscape of Refractory, Early, and Late Relapse Groups

We then grouped diagnostic and relapse cohorts to determine the differences in the genes driving disease progression in REFR, ER, and LR groups. REFR samples had high rates of *TP53*, *BCL2*, *MYC*, *B2M*, *FAS* and *FAT4* mutations (Figure 6A). The appearance of *MYC* and *BCL2* is reminiscent of double-hit lymphomas, but these occurred as a result of SNVs and in refractory samples without *MYC* and *BCL2* translocations by FISH. In addition to *CREBBP*, its transcriptional partner *EP300* is well represented in REFR samples from the relapse cohort. There is also an increased presence of *KMT2D*, as well as *BTG1* mutations in samples after therapy in REFR disease. Groupwise comparison between all groups revealed that *MAP2K1* was significantly enriched in REFR DLBCL (Figure 6C, $p < 0.05$).

EP300 mutations are also supported in ER samples, which display similar mutational profiles to REFR cases (Figure 6B). While *BCL2* and *MYC* are prominently mutated in REFR cases at both diagnosis and relapse, they are more prominent in ER cases at relapse. ER and REFR DLBCL appear prone to alterations to extrinsic apoptosis via *FAS* and *B2M* (Figure 6B). ER cases in both cohorts have increased variants in *BCOR* as well as *CD83*, which was statistically enriched (Figure 6C). Pathway enrichment analysis revealed that REFR and ER shared similar dysfunction in genes related to *TP53* expression, apoptosis and the *TP53* modulated regulation of cell death (Figure S6A-B). REFR cases also were highly enriched in mutations affecting IL-13 and IL-4 signaling, notably in the JAK/STAT pathway (*STAT3* and *STAT6* mutations).

Although there are fewer cases, LR DLBCL displays a markedly different mutational profile than REFR/ER DLBCL, with rise in the presence of *EZH2* and *DNMT3A* variants, indicative of a more pronounced dysfunction to epigenetic regulation (Figure 6B). This was also reflected in pathway analysis in which the most significant pathways affected revolved around chromatin modification (Figure S6C). The mutational profiles of LR DLBCL are the most discordant between diagnosis and relapse of all relapse groups, sharing only 30% of genes between timepoints. Common mutations are seen in *KTM2D*, *CREBBP*, *EZH2*, *IRF8*. However, there are additional mutations in *BCL6*, *BCL10*, *FAT4* and *IGLL5*.

Lastly, CR samples show a much more diverse set of variants calls than relapsed cases. Their mutational profile is striking due to its prognostic implications, and it encompasses genes more associated with increased survival, which include *NOTCH2*, *TMEM30A*, *DTX1*, *BTG2*, and *TNFAIP3* (Figure 6C, $p < 0.05$). Our diagnostic cohort shows 50% of CR samples have mutations in one of these 5 genes (Figure S4D). *TNFAIP3* was significantly likely to be co-mutated with *DTX1*, while being mutually exclusive from *TP53*. Meanwhile, *BTG2* also was co-mutated with *DTX1*, and exclusive from *CREBBP* ($p < 0.05$). This translated to improvements in PFS in cases with mutated *TNFAIP3* and *BTG2*, indicating these genes may be highly prognostic for favorable outcomes (Figure 6D).

4.5.6: Evolution of DLBCL in Response to Immunotherapy

Our relapse cohort also has a large number of samples collected before, during, and after treatments with immunotherapy in the context of clinical trials in >2L (Table S2), most notably PD-1 inhibitors or bispecific T cell engagers (BiTE) targeting CD20 and CD3. PD-1 inhibitors are used for Hodgkin lymphoma and have poor response rates in DLBCL [32,33]. Therefore, we

sought to focus on whether key elements in the genotype of these cases could help identify mechanisms by which rrDLBCL may overcome these therapies.

Overall, we had 54 samples taken during therapy with anti CD20-CD3 BiTE and 24 samples during PD-1 therapy. 19/54 BiTE samples and 6/24 PD-1 samples were taken after the completion of therapy with the remaining being taken before treatment start or mid-therapy. Analysis of end of treatment samples in both groups revealed that they carried a high mutational burden in *KMT2D*, *TP53*, and *CREBBP* (Figure 7A). 25% of samples after BiTE therapy had mutations in *BCL2* and *DNMT3A*, a gene that has not been described in the context of resistance to immunotherapy in DLBCL. Another 2 samples carried mutations in *MS4AI*, the gene responsible for CD20 expression. This may represent the loss of the antigen required for BiTE therapy, which would be a clear indication of resistant malignant clones, but corresponding tissue to assess the expression of CD20 is not available in these cases. ctDNA detection was present in 83% of samples after the completion of BiTE regimens, and this corresponded with an inferior PFS after the start of therapy (Figure 7B, $p=0.0295$).

One of the most prominently mutated genes after PD-1 therapy was *BIRC6*, which is not commonly seen at diagnosis (<5%) but was mutated in 3/6 PD-1 samples. *BIRC6* is an inhibitor of apoptosis and its overexpression has been associated with aggressive disease course in solid cancer [34]. In the context of multiple relapsed DLBCL, *BIRC6* mutated cases may identify patients with highly resistant malignant clones. Patient 1470 underwent PD-1 therapy and after experiencing progressive disease, was found to have mutated *BIRC6*. Pyclone is a computational tool that infers clonality from serial sampling and can be used to study clonal dynamics in disease [35]. Pyclone analysis of this case reveals that *BIRC6* was part of the dominant malignant cluster (2), even before PD-1 targeted therapy (Figure 7C). This revealed a stable clonal

structure that persisted even after 3 cycles of PD-1 therapy. Although the patient had a partial response to PD-1 after finishing treatment, the *BIRC6* clone was still detectable and returned at an even higher cellular prevalence than prior to therapy start. With regards to ctDNA surveillance during immunotherapy, we have demonstrated its use as a prognostic tool at the end of treatment regardless of line of therapy, and the ability to monitor mutational changes after treatment resistance in multiple contexts.

4.6: Discussion

Using a novel custom panel targeting rrDLBCL, we confirmed that detection of ctDNA is more likely to occur in refractory patients during therapy. This is supported by increased levels of ctDNA before, during, and after treatment in REFR DLBCL. Our cohort provides a large number of longitudinally collected samples over a period of 10 years. As such, we are able to demonstrate the use of this panel over a range of clinical settings: frontline, relapse, and even in novel immunotherapies. Therefore, ctDNA quantification under this panel serves as a valuable tool in standard of care scenarios, but also in the context of >2L treatments or clinical trials. The use of ctDNA as a prognostic tool has becoming increasingly relevant in hematological malignancies. Multiple groups have confirmed this in the context of R-CHOP therapy, as evidenced by detection of ctDNA during therapy and particularly at the end of therapy [25,27,36,37]. We clearly identify cases of detectable disease by CAPP-Seq, when clinically these patients are considered disease free by imaging. Interestingly, 6/9 samples with detectable ctDNA at EOT were considered in CR by PET imaging, indicating an increased sensitivity to disease detection via ctDNA analysis. This has been supported by additional studies showing improved PFS in DLBCL that is ctDNA negative compared to disease free by PET/CT [38,39]. Our panel does not involve tumor informed sequencing, and is smaller in size than many others.

This highlights a potential ease of use in implementing ctDNA analysis in clinic, as more complex or individualized panel designs may not be necessary to identify high-risk patients prior to treatment. Moreover, this assay is completely non-invasive and provides a universal platform that can be applied to any patient, regardless of tumor biopsy availability. This implementation in 1L is confirmed by our high success rate at diagnosis, as 95% of samples had detectable ctDNA pretreatment. However, in the 2L setting, only 74% of samples had detectable ctDNA at relapse. Reduction in ctDNA detection performance at relapse was unexpected, but further analysis revealed that four of these cases were CNS disease and may need more sensitive detection of plasma ctDNA [40,41]. LR samples had the worst detection in relapse setting, indicating these samples may belong to less aggressive lymphomas and that our detection is preferential to REFR and ER DLBCL.

Our cohort largely reflects known variants in diagnostic DLBCL, however, the large number of *TP53* mutations in our cohort was surprising. The distribution of variants highlights how important the type of *TP53* mutation may be to establish its prognostic effect, as LSH mutations have been described previously as being associated with inferior prognosis in DLBCL, while L2 mutations are not [42–44]. LSH motifs are important for maintaining proper DNA binding in the major groove of TP53 and mutations in this region appear to be a driver of relapsed disease in our cohort occurring exclusively in patients with inferior PFS at diagnosis. That not all *TP53* mutations have equal prognostic effects is clinically relevant. Detection of mutations in the LSH domain may identify early treatment failure by ctDNA sequencing. As *TP53* mutations are associated with an inferior response to CART therapy [45], it would be important to determine if LSH domain mutants underline a disease biology that is inherently resistant to apoptosis even after exposure to CART or if they are associated with refractory

disease that is usually associated with a high tumor burden, in which early detection may improve responses to CART.

Mutational data surrounding REFR DLBCL is lacking because patients die before providing germline DNA and consent. We have provided important insights into the mutational landscape of REFR DLBCL and genes implicated in aggressive therapeutic resistance. REFR DLBCL was highly dependent on *BCL2* and *MYC* alterations, which may belong to the DHIT gene expression signature (also DZsig) in GCB DLBCL as these cases had no rearrangements of these genes [46,47]. *BTG1* was mostly mutated in REFR cases after R-CHOP, which has been associated with aggressive lymphoma and inferior outcomes [48,49]. There is also an apparent switch away from NOTCH2 pathway mutations in more resistant DLBCL, as these mutations disappear by relapse and are mostly confined to patients in CR. Notably, when comparing all samples, there is a preference for NOTCH1 signaling dysfunction in refractory cases (only a few mutations), while *NOTCH2* is preferentially mutated in cases who achieve remission. This seems to support the classification and survivability of N1 vs BN2 genetic subgroups of DLBCL, in which BN2 subgroups usually have favorable prognosis [16]. In fact, the most significant finding from our diagnostic cohort was the highly favorable mutations seen in the CR group. Mutations in *TNFAIP3*, *BTG2*, and *DTX1* are all components of BN2 classification, and should warrant further study as prognostic identifiers for responsive patients prior to treatment. *TNFAIP3* was also common in our non-GCB cases at diagnosis, potentially highlighting a favorable profile for the normally inferior outcomes associated with non-GCB cases.

Limitations of our study include limited starting material, as the plasma samples used in this study ranged from 0.5-1.5 mL in total volume. Other studies in plasma ctDNA have used up to 5 mL of plasma, already a limiting factor at this volume [50,51]. This severely limits our

starting number of genome copies used in each analysis, and subsequently limits our ability to detect ctDNA at very low allele fractions (<1%). However, the results of this study are very promising, because we easily detected ctDNA pre-treatment with very little plasma using blood collected in EDTA-coated tubes, which are routinely used in clinical laboratories. Importantly, it could detect early rrDLBCL, especially in REFR cases or ER before overt clinical relapse. Unfortunately, we were not able to use more sensitive methods for detection such as Phased-Seq [52]. Future panel design should include phased variant regions to increase detection of ctDNA, particularly in the context of MRD. Increased sensitivity is needed after treatment if a clinical decision is made based on MRD status. In surveillance monitoring, our panel was able to detect loss of MRD prior to disease relapse.

The emergence of *DNMT3A* and *BIRC6* mutations in the context of immunotherapy resistance is intriguing and hypothesis generating. *BIRC6* is a rarer mutation in DLBCL and may have profound impacts on malignant cell survival in the context of multiple therapies. It has been described in gray zone lymphomas with more DLBCL patterns and may be important for future immunotherapy studies [53]. These factors should be investigated further for use as prognostic markers to these therapies. Our study supports the use of ctDNA analysis in the context of clinical trials in order to study the clonal dynamics and genetics of therapeutic resistance.

Overall, we validate the use of ctDNA in both frontline and relapsed settings. Our panel provides numerous advantages to current workflows in ctDNA analysis, which include completely non-invasive disease monitoring without requiring tumor tissue and focuses on rrDLBCL detection. This work highlights the use of ctDNA in serial sample studies, by identifying chemotherapy resistance by increased levels of ctDNA by C2 of 1L therapy. We also reveal mutational profiles associated with REFR DLBCL (*BCL2*, *MYC*, *BTG1*, *EP300*,

MAP2K1). These may contribute to increased prognostic and actionable profiling when analyzed in a larger cohort of REFR DLBCL. Even in DLBCL responding to treatment, we also show the utility of ctDNA monitoring during routine clinical follow-up, where our panel detects disease as early as 7 months prior to clinical relapse and could potentially be used to influence treatment management decisions in the future.

4.7: Acknowledgements

We would like to acknowledge all the patients and their families who consented to participate in tissue biobanking at the Banque de cellules leucémiques du Québec (BCLQ) and the Jewish General Hospital (Montreal, QC).

4.8: Funding

This study was supported by funding from CIHR, CQDM, and Roche. Funding for tumor banking was provided from Incyte, Gilead and JGH foundation.

4.9: Authorship Contributions

Contribution: NAJ and RDM conceptualized the study; RNR and AA performed the experiments; RNR, CKR, and ER analyzed the data; EB provided clinical data; NAJ, RDM, DWS, and CS supervised the study and contributed to experimental design; RNR and NAJ wrote the original manuscript; all authors reviewed, edited, and approved the final manuscript.

4.10: Disclosure of Conflicts of Interest

CKR is currently employed by SAGA Diagnostics (Sweden). ER is currently employed by AbCellera (Vancouver, BC). NAJ reports consultancy for AbbVie, AstraZeneca, Incyte, Beigene, Roche, Gilead, Merck and BMS. CS reports consultancy for AbbVie, Bayer, and Seattle Genetics; research funds from Trillium Therapeutics, BMS, and Epizyme. DWS reports

consultancy for AbbVie, AstraZeneca, Incyte, and Janssen; research funds from Janssen and Roche/Genentech. All other authors have no conflicts of interest to disclose.

4.11: References

1. Canadian Cancer Statistics Advisory Committee in collaboration with the Canadian Cancer Society, S.C. and the P.H.A. of C. *Canadian Cancer Statistics 2023*; Toronto, ON, 2023;
2. Swerdlow, S.H.; Campo, E.; Pileri, S.A.; Harris, N.L.; Stein, H.; Siebert, R.; Advani, R.; Ghielmini, M.; Salles, G.A.; Zelenetz, A.D.; et al. The 2016 Revision of the World Health Organization Classification of Lymphoid Neoplasms. *Blood* **2016**, *127*, 2375–2390, doi:10.1182/blood-2016-01-643569.
3. Alaggio, R.; Amador, C.; Anagnostopoulos, I.; Attygalle, A.D.; Araujo, I.B. de O.; Berti, E.; Bhagat, G.; Borges, A.M.; Boyer, D.; Calaminici, M.; et al. The 5th Edition of the World Health Organization Classification of Haematolymphoid Tumours: Lymphoid Neoplasms. *Leukemia* **2022**, *36*, 1720–1748, doi:10.1038/s41375-022-01620-2.
4. Coiffier, B.; Lepage, E.; Brière, J.; Herbrecht, R.; Tilly, H.; Bouabdallah, R.; Morel, P.; Van Den Neste, E.; Salles, G.; Gaulard, P.; et al. CHOP Chemotherapy plus Rituximab Compared with CHOP Alone in Elderly Patients with Diffuse Large-B-Cell Lymphoma. *N. Engl. J. Med.* **2002**, *346*, 235–242, doi:10.1056/NEJMoa011795.
5. Roschewski, M.; Staudt, L.M.; Wilson, W.H. Diffuse Large B-Cell Lymphoma - Treatment Approaches in the Molecular Era. *Nat. Rev. Clin. Oncol.* **2014**, *11*, 12–23, doi:10.1038/nrclinonc.2013.197.
6. Tilly, H.; Morschhauser, F.; Sehn, L.H.; Friedberg, J.W.; Trněný, M.; Sharman, J.P.;

- Herbaux, C.; Burke, J.M.; Matasar, M.; Rai, S.; et al. Polatuzumab Vedotin in Previously Untreated Diffuse Large B-Cell Lymphoma. *N. Engl. J. Med.* **2022**, *386*, 351–363, doi:10.1056/nejmoa2115304.
7. Crump, M.; Neelapu, S.S.; Farooq, U.; Van Den Neste, E.; Kuruvilla, J.; Westin, J.; Link, B.K.; Hay, A.; Cerhan, J.R.; Zhu, L.; et al. Outcomes in Refractory Diffuse Large B-Cell Lymphoma: Results from the International SCHOLAR-1 Study. *Blood* **2017**, *130*, 1800–1808, doi:10.1182/blood-2017-03-769620.
 8. Crump, M.; Kuruvilla, J.; Couban, S.; MacDonald, D.A.; Kukreti, V.; Kouroukis, C.T.; Rubinger, M.; Buckstein, R.; Imrie, K.R.; Federico, M.; et al. Randomized Comparison of Gemcitabine, Dexamethasone, and Cisplatin Versus Dexamethasone, Cytarabine, and Cisplatin Chemotherapy Before Autologous Stem-Cell Transplantation for Relapsed and Refractory Aggressive Lymphomas: NCIC-CTG LY.12. *J. Clin. Oncol.* **2014**, *32*, 3490–3496, doi:10.1200/JCO.2013.53.9593.
 9. Vardhana, S.A.; Sauter, C.S.; Matasar, M.J.; Zelenetz, A.D.; Galasso, N.; Woo, K.M.; Zhang, Z.; Moskowitz, C.H. Outcomes of Primary Refractory Diffuse Large B-Cell Lymphoma (DLBCL) Treated with Salvage Chemotherapy and Intention to Transplant in the Rituximab Era. *Br. J. Haematol.* **2017**, *176*, 591–599, doi:https://doi.org/10.1111/bjh.14453.
 10. Nagle, S.J.; Woo, K.; Schuster, S.J.; Nasta, S.D.; Stadtmauer, E.; Mick, R.; Svoboda, J. Outcomes of Patients with Relapsed/Refractory Diffuse Large B-Cell Lymphoma with Progression of Lymphoma after Autologous Stem Cell Transplantation in the Rituximab Era. *Am. J. Hematol.* **2013**, *88*, 890–894, doi:https://doi.org/10.1002/ajh.23524.

11. Schuster, S.J.; Bishop, M.R.; Tam, C.S.; Waller, E.K.; Borchmann, P.; McGuirk, J.P.; Jäger, U.; Jaglowski, S.; Andreadis, C.; Westin, J.R.; et al. Tisagenlecleucel in Adult Relapsed or Refractory Diffuse Large B-Cell Lymphoma. *N. Engl. J. Med.* **2019**, *380*, 45–56, doi:10.1056/nejmoa1804980.
12. Abramson, J.S.; Palomba, M.L.; Gordon, L.I.; Lunning, M.A.; Wang, M.; Arnason, J.; Mehta, A.; Purev, E.; Maloney, D.G.; Andreadis, C.; et al. Lisocabtagene Maraleucel for Patients with Relapsed or Refractory Large B-Cell Lymphomas (TRANSCEND NHL 001): A Multicentre Seamless Design Study. *Lancet* **2020**, *396*, 839–852, doi:10.1016/S0140-6736(20)31366-0.
13. Kamdar, M.; Solomon, S.R.; Arnason, J.; Johnston, P.B.; Glass, B.; Bachanova, V.; Ibrahimi, S.; Mielke, S.; Mutsaers, P.; Hernandez-Ilizaliturri, F.; et al. Lisocabtagene Maraleucel versus Standard of Care with Salvage Chemotherapy Followed by Autologous Stem Cell Transplantation as Second-Line Treatment in Patients with Relapsed or Refractory Large B-Cell Lymphoma (TRANSFORM): Results from an Interim Analys. *Lancet (London, England)* **2022**, *399*, 2294–2308, doi:10.1016/S0140-6736(22)00662-6.
14. Locke, F.L.; Ghobadi, A.; Jacobson, C.A.; Miklos, D.B.; Lekakis, L.J.; Oluwole, O.O.; Lin, Y.; Braunschweig, I.; Hill, B.T.; Timmerman, J.M.; et al. Long-Term Safety and Activity of Axicabtagene Ciloleucel in Refractory Large B-Cell Lymphoma (ZUMA-1): A Single-Arm, Multicentre, Phase 1–2 Trial. *Lancet Oncol.* **2019**, *20*, 31–42, doi:10.1016/S1470-2045(18)30864-7.
15. Locke, F.L.; Miklos, D.B.; Jacobson, C.A.; Perales, M.-A.; Kersten, M.-J.; Oluwole, O.O.;

- Ghobadi, A.; Rapoport, A.P.; McGuirk, J.; Pagel, J.M.; et al. Axicabtagene Ciloleucel as Second-Line Therapy for Large B-Cell Lymphoma. *N. Engl. J. Med.* **2022**, *386*, 640–654, doi:10.1056/nejmoa2116133.
16. Wright, G.W.; Huang, D.W.; Phelan, J.D.; Coulibaly, Z.A.; Roulland, S.; Young, R.M.; Wang, J.Q.; Schmitz, R.; Morin, R.D.; Tang, J.; et al. A Probabilistic Classification Tool for Genetic Subtypes of Diffuse Large B Cell Lymphoma with Therapeutic Implications. *Cancer Cell* **2020**, *37*, 551-568.e14, doi:10.1016/j.ccell.2020.03.015.
17. Chapuy, B.; Stewart, C.; Dunford, A.J.; Kim, J.; Kamburov, A.; Redd, R.A.; Lawrence, M.S.; Roemer, M.G.M.; Li, A.J.; Ziepert, M.; et al. Molecular Subtypes of Diffuse Large B Cell Lymphoma Are Associated with Distinct Pathogenic Mechanisms and Outcomes. *Nat. Med.* **2018**, *24*, 679–690, doi:10.1038/s41591-018-0016-8.
18. Schmitz, R.; Wright, G.W.; Huang, D.W.; Johnson, C.A.; Phelan, J.D.; Wang, J.Q.; Roulland, S.; Kasbekar, M.; Young, R.M.; Shaffer, A.L.; et al. Genetics and Pathogenesis of Diffuse Large B-Cell Lymphoma. *N. Engl. J. Med.* **2018**, *378*, 1396–1407, doi:10.1056/NEJMoa1801445.
19. Caballero, A.C.; Escribà-Garcia, L.; Alvarez-Fernández, C.; Briones, J. CAR T-Cell Therapy Predictive Response Markers in Diffuse Large B-Cell Lymphoma and Therapeutic Options After CART19 Failure. *Front. Immunol.* **2022**, *13*, 1–19, doi:10.3389/fimmu.2022.904497.
20. Cappell, K.M.; Kochenderfer, J.N. Long-Term Outcomes Following CAR T Cell Therapy: What We Know so Far. *Nat. Rev. Clin. Oncol.* **2023**, *20*, 359–371, doi:10.1038/s41571-023-00754-1.

21. Bishop, M.R.; Maziarz, R.T.; Waller, E.K.; Jäger, U.; Westin, J.R.; McGuirk, J.P.; Fleury, I.; Holte, H.; Borchmann, P.; del Corral, C.; et al. Tisagenlecleucel in Relapsed/Refractory Diffuse Large B-Cell Lymphoma Patients without Measurable Disease at Infusion. *Blood Adv.* **2019**, *3*, 2230–2236, doi:10.1182/bloodadvances.2019000151.
22. Wudhikarn, K.; Tomas, A.A.; Flynn, J.R.; Devlin, S.M.; Brower, J.; Bachanova, V.; Nastoupil, L.J.; McGuirk, J.P.; Maziarz, R.T.; Oluwole, O.O.; et al. Low Toxicity and Excellent Outcomes in Patients with DLBCL without Residual Lymphoma at the Time of CD19 CAR T-Cell Therapy. *Blood Adv.* **2023**, *7*, 3192–3198, doi:10.1182/bloodadvances.2022008294.
23. Newman, A.M.; Bratman, S. V.; To, J.; Wynne, J.F.; Eclov, N.C.W.; Modlin, L.A.; Liu, C.L.; Neal, J.W.; Wakelee, H.A.; Merritt, R.E.; et al. An Ultrasensitive Method for Quantitating Circulating Tumor DNA with Broad Patient Coverage. *Nat. Med.* **2014**, *20*, 548–554, doi:10.1038/nm.3519.
24. Newman, A.M.; Lovejoy, A.F.; Klass, D.M.; Kurtz, D.M.; Chabon, J.J.; Scherer, F.; Stehr, H.; Liu, C.L.; Bratman, S. V.; Say, C.; et al. Integrated Digital Error Suppression for Improved Detection of Circulating Tumor DNA. *Nat. Biotechnol.* **2016**, *34*, 547–555, doi:10.1038/nbt.3520.
25. Kurtz, D.M.; Scherer, F.; Jin, M.C.; Soo, J.; Craig, A.F.M.; Esfahani, M.S.; Chabon, J.J.; Stehr, H.; Liu, C.L.; Tibshirani, R.; et al. Circulating Tumor DNA Measurements as Early Outcome Predictors in Diffuse Large B-Cell Lymphoma. *J. Clin. Oncol.* **2018**, *36*, 2845–2853, doi:10.1200/JCO.2018.78.5246.
26. Sidaway, P. CtDNA Predicts Outcomes in DLBCL. *Nat. Rev. Clin. Oncol.* **2018**, *15*, 655.

27. Meriranta, L.; Alkodsı, A.; Pasanen, A.; Lepistö, M.; Mapar, P.; Blaker, Y.N.; Jørgensen, J.; Karjalainen-Lindsberg, M.-L.; Fiskvik, I.; Mikalsen, L.T.G.; et al. Molecular Features Encoded in the CtDNA Reveal Heterogeneity and Predict Outcome in High-Risk Aggressive B-Cell Lymphoma. *Blood* **2022**, *139*, 1863–1877, doi:10.1182/blood.2021012852.
28. Hilton, L.K.; Ngu, H.S.; Collinge, B.; Dreval, K.; Ben-Neriah, S.; Rushton, C.K.; Wong, J.C.H.; Cruz, M.; Roth, A.; Boyle, M.; et al. Relapse Timing Is Associated With Distinct Evolutionary Dynamics in Diffuse Large B-Cell Lymphoma. *J. Clin. Oncol. Off. J. Am. Soc. Clin. Oncol.* **2023**, *41*, 4164–4177, doi:10.1200/JCO.23.00570.
29. Li, H.; Durbin, R. Fast and Accurate Short Read Alignment with Burrows-Wheeler Transform. *Bioinformatics* **2009**, *25*, 1754–1760, doi:10.1093/bioinformatics/btp324.
30. Morin, R.D.; Assouline, S.; Alcaide, M.; Mohajeri, A.; Johnston, R.L.; Chong, L.; Grewal, J.; Yu, S.; Fornika, D.; Bushell, K.; et al. Genetic Landscapes of Relapsed and Refractory Diffuse Large B-Cell Lymphomas. *Clin. Cancer Res.* **2016**, *22*, 2290–2300, doi:10.1158/1078-0432.CCR-15-2123.
31. Rushton, C.K.; Arthur, S.E.; Alcaide, M.; Cheung, M.; Jiang, A.; Coyle, K.M.; Cleary, K.L.S.; Thomas, N.; Hilton, L.K.; Michaud, N.; et al. Genetic and Evolutionary Patterns of Treatment Resistance in Relapsed B-Cell Lymphoma. *Blood Adv.* **2020**, *4*, 2886–2898, doi:10.1182/bloodadvances.2020001696.
32. Ansell, S.M.; Lesokhin, A.M.; Borrello, I.; Halwani, A.; Scott, E.C.; Gutierrez, M.; Schuster, S.J.; Millenson, M.M.; Cattry, D.; Freeman, G.J.; et al. PD-1 Blockade with Nivolumab in Relapsed or Refractory Hodgkin’s Lymphoma. *N. Engl. J. Med.* **2015**, *372*,

- 311–319, doi:10.1056/nejmoa1411087.
33. Ansell, S.M.; Minnema, M.C.; Johnson, P.; Timmerman, J.M.; Armand, P.; Shipp, M.A.; Rodig, S.J.; Ligon, A.H.; Roemer, M.G.M.; Reddy, N.; et al. Nivolumab for Relapsed/Refractory Diffuse Large B-Cell Lymphoma in Patients Ineligible for or Having Failed Autologous Transplantation: A Single-Arm, Phase II Study. *J. Clin. Oncol.* **2019**, *37*, 481–489, doi:10.1200/JCO.18.00766.
 34. Saleem, M.; Qadir, M.I.; Perveen, N.; Ahmad, B.; Saleem, U.; Irshad, T.; Ahmad, B. Inhibitors of Apoptotic Proteins: New Targets for Anticancer Therapy. *Chem. Biol. Drug Des.* **2013**, *82*, 243–251, doi:https://doi.org/10.1111/cbdd.12176.
 35. Roth, A.; Khattra, J.; Yap, D.; Wan, A.; Laks, E.; Biele, J.; Ha, G.; Aparicio, S.; Bouchard-Côté, A.; Shah, S.P. PyClone: Statistical Inference of Clonal Population Structure in Cancer. *Nat. Methods* **2014**, *11*, 396–398, doi:10.1038/nmeth.2883.
 36. Kurtz, D.M.; Esfahani, M.S.; Scherer, F.; Soo, J.; Jin, M.C.; Liu, C.L.; Newman, A.M.; Dührsen, U.; Hüttmann, A.; Casasnovas, O.; et al. Dynamic Risk Profiling Using Serial Tumor Biomarkers for Personalized Outcome Prediction. *Cell* **2019**, *178*, 699-713.e19, doi:10.1016/j.cell.2019.06.011.
 37. Alig, S.; Macaulay, C.W.; Kurtz, D.M.; Dührsen, U.; Hüttmann, A.; Schmitz, C.; Jin, M.C.; Sworder, B.J.; Garofalo, A.; Shahrokh Esfahani, M.; et al. Short Diagnosis-to-Treatment Interval Is Associated With Higher Circulating Tumor DNA Levels in Diffuse Large B-Cell Lymphoma. *J. Clin. Oncol. Off. J. Am. Soc. Clin. Oncol.* **2021**, *39*, 2605–2616, doi:10.1200/JCO.20.02573.
 38. Herrera, A.F.; Tracy, S.; Sehn, L.H.; Jardin, F.; Lenz, G.; Trneny, M.; Salles, G.A.;

- Flowers, C.; Tilly, H.; Sharman, J.P.; et al. Circulating Tumor DNA (CtDNA) Status and Clinical Outcomes in Patients (Pts) with Previously Untreated Diffuse Large B-Cell Lymphoma (DLBCL) in the POLARIX Study. *J. Clin. Oncol.* **2023**, *41*, 7523, doi:10.1200/JCO.2023.41.16_suppl.7523.
39. Roschewski, M.; Lindenberg, L.; Mena, E.; Lakhotia, R.; Melani, C.; Steinberg, S.M.; Schultz, A.; Hogan, G.; Chabon, J.J.; Close, S.; et al. End-of-Treatment Response Assessment after Frontline Therapy for Aggressive B-Cell Lymphoma: Landmark Comparison of a Singular PET/CT Scan Versus Ultrasensitive Circulating Tumor DNA. *Blood* **2023**, *142*, 192, doi:https://doi.org/10.1182/blood-2023-180007.
40. Mutter, J.A.; Alig, S.K.; Esfahani, M.S.; Lauer, E.M.; Mitschke, J.; Kurtz, D.M.; Kühn, J.; Bleul, S.; Olsen, M.; Liu, C.L.; et al. Circulating Tumor DNA Profiling for Detection, Risk Stratification, and Classification of Brain Lymphomas. *J. Clin. Oncol. Off. J. Am. Soc. Clin. Oncol.* **2023**, *41*, 1684–1694, doi:10.1200/JCO.22.00826.
41. Heger, J.-M.; Mattlener, J.; Schneider, J.; Gödel, P.; Sieg, N.; Ullrich, F.; Lewis, R.; Bucaciuc-Mracica, T.; Schwarz, R.F.; Rueß, D.; et al. Entirely Noninvasive Outcome Prediction in Central Nervous System Lymphomas Using Circulating Tumor DNA. *Blood* **2024**, *143*, 522–534, doi:10.1182/blood.2023022020.
42. Xu-Monette, Z.Y.; Wu, L.; Visco, C.; Tai, Y.C.; Tzankov, A.; Liu, W.; Montes-Moreno, S.; Dybkær, K.; Chiu, A.; Orazi, A.; et al. Mutational Profile and Prognostic Significance of TP53 in Diffuse Large B-Cell Lymphoma Patients Treated with R-CHOP: Report from an International DLBCL Rituximab-CHOP Consortium Program Study. *Blood* **2012**, *120*, 3986–3996, doi:10.1182/blood-2012-05-433334.

43. Young, K.H.; Leroy, K.; Møller, M.B.; Colleoni, G.W.B.; Sánchez-Beato, M.; Kerbaudy, F.R.; Haioun, C.; Eickhoff, J.C.; Young, A.H.; Gaulard, P.; et al. Structural Profiles of TP53 Gene Mutations Predict Clinical Outcome in Diffuse Large B-Cell Lymphoma: An International Collaborative Study. *Blood* **2008**, *112*, 3088–3098, doi:10.1182/blood-2008-01-129783.
44. Peroja, P.; Pedersen, M.; Mantere, T.; Nørgaard, P.; Peltonen, J.; Haapasaari, K.M.; Böhm, J.; Jantunen, E.; Turpeenniemi-Hujanen, T.; Rapakko, K.; et al. Mutation of TP53, Translocation Analysis and Immunohistochemical Expression of MYC, BCL-2 and BCL-6 in Patients with DLBCL Treated with R-CHOP. *Sci. Rep.* **2018**, *8*, 1–9, doi:10.1038/s41598-018-33230-3.
45. Shouval, R.; Alarcon Tomas, A.; Fein, J.A.; Flynn, J.R.; Markovits, E.; Mayer, S.; Olaide Afuye, A.; Alperovich, A.; Anagnostou, T.; Besser, M.J.; et al. Impact of TP53 Genomic Alterations in Large B-Cell Lymphoma Treated With CD19-Chimeric Antigen Receptor T-Cell Therapy. *J. Clin. Oncol. Off. J. Am. Soc. Clin. Oncol.* **2022**, *40*, 369–381, doi:10.1200/JCO.21.02143.
46. Alduaij, W.; Collinge, B.; Ben-Neriah, S.; Jiang, A.; Hilton, L.K.; Boyle, M.; Meissner, B.; Chong, L.; Miyata-Takata, T.; Slack, G.W.; et al. Molecular Determinants of Clinical Outcomes in a Real-World Diffuse Large B-Cell Lymphoma Population. *Blood* **2023**, *141*, 2493–2507, doi:10.1182/blood.2022018248.
47. Ennishi, D.; Jiang, A.; Boyle, M.; Collinge, B.; Grande, B.M.; Ben-Neriah, S.; Rushton, C.; Tang, J.; Thomas, N.; Slack, G.W.; et al. Double-Hit Gene Expression Signature Defines a Distinct Subgroup of Germinal Center B-Cell-Like Diffuse Large B-Cell

- Lymphoma. *J. Clin. Oncol. Off. J. Am. Soc. Clin. Oncol.* **2019**, *37*, 190–201, doi:10.1200/JCO.18.01583.
48. Mlynarczyk, C.; Teater, M.; Pae, J.; Chin, C.R.; Wang, L.; Arulraj, T.; Barisic, D.; Papin, A.; Hoehn, K.B.; Kots, E.; et al. BTG1 Mutation Yields Supercompetitive B Cells Primed for Malignant Transformation. *Science (80-.)*. **2024**, *379*, eabj7412, doi:10.1126/science.abj7412.
49. Delage, L.; Lambert, M.; Bardel, É.; Kundlacz, C.; Chartoire, D.; Conchon, A.; Peugnet, A.-L.; Gorka, L.; Auberger, P.; Jacquet, A.; et al. BTG1 Inactivation Drives Lymphomagenesis and Promotes Lymphoma Dissemination through Activation of BCAR1. *Blood* **2023**, *141*, 1209–1220, doi:10.1182/blood.2022016943.
50. Keller, L.; Belloum, Y.; Wikman, H.; Pantel, K. Clinical Relevance of Blood-Based CtDNA Analysis: Mutation Detection and Beyond. *Br. J. Cancer* **2021**, *124*, 345–358, doi:10.1038/s41416-020-01047-5.
51. Abbosh, C.; Birkbak, N.J.; Swanton, C. Early Stage NSCLC — Challenges to Implementing CtDNA-Based Screening and MRD Detection. *Nat. Rev. Clin. Oncol.* **2018**, *15*, 577–586, doi:10.1038/s41571-018-0058-3.
52. Kurtz, D.M.; Soo, J.; Co Ting Keh, L.; Alig, S.; Chabon, J.J.; Sworder, B.J.; Schultz, A.; Jin, M.C.; Scherer, F.; Garofalo, A.; et al. Enhanced Detection of Minimal Residual Disease by Targeted Sequencing of Phased Variants in Circulating Tumor DNA. *Nat. Biotechnol.* **2021**, *39*, 1537–1547, doi:10.1038/s41587-021-00981-w.
53. Sarkozy, C.; Hung, S.S.; Chavez, E.A.; Duns, G.; Takata, K.; Chong, L.C.; Aoki, T.; Jiang, A.; Miyata-Takata, T.; Telenius, A.; et al. Mutational Landscape of Gray Zone

- Lymphoma. *Blood* **2021**, *137*, 1765–1776, doi:10.1182/blood.2020007507.
54. McLaren, W.; Gil, L.; Hunt, S.E.; Riat, H.S.; Ritchie, G.R.S.; Thormann, A.; Flicek, P.; Cunningham, F. The Ensembl Variant Effect Predictor. *Genome Biol.* **2016**, *17*, 122, doi:10.1186/s13059-016-0974-4.
55. Mayakonda, A.; Lin, D.-C.; Assenov, Y.; Plass, C.; Koeffler, H.P. Maftools: Efficient and Comprehensive Analysis of Somatic Variants in Cancer. *Genome Res.* **2018**, *28*, 1747–1756, doi:10.1101/gr.239244.118.
56. Zhou, X.; Edmonson, M.N.; Wilkinson, M.R.; Patel, A.; Wu, G.; Liu, Y.; Li, Y.; Zhang, Z.; Rusch, M.C.; Parker, M.; et al. Exploring Genomic Alteration in Pediatric Cancer Using ProteinPaint. *Nat. Genet.* 2016, *48*, 4–6.
57. Reimand, J.; Isserlin, R.; Voisin, V.; Kucera, M.; Tannus-Lopes, C.; Rostamianfar, A.; Wadi, L.; Meyer, M.; Wong, J.; Xu, C.; et al. Pathway Enrichment Analysis and Visualization of Omics Data Using g:Profiler, GSEA, Cytoscape and EnrichmentMap. *Nat. Protoc.* **2019**, *14*, 482–517, doi:10.1038/s41596-018-0103-9.

4.11: Tables

Table 4.1: Clinical Characteristics of Cohorts

Clinical Variable	All Patients (n=237)	%	Diagnosis Cohort (n=170)	%	Relapse Cohort (n=107)	%
Median age, years	67		69		63	
Diagnosis						
DLBCL	175	73.8	130	76.5	69	64.5
DLBCL transformed from indolent lymphoma	33	13.9	21	12.4	21	19.6
Composite DLBCL	14	5.9	10	5.9	9	8.4
PMBCL	4	1.7	3	1.8	1	0.9
TCRBCL	2	0.8	1	0.6	2	1.9
PBL	1	0.4	0	0	1	0.9
HGBL-DH (<i>BCL2/BCL6</i> and <i>MYC</i>)	8	3.4	5	2.9	4	3.7
Stage						
I	17	7.2	15	8.8	3	2.8
II	27	11.4	21	12.4	10	9.3
III	32	13.5	18	10.6	19	17.8
IV	148	62.4	109	64.1	67	62.6
Unknown	13	5.5	7	4.1	8	7.5
IPI						
0-1	28	11.8	21	12.4	8	7.5
2	46	19.4	35	20.6	19	17.8
3	59	24.9	44	25.9	31	29.0
4-5	70	29.5	58	34.1	25	23.4
Unknown	34	14.3	12	7.1	24	22.4
Molecular Features						
GCB	127	53.6	89	52.4	57	53.3
Non-GCB	79	33.3	56	32.9	41	38.3
Unknown	31	13.1	25	14.7	9	8.4
Double hit (<i>BCL2/BCL6</i> and <i>MYC</i>)	8	3.4	5	2.9	4	3.7
Relapse Group						
Refractory (relapse <9 months after diagnosis)	58	24.5	25	14.7	44	41.1
Early Relapse (9-24 months)	49	20.7	31	18.2	39	36.4
Late Relapse (>24 months)	29	12.2	13	7.6	24	22.4
Clinical Remission (CR > 24 months)	96	40.5	96	56.5	0	0
Unknown	5	2.1	5	2.9	0	0

Table 4.1: Clinical variables for all patients shown at diagnosis prior to treatment. 40 patients have samples that span both diagnosis and relapse cohorts. Unknown patients under relapse groups could not be assigned to a group

due to death unrelated to DLBCL. Abbreviations: DLBCL, diffuse large B cell lymphoma; PMBCL, primary mediastinal B cell lymphoma; TCRBCL, T cell rich B cell lymphoma; PBL, plasmablastic lymphoma; HGBL-DH, high-grade B cell lymphoma-double hit; IPI, international prognostic index; GCB, germinal center B cell-like; CR, complete response to R-CHOP.

Table 4.2: Sample Collection Characteristics

R-CHOP Therapy	Number	Cohort
DLBCL Diagnosis	99	Diagnosis
Mid R-CHOP (C1-5)	155	Diagnosis
End of R-CHOP	32	Diagnosis
Post R-CHOP Surveillance	38	Diagnosis
Post R-CHOP Relapse	46	Relapse
Salvage Therapy		Relapse
R-based Salvage Chemotherapy	39	Relapse
Radiation	3	Relapse
BR	3	Relapse
Transplant and CART Therapy		Relapse
ASCT	11	Relapse
CART	2	Relapse
Alternative Therapy		Relapse
CNS (HDMTX)	6	Relapse
BiTE (anti CD3 and CD20)	54	Relapse
PD-1 Inhibitor	24	Relapse
EZH2 Inhibitor	4	Relapse
Pola-BR	16	Relapse
Syk Inhibitor	8	Relapse
Other	3	Relapse

Table 4.2: Distribution of plasma samples collected and during which treatment regimens. Other samples include dasatinib (kinase inhibitor), IRD, and venetoclax (BCL2 inhibitor). Abbreviations: R-CHOP, rituximab-cyclophosphamide-doxorubicin-vincristine-prednisone; DLBCL, diffuse large B cell lymphoma; R-GDP, rituximab-gemcitabine-dexamethasone-cisplatin; R-ESHAP, rituximab-etoposide-methylprednisolone-cytarabine-cisplatin; R-EPOCH, rituximab-etoposide-doxorubicin-vincristine-prednisone-cyclophosphamide; R-GEMOX, rituximab-gemcitabine-oxaliplatin; IRD, ixazomib-lenalidomide-dexamethasone; BR, bendamustine-rituximab; CNS, central nervous system; HDMTX, high-dose methotrexate; BiTE, bispecific T cell engager; Pola-BR, polatuzamab vedotin-bendamustine-rituximab; Syk, spleen tyrosine kinase.

Table 4.3: CAPP-Seq Panel for rrDLBCL

rrDLBCL Gene Panel								
ACTB	C10orf137	DTX1	GNAI2	IRF4	MYC	PPP1R9B	SPEN	TRAF2
ACTG1	CARD11	DUSP2	GRHRP	IRF8	MYD88	PRDM1	SPIB	TRIP12
ALDH18A1	CCND1	EBF1	HIST1H1C	ITPKB	MYO1E	PRKCB	STAT3	TRRAP
ARID1A	CCND3	EDRF1	HIST1H1D	JAK3	NCOA3	PRRC2C	STAT5B	TSPOAP1
ARID5B	CD19	EIF4A2	HIST1H1E	JUNB	NEAT1	PTEN	STAT6	UBE2A
ATM	CD58	EP300	HIST1H2BK	KLF2	NFKB1	PTPN1	ST6GAL1	UBR5
BACH	CD70	EPB41	HLA-A	KLHL14	NFKBIA	RAC2	TAP1	USP7
B2M	CD74	ETS1	HLA-B	KLHL21	NFKBIE	RB1	TBL1XR1	VMP1
BCL10	CD79B	ETV6	HLA-C	KLHL42	NFKBIZ	REL	TCF3	WDR24
BCL11A	CD83	EZH2	HLA-DMB	KLHL6	NKRF	RFTN1	TCL1A	WEE1
BCL2	CDKN2A	FAS	HNRNPD	KMT2D	NOL9	RHOA	TCTN1	XBP1
BCL2L1	CHD2	FAT4	HNRNPU	LCOR	NOTCH1	RHOH	TET2	XPO1
BCL6	CHST2	FBXO11	HVCN1	LPP	NOTCH2	RRAGC	TMEM30A	ZC3H12A
BCL7A	CIITA	FCGR2A	ID3	LRMP	OSBPL10	S1PR2	TMSB4X	ZC3H12D
BCOR	CLTC	FCGR2B	IDH2	LTB	PAX5	SEC24C	TNFAIP3	ZCCHC7
BIRC3	CREBBP	FCGR2C	IGLL5	MALAT1	P2RY8	SERPINA9	TNFRSF14	ZFP36L1
BIRC6	CTA2	FCRLA	IKBKB	MAP2K1	PABPC1	SETD1B	TNRC18	ZNF516
BRAF	CXCR4	FOXC1	IL10RA	MED16	PIM1	SETD2	TOX	ZNF608
BTG1	DAZAP1	FOXO1	IL16	MEF2B	PIM2	SF3B1	TP53	
BTG2	DDX3X	FOXP1	IL4R	MIR17HG	PLCG2	SGK1	TP53BP1	
BTK	DNMT3A	GNA12	ING1	MPEG1	POT1	SLC1A5	TP63	
C10orf12	DOCK8	GNA13	IRF2BP2	MS4A1	POU2AF1	SOCS1	TP73	

Table 4.3: List of all genes included in the CAPP-Seq panel used for targeted sequencing and subsequent analysis of ctDNA content.

4.12: Figure Legends

Figure 4.1: Overview of Sample Collection and Cohort Development. Plasma samples were collected for patients in a serial fashion starting at either diagnosis or relapse. The retrospective samples were heterogenous, and therefore we separated the samples into 2 cohorts to help adjust for sampling bias. This included a diagnostic cohort, with samples taken pretreatment, during frontline treatment, and after treatment was completed. The relapse cohort consisted of samples taken at relapse and then during/after subsequent therapies.

Figure 4.2: ctDNA Quantification During R-CHOP. Average log hGE/mL for patients with DLBCL is shown at pretreatment, cycle 2 of R-CHOP, and end of R-CHOP regimen. Bars represent minimum and maximum values of data points. Analysis was carried out using one-way ANOVA or unpaired t-test with Welch's correction. A) ctDNA levels are correlated with IPI scores (0-5) ($p=0.0148$). B) ctDNA pretreatment levels grouped by response to R-CHOP. CR = complete response, PR = partial response, PD = progressive disease. ($p=0.0133$). C) ctDNA levels following cycle 2 of R-CHOP. REFR = refractory, ER = early relapse, CR = complete response. ($p=0.0395$). D) ctDNA levels assessed after the completion of R-CHOP. All samples are within 3 months of end of treatment, corresponding to the PET/CT scan visits. REFR = refractory, ER = early relapse, LR = late relapse, CR = complete response. ($p=0.0010$). E) Kaplan-Meier survival curve of DLBCL specific progression free survival for samples based on ctDNA status at the end of R-CHOP. ($p<0.0001$, HR: 19.25).

Figure 4.3: Log Fold Changes in ctDNA in Paired Diagnostic and Post Cycle 2 Samples. A) Log fold decreases in ctDNA are plotted for REFR/ER and CR groups. Average decrease of samples is shown with error bars representing standard error of the mean. ND (non-detectable)

samples were assigned a value of -6, outside the range of this assay. $P=0.0443$. B) Progression free survival of patients based on a log fold threshold of 2.5. ($p=0.0798$, HR:3.499)

Figure 4.4: Tracking Measurable Residual Disease in REFR and ER DLBCL. Using high confidence variants from diagnosis ctDNA, the same mutations are tracked at the same position in subsequent samples. ctDNA fraction is the average allele fraction of all somatic mutations in a given timepoint. A) Case 970 displays stable ctDNA detection in response to therapy, indicative of refractory disease. MTX = methotrexate. B) Case 2288 shows an initial response to therapy but low detection at end of R-CHOP and later increase in allele fraction as the samples get closer to clinical relapse. ER may show promising ctDNA dynamics initially, but re-emergence of disease happens quickly after end of therapy.

Figure 4.5: Mutational Overview of SNVs in Diagnostic and Relapse Cohorts. A) Oncoplot of the top 25 variants in diagnostic samples ($n=87$). Synonymous variants are removed from this analysis. Each column represents a single sample, with genes listed on the left and mutational prevalence on the right. Relapse groups (REFR, ER, LR, CR) and types of mutations are displayed below and tumor mutational burden (TMB) is shown above. B) Lollipop plot of *TP53* with mutations at diagnosis (top) and relapse (bottom) shown. C) Oncoplot of the top 25 variants in samples after completion of R-CHOP therapy ($n=32$). Synonymous variants are removed from this analysis. D) Forest plot comparing the mutational prevalence of genes at diagnosis and relapse. Odds ratio (OR) and p-values are shown, NS = non-significant ($p<0.1$), * = $p<0.05$.

Figure 4.6: Genetic Landscape of Relapse Groups. A) Co-Bar plot of top mutated genes in REFR DLBCL at Diagnosis ($n=11$) and after progressive disease post R-CHOP ($n=12$). Samples are unpaired and without synonymous variants. B) Oncoplot of the top 30 variants of all samples at diagnosis and relapse post R-CHOP ($n=119$), sorted by relapse group. Synonymous variants

are removed from this analysis. Each column represents a single sample, with genes listed on the left and mutational prevalence on the right. Relapse groups (REFR, ER, LR, CR) and types of mutations are displayed below and tumor mutational burden (TMB) is shown above. C) Groupwise comparison of genes enriched in relapse groups. X-axis shows genes, y-axis shows percentage mutated. Every gene shown is statistically enriched in the relevant group shown ($p < 0.05$). D) Progression free survival curve of diagnostic samples that are either mutated in *TNFAIP3* or *BTG2*, compared to all other cases. $p = 0.0005$.

Figure 4.7: Mechanisms of Resistance in rrDLBCL Treated with Immunotherapy. A)

Oncoplot of the top 25 variants in post BiTE (red) and post PD-1 (blue) samples ($n = 25$). Synonymous variants are removed from this analysis. Each column represents a single sample, with genes listed on the left and mutational prevalence on the right. Sample type (BiTE or PD-1) and types of mutations are displayed below and tumor mutational burden (TMB) is shown above. B) Progression free survival curve of patients based on ctDNA status at the end of BiTE therapy. $p = 0.0070$. C) Pyclone analysis of patient 1470. Sample timepoint is shown on the x-axis with cellular prevalence (allele fraction of each mutation) is plotted on the y-axis. Pyclone identifies 3 clonal structures from the serial sampling through PD-1 therapy.

Figure 4.S1: Survival based on ctDNA level at diagnosis. A) Overall survival of patients at diagnosis based on ctDNA status pretreatment. A cutoff of 2.0 log hGE/mL was used to discriminate between ctDNA high and low samples. $p = 0.2188$, HR: 1.736. B) Progression free survival of patients at diagnosis using the same parameters as panel A. $p = 0.0915$, HR: 1.1792.

Figure 4.S2: ctDNA Quantification at Relapse. A) Average log hGE/mL for patients with at relapse is shown. Bars represent minimum and maximum values of data points. Analysis was carried out using one-way ANOVA or unpaired t-test with Welch's correction. A) ctDNA levels

separated based on relapse group (REFR, ER, LR). No difference was seen between groups (ANOVA, $p=0.7760$). B) ctDNA levels correlate with IPI scores calculated at relapse, similar to diagnosis (ANOVA, $p=0.0156$). Samples were grouped together based on low (0-2), intermediate (3), and high-risk (4-5) IPI groups due to the reduced number of samples available at relapse. C) Progression free survival of patients at relapse based on ctDNA status. A cutoff of 1.0 log hGE/mL was used to discriminate between ctDNA high and low samples. $p=0.0379$, HR: 2.812. D) Overall survival of patients at relapse using the same parameters as panel C. $p=0.0205$, HR: 3.338.

Figure 4.S3: Variant Calling Based on Cell of Origin. A) Oncoplot of the top 25 variants in diagnostic GCB samples ($n=49$). Synonymous variants are removed from this analysis. Each column represents a single sample, with genes listed on the left and mutational prevalence on the right. Types of mutations are displayed below and tumor mutational burden (TMB) is shown above. B) Oncoplot of the top 25 variants in diagnostic non-GCB samples ($n=26$). Synonymous variants are removed from this analysis. Each column represents a single sample, with genes listed on the left and mutational prevalence on the right. Types of mutations are displayed below and tumor mutational burden (TMB) is shown above.

Figure 4.S4: Variant Calling of Relapse Groups at Diagnosis. Oncoplots of the top 25 variants in diagnostic samples from REFR (A, $n=11$), ER (B, $n=13$), LR (C, $n=5$), and CR (D, $n=54$). Synonymous variants are removed from this analysis. Each column represents a single sample, with genes listed on the left and mutational prevalence on the right. Types of mutations are displayed below and tumor mutational burden (TMB) is shown above.

Figure 4.S5: Variant Calling of Relapse Groups after R-CHOP. Oncoplots of the top 25 variants in post R-CHOP samples from REFR (A, $n=12$), ER (B, $n=13$), and LR (C, $n=7$).

Synonymous variants are removed from this analysis. Each column represents a single sample, with genes listed on the left and mutational prevalence on the right. Types of mutations are displayed below and tumor mutational burden (TMB) is shown above.

Figure 4.S6: Pathway Enrichment Analysis of Relapse Groups at Diagnosis. The top 25 genes at diagnosis for each group (REFR, A; ER, B; LR, C; CR, D) was used in gProfiler to establish which Reactome pathways were most significantly affected by the genes in question.

4.13: Figures

Figure 1

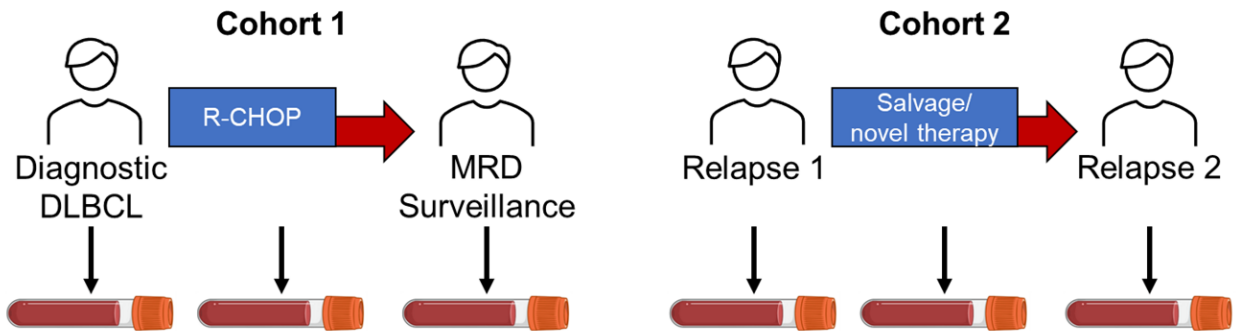


Figure 2

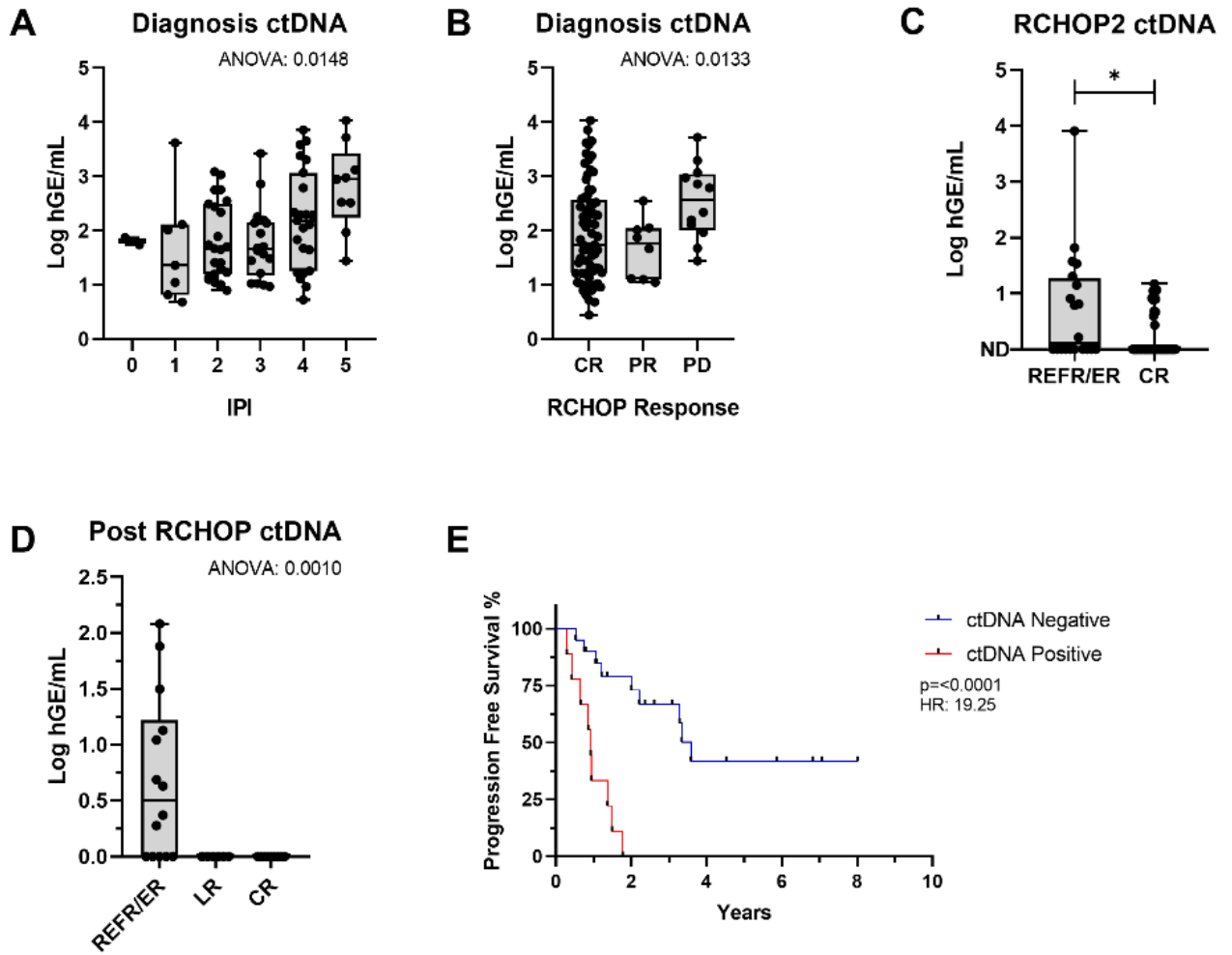


Figure 3

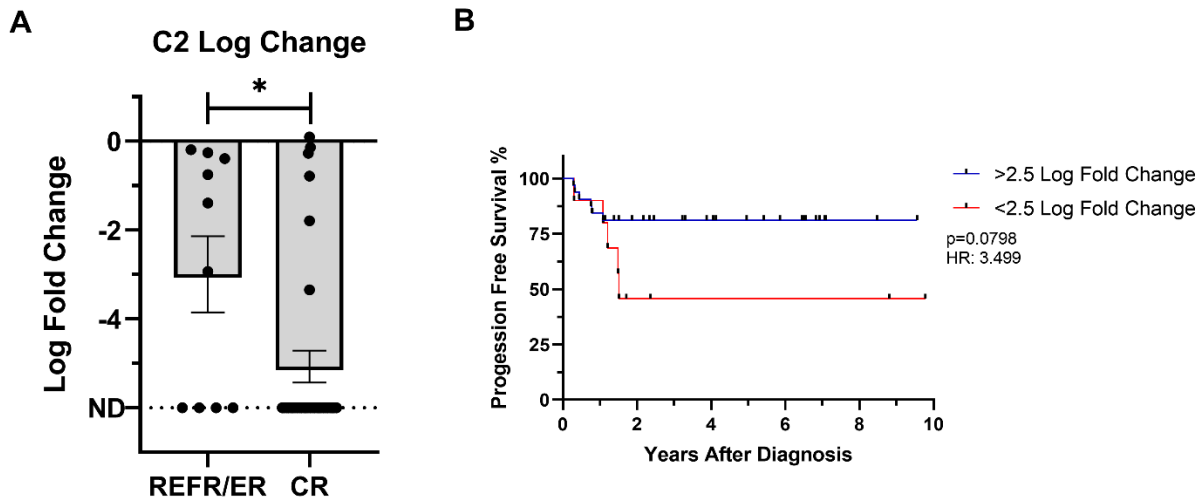


Figure 4

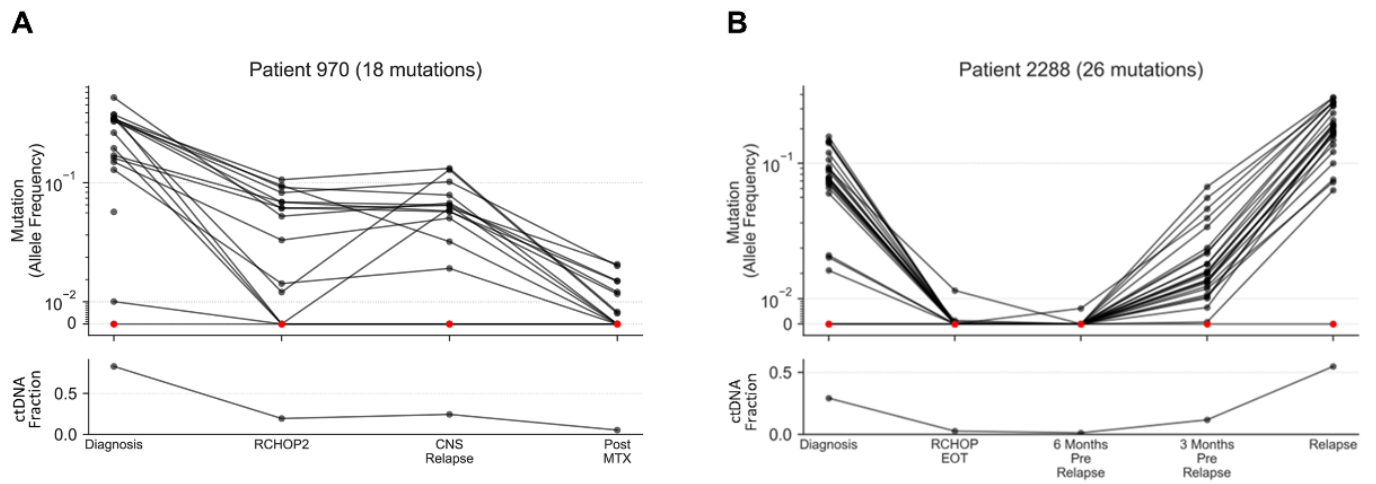


Figure 5

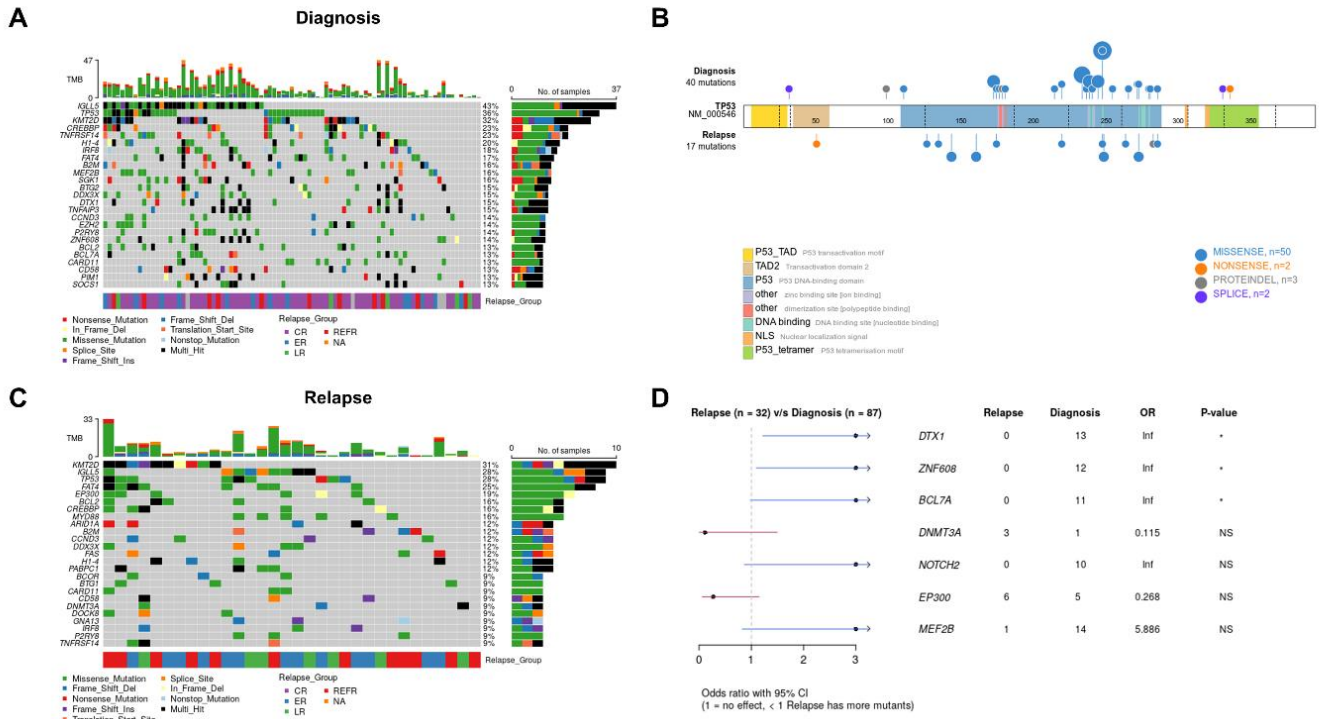


Figure 6

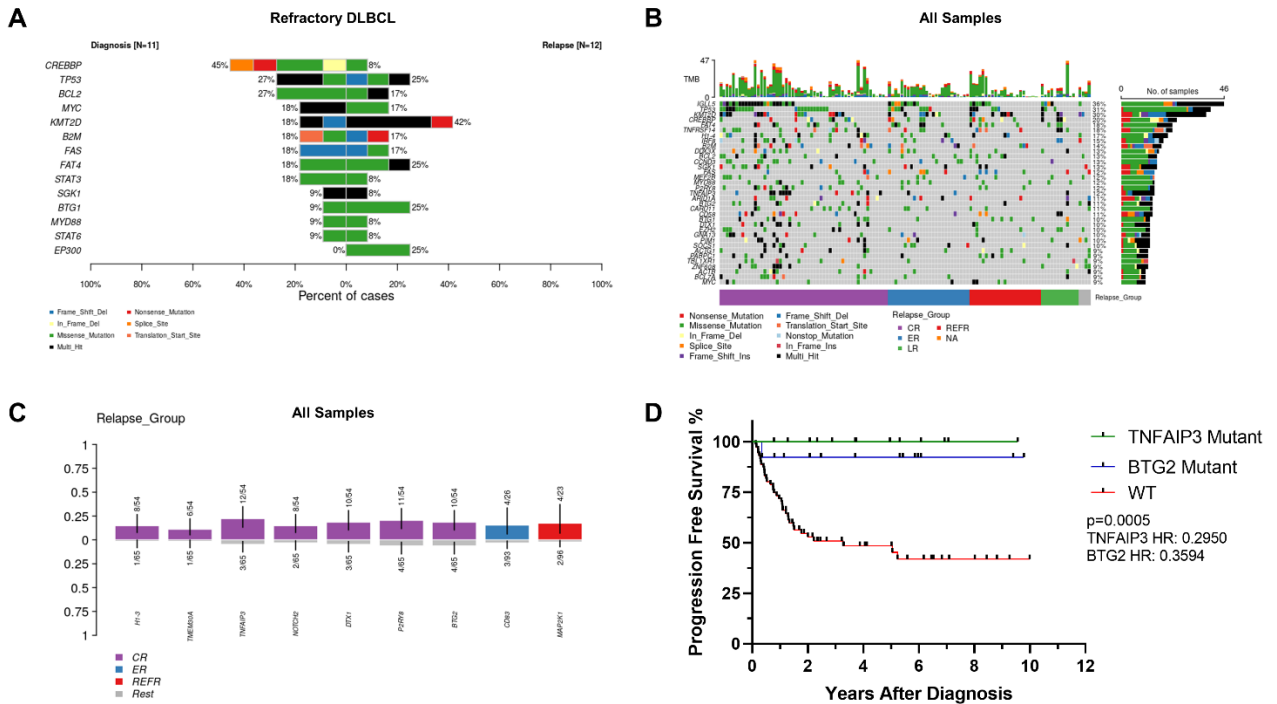
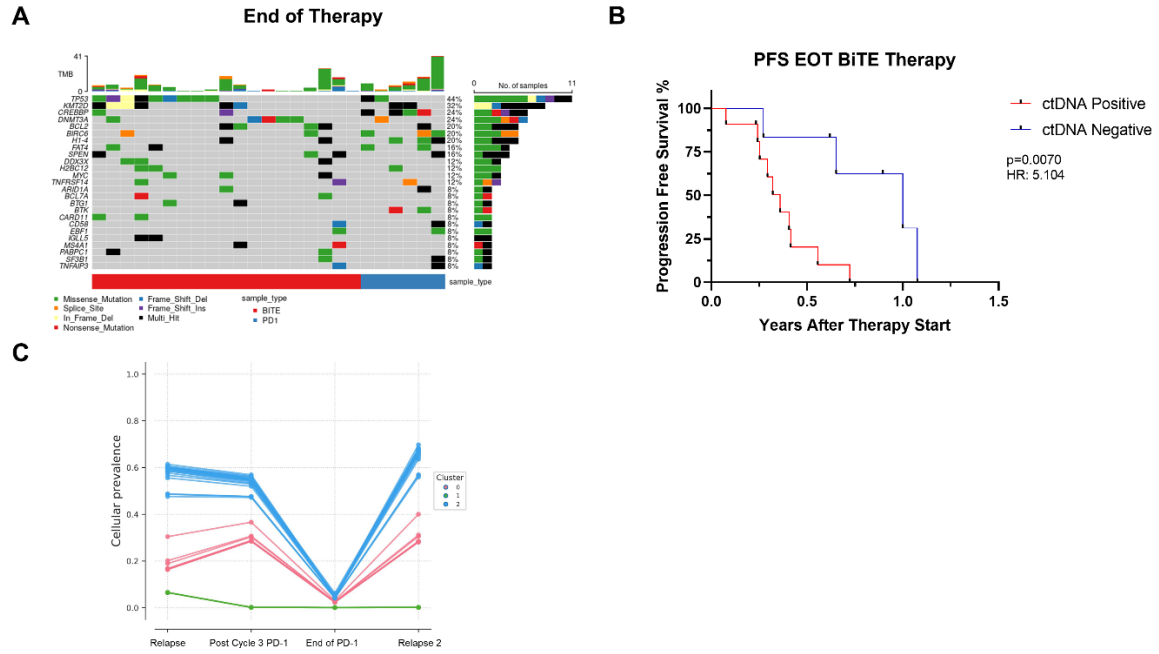


Figure 7



4.14: Supplemental Figures

Figure S1

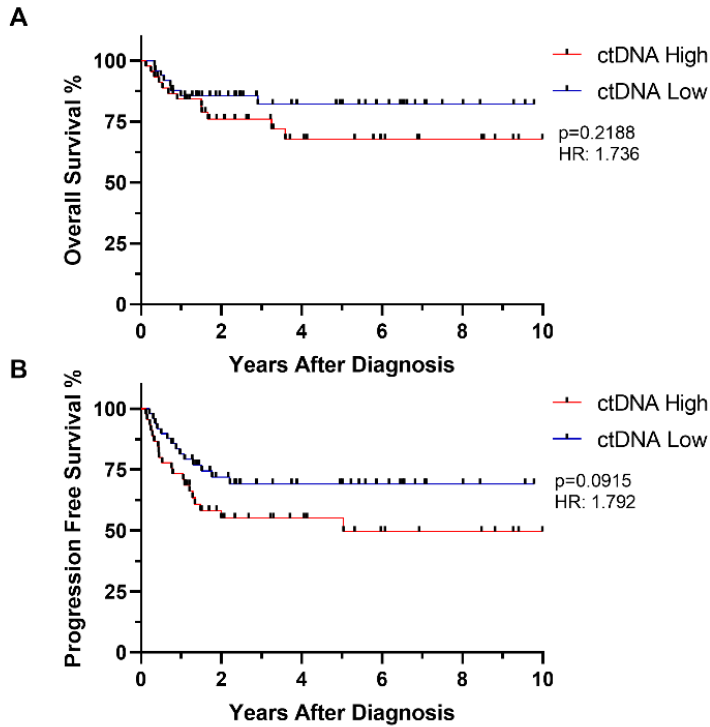


Figure S4

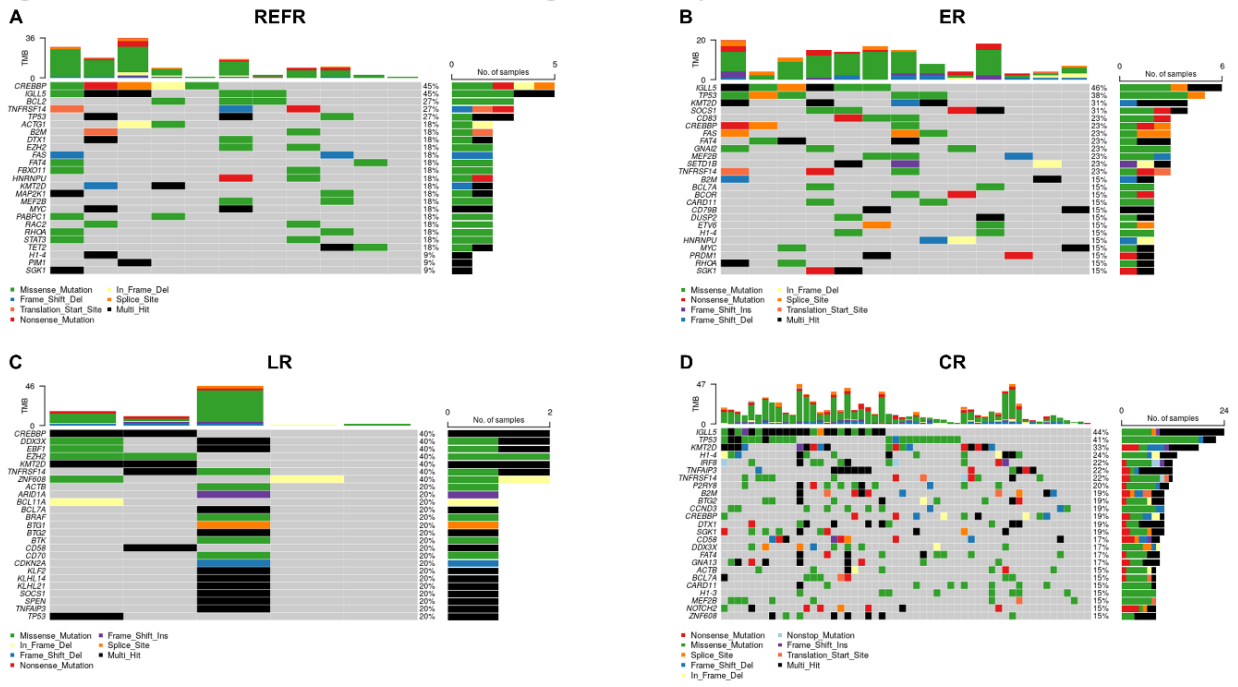


Figure S5

Post R-CHOP Relapse Groups

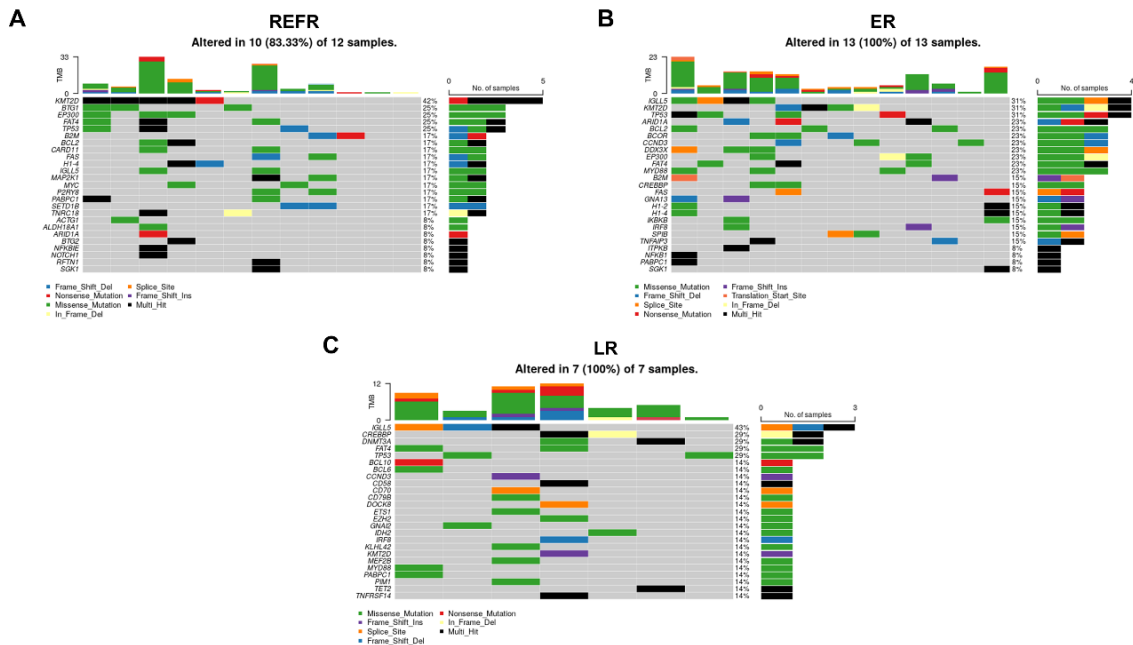
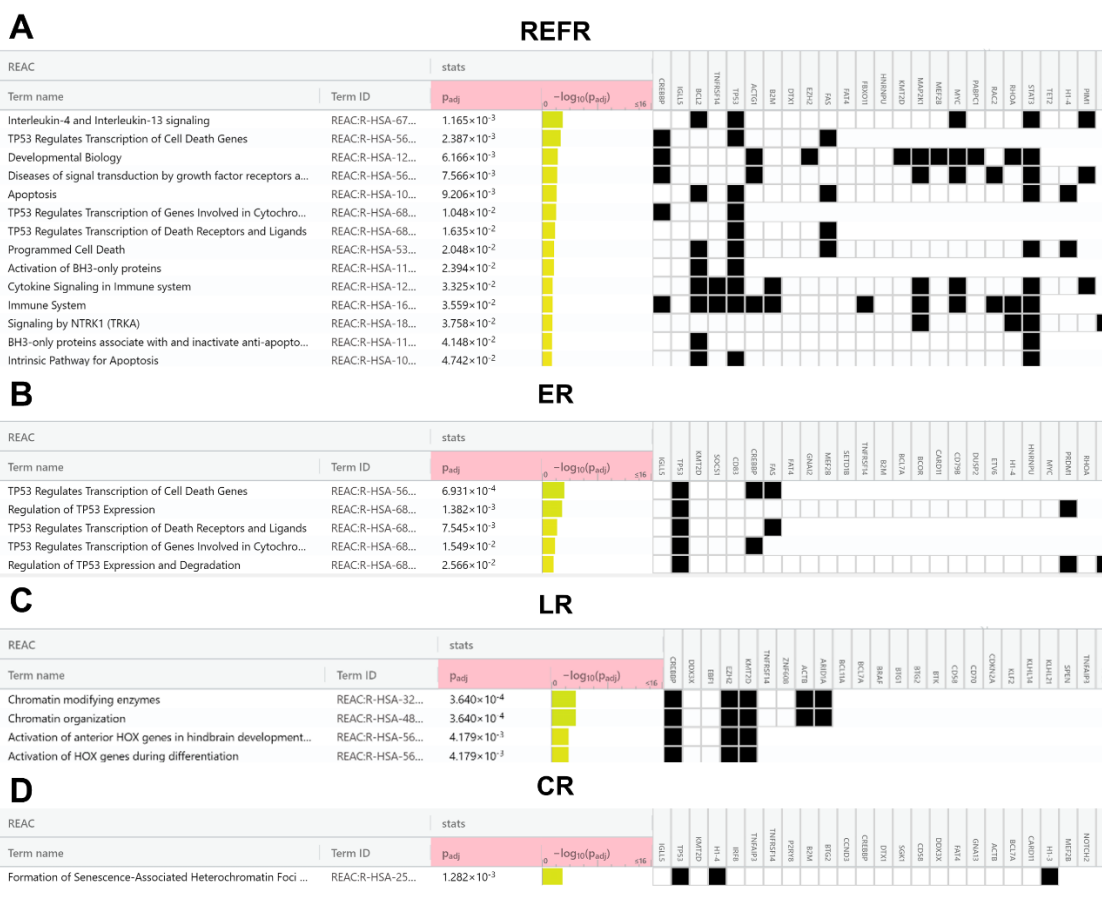


Figure S6 Pathway Enrichment Analysis



4.15: Supplemental Methods

4.15.1: cfDNA Extraction and Library Construction

cfDNA extraction was carried out on samples using the MAGMAX cfDNA isolation kit (ThermoFisher Scientific), which uses magnetic bead technology to bind small fragmented cfDNA. cfDNA was isolated from 0.5-1.5 mL of plasma depending on availability. After extraction, samples were quantified using Qubit fluorometer (ThermoFisher Scientific) and expressed as ng/ μ L.

Library construction was carried out using xGenTM cfDNA & FFPE DNA Library Preparation Kit (Integrated DNA Technologies, #10010207) in combination with xGenTM UDI

10nt primer pairs (Integrated DNA Technologies, #10008052) for sample pooling and demultiplexing. Briefly, 15 μ L of cfDNA sample (between 1-250ng) underwent end repair and subsequent ligation of the sequencing adapters. This kit utilizes a 2-step ligation which first adds single stranded adapters to the 3' end of the fragmented DNA, and then an additional ligation of 5' end. These adaptors incorporate unique molecular identifiers (UMI) on each strand that are later used for bioinformatic error correction. Following ligation, PCR amplification was carried out using UDI primer pairs and xGen 2x HiFi PCR mix to create a final cfDNA library with incorporated dual sample indexes and UMI.

4.15.2: UMI Processing and Single Nucleotide Variant Calling

UMIs were processed using the fgbio toolkit (<https://github.com/fulcrum-genomics/fgbio>). In brief, duplicate reads stemming from the same parental molecule were identified via shared UMI sequences and collapsed to form a consensus read pair. Error correction was also subsequently performed on overlapping bases within each read pair. Following error correction, bases with a quality score <20 were masked as “N” for the purposes of downstream analyses. The average read depth following UMI-based consensus and correction was ~500X per sample. Quality control and sequencing metrics were calculated using the Picard toolkit (<https://broadinstitute.github.io/picard/>) and UMI-specific metrics were calculated using the fgbio toolkit. As matched normal were sequenced without UMIs, a similar workflow was used but UMI-processing steps were excluded, with duplicate reads marked using Picard MarkDuplicates. Single nucleotide variants were called in matched tumor-normal mode using SAGE (<https://github.com/hartwigmedical/hmftools/tree/master/sage>), and annotated using ensembl VEP version 96 [54] and vcf2maf (<https://github.com/mskcc/vcf2maf>). Custom post-filtering was applied to remove 1) Variants with fewer than 5 supporting molecules, 2) Variants

at loci with less than 8 unique read pairs in the normal (and thus not assigned as germline or somatic), 3) Variants at positions where more than 5% of bases were masked, 4) SNVs or small insertions/deletions which are an extension/contraction of a repeat occurring more than 6 times, and 5) Variants observed in more than 10% of samples and not previously established as known lymphoma hotspots.

4.15.3: Measurable Disease Tracking

In cases of serial samples, we utilized high confidence variants from gross disease timepoints (diagnosis or relapse) and tracked the same mutations in subsequent samples. Briefly, the same mutation was tracked over subsequent timepoints and the alternate allele count was measured for each mutation at the same position in later timepoints. This allowed a more in-depth tracking of changes in VAF regardless of limit of detection by using the raw read counts after UMI processing.

4.15.4: Statistics and Visualization

Statistics were performed using functions from both Maftools [55], R Studio and, GraphPad Prism (Version 8). Comparisons across multiple groups was performed by Brown-Forsythe one-way ANOVA, while comparisons between 2 groups was performed using student's t-test with Welch's correction. Binary comparisons of grouped variables were analyzed using Fisher's exact test. Survival curves were generated using GraphPad Prism and analyzed via Log-Rank test. Oncoplots were generated via Maftools while lollipop plots for specific genes were made with ProteinPaint [56]. Pathway enrichment analysis was performed as described previously, using g:Profiler [57]. Pyclone analysis was used to infer clonality and plot cellular prevalence of clones of interest [35]. All other plots were generated in GraphPad Prism or R.

Chapter 5: Discussion & Conclusion

5.1: DLBCL Therapeutic Resistance and Apoptosis

rrDLBCL shows a markedly reduced ability to respond to 1L treatment, and this is reflected in the apoptotic dysfunction outlined in chapter 3. While the overexpression of anti-apoptotic BCL2 is a well-known mechanism of resistance in multiple lymphomas, the failure of pro-apoptotic effectors (BAX/BAK) to initiate apoptosis under direct pro-apoptotic activation is a novel phenotype of DLBCL cell survival. Pro-apoptotic defects create an aggressive disease that is likely to be refractory to any treatment. This is a unique phenomenon, as genetic lesions in pro-apoptotic proteins BAX and BAK are extremely rare and unlikely to directly contribute to this effect[169]. Moreover, while we have shown that MCL1 is the primary contributor to resistance in NHL after targeting BCL2, other studies have shown that MCL1 inhibition is mediated by BAX[250–252]. Class B samples may fail to initiate apoptosis because targeting MCL1 and BCL2 depends on functional BAX. This also shows the difficulty in treating such cases, which are likely to be refractory to any treatment that primarily relies on intrinsic apoptosis as a means of cell death.

Investigation into the mechanisms underlying the profound apoptotic dysfunction of class B is underway. Given the frequency with which these blocks occurred, it is likely that additional proteins and/or mutations are involved in preventing apoptotic activation. BAX/BAK protein expression by immunofluorescence in class B samples were similar to class C samples, indicating that other mechanisms are at play. After BAX/BAK initiate the release of cytochrome c from the mitochondria, downstream proteins may also interfere with the induction of apoptosis. Impairment of caspase activity after cytochrome c release could contribute to resistance in these cases. Additional over-activation of inhibitors of apoptosis proteins (IAPs) may also impair

BAX-mediated apoptosis[253–255]. However, these still unlikely to completely explain class B effects given that cytochrome c was retained in the mitochondria during staining, indicating a failure for BAX/BAK to permeabilize the mitochondrial membrane. Novel studies exploring the relationship between effector dysfunction in the context of large-scale apoptotic activation are needed and can help to elucidate mechanisms by which BAX/BAK is prevented from releasing cytochrome c.

Future studies should focus on the protein-protein interactions that may interfere with either homo- or heterodimer formation between BAX and BAK, or their subsequent anchoring to the mitochondrial membrane. This is made difficult by the fact that these observations were made in primary tissues that may be depleted. One B cell lymphoma cell line, SU-DHL10, was confirmed to have a class B block, as was an additional cell-line derived from BL[256,257]. These were both attributed to a lack of BAX and BAK protein expression, which is not the case for many samples in our study. New models of effector dysfunction either through inhibition or genetic knockouts will help to explain the class B phenomenon and potentially provide novel targets for therapy. BAX/BAK have multiple binding partners that can either produce pro- or anti-apoptotic effects outside of anti-apoptotic proteins, so additional analysis of the involvement of these partners should be examined in the context of mitochondrial membrane permeabilization. Voltage dependent anion channels (VDAC1, VDAC2, VDAC3) are involved in ATP transport from the mitochondria but have also been shown to interact with apoptotic proteins to mediate mitochondrial membrane permeabilization (MOMP)[258]. For example, VDAC2 was shown to be necessary for properly functioning BAX and mediate apoptosis[259]. Class B apoptotic blocks may be a consequence of inappropriate BH3 protein localization to the mitochondrial membrane and/or lack of pore formation preventing cytochrome c release. This

provides evidence for further exploration of dysfunctional MOMP in the context of malignant cells and the interaction between mitochondrial membrane proteins and BH3 effectors in these cases.

5.2: Early Detection of rrDLBCL using ctDNA

Chapter 4 of this thesis established the use of our novel gene panel using previously detailed methodology (CAPP-Seq)[232,233] to detect ctDNA and rrDLBCL as early as possible in 1L therapy. REFR and ER DLBCL have significantly reduced survival and represents a subset of patients that could be candidates for early transition into 2L therapies such as CART cell therapy. Due to the effectiveness of CART in patients with reduced tumor burden, identifying these cases early requires novel assays with increased turnaround times. The non-invasive nature of ctDNA sampling is an attractive solution to this problem. Our panel provides a quick and effective measurement of ctDNA levels at various treatment timepoints, and could potentially contribute to both identification of refractory disease and disease reoccurrence in responding patients. The two most predictive factors for rrDLBCL using ctDNA in this study were detection of ctDNA after either C2 or end of R-CHOP. These represent potential treatment landmarks where monitoring of ctDNA dynamics is particularly useful in making potential changes in clinical course. The incorporation of these prognostic markers in a clinical setting still requires extensive validation in clinical trials and larger cohorts. We are continually exploring the involvement of multiple prognostic variables in predicting rrDLBCL, and it may be that a combination of IPI, specific mutations, and ctDNA dynamics provides a more robust prognostic classification than current methods. Mutations in *TNFAIP3*, *BTG2*, or *DTX1* are good candidates for further validation, as they confer a favorable prognosis in our data. Whereas mutations in

BCL2, *MYC*, *EP300*, and *BTG1* are potentially useful for identifying REFR DLBCL due to the prevalence of these mutations during treatment in resistant cases.

5.3: Mutational Profile of REFR DLBCL

rrDLBCL cases vary by response to therapy and time to relapse, but our data suggests that these differences are underlined by distinct mutational profiles. *BCL2* and *MYC* mutations are more prevalent in REFR DLBCL, reminiscent of HGBCL-DH which is notorious for inferior prognosis. This data supports the classification of DZsig DLBCL, and potentially its incorporation into the identification of REFR DLBCL without *BCL2* and *MYC* rearrangements by FISH[8]. Follow up analysis of the gene expression profiles of these samples will confirm their DZsig status and identify the extent to which genetic classification corresponds to differing relapse groups in our cohort.

Further investigation into the oncogenic potential of *BTG1* and *EP300* mutations is warranted due to the large percentage of mutated cases in REFR DLBCL at 2L therapy. *BTG1* dysfunction has been highlighted as a key mutational event in MCD subtypes and was recently implicated as an important driver of lymphogenesis via overexpression of *BCL2*, *MYC*, and increased cellular migration[260,261]. *EP300* is well known for its role as part of the p300-CBP coactivator family with *CREBBP*, another common driver of DLBCL[107,115]. While *CREBBP* is commonly mutated in diagnostic DLBCL cohorts, *EP300* became a top ten mutated gene in our relapse cohort. This suggests that additional epigenetic dysfunction may be acquired after therapeutic pressure in aggressive DLBCL in addition to refractory cases. In anaplastic and Hodgkin lymphoma, *EP300* preferentially affected *MYC* expression, a phenomenon that may also be explored in DLBCL[262]. Further implications have been made in *CREBBP/EP300* involvement in NOTCH signaling and altering the tumor-immune interaction[263]. Dysfunction

in these genes also interferes with MHC-II expression, promotes Treg function, and thereby promotes immune escape[264–266]. *EP300* is preferential to dark zone GC function[267], adding to the growing association between REFR DLBCL and dark zone signatures. Mutations are usually mutually exclusive between these two, but there may be certain rare epigenetic profiles (e.g. co-mutation in *EP300* and *CREBBP*) that result in more resistant disease, which is the case in two of our rrDLBCL cases at relapse. The use of histone deacetylase inhibitors (HDACi) has been explored in DLBCL, although response rates are generally modest[118,268–270].

Lastly, enrichment analysis of REFR DLBCL from diagnostic and relapse cohorts showed increases in *MAP2K1* mutations. *MAP2K1* encodes for a kinase that is involved in ERK signaling and subsequently many cell processes including proliferation, transcriptional regulation, and apoptosis[271]. It is rarely mutated in DLBCL, but is associated with ERK activation in pediatric-type FL, as well as hairy cell leukemia and progression of splenic diffuse red pulp lymphoma[272–275]. It was highlighted as a genetic event in the TET2/SGK1 cluster of DLBCL similar to ST2 by LymphGen, with common mutations in ERK activation being prominent in these cases[276]. The increase in mutations seen in REFR DLBCL may implicate *MAP2K1* mutations in resistance and apoptotic dysfunction, an underreported genetic phenomenon in DLBCL.

In summary, REFR DLBCL exhibits alterations in genes known to be recurrently mutated in lymphoma and appear to be related to dark zone signatures focusing on upregulation of BCL2 and MYC activity via numerous pathways (e.g. *BTG1*, *CREBBP/EP300*) or previously underreported genetic mutations (*MAP2K1*). These genes may be important factors in determining refractory status of patients in addition to ctDNA dynamics and apoptotic response.

5.4: Mutational Profiles of ER and LR DLBCL

ER DLBCL displayed similar mutational profiles as REFR cases, with more emphasis on immune interaction and less on cell survival (e.g. fewer mutations in *MYC* and *BCL2*). Shared amongst ER and REFR cases are variants in both *B2M* and *FAS*, important for antigen presentation and extrinsic apoptosis. These have been thoroughly described as recurrently mutated in DLBCL, particularly *FAS* in rrDLBCL[169], and contribute to immune evasion. These mutations contribute to overlapping genetic signatures in ER and REFR characterized by dysfunction in TP53 mediated transcription of genes involved in cell death signaling (Chapter 4, Figure S6). Analysis of significantly enriched samples at both diagnosis and relapse revealed *CD83* mutations that were overrepresented by ER DLBCL. *CD83* mutations are rare variants that occur in roughly 5% of all cases, but are present in 15% of ER samples. *CD83* is an important regulator of immune interaction and helps to stabilize MHC-II function[277]. Mutations in *CD83* have been implicated in a PMBL-like genetic signature that identifies a particular novel subgroup of DLBCL with upregulated JAK/STAT and NF- κ B signaling[278]. This contributes to dysfunctional immune interaction in ER DLBCL, in addition to mutations previously mentioned (*B2M*, *FAS*). Interestingly in genetic classification, *CD83* was identified in a SOCS1/SGK1 based cluster (Lacy et al.[276]) or cluster C4 (Chapuy et al.[5]) and both had relatively high survival compared to other cohorts. Our data implies *CD83* mutations are common in patients with worse prognosis and early disease progression. This highlights that while many genes are implicated in novel genetic subgroups of DLBCL, differences in classification methodology require further harmonization and additional cohort studies to accurately define subtypes that could be used clinically for patient evaluation.

LR DLBCL was unique from REFR or ER DLBCL in that there was a preference towards dysfunctional epigenetic regulation. This was supported primarily by mutations in epigenetic regulators *KTM2D*, *EZH2* and *DNMT3A*. These potentially highlight an important role for *DNMT3A* in rrDLBCL, which has previously been more associated with acute myeloid leukemia[279,280]. Epigenetic dysfunction is a known driver of DLBCL⁴¹, but our results support a more prominent role for this in LR cases. Frequently, studies follow patients for 2 years or less, but this may not sufficiently capture the evolution of patients in the LR category and warrants further exploration. Differences between late and early relapses have been highlighted previously by separate evolutionary pathways in disease progression at relapse[281]. Considered a branched evolution of malignant cells, LR indeed showed the highest change in mutations between diagnostic and relapse cohort, albeit in a limited number of samples. This would need to be confirmed in paired sample biopsies for these cases to demonstrate clear evolution between timepoints. Our data supports that LR are divergent from REFR/ER disease and are lacking key oncogenic mutations in cell survival pathways. Incorporating the mutational data shown here into genetic classifiers such as LymphGen will be important in correlating our relapse groups with DLBCL genetic subgroups and establishing additional variables for rrDLBCL detection. This will also help to highlight any novel signatures in our data that may contribute to poor survival even within established subgroups of DLBCL.

In summary, the distinct mutational profiles detailed here, coupled with the analysis of ctDNA dynamics during therapy, serve as important observations and can contribute to further identification of differing types of rrDLBCL prior to treatment and as patients are monitored in clinic. Future studies should aim to incorporate additional mutational data such as copy number

events, structural variants, and fragmentomic analysis to help further define the mutational landscape of REFR, ER, and LR DLBCL.

5.5: Technical Advantages of rrDLBCL Panel Sequencing

Our gene panel, which focuses on genes implicated in rrDLBCL, has significant advantages with regards to implementation. These are important considerations when assessing the use of ctDNA assays in patient assessments and the transition of these studies from the lab to the clinic. This includes the size of the panel, *de novo* sequencing without the need of a matched tissue biopsy, and ease of detection from relatively small amounts of material. Our panel measures to ~700 kb, which is small in comparison to ctDNA panels being explored in industry. This is a result of targeting highly impactful genes that are more likely to have direct implications in rrDLBCL progression. This allows us to pool more samples together for a single sequencing run. As such, we can reduce costs significantly and increase our throughput of cases in a more economical manner. For detecting refractory disease, our approach is much simpler than other proposed techniques which often involve sequencing of matched tumor biopsies in order to identify high confidence variants for subsequent ctDNA tracking. This approach has some drawbacks, as the focus on known mutations is good for high depth MRD testing, but loses the ability to track emergent, novel mutations as well as variants not detected in the biopsy. One of the benefits of ctDNA is capturing the entire systemic disease, regardless of tumor sites. These can be quite different in patients with DLBCL, especially those exhibiting features of composite lymphoma (e.g. FL and DLBCL). Lastly, one of the limits of our study was the lack of sufficient starting material. Our study utilized retrospective samples of plasma measuring between 0.5-1.5 mL. This leads to small amounts of starting DNA molecules for analysis. However, this study also shows that detection of ctDNA can be achieved even with minute quantities of DNA. While

our results here are very promising, it is expected that the level of detection in our panel will only increase with more starting DNA. Therefore, future sample collection in our lab will aim to increase the amount of plasma archived and bio-banked for studies. This will be an important factor to consider for potential prospective studies that are needed as well.

5.6: ctDNA Analysis of BH3 Profiles

To combine the functional defects in DLBCL with the mutational landscape observed by ctDNA monitoring, we set out to sequence BH3 samples as part of the Marathon of Hope Cancer Network, but this data is not yet available. However, several patients who were part of the ctDNA study presented here, were also part of the BH3 study. While we studied plasma cfDNA in these cases and not tumor biopsies, there may still be some correlation between mutations present in ctDNA and our classes of apoptotic block. Therefore, outside the context of these two manuscripts, mutational profiles of available patients at diagnosis with class A, B, and C blocks were assessed (Figure 5.1). The number of samples available for analysis was low (n= 1 A, 2 B, 4 C), but there were some mutations implicated in resistance to apoptosis within these samples.

Class C samples were mostly rrDLBCL cases with 2 ER and 1 LR case among them. It is important to realize that while class C DLBCL is more responsive to apoptotic stimuli than class A/B DLBCL, as shown by their initial response to RCHOP, these are still capable of additional mechanisms to promote tumor growth and survival. Class C samples had mutations in common drivers of DLBCL seen in diagnostic cohorts (*CREBBP*, *KMT2D*, *TP53*). However, 3/4 samples also exhibited SNVs in *IRF8*, which is an important transcription factor for myeloid cell differentiation and is mutated in various subtypes of DLBCL[154,282]. Interestingly, *IRF8* was also important for BAX transcription in myeloid cells[283], but considering these mutations occurred in class C samples, BAX is likely functional in these DLBCL. *IRF8* is also one of the

defining features of EZB DLBCL as identified by LymphGen. These DLBCL were identified as having common mutations in epigenetic regulation, and we see that in class C samples as well (*CREBBP*, *KMT2D*, *IRF8*). Therefore, they may be an association with EZB DLBCL and class C samples, however additional EZB mutations are also found in class A/B samples here. Further analysis of additional samples and application of the LymphGen algorithm to future data can help further elaborate on the association between genetic classification and apoptotic dysfunction.

SNV mutations in pro-apoptotic blocks showed similar dysfunction to pathways implicated in REFR mutational analysis. All three cases of class A and B block were considered part of the refractory group, again supporting the aggressive resistance to therapy seen in these defects. The class A sample only had one detectable mutation in *CREBBP*, and therefore was not very informative on any potential novel mechanisms of therapy resistance. Similar mutations were seen in class B and C samples, with *TP53*, *FAS*, and *BCL2* mutations possibly contributing to apoptotic inhibition and cell survival in these DLBCL. TP53 is one of the mediators of BAX protein function[284], but mutations occur in both class C and B samples, pointing to additional mutations that may contribute to loss of apoptotic function. Such mutations have been seen before in resistant DLBCL, as Class B samples displayed mutations in *BIRC6* and *BTG1*. These mutations were noted in the ctDNA study as being associated with REFR DLBCL (*BTG1*) or with potential aggressive disease in the relapse setting (*BIRC6*). There appears to be a link between common genes in refractory patients and class B apoptotic block. Unfortunately, not every refractory case was BH3 profiled, but it is likely that class B cases and REFR status based on time to relapse identify similar patient groups. This is not surprising, as these are by definition resistant to therapy, but the overlap between them reveals a complex relationship between

genetic alterations and functional activity. This was also supported by pathway enrichment analysis (Figure 4.S6), which identified REFR DLCL as having mutations commonly associated with BH3-only protein activation and function. This is a very small sample size, but continued exploration of the class B phenotype on a broad genetic level is needed. Given the targeted nature of this panel, novel genes may be implicated in class B mutational status and be revealed by WGS or WES sequencing.

The overlap between REFR DLBCL and class B profiles is identified by their association with mutations identified in chapter 4 (*BCL2*, *BTG1*, *BIRC6*) and furthers our understanding of the closely related phenomena of intrinsic apoptotic dysfunction and refractory disease. Interestingly, class A, B, and C samples have shared mutations typical of EZB genetic classification (e.g. *KMT2D*, *CREBBP*, *BCL2*, *FAS*). This underscores the inability of current genetic classification to sufficiently capture refractory disease, as large differences in apoptotic competency are demonstrated within genetic subtypes. Additionally, it has been shown that refractory DLBCL can be assigned to different subtypes, including EZB, MCD, or unclassifiable[281]. Although assessing viable tumor cells using BH3 profiling is not realistic in clinical settings, potential exists in the future for a combination of both genetic and functional assays in identifying REFR DLBCL. These cases may be candidates for therapies that induce cell death outside of intrinsic apoptosis, such as CART or BiTE therapy, and would be aided by early identification.

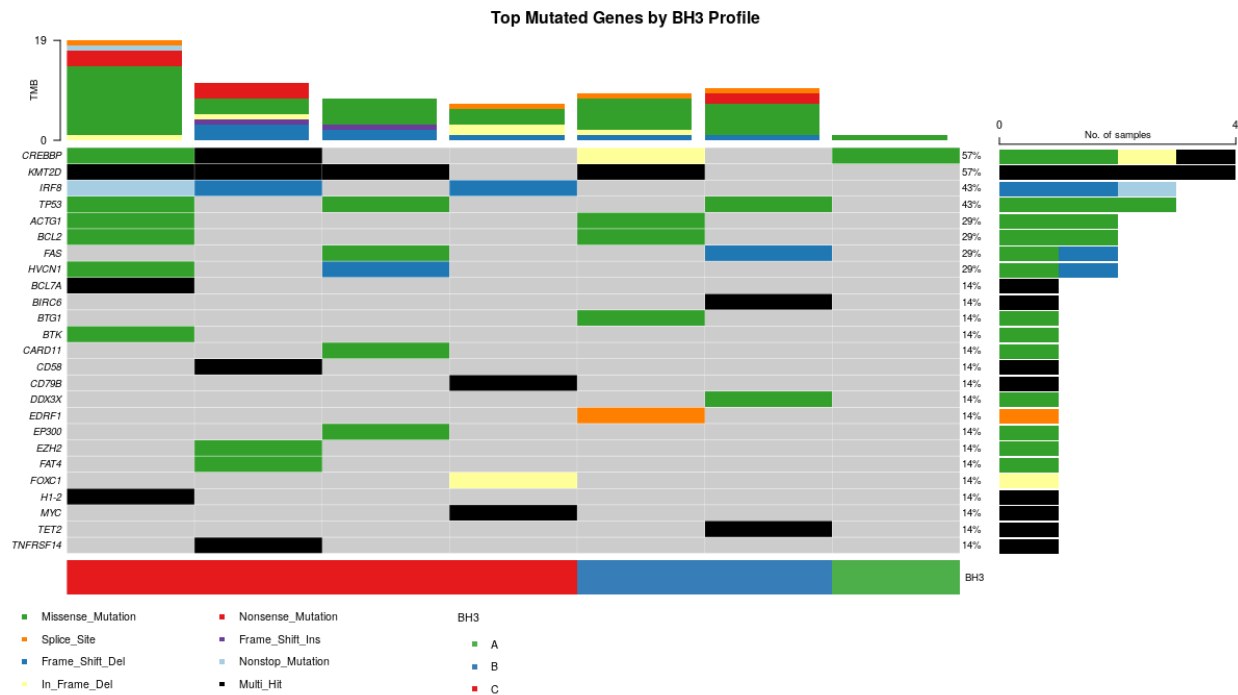


Figure 5.1: Comparison of Diagnostic ctDNA Mutations and BH3 Profiles. Oncoplot of the top 25 variants in diagnostic samples from cases that also had BH3 profiling. Class A, B, and C apoptotic blocks were $n = 1, 2$ and 4 , respectively. Synonymous variants are removed from this analysis. Each column represents a single sample, with genes listed on the left and mutational prevalence on the right. Types of mutations are displayed below and tumor mutational burden (TMB) is shown above.

5.7: Future Directions in rrDLBCL Clinical Management

Currently, rrDLBCL poses serious clinical problems due to the lack of validated prognostic tools in identifying refractory disease with greater accuracy. This may be changing, as the era of personalized medicine will result in more specific treatment measures based both on genetic subtyping and changes in cellular function. Assays such as the novel rrDLBCL gene panel described in this thesis may contribute to improved detection of refractory disease, crucially at earlier stages than what is presently available in clinics. The largest hurdle to

implementing these into clinical practice is the consolidation of mutational signatures identified by multiple different genetic classifiers and sequencing studies [285]. While a significant amount of overlap is evident between them, differences arise due to changes in computational methodology, as well as the cohorts being analyzed. Key mutational events in these genetic classifications are clear, but there is less understanding in when one subtype ends and another begins. Additionally, many patients still remain unclassifiable by these methods and therefore would be provided no benefit in clinical scenarios. It will be important to see how many of the REFR DLBCL analyzed in this thesis may fall under this unclassifiable umbrella.

The next steps in bringing these tools to patient management needs to involve validation in real-time, prospective studies. These will firstly establish the feasibility of these assays in implementation with regards to processing times, costs, and failure rates. Following this, landmark clinical trials incorporating mutational profiles and ctDNA dynamics into treatment selection will be needed. It is not hard to envision a future where standard of care is centered around ultra-specific treatment regimens informed by genetic profiling in the context of complex clinical presentation, combined with continued follow-up via the non-invasive ctDNA methodology we have described here.

5.8: Conclusion & Summary

Following the examination of apoptotic defects and the monitoring of ctDNA during treatment, we have expanded the knowledge of treatment resistance in DLBCL. rrDLBCL is well-known for its aggressive disease course and the extremely poor outcomes for patients after relapse. While this is still the case in most settings, the treatment landscape of DLBCL is changing rapidly. Novel immunotherapies are making remarkable strides in the relapsed setting, with CAR-T cell therapy likely to be the new standard of care in 2L. BiTE immunotherapy is

also being explored and new clinical trials are assessing its use in 1L clinical regimens. For these therapies to be effective, there needs to be a better understanding of how refractory disease can avoid cell death and how we can optimize the treatment intervention plan.

To that effect, this thesis has outlined two factors that are key to understanding rrDLBCL responses during therapy, apoptotic dysfunction and ctDNA dynamics during treatment.

rrDLBCL is characterized by reduced ability to initiate apoptosis, and this is partially due to reduced effector function in pro-apoptotic proteins such as BAX or BAK. This is an important observation that implicates intrinsic ability to avoid cell death in refractory DLBCL and may be an important consideration for therapy choice, opting for treatments that use mechanisms outside of mitochondrial apoptosis to kill cells. Refractory DLBCL is also consistent with increased levels of ctDNA before, during and end of therapy, which highlights persistent disease in response to treatment. Serial sampling using our novel gene panel has clearly identified the ability to track stable and/or progressive disease in response to treatment and supports the exploration of ctDNA monitoring in routine clinical follow up. Finally, we have also identified genetic lesions common to REFR DLBCL that may contribute to an underlying mutational profile. These include genes implicated in cell survival and disease progression: *MYC*, *BCL2*, *EP300*, *MAP2K1*, and *BTG1*. Further analysis of potential combinations of genetic and phenotypic observations made here is ongoing to help define rrDLBCL as early as possible in the clinical setting.

Future challenges in the identification of REFR DLBCL include the application of either functional assays (e.g. BH3 profiling) or ctDNA analysis to clinical settings, which will require extensive validation and standardization. While apoptotic resistance and pro-apoptotic defects appear to be an innate characteristic of REFR DLBCL, additional experiments are needed to

fully elucidate the mechanism of dysfunctional BAX/BAK. These will include previously mentioned genomic (WGS) and transcriptomic analysis of class A, B, and C samples used in our BH3 study. These results will identify potential mutations or additional proteins involved in dysfunctional anchoring and/or pore formation of BAX/BAK to the mitochondrial membrane, or other unknown mechanisms contributing to this phenotype. Moreover, as additional samples are analyzed using our novel rrDLBCL ctDNA panel, follow-up studies may help develop mutational signatures associated specifically with REFR DLBCL or chemo-resistance, as well as chemo-sensitive DLBCL. These signatures should then be compared to existing genetic classification (e.g. LymphGen) or gene expression profiles (DZsig) to further elaborate on subtypes of DLBCL that are likely to be refractory to frontline treatment.

In conclusion, this thesis has contributed to the growing understanding of rrDLBCL in the context of DLBCL apoptotic function, as well as the translation of ctDNA analysis in identifying refractory cases during multiple treatment settings, which display specific ctDNA dynamics and mutations implicated in aggressive therapeutic resistance. These findings should help design improved rrDLBCL management strategies after further validation of refractory mutational profiles and prognostic ctDNA monitoring is established for clinical use.

Chapter 6: References

1. Coiffier, B.; Lepage, E.; Brière, J.; Herbrecht, R.; Tilly, H.; Bouabdallah, R.; Morel, P.; Van Den Neste, E.; Salles, G.; Gaulard, P.; et al. CHOP Chemotherapy plus Rituximab Compared with CHOP Alone in Elderly Patients with Diffuse Large-B-Cell Lymphoma. *N. Engl. J. Med.* **2002**, *346*, 235–242, doi:10.1056/NEJMoa011795.
2. Shipp, M.A.; Ross, K.N.; Tamayo, P.; Weng, A.P.; Kutok, J.L.; Aguiar, R.C.T.; Gaasenbeek, M.; Angelo, M.; Reich, M.; Pinkus, G.S.; et al. Diffuse Large B-Cell Lymphoma Outcome Prediction by Gene-Expression Profiling and Supervised Machine Learning. *Nat. Med.* **2002**, *8*, 68–74, doi:10.1038/nm0102-68.
3. Aukema, S.M.; Siebert, R.; Schuurin, E.; van Imhoff, G.W.; Kluin-Nelemans, H.C.; Boerma, E.-J.; Kluin, P.M. Double-Hit B-Cell Lymphomas. *Blood* **2011**, *117*, 2319–2331, doi:10.1182/blood-2010-09-297879.
4. Alaggio, R.; Amador, C.; Anagnostopoulos, I.; Attygalle, A.D.; Araujo, I.B. de O.; Berti, E.; Bhagat, G.; Borges, A.M.; Boyer, D.; Calaminici, M.; et al. The 5th Edition of the World Health Organization Classification of Haematolymphoid Tumours: Lymphoid Neoplasms. *Leukemia* **2022**, *36*, 1720–1748, doi:10.1038/s41375-022-01620-2.
5. Chapuy, B.; Stewart, C.; Dunford, A.J.; Kim, J.; Kamburov, A.; Redd, R.A.; Lawrence, M.S.; Roemer, M.G.M.; Li, A.J.; Ziepert, M.; et al. Molecular Subtypes of Diffuse Large B Cell Lymphoma Are Associated with Distinct Pathogenic Mechanisms and Outcomes. *Nat. Med.* **2018**, *24*, 679–690, doi:10.1038/s41591-018-0016-8.
6. Wright, G.W.; Huang, D.W.; Phelan, J.D.; Coulibaly, Z.A.; Roulland, S.; Young, R.M.; Wang, J.Q.; Schmitz, R.; Morin, R.D.; Tang, J.; et al. A Probabilistic Classification Tool

- for Genetic Subtypes of Diffuse Large B Cell Lymphoma with Therapeutic Implications. *Cancer Cell* **2020**, *37*, 551-568.e14, doi:10.1016/j.ccell.2020.03.015.
7. Ennishi, D.; Jiang, A.; Boyle, M.; Collinge, B.; Grande, B.M.; Ben-Neriah, S.; Rushton, C.; Tang, J.; Thomas, N.; Slack, G.W.; et al. Double-Hit Gene Expression Signature Defines a Distinct Subgroup of Germinal Center B-Cell-Like Diffuse Large B-Cell Lymphoma. *J. Clin. Oncol. Off. J. Am. Soc. Clin. Oncol.* **2019**, *37*, 190–201, doi:10.1200/JCO.18.01583.
 8. Alduaij, W.; Collinge, B.; Ben-Neriah, S.; Jiang, A.; Hilton, L.K.; Boyle, M.; Meissner, B.; Chong, L.; Miyata-Takata, T.; Slack, G.W.; et al. Molecular Determinants of Clinical Outcomes in a Real-World Diffuse Large B-Cell Lymphoma Population. *Blood* **2023**, *141*, 2493–2507, doi:10.1182/blood.2022018248.
 9. Morin, R.D.; Assouline, S.; Alcaide, M.; Mohajeri, A.; Johnston, R.L.; Chong, L.; Grewal, J.; Yu, S.; Fornika, D.; Bushell, K.; et al. Genetic Landscapes of Relapsed and Refractory Diffuse Large B-Cell Lymphomas. *Clin. Cancer Res.* **2016**, *22*, 2290–2300, doi:10.1158/1078-0432.CCR-15-2123.
 10. Rushton, C.K.; Arthur, S.E.; Alcaide, M.; Cheung, M.; Jiang, A.; Coyle, K.M.; Cleary, K.L.S.; Thomas, N.; Hilton, L.K.; Michaud, N.; et al. Genetic and Evolutionary Patterns of Treatment Resistance in Relapsed B-Cell Lymphoma. *Blood Adv.* **2020**, *4*, 2886–2898, doi:10.1182/bloodadvances.2020001696.
 11. Kennedy, G.A.; Tey, S.-K.; Cobcroft, R.; Marlton, P.; Cull, G.; Grimmett, K.; Thomson, D.; Gill, D. Incidence and Nature of CD20-Negative Relapses Following Rituximab Therapy in Aggressive B-Cell Non-Hodgkin's Lymphoma: A Retrospective Review. *Br.*

- J. Haematol.* **2002**, *119*, 412–416, doi:10.1046/j.1365-2141.2002.03843.x.
12. Hiraga, J.; Tomita, A.; Sugimoto, T.; Shimada, K.; Ito, M.; Nakamura, S.; Kiyoi, H.; Kinoshita, T.; Naoe, T. Down-Regulation of CD20 Expression in B-Cell Lymphoma Cells after Treatment with Rituximab-Containing Combination Chemotherapies: Its Prevalence and Clinical Significance. *Blood* **2009**, *113*, 4885–4893, doi:10.1182/blood-2008-08-175208.
 13. Johnson, N.A.; Boyle, M.; Bashashati, A.; Leach, S.; Brooks-Wilson, A.; Sehn, L.H.; Chhanabhai, M.; Brinkman, R.R.; Connors, J.M.; Weng, A.P.; et al. Diffuse Large B-Cell Lymphoma: Reduced CD20 Expression Is Associated with an Inferior Survival. *Blood* **2009**, *113*, 3773–3780, doi:10.1182/blood-2008-09-177469.
 14. Rys, R.N.; Geoffrion, D.; Rushton, C.; Alcaide, M.; Santiago, R.; Mann, K.K.; Dmitrienko, S.; Petrogiannis-Haliois, T.; Assouline, S.; Morin, R.D.; et al. CD20 Is an Unstable Target in Primary-Refractory High-Grade Lymphomas. *Blood* **2019**, *134*, 1608, doi:10.1182/blood-2019-127129.
 15. Wilson, W.H.; Young, R.M.; Schmitz, R.; Yang, Y.; Pittaluga, S.; Wright, G.; Lih, C.J.; Williams, P.M.; Shaffer, A.L.; Gerecitano, J.; et al. Targeting B Cell Receptor Signaling with Ibrutinib in Diffuse Large B Cell Lymphoma. *Nat. Med.* **2015**, *21*, 922–926, doi:10.1038/nm.3884.
 16. Wilson, W.H.; Wright, G.W.; Huang, D.W.; Hodgkinson, B.; Balasubramanian, S.; Fan, Y.; Vermeulen, J.; Shreeve, M.; Staudt, L.M. Effect of Ibrutinib with R-CHOP Chemotherapy in Genetic Subtypes of DLBCL. *Cancer Cell* **2021**, *39*, 1643-1653.e3, doi:10.1016/j.ccell.2021.10.006.

17. Sehn, L.H.; Herrera, A.F.; Flowers, C.R.; Kamdar, M.K.; McMillan, A.; Hertzberg, M.; Assouline, S.; Kim, T.M.; Kim, W.S.; Ozcan, M.; et al. Polatuzumab Vedotin in Relapsed or Refractory Diffuse Large B-Cell Lymphoma. *J. Clin. Oncol. Off. J. Am. Soc. Clin. Oncol.* **2020**, *38*, 155–165, doi:10.1200/JCO.19.00172.
18. Tilly, H.; Morschhauser, F.; Sehn, L.H.; Friedberg, J.W.; Trněný, M.; Sharman, J.P.; Herbaux, C.; Burke, J.M.; Matasar, M.; Rai, S.; et al. Polatuzumab Vedotin in Previously Untreated Diffuse Large B-Cell Lymphoma. *N. Engl. J. Med.* **2022**, *386*, 351–363, doi:10.1056/nejmoa2115304.
19. Brown, J.R.; Hamadani, M.; Hayslip, J.; Janssens, A.; Wagner-Johnston, N.; Ottmann, O.; Arnason, J.; Tilly, H.; Millenson, M.; Offner, F.; et al. Voxtalisib (XL765) in Patients with Relapsed or Refractory Non-Hodgkin Lymphoma or Chronic Lymphocytic Leukaemia: An Open-Label, Phase 2 Trial. *Lancet Haematol.* **2018**, *5*, e170–e180, doi:10.1016/S2352-3026(18)30030-9.
20. Davids, M.S.; Roberts, A.W.; Seymour, J.F.; Pagel, J.M.; Kahl, B.S.; Wierda, W.G.; Puvvada, S.; Kipps, T.J.; Anderson, M.A.; Salem, A.H.; et al. Phase I First-in-Human Study of Venetoclax in Patients With Relapsed or Refractory Non-Hodgkin Lymphoma. *J. Clin. Oncol.* **2017**, *35*, 826–833, doi:10.1200/JCO.2016.70.4320.
21. Gerecitano, J.F.; Roberts, A.W.; Seymour, J.F.; Wierda, W.G.; Kahl, B.S.; Pagel, J.M.; Puvvada, S.; Kipps, T.J.; Anderson, M.A.; Dunbar, M. A Phase 1 Study of Venetoclax (ABT-199/GDC-0199) Monotherapy in Patients with Relapsed/Refractory Non-Hodgkin Lymphoma. *Blood* **2015**, *126*, 254.
22. Lejeune, M.; Köse, M.C.; Duray, E.; Einsele, H.; Beguin, Y.; Caers, J. Bispecific, T-Cell-

- Recruiting Antibodies in B-Cell Malignancies. *Front. Immunol.* **2020**, *11*, doi:10.3389/fimmu.2020.00762.
23. Einsele, H.; Borghaei, H.; Orlowski, R.Z.; Subklewe, M.; Roboz, G.J.; Zugmaier, G.; Kufer, P.; Iskander, K.; Kantarjian, H.M. The BiTE (Bispecific T-Cell Engager) Platform: Development and Future Potential of a Targeted Immuno-Oncology Therapy across Tumor Types. *Cancer* **2020**, *126*, 3192–3201, doi:https://doi.org/10.1002/cncr.32909.
24. Goebeler, M.E.; Knop, S.; Viardot, A.; Kufer, P.; Topp, M.S.; Einsele, H.; Noppeney, R.; Hess, G.; Kallert, S.; Mackensen, A.; et al. Bispecific T-Cell Engager (BiTE) Antibody Construct Blinatumomab for the Treatment of Patients with Relapsed/Refractory Non-Hodgkin Lymphoma: Final Results from a Phase I Study. *J. Clin. Oncol.* **2016**, *34*, 1104–1111, doi:10.1200/JCO.2014.59.1586.
25. Dickinson, M.; Carlo-Stella, C.; Morschhauser, F.; Bachy, E.; Corradini, P.; Iacoboni, G.; Khan, C.; Wrobel, T.; Offner, F.; Trneny, M. Glofitamab in Patients with Relapsed/Refractory (R/R) Diffuse Large B-Cell Lymphoma (DLBCL) And ≥ 2 Prior Therapies: Pivotal Phase II Expansion Results. *J Clin Oncol* **2022**, *40*, 7500.
26. Falchi, L.; Vardhana, S.A.; Salles, G.A. Bispecific Antibodies for the Treatment of B-Cell Lymphoma: Promises, Unknowns, and Opportunities. *Blood* **2023**, *141*, 467–480, doi:10.1182/blood.2021011994.
27. Falchi, L.; Jardin, F.; Haioun, C.; Wrobel, T.; Joergensen, J.M.; Bastos-Oreiro, M.; Mou, E.; Martinez-Lopez, J.; Budde, L.E.; Bartlett, N.L.; et al. Glofitamab (Glofit) Plus R-CHOP Has a Favorable Safety Profile and Induces High Response Rates in Patients with Previously Untreated (1L) Large B-Cell Lymphoma (LBCL) Defined As High Risk By

- Circulating Tumor DNA (CtDNA) Dynamics: Preliminary Safety and E. *Blood* **2023**, *142*, 858, doi:10.1182/blood-2023-173953.
28. June, C.H.; O'Connor, R.S.; Kawalekar, O.U.; Ghassemi, S.; Milone, M.C. CAR T Cell Immunotherapy for Human Cancer. *Science (80-.)*. **2018**, *359*, 1361–1365, doi:10.1126/science.aar6711.
 29. Locke, F.L.; Ghobadi, A.; Jacobson, C.A.; Miklos, D.B.; Lekakis, L.J.; Oluwole, O.O.; Lin, Y.; Braunschweig, I.; Hill, B.T.; Timmerman, J.M.; et al. Long-Term Safety and Activity of Axicabtagene Ciloleucel in Refractory Large B-Cell Lymphoma (ZUMA-1): A Single-Arm, Multicentre, Phase 1–2 Trial. *Lancet Oncol.* **2019**, *20*, 31–42, doi:10.1016/S1470-2045(18)30864-7.
 30. Schuster, S.J.; Bishop, M.R.; Tam, C.S.; Waller, E.K.; Borchmann, P.; McGuirk, J.P.; Jäger, U.; Jaglowski, S.; Andreadis, C.; Westin, J.R.; et al. Tisagenlecleucel in Adult Relapsed or Refractory Diffuse Large B-Cell Lymphoma. *N. Engl. J. Med.* **2019**, *380*, 45–56, doi:10.1056/nejmoa1804980.
 31. Abramson, J.S.; Palomba, M.L.; Gordon, L.I.; Lunning, M.A.; Wang, M.; Arnason, J.; Mehta, A.; Purev, E.; Maloney, D.G.; Andreadis, C.; et al. Lisocabtagene Maraleucel for Patients with Relapsed or Refractory Large B-Cell Lymphomas (TRANSCEND NHL 001): A Multicentre Seamless Design Study. *Lancet* **2020**, *396*, 839–852, doi:10.1016/S0140-6736(20)31366-0.
 32. Caballero, A.C.; Escribà-Garcia, L.; Alvarez-Fernández, C.; Briones, J. CAR T-Cell Therapy Predictive Response Markers in Diffuse Large B-Cell Lymphoma and Therapeutic Options After CART19 Failure. *Front. Immunol.* **2022**, *13*, 1–19,

doi:10.3389/fimmu.2022.904497.

33. Bishop, M.R.; Maziarz, R.T.; Waller, E.K.; Jäger, U.; Westin, J.R.; McGuirk, J.P.; Fleury, I.; Holte, H.; Borchmann, P.; del Corral, C.; et al. Tisagenlecleucel in Relapsed/Refractory Diffuse Large B-Cell Lymphoma Patients without Measurable Disease at Infusion. *Blood Adv.* **2019**, *3*, 2230–2236, doi:10.1182/bloodadvances.2019000151.
34. Wudhikarn, K.; Tomas, A.A.; Flynn, J.R.; Devlin, S.M.; Brower, J.; Bachanova, V.; Nastoupil, L.J.; McGuirk, J.P.; Maziarz, R.T.; Oluwole, O.O.; et al. Low Toxicity and Excellent Outcomes in Patients with DLBCL without Residual Lymphoma at the Time of CD19 CAR T-Cell Therapy. *Blood Adv.* **2023**, *7*, 3192–3198, doi:10.1182/bloodadvances.2022008294.
35. Cappell, K.M.; Kochenderfer, J.N. Long-Term Outcomes Following CAR T Cell Therapy: What We Know so Far. *Nat. Rev. Clin. Oncol.* **2023**, *20*, 359–371, doi:10.1038/s41571-023-00754-1.
36. Locke, F.L.; Miklos, D.B.; Jacobson, C.A.; Perales, M.-A.; Kersten, M.-J.; Oluwole, O.O.; Ghobadi, A.; Rapoport, A.P.; McGuirk, J.; Pagel, J.M.; et al. Axicabtagene Ciloleucel as Second-Line Therapy for Large B-Cell Lymphoma. *N. Engl. J. Med.* **2022**, *386*, 640–654, doi:10.1056/nejmoa2116133.
37. Kamdar, M.; Solomon, S.R.; Arnason, J.; Johnston, P.B.; Glass, B.; Bachanova, V.; Ibrahimi, S.; Mielke, S.; Mutsaers, P.; Hernandez-Ilizaliturri, F.; et al. Lisocabtagene Maraleucel versus Standard of Care with Salvage Chemotherapy Followed by Autologous Stem Cell Transplantation as Second-Line Treatment in Patients with Relapsed or Refractory Large B-Cell Lymphoma (TRANSFORM): Results from an

- Interim Analys. *Lancet (London, England)* **2022**, 399, 2294–2308, doi:10.1016/S0140-6736(22)00662-6.
38. Lebien, T.W.; Tedder, T.F. B Lymphocytes: How They Develop and Function. *Blood* **2008**, 112, 1570–1580, doi:10.1182/blood-2008-02-078071.
39. Brack, C.; Hirama, M.; Lenhard-Schuller, R.; Tonegawa, S. A Complete Immunoglobulin Gene Is Created by Somatic Recombination. *Cell* **1978**, 15, 1–14, doi:10.1016/0092-8674(78)90078-8.
40. HONJO, T. Immunoglobulin Genes. *Annu. Rev. Immunol.* **1983**, 1, 499–528.
41. Bengtén, E.; Wilson, M.; Miller, N.; Clem, L.W.; Pilström, L.; Warr, G.W. Immunoglobulin Isotypes: Structure, Function, and Genetics. *Curr. Top. Microbiol. Immunol.* **2000**, 248, 189–219, doi:10.1007/978-3-642-59674-2_9.
42. Dal Porto, J.M.; Gauld, S.B.; Merrell, K.T.; Mills, D.; Pugh-Bernard, A.E.; Cambier, J. B Cell Antigen Receptor Signaling 101. *Mol. Immunol.* **2004**, 41, 599–613, doi:10.1016/j.molimm.2004.04.008.
43. Lam, K.P.; Kühn, R.; Rajewsky, K. In Vivo Ablation of Surface Immunoglobulin on Mature B Cells by Inducible Gene Targeting Results in Rapid Cell Death. *Cell* **1997**, 90, 1073–1083, doi:10.1016/s0092-8674(00)80373-6.
44. Xu, W.; Berning, P.; Lenz, G. Targeting B-Cell Receptor and PI3K Signaling in Diffuse Large B-Cell Lymphoma. *Blood* **2021**, 138, 1110–1119, doi:10.1182/blood.2020006784.
45. Rickert, R.C. New Insights into Pre-BCR and BCR Signalling with Relevance to B Cell Malignancies. *Nat. Rev. Immunol.* **2013**, 13, 578–591, doi:10.1038/nri3487.

46. Wilson, W.H.; Young, R.M.; Schmitz, R.; Yang, Y.; Pittaluga, S.; Wright, G.; Lih, C.-J.; Williams, P.M.; Shaffer, A.L.; Gerecitano, J.; et al. Targeting B Cell Receptor Signaling with Ibrutinib in Diffuse Large B Cell Lymphoma. *Nat. Med.* **2015**, *21*, 922–926, doi:10.1038/nm.3884.
47. Hardy, R.R.; Hayakawa, K. B Cell Development Pathways. *Annu. Rev. Immunol.* **2001**, *19*, 595–621, doi:10.1146/annurev.immunol.19.1.595.
48. Zhang, M.; Srivastava, G.; Lu, L. The Pre-B Cell Receptor and Its Function during B Cell Development. *Cell. Mol. Immunol.* **2004**, *1*, 89–94.
49. Tedder, T.F.; Zhou, L.J.; Engel, P. The CD19/CD21 Signal Transduction Complex of B Lymphocytes. *Immunol. Today* **1994**, *15*, 437–442, doi:10.1016/0167-5699(94)90274-7.
50. Stashenko, P.; Nadler, L.M.; Hardy, R.; Schlossman, S.F. Characterization of a Human B Lymphocyte-Specific Antigen. *J. Immunol.* **1980**, *125*, 1678–1685.
51. Smith, M.R. Rituximab (Monoclonal Anti-CD20 Antibody): Mechanisms of Action and Resistance. *Oncogene* **2003**, *22*, 7359–7368, doi:10.1038/sj.onc.1206939.
52. Reff, M.E.; Carner, K.; Chambers, K.S.; Chinn, P.C.; Leonard, J.E.; Raab, R.; Newman, R.A.; Hanna, N.; Anderson, D.R. Depletion of B Cells in Vivo by a Chimeric Mouse Human Monoclonal Antibody to CD20. *Blood* **1994**, *83*, 435–445, doi:10.1182/blood.v83.2.435.bloodjournal832435.
53. Stavnezer, J.; Guikema, J.E.J.; Schrader, C.E. Mechanism and Regulation of Class Switch Recombination. *Annu. Rev. Immunol.* **2008**, *26*, 261–292, doi:10.1146/annurev.immunol.26.021607.090248.

54. Stavnezer, J. Immunoglobulin Class Switching Cytokines Direct Switching by Regulating Germline Transcription. *Curr. Opin. Immunol.* **1996**, *8*, 199–205.
55. Muramatsu, M.; Kinoshita, K.; Fagarasan, S.; Yamada, S.; Shinkai, Y.; Honjo, T. Class Switch Recombination and Hypermutation Require Activation-Induced Cytidine Deaminase (AID), a Potential RNA Editing Enzyme. *Cell* **2000**, *102*, 553–563, doi:10.1016/S0092-8674(00)00078-7.
56. Okazaki, I.; Kotani, A.; Honjo, T. Role of AID in Tumorigenesis. *Adv. Immunol.* **2007**, *94*, 245–273, doi:10.1016/S0065-2776(06)94008-5.
57. Pasqualucci, L.; Bhagat, G.; Jankovic, M.; Compagno, M.; Smith, P.; Muramatsu, M.; Honjo, T.; Morse, H.C.; Nussenzweig, M.C.; Dalla-Favera, R. AID Is Required for Germinal Center-Derived Lymphomagenesis. *Nat. Genet.* **2008**, *40*, 108–112, doi:10.1038/ng.2007.35.
58. Mesin, L.; Ersching, J.; Victora, G.D. Germinal Center B Cell Dynamics. *Immunity* **2016**, *45*, 471–482, doi:10.1016/j.immuni.2016.09.001.
59. Klein, U.; Dalla-Favera, R. Germinal Centres: Role in B-Cell Physiology and Malignancy. *Nat. Rev. Immunol.* **2008**, *8*, 22–33, doi:10.1038/nri2217.
60. Victora, G.D.; Dominguez-Sola, D.; Holmes, A.B.; Deroubaix, S.; Dalla-Favera, R.; Nussenzweig, M.C. Identification of Human Germinal Center Light and Dark Zone Cells and Their Relationship to Human B-Cell Lymphomas. *Blood* **2012**, *120*, 2240–2248, doi:10.1182/blood-2012-03-415380.
61. Pelengaris, S.; Khan, M.; Evan, G. C-MYC: More than Just a Matter of Life and Death.

- Nat. Rev. Cancer* **2002**, *2*, 764–776, doi:10.1038/nrc904.
62. Calado, D.P.; Sasaki, Y.; Godinho, S.A.; Pellerin, A.; Köchert, K.; Sleckman, B.P.; de Alborán, I.M.; Janz, M.; Rodig, S.; Rajewsky, K. The Cell-Cycle Regulator c-Myc Is Essential for the Formation and Maintenance of Germinal Centers. *Nat. Immunol.* **2012**, *13*, 1092–1100, doi:10.1038/ni.2418.
63. Dominguez-Sola, D.; Vitoria, G.D.; Ying, C.Y.; Phan, R.T.; Saito, M.; Nussenzweig, M.C.; Dalla-Favera, R. The Proto-Oncogene MYC Is Required for Selection in the Germinal Center and Cyclic Reentry. *Nat. Immunol.* **2012**, *13*, 1083–1091, doi:10.1038/ni.2428.
64. Canadian Cancer Statistics Advisory Committee in collaboration with the Canadian Cancer Society, S.C. and the P.H.A. of C. *Canadian Cancer Statistics 2023*; Toronto, ON, 2023;
65. Siegel, R.L.; Miller, K.D.; Jemal, A. Cancer Statistics, 2019. *CA. Cancer J. Clin.* **2019**, *69*, 7–34, doi:10.3322/caac.21551.
66. Grogg, K.L.; Miller, R.F.; Dogan, A. HIV Infection and Lymphoma. *J. Clin. Pathol.* **2007**, *60*, 1365–1372, doi:10.1136/jcp.2007.051953.
67. Vockerodt, M.; Yap, L.-F.; Shannon-Lowe, C.; Curley, H.; Wei, W.; Vrzalikova, K.; Murray, P.G. The Epstein–Barr Virus and the Pathogenesis of Lymphoma. *J. Pathol.* **2015**, *235*, 312–322, doi:https://doi.org/10.1002/path.4459.
68. Swerdlow, S.H.; Campo, E.; Pileri, S.A.; Harris, N.L.; Stein, H.; Siebert, R.; Advani, R.; Ghielmini, M.; Salles, G.A.; Zelenetz, A.D.; et al. The 2016 Revision of the World Health

- Organization Classification of Lymphoid Neoplasms. *Blood* **2016**, *127*, 2375–2390, doi:10.1182/blood-2016-01-643569.
69. Shankland, K.R.; Armitage, J.O.; Hancock, B.W.; Park, W. Non-Hodgkin Lymphoma. **2012**.
70. Li, S.; Young, K.H.; Medeiros, L.J. Diffuse Large B-Cell Lymphoma. *Pathology* **2018**, *50*, 74–87, doi:10.1016/j.pathol.2017.09.006.
71. Casulo, C.; Burack, W.R.; Friedberg, J.W. Transformed Follicular Non-Hodgkin Lymphoma. *Blood* **2015**, *125*, 40–47, doi:10.1182/blood-2014-04-516815.
72. Montoto, S.; Fitzgibbon, J. Transformation of Indolent B-Cell Lymphomas. *J. Clin. Oncol.* **2011**, *29*, 1827–1834.
73. A Predictive Model for Aggressive Non-Hodgkin’s Lymphoma. *N. Engl. J. Med.* **1993**, *329*, 987–994, doi:10.1056/NEJM199309303291402.
74. Zhou, Z.; Sehn, L.H.; Rademaker, A.W.; Gordon, L.I.; LaCasce, A.S.; Crosby-Thompson, A.; Vanderplas, A.; Zelenetz, A.D.; Abel, G.A.; Rodriguez, M.A.; et al. An Enhanced International Prognostic Index (NCCN-IPI) for Patients with Diffuse Large B-Cell Lymphoma Treated in the Rituximab Era. *Blood* **2014**, *123*, 837–842, doi:10.1182/blood-2013-09-524108.
75. Sehn, L.H.; Berry, B.; Chhanabhai, M.; Fitzgerald, C.; Gill, K.; Hoskins, P.; Klasa, R.; Savage, K.J.; Shenkier, T.; Sutherland, J.; et al. The Revised International Prognostic Index (R-IPI) Is a Better Predictor of Outcome than the Standard IPI for Patients with Diffuse Large B-Cell Lymphoma Treated with R-CHOP. *Blood* **2006**, *109*, 1857–1861,

doi:10.1182/blood-2006-08-038257.

76. Ruppert, A.S.; Dixon, J.G.; Salles, G.; Wall, A.; Cunningham, D.; Poeschel, V.; Haioun, C.; Tilly, H.; Ghesquieres, H.; Ziepert, M.; et al. International Prognostic Indices in Diffuse Large B-Cell Lymphoma: A Comparison of IPI, R-IPI, and NCCN-IPI. *Blood* **2020**, *135*, 2041–2048, doi:10.1182/blood.2019002729.
77. Sehn, L.H.; Salles, G. Diffuse Large B-Cell Lymphoma. *N. Engl. J. Med.* **2021**, *384*, 842–858, doi:10.1056/NEJMra2027612.
78. Liu, Y.; Barta, S.K. Diffuse Large B-Cell Lymphoma: 2019 Update on Diagnosis, Risk Stratification, and Treatment. *Am. J. Hematol.* **2019**, *94*, 604–616, doi:10.1002/ajh.25460.
79. Alizadeh, A.A.; Elsen, M.B.; Davis, R.E.; Ma, C.L.; Lossos, I.S.; Rosenwald, A.; Boldrick, J.C.; Sabet, H.; Tran, T.; Yu, X.; et al. Distinct Types of Diffuse Large B-Cell Lymphoma Identified by Gene Expression Profiling. *Nature* **2000**, *403*, 503–511, doi:10.1038/35000501.
80. Lenz, G.; Wright, G.; Dave, S.S.; Xiao, W.; Powell, J.; Zhao, H.; Xu, W.; Tan, B.; Goldschmidt, N.; Iqbal, J.; et al. Stromal Gene Signatures in Large-B-Cell Lymphomas. *N. Engl. J. Med.* **2008**, *359*, 2313–2323, doi:10.1056/NEJMoa0802885.
81. Scott, D.W.; Mottok, A.; Ennishi, D.; Wright, G.W.; Farinha, P.; Ben-Neriah, S.; Kridel, R.; Barry, G.S.; Hother, C.; Abrisqueta, P.; et al. Prognostic Significance of Diffuse Large B-Cell Lymphoma Cell of Origin Determined by Digital Gene Expression in Formalin-Fixed Paraffin-Embedded Tissue Biopsies. *J. Clin. Oncol. Off. J. Am. Soc. Clin. Oncol.* **2015**, *33*, 2848–2856, doi:10.1200/JCO.2014.60.2383.

82. Meyer, P.N.; Fu, K.; Greiner, T.C.; Smith, L.M.; Delabie, J.; Gascoyne, R.D.; Ott, G.; Rosenwald, A.; Braziel, R.M.; Campo, E.; et al. Immunohistochemical Methods for Predicting Cell of Origin and Survival in Patients with Diffuse Large B-Cell Lymphoma Treated with Rituximab. *J. Clin. Oncol. Off. J. Am. Soc. Clin. Oncol.* **2011**, *29*, 200–207, doi:10.1200/JCO.2010.30.0368.
83. Kawasaki, C.; Ohshima, K.; Suzumtya, J.; Kanda, M.; Tsuchiya, T.; Tamura, K.; Kikuchi, M. Rearrangements of Bcl-1, Bcl-2, Bcl-6, and c-Myc in Diffuse Large B-Cell Lymphomas. *Leuk. Lymphoma* **2001**, *42*, 1099–1106.
84. Kramer, M.H.; Hermans, J.; Wijburg, E.; Philippo, K.; Geelen, E.; van Krieken, J.H.; de Jong, D.; Maartense, E.; Schuurin, E.; Kluin, P.M. Clinical Relevance of BCL2, BCL6, and MYC Rearrangements in Diffuse Large B-Cell Lymphoma. *Blood* **1998**, *92*, 3152–3162.
85. Wiktor, A.E.; Van Dyke, D.L.; Stupca, P.J.; Ketterling, R.P.; Thorland, E.C.; Shearer, B.M.; Fink, S.R.; Stockero, K.J.; Majorowicz, J.R.; Dewald, G.W. Preclinical Validation of Fluorescence in Situ Hybridization Assays for Clinical Practice. *Genet. Med.* **2006**, *8*, 16–23, doi:10.1097/01.gim.0000195645.00446.61.
86. Scott, D.W.; King, R.L.; Staiger, A.M.; Ben-Neriah, S.; Jiang, A.; Horn, H.; Mottok, A.; Farinha, P.; Slack, G.W.; Ennishi, D.; et al. High-Grade B-Cell Lymphoma with MYC and BCL2 and/or BCL6 Rearrangements with Diffuse Large B-Cell Lymphoma Morphology. *Blood* **2018**, *131*, 2060–2064, doi:10.1182/blood-2017-12-820605.
87. Rosenwald, A.; Bens, S.; Advani, R.; Barrans, S.; Copie-Bergman, C.; Elsensohn, M.-H.; Natkunam, Y.; Calaminici, M.; Sander, B.; Baia, M.; et al. Prognostic Significance of

- MYC Rearrangement and Translocation Partner in Diffuse Large B-Cell Lymphoma: A Study by the Lunenburg Lymphoma Biomarker Consortium. *J. Clin. Oncol. Off. J. Am. Soc. Clin. Oncol.* **2019**, *37*, 3359–3368, doi:10.1200/JCO.19.00743.
88. Johnson, N.A.; Slack, G.W.; Savage, K.J.; Connors, J.M.; Ben-Neriah, S.; Rogic, S.; Scott, D.W.; Tan, K.L.; Steidl, C.; Sehn, L.H.; et al. Concurrent Expression of MYC and BCL2 in Diffuse Large B-Cell Lymphoma Treated with Rituximab plus Cyclophosphamide, Doxorubicin, Vincristine, and Prednisone. *J. Clin. Oncol.* **2012**, *30*, 3452–3459, doi:10.1200/JCO.2011.41.0985.
89. Savage, K.J.; Slack, G.W.; Mottok, A.; Sehn, L.H.; Villa, D.; Kansara, R.; Kridel, R.; Steidl, C.; Ennishi, D.; Tan, K.L.; et al. Impact of Dual Expression of MYC and BCL2 by Immunohistochemistry on the Risk of CNS Relapse in DLBCL. *Blood* **2016**, *127*, 2182–2188, doi:10.1182/blood-2015-10-676700.
90. Hu, S.; Xu-Monette, Z.Y.; Tzankov, A.; Green, T.; Wu, L.; Balasubramanyam, A.; Liu, W.; Visco, C.; Li, Y.; Miranda, R.N.; et al. MYC/BCL2 Protein Coexpression Contributes to the Inferior Survival of Activated B-Cell Subtype of Diffuse Large B-Cell Lymphoma and Demonstrates High-Risk Gene Expression Signatures: A Report from The International DLBCL Rituximab-CHOP Consortium Program. *Blood* **2013**, *121*, 4021–4031, doi:10.1182/blood-2012-10-460063.
91. Riedell, P.A.; Smith, S.M. Double Hit and Double Expressors in Lymphoma: Definition and Treatment. *Cancer* **2018**, *124*, 4622–4632, doi:https://doi.org/10.1002/cncr.31646.
92. Morin, R.D.; Mungall, K.; Pleasance, E.; Mungall, A.J.; Goya, R.; Huff, R.D.; Scott, D.W.; Ding, J.; Roth, A.; Chiu, R.; et al. Mutational and Structural Analysis of Diffuse

- Large B-Cell Lymphoma Using Whole-Genome Sequencing. *Blood* **2013**, *122*, 1256–1265, doi:10.1182/blood-2013-02-483727.
93. Pasqualucci, L.; Dalla-Favera, R. Genetics of Diffuse Large B-Cell Lymphoma. *Blood* **2018**, *131*, 2307–2319, doi:10.1182/blood-2017-11-764332.
94. Davis, R.E.; Ngo, V.N.; Lenz, G.; Tolar, P.; Young, R.M.; Romesser, P.B.; Kohlhammer, H.; Lamy, L.; Zhao, H.; Yang, Y.; et al. Chronic Active B-Cell-Receptor Signalling in Diffuse Large B-Cell Lymphoma. *Nature* **2010**, *463*, 88–92, doi:10.1038/nature08638.
95. Lenz, G.; Davis, R.E.; Ngo, V.N.; Lam, L.; George, T.C.; Wright, G.W.; Dave, S.S.; Zhao, H.; Xu, W.; Rosenwald, A.; et al. Oncogenic CARD11 Mutations in Human Diffuse Large B Cell Lymphoma. *Science* **2008**, *319*, 1676–1679, doi:10.1126/science.1153629.
96. ten Hacken, E.; Burger, J.A. Molecular Pathways: Targeting the Microenvironment in Chronic Lymphocytic Leukemia--Focus on the B-Cell Receptor. *Clin. Cancer Res.* **2014**, *20*, 548–556, doi:10.1158/1078-0432.CCR-13-0226.
97. Jain, N.; Keating, M.; Thompson, P.; Ferrajoli, A.; Burger, J.; Borthakur, G.; Takahashi, K.; Estrov, Z.; Fowler, N.; Kadia, T.; et al. Ibrutinib and Venetoclax for First-Line Treatment of CLL. *N. Engl. J. Med.* **2019**, *380*, 2095–2103, doi:10.1056/NEJMoa1900574.
98. Younes, A.; Brody, J.; Carpio, C.; Lopez-Guillermo, A.; Ben-Yehuda, D.; Ferhanoglu, B.; Nagler, A.; Ozcan, M.; Avivi, I.; Bosch, F.; et al. Safety and Activity of Ibrutinib in Combination with Nivolumab in Patients with Relapsed Non-Hodgkin Lymphoma or Chronic Lymphocytic Leukaemia: A Phase 1/2a Study. *Lancet Haematol.* **2019**, *6*, e67–e78, doi:10.1016/S2352-3026(18)30217-5.

99. Sauter, C.S.; Matasar, M.J.; Schoder, H.; Devlin, S.M.; Drullinsky, P.; Gerecitano, J.; Kumar, A.; Noy, A.; Palomba, M.L.; Portlock, C.S.; et al. A Phase 1 Study of Ibrutinib in Combination with R-ICE in Patients with Relapsed or Primary Refractory DLBCL. *Blood* **2018**, *131*, 1805–1808, doi:10.1182/blood-2017-08-802561.
100. Morschhauser, F.; Flinn, I.W.; Advani, R.; Sehn, L.H.; Diefenbach, C.; Kolibaba, K.; Press, O.W.; Salles, G.; Tilly, H.; Chen, A.I.; et al. Polatuzumab Vedotin or Pinatuzumab Vedotin plus Rituximab in Patients with Relapsed or Refractory Non-Hodgkin Lymphoma: Final Results from a Phase 2 Randomised Study (ROMULUS). *Lancet Haematol.* **2019**, *6*, e254–e265, doi:10.1016/S2352-3026(19)30026-2.
101. Tilly, H.; Morschhauser, F.; Bartlett, N.L.; Mehta, A.; Salles, G.; Haioun, C.; Munoz, J.; Chen, A.I.; Kolibaba, K.; Lu, D.; et al. Polatuzumab Vedotin in Combination with Immunochemotherapy in Patients with Previously Untreated Diffuse Large B-Cell Lymphoma: An Open-Label, Non-Randomised, Phase 1b-2 Study. *Lancet. Oncol.* **2019**, *20*, 998–1010, doi:10.1016/S1470-2045(19)30091-9.
102. Sehn, L.H.; Hertzberg, M.; Opat, S.; Herrera, A.F.; Assouline, S.; Flowers, C.R.; Kim, T.M.; McMillan, A.; Ozcan, M.; Safar, V.; et al. Polatuzumab Vedotin plus Bendamustine and Rituximab in Relapsed/Refractory DLBCL: Survival Update and New Extension Cohort Data. *Blood Adv.* **2022**, *6*, 533–543, doi:10.1182/bloodadvances.2021005794.
103. Ngo, V.N.; Young, R.M.; Schmitz, R.; Jhavar, S.; Xiao, W.; Lim, K.-H.; Kohlhammer, H.; Xu, W.; Yang, Y.; Zhao, H.; et al. Oncogenically Active MYD88 Mutations in Human Lymphoma. *Nature* **2011**, *470*, 115–119, doi:10.1038/nature09671.
104. Knittel, G.; Liedgens, P.; Korovkina, D.; Seeger, J.M.; Al-Baldawi, Y.; Al-Maarri, M.;

- Fritz, C.; Vlantis, K.; Bezhanova, S.; Scheel, A.H.; et al. B-Cell-Specific Conditional Expression of Myd88p.L252P Leads to the Development of Diffuse Large B-Cell Lymphoma in Mice. *Blood* **2016**, *127*, 2732–2741, doi:10.1182/blood-2015-11-684183.
105. Morin, R.D.; Assouline, S.; Alcaide, M.; Mohajeri, A.; Johnston, R.L.; Chong, L.; Grewal, J.; Yu, S.; Fornika, D.; Bushell, K.; et al. Genetic Landscapes of Relapsed and Refractory Diffuse Large B-Cell Lymphomas. *Clin. Cancer Res.* **2016**, *22*, 2290–2300, doi:10.1158/1078-0432.CCR-15-2123.
106. Ok, C.Y.; Chen, J.; Xu-Monette, Z.Y.; Tzankov, A.; Manyam, G.C.; Li, L.; Visco, C.; Montes-Moreno, S.; Dybkær, K.; Chiu, A.; et al. Clinical Implications of Phosphorylated STAT3 Expression in De Novo Diffuse Large B-Cell Lymphoma. *Clin. Cancer Res.* **2014**, *20*, 5113–5123, doi:10.1158/1078-0432.CCR-14-0683.
107. Morin, R.D.; Mendez-Lago, M.; Mungall, A.J.; Goya, R.; Mungall, K.L.; Corbett, R.D.; Johnson, N.A.; Severson, T.M.; Chiu, R.; Field, M.; et al. Frequent Mutation of Histone-Modifying Genes in Non-Hodgkin Lymphoma. *Nature* **2011**, *476*, 298–303, doi:10.1038/nature10351.
108. Zhang, J.; Dominguez-Sola, D.; Hussein, S.; Lee, J.-E.; Holmes, A.B.; Bansal, M.; Vlasevska, S.; Mo, T.; Tang, H.; Basso, K.; et al. Disruption of KMT2D Perturbs Germinal Center B Cell Development and Promotes Lymphomagenesis. *Nat. Med.* **2015**, *21*, 1190–1198, doi:10.1038/nm.3940.
109. Ortega-Molina, A.; Boss, I.W.; Canela, A.; Pan, H.; Jiang, Y.; Zhao, C.; Jiang, M.; Hu, D.; Agirre, X.; Niesvizky, I.; et al. The Histone Lysine Methyltransferase KMT2D Sustains a Gene Expression Program That Represses B Cell Lymphoma Development. *Nat. Med.*

- 2015**, *21*, 1199–1208, doi:10.1038/nm.3943.
110. Chambwe, N.; Kormaksson, M.; Geng, H.; De, S.; Michor, F.; Johnson, N.A.; Morin, R.D.; Scott, D.W.; Godley, L.A.; Gascoyne, R.D.; et al. Variability in DNA Methylation Defines Novel Epigenetic Subgroups of DLBCL Associated with Different Clinical Outcomes. *Blood* **2014**, *123*, 1699–1708, doi:10.1182/blood-2013-07-509885.
111. Caganova, M.; Carrisi, C.; Varano, G.; Mainoldi, F.; Zanardi, F.; Germain, P.-L.; George, L.; Alberghini, F.; Ferrarini, L.; Talukder, A.K.; et al. Germinal Center Dysregulation by Histone Methyltransferase EZH2 Promotes Lymphomagenesis. *J. Clin. Invest.* **2013**, *123*, 5009–5022, doi:10.1172/JCI70626.
112. Morin, R.D.; Johnson, N.A.; Severson, T.M.; Mungall, A.J.; An, J.; Goya, R.; Paul, J.E.; Boyle, M.; Woolcock, B.W.; Kuchenbauer, F.; et al. Somatic Mutations Altering EZH2 (Tyr641) in Follicular and Diffuse Large B-Cell Lymphomas of Germinal-Center Origin. *Nat. Genet.* **2010**, *42*, 181–185, doi:10.1038/ng.518.
113. McCabe, M.T.; Ott, H.M.; Ganji, G.; Korenchuk, S.; Thompson, C.; Van Aller, G.S.; Liu, Y.; Graves, A.P.; Della Pietra, A. 3rd; Diaz, E.; et al. EZH2 Inhibition as a Therapeutic Strategy for Lymphoma with EZH2-Activating Mutations. *Nature* **2012**, *492*, 108–112, doi:10.1038/nature11606.
114. Italiano, A.; Soria, J.-C.; Toulmonde, M.; Michot, J.-M.; Lucchesi, C.; Varga, A.; Coindre, J.-M.; Blakemore, S.J.; Clawson, A.; Suttle, B.; et al. Tazemetostat, an EZH2 Inhibitor, in Relapsed or Refractory B-Cell Non-Hodgkin Lymphoma and Advanced Solid Tumours: A First-in-Human, Open-Label, Phase 1 Study. *Lancet. Oncol.* **2018**, *19*, 649–659, doi:10.1016/S1470-2045(18)30145-1.

115. Pasqualucci, L.; Dominguez-Sola, D.; Chiarenza, A.; Fabbri, G.; Grunn, A.; Trifonov, V.; Kasper, L.H.; Lerach, S.; Tang, H.; Ma, J.; et al. Inactivating Mutations of Acetyltransferase Genes in B-Cell Lymphoma. *Nature* **2011**, *471*, 189–195, doi:10.1038/nature09730.
116. Zhang, J.; Vlasevska, S.; Wells, V.A.; Nataraj, S.; Holmes, A.B.; Duval, R.; Meyer, S.N.; Mo, T.; Basso, K.; Brindle, P.K.; et al. The CREBBP Acetyltransferase Is a Haploinsufficient Tumor Suppressor in B-Cell Lymphoma. *Cancer Discov.* **2017**, *7*, 322–337, doi:10.1158/2159-8290.CD-16-1417.
117. Guan, X.-W.; Wang, H.-Q.; Ban, W.-W.; Chang, Z.; Chen, H.-Z.; Jia, L.; Liu, F.-T. Novel HDAC Inhibitor Chidamide Synergizes with Rituximab to Inhibit Diffuse Large B-Cell Lymphoma Tumour Growth by Upregulating CD20. *Cell Death Dis.* **2020**, *11*, 20, doi:10.1038/s41419-019-2210-0.
118. Batlevi, C.L.; Crump, M.; Andreadis, C.; Rizzieri, D.; Assouline, S.E.; Fox, S.; van der Jagt, R.H.C.; Copeland, A.; Potvin, D.; Chao, R.; et al. A Phase 2 Study of Mocetinostat, a Histone Deacetylase Inhibitor, in Relapsed or Refractory Lymphoma. *Br. J. Haematol.* **2017**, *178*, 434–441, doi:10.1111/bjh.14698.
119. Barnes, J.A.; Redd, R.; Fisher, D.C.; Hochberg, E.P.; Takvorian, T.; Neuberg, D.; Jacobsen, E.; Abramson, J.S. Panobinostat in Combination with Rituximab in Heavily Pretreated Diffuse Large B-Cell Lymphoma: Results of a Phase II Study. *Hematol. Oncol.* **2018**, *36*, 633–637, doi:10.1002/hon.2515.
120. Ocio, E.M.; Moreau, P.; Veskovski, L.; Warzocha, K.; White, D.; Chuncharunee, S.; de la Rubia, J.; Wang, M.-C.; Pulini, S.; Shelekhova, T.; et al. Panobinostat plus Bortezomib

- and Dexamethasone versus Placebo plus Bortezomib and Dexamethasone in Patients with Relapsed or Relapsed and Refractory Multiple Myeloma: A Multicentre, Randomised, Double-Blind Phase 3 Trial. *Lancet Oncol.* **2014**, *15*, 1195–1206, doi:10.1016/s1470-2045(14)70440-1.
121. Horn, H.; Ziepert, M.; Becher, C.; Barth, T.F.E.; Bernd, H.-W.; Feller, A.C.; Klapper, W.; Hummel, M.; Stein, H.; Hansmann, M.-L.; et al. MYC Status in Concert with BCL2 and BCL6 Expression Predicts Outcome in Diffuse Large B-Cell Lymphoma. *Blood* **2013**, *121*, 2253–2263, doi:10.1182/blood-2012-06-435842.
122. Epperla, N.; Maddocks, K.J.; Salhab, M.; Chavez, J.C.; Reddy, N.; Karmali, R.; Umyarova, E.; Bachanova, V.; Costa, C.; Glenn, M.; et al. C-MYC–Positive Relapsed and Refractory, Diffuse Large B-Cell Lymphoma: Impact of Additional “Hits” and Outcomes with Subsequent Therapy. *Cancer* **2017**, *123*, 4411–4418, doi:10.1002/ncr.30895.
123. Barrans, S.; Crouch, S.; Smith, A.; Turner, K.; Owen, R.; Patmore, R.; Roman, E.; Jack, A. Rearrangement of MYC Is Associated with Poor Prognosis in Patients with Diffuse Large B-Cell Lymphoma Treated in the Era of Rituximab. *J. Clin. Oncol. Off. J. Am. Soc. Clin. Oncol.* **2010**, *28*, 3360–3365, doi:10.1200/JCO.2009.26.3947.
124. Savage, K.J.; Johnson, N.A.; Ben-Neriah, S.; Connors, J.M.; Sehn, L.H.; Farinha, P.; Horsman, D.E.; Gascoyne, R.D. Myc Gene Rearrangements Are Associated with a Poor Prognosis in Diffuse Large B-Cell Lymphoma Patients Treated with R-CHOP Chemotherapy. *Blood* **2009**, *114*, 3533 LP – 3537, doi:10.1182/blood-2009-05-220095.
125. Das, S.K.; Lewis, B.A.; Levens, D. MYC: A Complex Problem. *Trends Cell Biol.* **2023**, *33*, 235–246, doi:10.1016/j.tcb.2022.07.006.

126. Quesada, A.E.; Medeiros, L.J.; Desai, P.A.; Lin, P.; Westin, J.R.; Hawsawi, H.M.; Wei, P.; Tang, G.; Seegmiller, A.C.; Reddy, N.M.; et al. Increased MYC Copy Number Is an Independent Prognostic Factor in Patients with Diffuse Large B-Cell Lymphoma. *Mod. Pathol. an Off. J. United States Can. Acad. Pathol. Inc* **2017**, *30*, 1688–1697, doi:10.1038/modpathol.2017.93.
127. Nguyen, L.; Papenhausen, P.; Shao, H. The Role of C-MYC in B-Cell Lymphomas: Diagnostic and Molecular Aspects. *Genes (Basel)*. 2017, *8*.
128. Slack, G.W.; Gascoyne, R.D. MYC and Aggressive B-Cell Lymphomas. *Adv. Anat. Pathol.* **2011**, *18*.
129. Kluk, M.J.; Chapuy, B.; Sinha, P.; Roy, A.; Dal Cin, P.; Neuberg, D.S.; Monti, S.; Pinkus, G.S.; Shipp, M.A.; Rodig, S.J. Immunohistochemical Detection of MYC-Driven Diffuse Large B-Cell Lymphomas. *PLoS One* **2012**, *7*, doi:10.1371/journal.pone.0033813.
130. Ennishi, D.; Mottok, A.; Ben-Neriah, S.; Shulha, H.P.; Farinha, P.; Chan, F.C.; Meissner, B.; Boyle, M.; Hother, C.; Kridel, R.; et al. Genetic Profiling of MYC and BCL2 in Diffuse Large B-Cell Lymphoma Determines Cell-of-Origin–Specific Clinical Impact. *Blood* **2017**, *129*, 2760–2770, doi:10.1182/blood-2016-11-747022.
131. Collinge, B.; Ben-Neriah, S.; Chong, L.; Boyle, M.; Jiang, A.; Miyata-Takata, T.; Farinha, P.; Craig, J.W.; Slack, G.W.; Ennishi, D.; et al. The Impact of MYC and BCL2 Structural Variants in Tumors of DLBCL Morphology and Mechanisms of False-Negative MYC IHC. *Blood* **2021**, *137*, 2196–2208, doi:10.1182/blood.2020007193.
132. Davies, J.R.; Hilton, L.K.; Jiang, A.; Barrans, S.; Burton, C.; Johnson, P.W.M.; Davies, A.J.; Du, M.-Q.; Tooze, R.; Cucco, F.; et al. Comparison of MHG and DZsig Reveals

- Shared Biology and a Core Overlap Group with Inferior Prognosis in DLBCL. *Blood Adv.* **2023**, *7*, 6156–6162, doi:10.1182/bloodadvances.2023010673.
133. Hilton, L.K.; Tang, J.; Ben-Neriah, S.; Alcaide, M.; Jiang, A.; Grande, B.M.; Rushton, C.K.; Boyle, M.; Meissner, B.; Scott, D.W.; et al. The Double-Hit Signature Identifies Double-Hit Diffuse Large B-Cell Lymphoma with Genetic Events Cryptic to FISH. *Blood* **2019**, *134*, 1528–1532, doi:https://doi.org/10.1182/blood.2019002600.
134. Sha, C.; Barrans, S.; Cucco, F.; Bentley, M.A.; Care, M.A.; Cummin, T.; Kennedy, H.; Thompson, J.S.; Uddin, R.; Worrillow, L.; et al. Molecular High-Grade B-Cell Lymphoma: Defining a Poor-Risk Group That Requires Different Approaches to Therapy. *J. Clin. Oncol. Off. J. Am. Soc. Clin. Oncol.* **2019**, *37*, 202–212, doi:10.1200/JCO.18.01314.
135. Petitjean, A.; Achatz, M.I.W.; Borresen-Dale, A.L.; Hainaut, P.; Olivier, M. TP53 Mutations in Human Cancers: Functional Selection and Impact on Cancer Prognosis and Outcomes. *Oncogene* **2007**, *26*, 2157–2165, doi:10.1038/sj.onc.1210302.
136. Young, K.H.; Weisenburger, D.D.; Dave, B.J.; Smith, L.; Sanger, W.; Iqbal, J.; Campo, E.; Delabie, J.; Gascoyne, R.D.; Ott, G.; et al. Mutations in the DNA-Binding Codons of TP53, Which Are Associated with Decreased Expression of TRAIL Receptor-2, Predict for Poor Survival in Diffuse Large B-Cell Lymphoma. *Blood* **2007**, *110*, 4396–4405, doi:10.1182/blood-2007-02-072082.
137. Young, K.H.; Leroy, K.; Møller, M.B.; Colleoni, G.W.B.; Sánchez-Beato, M.; Kerbauy, F.R.; Haioun, C.; Eickhoff, J.C.; Young, A.H.; Gaulard, P.; et al. Structural Profiles of TP53 Gene Mutations Predict Clinical Outcome in Diffuse Large B-Cell Lymphoma: An

- International Collaborative Study. *Blood* **2008**, *112*, 3088–3098, doi:10.1182/blood-2008-01-129783.
138. Xu-Monette, Z.Y.; Medeiros, L.J.; Li, Y.; Orłowski, R.Z.; Andreeff, M.; Bueso-Ramos, C.E.; Greiner, T.C.; McDonnell, T.J.; Young, K.H. Dysfunction of the TP53 Tumor Suppressor Gene in Lymphoid Malignancies. *Blood* **2012**, *119*, 3668–3683, doi:10.1182/blood-2011-11-366062.
139. Wright, G.W.; Huang, D.W.; Phelan, J.D.; Coulibaly, Z.A.; Roulland, S.; Young, R.M.; Wang, J.Q.; Schmitz, R.; Morin, R.D.; Tang, J.; et al. A Probabilistic Classification Tool for Genetic Subtypes of Diffuse Large B Cell Lymphoma with Therapeutic Implications. *Cancer Cell* **2020**, *37*, 551-568.e14, doi:10.1016/j.ccell.2020.03.015.
140. Soussi, T.; Wiman, K.G. TP53: An Oncogene in Disguise. *Cell Death Differ.* **2015**, *22*, 1239–1249, doi:10.1038/cdd.2015.53.
141. Xu-Monette, Z.Y.; Wu, L.; Visco, C.; Tai, Y.C.; Tzankov, A.; Liu, W.; Montes-Moreno, S.; Dybkær, K.; Chiu, A.; Orazi, A.; et al. Mutational Profile and Prognostic Significance of TP53 in Diffuse Large B-Cell Lymphoma Patients Treated with R-CHOP: Report from an International DLBCL Rituximab-CHOP Consortium Program Study. *Blood* **2012**, *120*, 3986–3996, doi:10.1182/blood-2012-05-433334.
142. Lu, T.X.; Young, K.H.; Xu, W.; Li, J.Y. TP53 Dysfunction in Diffuse Large B-Cell Lymphoma. *Crit. Rev. Oncol. Hematol.* **2016**, *97*, 47–55, doi:10.1016/j.critrevonc.2015.08.006.
143. Peroja, P.; Pedersen, M.; Mantere, T.; Nørgaard, P.; Peltonen, J.; Haapasaari, K.M.; Böhm, J.; Jantunen, E.; Turpeenniemi-Hujanen, T.; Rapakko, K.; et al. Mutation of TP53,

- Translocation Analysis and Immunohistochemical Expression of MYC, BCL-2 and BCL-6 in Patients with DLBCL Treated with R-CHOP. *Sci. Rep.* **2018**, *8*, 1–9, doi:10.1038/s41598-018-33230-3.
144. Schuetz, J.M.; Johnson, N.A.; Morin, R.D.; Scott, D.W.; Tan, K.; Ben-Nierah, S.; Boyle, M.; Slack, G.W.; Marra, M.A.; Connors, J.M.; et al. BCL2 Mutations in Diffuse Large B-Cell Lymphoma. *Leukemia* **2012**, *26*, 1383–1390, doi:10.1038/leu.2011.378.
145. Inoue-Yamauchi, A.; Jeng, P.S.; Kim, K.; Chen, H.-C.; Han, S.; Ganesan, Y.T.; Ishizawa, K.; Jebiwott, S.; Dong, Y.; Pietanza, M.C.; et al. Targeting the Differential Addiction to Anti-Apoptotic BCL-2 Family for Cancer Therapy. *Nat. Commun.* **2017**, *8*, 16078, doi:10.1038/ncomms16078.
146. Stilgenbauer, S.; Eichhorst, B.; Schetelig, J.; Coutre, S.; Seymour, J.F.; Munir, T.; Puvvada, S.D.; Wendtner, C.-M.; Roberts, A.W.; Jurczak, W.; et al. Venetoclax in Relapsed or Refractory Chronic Lymphocytic Leukaemia with 17p Deletion: A Multicentre, Open-Label, Phase 2 Study. *Lancet. Oncol.* *17*, 768–778, doi:10.1016/s1470-2045(16)30212-1.
147. Morschhauser, F.; Feugier, P.; Flinn, I.W.; Gasiowski, R.E.; Greil, R.; Johnson, N.A.; Larouche, J.-F.; Lugtenburg, P.J.; Patti, C.; Salles, G.; et al. Venetoclax Plus Rituximab, Cyclophosphamide, Doxorubicin, Vincristine and Prednisolone (R-CHOP) Improves Outcomes in BCL2-Positive First-Line Diffuse Large B-Cell Lymphoma (DLBCL): First Safety, Efficacy and Biomarker Analyses from the Phase II CAVALLI St. In Proceedings of the 60th ASH Annual Meeting & Exposition; December 1-4, 2018; ASH: San Diego, CA, December 2018; p. Abstract nr 782.

148. Mottok, A.; Woolcock, B.; Chan, F.C.; Tong, K.M.; Chong, L.; Farinha, P.; Telenius, A.; Chavez, E.; Ramchandani, S.; Drake, M.; et al. Genomic Alterations in CIITA Are Frequent in Primary Mediastinal Large B Cell Lymphoma and Are Associated with Diminished MHC Class II Expression. *Cell Rep.* **2015**, *13*, 1418–1431, doi:10.1016/j.celrep.2015.10.008.
149. Rimsza, L.M.; Roberts, R.A.; Miller, T.P.; Unger, J.M.; LeBlanc, M.; Braziel, R.M.; Weisenberger, D.D.; Chan, W.C.; Muller-Hermelink, H.K.; Jaffe, E.S.; et al. Loss of MHC Class II Gene and Protein Expression in Diffuse Large B-Cell Lymphoma Is Related to Decreased Tumor Immunosurveillance and Poor Patient Survival Regardless of Other Prognostic Factors: A Follow-up Study from the Leukemia and Lymphoma Molecula. *Blood* **2004**, *103*, 4251–4258, doi:10.1182/blood-2003-07-2365.
150. Challa-Malladi, M.; Lieu, Y.K.; Califano, O.; Holmes, A.B.; Bhagat, G.; Murty, V. V.; Dominguez-Sola, D.; Pasqualucci, L.; Dalla-Favera, R. Combined Genetic Inactivation of B2-Microglobulin and CD58 Reveals Frequent Escape from Immune Recognition in Diffuse Large B Cell Lymphoma. *Cancer Cell* **2011**, *20*, 728–740, doi:10.1016/j.ccr.2011.11.006.
151. Trinh, D.L.; Scott, D.W.; Morin, R.D.; Mendez-Lago, M.; An, J.; Jones, S.J.M.; Mungall, A.J.; Zhao, Y.; Schein, J.; Steidl, C.; et al. Analysis of FOXO1 Mutations in Diffuse Large B-Cell Lymphoma. *Blood* **2013**, *121*, 3666–3674, doi:10.1182/blood-2013-01-479865.
152. Sander, S.; Chu, V.T.; Yasuda, T.; Franklin, A.; Graf, R.; Calado, D.P.; Li, S.; Imami, K.; Selbach, M.; Di Virgilio, M.; et al. PI3 Kinase and FOXO1 Transcription Factor Activity Differentially Control B Cells in the Germinal Center Light and Dark Zones. *Immunity*

- 2015**, *43*, 1075–1086, doi:10.1016/j.immuni.2015.10.021.
153. Cheung, K.-J.J.; Johnson, N.A.; Affleck, J.G.; Severson, T.; Steidl, C.; Ben-Neriah, S.; Schein, J.; Morin, R.D.; Moore, R.; Shah, S.P.; et al. Acquired TNFRSF14 Mutations in Follicular Lymphoma Are Associated with Worse Prognosis. *Cancer Res.* **2010**, *70*, 9166–9174, doi:10.1158/0008-5472.CAN-10-2460.
154. de Groen, R.A.L.; van Eijk, R.; Böhringer, S.; van Wezel, T.; Raghoo, R.; Ruano, D.; Jansen, P.M.; Briaire-de Bruijn, I.; de Groot, F.A.; Kleiverda, K.; et al. Frequent Mutated B2M, EZH2, IRF8, and TNFRSF14 in Primary Bone Diffuse Large B-Cell Lymphoma Reflect a GCB Phenotype. *Blood Adv.* **2021**, *5*, 3760–3775, doi:10.1182/bloodadvances.2021005215.
155. Wherry, E.J. T Cell Exhaustion. *Nat. Immunol.* **2011**, *12*, 492–499, doi:10.1038/ni.2035.
156. Chong, L.C.; Twa, D.D.W.; Mottok, A.; Ben-Neriah, S.; Woolcock, B.W.; Zhao, Y.; Savage, K.J.; Marra, M.A.; Scott, D.W.; Gascoyne, R.D.; et al. Comprehensive Characterization of Programmed Death Ligand Structural Rearrangements in B-Cell Non-Hodgkin Lymphomas. *Blood* **2016**, *128*, 1206–1213, doi:10.1182/blood-2015-11-683003.
157. Georgiou, K.; Chen, L.; Berglund, M.; Ren, W.; de Miranda, N.F.C.C.; Lisboa, S.; Fangazio, M.; Zhu, S.; Hou, Y.; Wu, K.; et al. Genetic Basis of PD-L1 Overexpression in Diffuse Large B-Cell Lymphomas. *Blood* **2016**, *127*, 3026–3034, doi:10.1182/blood-2015-12-686550.
158. Kline, J.; Godfrey, J.; Ansell, S.M. The Immune Landscape and Response to Immune Checkpoint Blockade Therapy in Lymphoma. *Blood* **2020**, *135*, 523–533, doi:10.1182/blood.2019000847.

159. Ansell, S.M.; Minnema, M.C.; Johnson, P.; Timmerman, J.M.; Armand, P.; Shipp, M.A.; Rodig, S.J.; Ligon, A.H.; Roemer, M.G.M.; Reddy, N.; et al. Nivolumab for Relapsed/Refractory Diffuse Large B-Cell Lymphoma in Patients Ineligible for or Having Failed Autologous Transplantation: A Single-Arm, Phase II Study. *J. Clin. Oncol.* **2019**, *37*, 481–489, doi:10.1200/JCO.18.00766.
160. Frigault, M.J.; Armand, P.; Redd, R.A.; Jeter, E.; Merryman, R.W.; Coleman, K.C.; Herrera, A.F.; Dahi, P.; Nieto, Y.; LaCasce, A.S.; et al. PD-1 Blockade for Diffuse Large B-Cell Lymphoma after Autologous Stem Cell Transplantation. *Blood Adv.* **2020**, *4*, 122–126, doi:10.1182/bloodadvances.2019000784.
161. Xu-Monette, Z.Y.; Zhou, J.; Young, K.H. PD-1 Expression and Clinical PD-1 Blockade in B-Cell Lymphomas. *Blood* **2018**, *131*, 68–83, doi:10.1182/blood-2017-07-740993.
162. Goodman, A.; Patel, S.P.; Kurzrock, R. PD-1-PD-L1 Immune-Checkpoint Blockade in B-Cell Lymphomas. *Nat. Rev. Clin. Oncol.* **2017**, *14*, 203–220, doi:10.1038/nrclinonc.2016.168.
163. Tanaka, A.; Sakaguchi, S. Regulatory T Cells in Cancer Immunotherapy. *Cell Res.* **2017**, *27*, 109–118, doi:10.1038/cr.2016.151.
164. Zhang, J.; Medeiros, L.J.; Young, K.H. Cancer Immunotherapy in Diffuse Large B-Cell Lymphoma. *Front. Oncol.* **2018**, *8*, 1–12, doi:10.3389/fonc.2018.00351.
165. Kumar, D.; Xu, M.L. Microenvironment Cell Contribution to Lymphoma Immunity. *Front. Oncol.* **2018**, *8*, 288, doi:10.3389/fonc.2018.00288.
166. Schmitz, R.; Wright, G.W.; Huang, D.W.; Johnson, C.A.; Phelan, J.D.; Wang, J.Q.;

- Roulland, S.; Kasbekar, M.; Young, R.M.; Shaffer, A.L.; et al. Genetics and Pathogenesis of Diffuse Large B-Cell Lymphoma. *N. Engl. J. Med.* **2018**, *378*, 1396–1407, doi:10.1056/NEJMoa1801445.
167. Brunet, J.P.; Tamayo, P.; Golub, T.R.; Mesirov, J.P. Metagenes and Molecular Pattern Discovery Using Matrix Factorization. *Proc. Natl. Acad. Sci. U. S. A.* **2004**, *101*, 4164–4169, doi:10.1073/pnas.0308531101.
168. Berendsen, M.R.; Stevens, W.B.C.; van den Brand, M.; van Krieken, J.H.; Scheijen, B. Molecular Genetics of Relapsed Diffuse Large B-Cell Lymphoma: Insight into Mechanisms of Therapy Resistance. *Cancers (Basel)*. 2020, *12*.
169. Morin, R.D.; Assouline, S.; Alcaide, M.; Mohajeri, A.; Johnston, R.L.; Chong, L.; Grewal, J.; Yu, S.; Fornika, D.; Bushell, K.; et al. Genetic Landscapes of Relapsed and Refractory Diffuse Large B-Cell Lymphomas. *Clin. Cancer Res.* **2016**, *22*, 2290–2300, doi:10.1158/1078-0432.CCR-15-2123.
170. Benoit, A.; Abraham, M.J.; Li, S.; Kim, J.; Estrada-Tejedor, R.; Bakadlag, R.; Subramaniam, N.; Makhani, K.; Guilbert, C.; Tu, R.; et al. STAT6 Mutations Enriched at Diffuse Large B-Cell Lymphoma Relapse Reshape the Tumor Microenvironment. *Int. J. Hematol.* **2024**, doi:10.1007/s12185-023-03692-x.
171. Hiraga, J.; Tomita, A.; Sugimoto, T.; Shimada, K.; Ito, M.; Nakamura, S.; Kiyoi, H.; Kinoshita, T.; Naoe, T. Down-Regulation of CD20 Expression in B-Cell Lymphoma Cells after Treatment with Rituximab-Containing Combination Chemotherapies: Its Prevalence and Clinical Significance. *Blood* **2009**, *113*, 4885–4893, doi:10.1182/blood-2008-08-175208.

172. Schuster, S.J.; Huw, L.-Y.; Bolen, C.R.; Maximov, V.; Polson, A.G.; Hatzi, K.; Lasater, E.A.; Assouline, S.E.; Bartlett, N.L.; Budde, L.E.; et al. Loss of CD20 Expression as a Mechanism of Resistance to Mosunetuzumab in Relapsed/Refractory B-Cell Lymphomas. *Blood* **2024**, *143*, 822–832, doi:10.1182/blood.2023022348.
173. Rushton, C.K.; Rys, R.N.; Chavez, E.; Hilton, L.K.; Alcaide, M.; Dreval, K.; Cheung, M.; Cruz, M.; Coyle, K.M.; Meissner, B.; et al. Recurrent Copy Number Alterations Contribute to a Unique Genetic Landscape in Relapsed-Refractory DLBCL. *Blood* **2022**, *140*, 9259–9260, doi:10.1182/blood-2022-169623.
174. Tilly, H.; Gomes da Silva, M.; Vitolo, U.; Jack, A.; Meignan, M.; Lopez-Guillermo, A.; Walewski, J.; André, M.; Johnson, P.W.; Pfreundschuh, M.; et al. Diffuse Large B-Cell Lymphoma (DLBCL): ESMO Clinical Practice Guidelines for Diagnosis, Treatment and Follow-Up. *Ann. Oncol.* **2015**, *26*, vii78–vii82, doi:10.1093/annonc/mdv304.
175. Liu, Y.; Barta, S.K. Diffuse Large B-Cell Lymphoma: 2019 Update on Diagnosis, Risk Stratification, and Treatment. *Am. J. Hematol.* **2019**, *94*, 604–616, doi:10.1002/ajh.25460.
176. Roschewski, M.; Staudt, L.M.; Wilson, W.H. Diffuse Large B-Cell Lymphoma - Treatment Approaches in the Molecular Era. *Nat. Rev. Clin. Oncol.* **2014**, *11*, 12–23, doi:10.1038/nrclinonc.2013.197.
177. Weiner, G.J. Rituximab: Mechanism of Action. *Semin. Hematol.* **2010**, *47*, 115–123, doi:10.1053/j.seminhematol.2010.01.011.
178. Feugier, P.; Van Hoof, A.; Sebban, C.; Solal-Celigny, P.; Bouabdallah, R.; Fermé, C.; Christian, B.; Lepage, E.; Tilly, H.; Morschhauser, F.; et al. Long-Term Results of the R-CHOP Study in the Treatment of Elderly Patients with Diffuse Large B-Cell Lymphoma:

- A Study by the Groupe d'étude Des Lymphomes de l'adulte. *J. Clin. Oncol.* **2005**, *23*, 4117–4126, doi:10.1200/JCO.2005.09.131.
179. Habermann, T.M.; Weller, E.A.; Morrison, V.A.; Gascoyne, R.D.; Cassileth, P.A.; Cohn, J.B.; Dakhil, S.R.; Woda, B.; Fisher, R.I.; Peterson, B.A.; et al. Rituximab-CHOP versus CHOP Alone or with Maintenance Rituximab in Older Patients with Diffuse Large B-Cell Lymphoma. *J. Clin. Oncol.* **2006**, *24*, 3121–3127, doi:10.1200/JCO.2005.05.1003.
180. Bartlett, N.L.; Wilson, W.H.; Jung, S.-H.; Hsi, E.D.; Maurer, M.J.; Pederson, L.D.; Polley, M.-Y.C.; Pitcher, B.N.; Cheson, B.D.; Kahl, B.S.; et al. Dose-Adjusted EPOCH-R Compared With R-CHOP as Frontline Therapy for Diffuse Large B-Cell Lymphoma: Clinical Outcomes of the Phase III Intergroup Trial Alliance/CALGB 50303. *J. Clin. Oncol. Off. J. Am. Soc. Clin. Oncol.* **2019**, *37*, 1790–1799, doi:10.1200/JCO.18.01994.
181. Ng, A.K.; Yahalom, J.; Goda, J.S.; Constine, L.S.; Pinnix, C.C.; Kelsey, C.R.; Hoppe, B.; Oguchi, M.; Suh, C.-O.; Wirth, A.; et al. Role of Radiation Therapy in Patients With Relapsed/Refractory Diffuse Large B-Cell Lymphoma: Guidelines from the International Lymphoma Radiation Oncology Group. *Int. J. Radiat. Oncol.* **2018**, *100*, 652–669, doi:https://doi.org/10.1016/j.ijrobp.2017.12.005.
182. Morschhauser, F.; Feugier, P.; Flinn, I.W.; Gasiorowski, R.; Greil, R.; Illés, Á.; Johnson, N.A.; Larouche, J.F.; Lugtenburg, P.J.; Patti, C.; et al. A Phase 2 Study of Venetoclax plus R-CHOP as First-Line Treatment for Patients with Diffuse Large B-Cell Lymphoma. *Blood* **2021**, *137*, 600–609, doi:10.1182/blood.2020006578.
183. Philip, T.; Guglielmi, C.; Hagenbeek, A.; Somers, R.; Van Der Lelie, H.; Bron, D.; Sonneveld, P.; Gisselbrecht, C.; Cahn, J.-Y.; Harousseau, J.-L.; et al. Autologous Bone

- Marrow Transplantation as Compared with Salvage Chemotherapy in Relapses of Chemotherapy-Sensitive Non-Hodgkin's Lymphoma. *N. Engl. J. Med.* **1995**, *333*, 1540–1545, doi:10.1056/NEJM199512073332305.
184. Gisselbrecht, C.; Glass, B.; Mounier, N.; Singh Gill, D.; Linch, D.C.; Trneny, M.; Bosly, A.; Ketterer, N.; Shpilberg, O.; Hagberg, H.; et al. Salvage Regimens With Autologous Transplantation for Relapsed Large B-Cell Lymphoma in the Rituximab Era. *J. Clin. Oncol.* **2010**, *28*, 4184–4190, doi:10.1200/JCO.2010.28.1618.
185. Crump, M.; Kuruvilla, J.; Couban, S.; MacDonald, D.A.; Kukreti, V.; Kouroukis, C.T.; Rubinger, M.; Buckstein, R.; Imrie, K.R.; Federico, M.; et al. Randomized Comparison of Gemcitabine, Dexamethasone, and Cisplatin Versus Dexamethasone, Cytarabine, and Cisplatin Chemotherapy Before Autologous Stem-Cell Transplantation for Relapsed and Refractory Aggressive Lymphomas: NCIC-CTG LY.12. *J. Clin. Oncol.* **2014**, *32*, 3490–3496, doi:10.1200/JCO.2013.53.9593.
186. Moccia, A.A.; Hitz, F.; Hoskins, P.; Klasa, R.; Power, M.M.; Savage, K.J.; Shenkier, T.; Shepherd, J.D.; Slack, G.W.; Song, K.W.; et al. Gemcitabine, Dexamethasone, and Cisplatin (GDP) Is an Effective and Well-Tolerated Salvage Therapy for Relapsed/Refractory Diffuse Large B-Cell Lymphoma and Hodgkin Lymphoma. *Leuk. Lymphoma* **2017**, *58*, 324–332, doi:10.1080/10428194.2016.1193852.
187. Vercellino, L.; Di Blasi, R.; Kanoun, S.; Tessoulin, B.; Rossi, C.; D'Aveni-Piney, M.; Obéric, L.; Bodet-Milin, C.; Bories, P.; Olivier, P.; et al. Predictive Factors of Early Progression after CAR T-Cell Therapy in Relapsed/Refractory Diffuse Large B-Cell Lymphoma. *Blood Adv.* **2020**, *4*, 5607–5615, doi:10.1182/bloodadvances.2020003001.

188. Jacobson, C.A.; Hunter, B.D.; Redd, R.; Rodig, S.J.; Chen, P.-H.; Wright, K.; Lipschitz, M.; Ritz, J.; Kamihara, Y.; Armand, P.; et al. Axicabtagene Ciloleucel in the Non-Trial Setting: Outcomes and Correlates of Response, Resistance, and Toxicity. *J. Clin. Oncol.* **2020**, *38*, 3095–3106, doi:10.1200/JCO.19.02103.
189. Nastoupil, L.J.; Jain, M.D.; Feng, L.; Spiegel, J.Y.; Ghobadi, A.; Lin, Y.; Dahiya, S.; Lunning, M.; Lekakis, L.; Reagan, P.; et al. Standard-of-Care Axicabtagene Ciloleucel for Relapsed or Refractory Large B-Cell Lymphoma: Results From the US Lymphoma CAR T Consortium. *J. Clin. Oncol. Off. J. Am. Soc. Clin. Oncol.* **2020**, *38*, 3119–3128, doi:10.1200/JCO.19.02104.
190. Sesques, P.; Ferrant, E.; Safar, V.; Wallet, F.; Tordo, J.; Dhomps, A.; Karlin, L.; Brisou, G.; Vercasson, M.; Hospital-Gustem, C.; et al. Commercial Anti-CD19 CAR T Cell Therapy for Patients with Relapsed/Refractory Aggressive B Cell Lymphoma in a European Center. *Am. J. Hematol.* **2020**, *95*, 1324–1333, doi:https://doi.org/10.1002/ajh.25951.
191. Westin, J.; Jacobson, C.A.; Chavez, J.C.; Sureda, A.; Morschhauser, F.; Glaß, B.; Dickinson, M.; Davies, A.; Flinn, I.W.; Maloney, D.G.; et al. ZUMA-23: A Global, Phase 3, Randomized Controlled Study of Axicabtagene Ciloleucel versus Standard of Care as First-Line Therapy in Patients with High-Risk Large B-Cell Lymphoma. *J. Clin. Oncol.* **2023**, *41*, TPS7578–TPS7578, doi:10.1200/JCO.2023.41.16_suppl.TPS7578.
192. Neelapu, S.S.; Dickinson, M.; Munoz, J.; Ulrickson, M.L.; Thieblemont, C.; Oluwole, O.O.; Herrera, A.F.; Ujjani, C.S.; Lin, Y.; Riedell, P.A.; et al. Axicabtagene Ciloleucel as First-Line Therapy in High-Risk Large B-Cell Lymphoma: The Phase 2 ZUMA-12 Trial.

- Nat. Med.* **2022**, 28, 735–742, doi:10.1038/s41591-022-01731-4.
193. Palanca-Wessels, M.C.A.; Czuczman, M.; Salles, G.; Assouline, S.; Sehn, L.H.; Flinn, I.; Patel, M.R.; Sangha, R.; Hagenbeek, A.; Advani, R.; et al. Safety and Activity of the Anti-CD79B Antibody–Drug Conjugate Polatuzumab Vedotin in Relapsed or Refractory B-Cell Non-Hodgkin Lymphoma and Chronic Lymphocytic Leukaemia: A Phase 1 Study. *Lancet Oncol.* **2015**, 16, 704–715, doi:https://doi.org/10.1016/S1470-2045(15)70128-2.
194. Gribben, J.G.; Fowler, N.; Morschhauser, F. Mechanisms of Action of Lenalidomide in B-Cell Non-Hodgkin Lymphoma. *J. Clin. Oncol. Off. J. Am. Soc. Clin. Oncol.* **2015**, 33, 2803–2811, doi:10.1200/JCO.2014.59.5363.
195. Salles, G.; Duell, J.; González Barca, E.; Tournilhac, O.; Jurczak, W.; Liberati, A.M.; Nagy, Z.; Obr, A.; Gaidano, G.; André, M.; et al. Tafasitamab plus Lenalidomide in Relapsed or Refractory Diffuse Large B-Cell Lymphoma (L-MIND): A Multicentre, Prospective, Single-Arm, Phase 2 Study. *Lancet Oncol.* **2020**, 21, 978–988, doi:10.1016/S1470-2045(20)30225-4.
196. Duell, J.; Maddocks, K.J.; González-Barca, E.; Jurczak, W.; Liberati, A.M.; De Vos, S.; Nagy, Z.; Obr, A.; Gaidano, G.; Abrisqueta, P.; et al. Long-Term Outcomes from the Phase II L-MIND Study of Tafasitamab (MOR208) plus Lenalidomide in Patients with Relapsed or Refractory Diffuse Large B-Cell Lymphoma. *Haematologica* **2021**, 106, 2417–2426, doi:10.3324/haematol.2020.275958.
197. Carneiro, B.A.; El-Deiry, W.S. Targeting Apoptosis in Cancer Therapy. *Nat. Rev. Clin. Oncol.* **2020**, 17, 395–417, doi:10.1038/s41571-020-0341-y.
198. Gurudutta, G.U.; Verma, Y.K.; Singh, V.K.; Gupta, P.; Raj, H.G.; Sharma, R.K.; Chandra,

- R. Structural Conservation of Residues in BH1 and BH2 Domains of Bcl-2 Family Proteins. *FEBS Lett.* **2005**, *579*, 3503–3507, doi:10.1016/j.febslet.2005.05.015.
199. Singh, R.; Letai, A.; Sarosiek, K. Regulation of Apoptosis in Health and Disease: The Balancing Act of BCL-2 Family Proteins. *Nat. Rev. Mol. Cell Biol.* **2019**, *20*, 175–193, doi:10.1038/s41580-018-0089-8.
200. Krammer, P.H. CD95's Deadly Mission in the Immune System. *Nature* **2000**, *407*, 789–795, doi:10.1038/35037728.
201. Lavrik, I.N.; Krammer, P.H. Regulation of CD95/Fas Signaling at the DISC. *Cell Death Differ.* **2012**, *19*, 36–41, doi:10.1038/cdd.2011.155.
202. Leveille, E.; Johnson, N.A. Genetic Events Inhibiting Apoptosis in Diffuse Large B Cell Lymphoma. *Cancers (Basel)*. **2021**, *13*, 2167, doi:10.3390/cancers13092167.
203. Certo, M.; Del Gaizo Moore, V.; Nishino, M.; Wei, G.; Korsmeyer, S.; Armstrong, S.A.; Letai, A. Mitochondria Primed by Death Signals Determine Cellular Addiction to Antiapoptotic BCL-2 Family Members. *Cancer Cell* **2006**, *9*, 351–365, doi:10.1016/j.ccr.2006.03.027.
204. Ingela, V.; Sebastian, C.; Katja, L.; Victor, P.; J., J.P.; Stefan, G.; Meinrad, B.; Philippe, B.; Andreas, S.; L., N.S.; et al. Mcl-1 Is Essential for Germinal Center Formation and B Cell Memory. *Science (80-.)*. **2010**, *330*, 1095–1099, doi:10.1126/science.1191793.
205. Opferman, J.T.; Letai, A.; Beard, C.; Sorcinelli, M.D.; Ong, C.C.; Korsmeyer, S.J. Development and Maintenance of B and T Lymphocytes Requires Antiapoptotic MCL-1. *Nature* **2003**, *426*, 671–676, doi:10.1038/nature02067.

206. Wenzel, S.S.; Grau, M.; Mavis, C.; Hailfinger, S.; Wolf, A.; Madle, H.; Deeb, G.; Dörken, B.; Thome, M.; Lenz, P.; et al. MCL1 Is Deregulated in Subgroups of Diffuse Large B-Cell Lymphoma. *Leukemia* **2013**, *27*, 1381–1390, doi:10.1038/leu.2012.367.
207. Fernández-Marrero, Y.; Spinner, S.; Kaufmann, T.; Jost, P.J. Survival Control of Malignant Lymphocytes by Anti-Apoptotic MCL-1. *Leukemia* **2016**, *30*, 2152–2159, doi:10.1038/leu.2016.213.
208. Cho-Vega, J.H.; Rassidakis, G.Z.; Admirand, J.H.; Oyarzo, M.; Ramalingam, P.; Paraguya, A.; McDonnell, T.J.; Amin, H.M.; Medeiros, L.J. MCL-1 Expression in B-Cell Non-Hodgkin's Lymphomas. *Hum. Pathol.* **2004**, *35*, 1095–1100, doi:https://doi.org/10.1016/j.humpath.2004.04.018.
209. Klanova, M.; Kazantsev, D.; Pokorna, E.; Zikmund, T.; Karolova, J.; Behounek, M.; Renesova, N.; Sovilj, D.; Kelemen, C.D.; Helman, K.; et al. Anti-Apoptotic MCL1 Protein Represents Critical Survival Molecule for Most Burkitt Lymphomas and BCL2-Negative Diffuse Large B-Cell Lymphomas. *Mol. Cancer Ther.* **2022**, *21*, 89–99, doi:10.1158/1535-7163.MCT-21-0511.
210. Smith, V.M.; Dietz, A.; Henz, K.; Bruecher, D.; Jackson, R.; Kowald, L.; van Wijk, S.J.L.; Jayne, S.; Macip, S.; Fulda, S.; et al. Specific Interactions of BCL-2 Family Proteins Mediate Sensitivity to BH3-Mimetics in Diffuse Large B-Cell Lymphoma. *Haematologica* **2020**, *105*, 2150–2163, doi:10.3324/haematol.2019.220525.
211. Lasater, E.A.; Amin, D.N.; Bannerji, R.; Mali, R.S.; Barrett, K.; Rys, R.N.; Oeh, J.; Lin, E.; Sterne-Weiler, T.; Ingalla, E.R.; et al. Targeting MCL-1 and BCL-2 with Polatuzumab Vedotin and Venetoclax Overcomes Treatment Resistance in R/R Non-Hodgkin

- Lymphoma: Results from Preclinical Models and a Phase Ib Study. *Am. J. Hematol.* **2023**, 98, 449–463, doi:10.1002/ajh.26809.
212. Souers, A.J.; Levenson, J.D.; Boghaert, E.R.; Ackler, S.L.; Catron, N.D.; Chen, J.; Dayton, B.D.; Ding, H.; Enschede, S.H.; Fairbrother, W.J.; et al. ABT-199, a Potent and Selective BCL-2 Inhibitor, Achieves Antitumor Activity While Sparing Platelets. *Nat. Med.* **2013**, 19, 202–208, doi:10.1038/nm.3048.
213. Adams, C.M.; Mitra, R.; Gong, J.Z.; Eischen, C.M. Non-Hodgkin and Hodgkin Lymphomas Select for Overexpression of BCLW. *Clin. Cancer Res.* **2017**, 23, 7119–7129, doi:10.1158/1078-0432.CCR-17-1144.
214. Diepstraten, S.T.; Chang, C.; Tai, L.; Gong, J.; Lan, P.; Dowell, A.C.; Taylor, G.S.; Strasser, A.; Kelly, G.L. BCL-W Is Dispensable for the Sustained Survival of Select Burkitt Lymphoma and Diffuse Large B-Cell Lymphoma Cell Lines. *Blood Adv.* **2020**, 4, 356–366, doi:10.1182/bloodadvances.2019000541.
215. Ryan, J.; Montero, J.; Rocco, J.; Letai, A. IBH3: Simple, Fixable BH3 Profiling to Determine Apoptotic Priming in Primary Tissue by Flow Cytometry. *Biol. Chem.* **2016**, 397, 671–678, doi:10.1515/hsz-2016-0107.
216. Del Gaizo Moore, V.; Letai, A. BH3 Profiling--Measuring Integrated Function of the Mitochondrial Apoptotic Pathway to Predict Cell Fate Decisions. *Cancer Lett.* **2013**, 332, 202–205, doi:10.1016/j.canlet.2011.12.021.
217. Deng, J.; Carlson, N.; Takeyama, K.; Dal Cin, P.; Shipp, M.; Letai, A. BH3 Profiling Identifies Three Distinct Classes of Apoptotic Blocks to Predict Response to ABT-737 and Conventional Chemotherapeutic Agents. *Cancer Cell* **2007**, 12, 171–185,

doi:10.1016/j.ccr.2007.07.001.

218. Kim, H.; Rafiuddin-Shah, M.; Tu, H.C.; Jeffers, J.R.; Zambetti, G.P.; Hsieh, J.J.D.; Cheng, E.H.Y. Hierarchical Regulation of Mitochondrion-Dependent Apoptosis by BCL-2 Subfamilies. *Nat. Cell Biol.* **2006**, *8*, 1348–1358, doi:10.1038/ncb1499.
219. Kuwana, T.; Bouchier-Hayes, L.; Chipuk, J.E.; Bonzon, C.; Sullivan, B.A.; Green, D.R.; Newmeyer, D.D. BH3 Domains of BH3-Only Proteins Differentially Regulate Bax-Mediated Mitochondrial Membrane Permeabilization Both Directly and Indirectly. *Mol. Cell* **2005**, *17*, 525–535, doi:10.1016/j.molcel.2005.02.003.
220. Del Gaizo Moore, V.; Brown, J.R.; Certo, M.; Love, T.M.; Novina, C.D.; Letai, A. Chronic Lymphocytic Leukemia Requires BCL2 to Sequester Prodeath BIM, Explaining Sensitivity to BCL2 Antagonist ABT-737. *J. Clin. Invest.* **2007**, *117*, 112–121, doi:10.1172/JCI28281.
221. Touzeau, C.; Ryan, J.; Guerriero, J.; Moreau, P.; Chonghaile, T.N.; Le Gouill, S.; Richardson, P.; Anderson, K.; Amiot, M.; Letai, A. BH3 Profiling Identifies Heterogeneous Dependency on Bcl-2 Family Members in Multiple Myeloma and Predicts Sensitivity to BH3 Mimetics. *Leukemia* **2016**, *30*, 761–764.
222. Pan, R.; Hogdal, L.J.; Benito, J.M.; Bucci, D.; Han, L.; Borthakur, G.; Cortes, J.; Deangelo, D.J.; Debose, L.; Mu, H.; et al. Selective BCL-2 Inhibition by ABT-199 Causes on-Target Cell Death in Acute Myeloid Leukemia. *Cancer Discov.* **2014**, doi:10.1158/2159-8290.CD-13-0609.
223. Ni Chonghaile, T.; Roderick, J.E.; Glenfield, C.; Ryan, J.; Sallan, S.E.; Silverman, L.B.; Loh, M.L.; Hunger, S.P.; Wood, B.; DeAngelo, D.J.; et al. Maturation Stage of T-Cell

- Acute Lymphoblastic Leukemia Determines BCL-2 versus BCL-XL Dependence and Sensitivity to ABT-199. *Cancer Discov.* **2014**, *4*, 1074–1087, doi:10.1158/2159-8290.CD-14-0353.
224. De Vlaminck, I.; Valantine, H.A.; Snyder, T.M.; Strehl, C.; Cohen, G.; Luikart, H.; Neff, N.F.; Okamoto, J.; Bernstein, D.; Weisshaar, D.; et al. Circulating Cell-Free DNA Enables Noninvasive Diagnosis of Heart Transplant Rejection. *Sci. Transl. Med.* **2014**, *6*, 241ra77 LP-241ra77, doi:10.1126/scitranslmed.3007803.
225. Chang, C.P.-Y.; Chia, R.-H.; Wu, T.-L.; Tsao, K.-C.; Sun, C.-F.; Wu, J.T. Elevated Cell-Free Serum DNA Detected in Patients with Myocardial Infarction. *Clin. Chim. Acta.* **2003**, *327*, 95–101, doi:10.1016/s0009-8981(02)00337-6.
226. Volik, S.; Alcaide, M.; Morin, R.D.; Collins, C. Cell-Free DNA (CfDNA): Clinical Significance and Utility in Cancer Shaped By Emerging Technologies. *Mol. Cancer Res.* **2016**, *14*, 898 LP – 908, doi:10.1158/1541-7786.MCR-16-0044.
227. Shaw, J.A.; Page, K.; Blighe, K.; Hava, N.; Guttery, D.; Ward, B.; Brown, J.; Ruangpratheep, C.; Stebbing, J.; Payne, R.; et al. Genomic Analysis of Circulating Cell-Free DNA Infers Breast Cancer Dormancy. *Genome Res.* **2012**, *22*, 220–231, doi:10.1101/gr.123497.111.
228. Schwarzenbach, H.; Alix-Panabières, C.; Müller, I.; Letang, N.; Vendrell, J.-P.; Rebillard, X.; Pantel, K. Cell-Free Tumor DNA in Blood Plasma As a Marker for Circulating Tumor Cells in Prostate Cancer. *Clin. Cancer Res.* **2009**, *15*, 1032 LP – 1038, doi:10.1158/1078-0432.CCR-08-1910.
229. Scherer, F.; Kurtz, D.M.; Diehn, M.; Alizadeh, A.A. High-Throughput Sequencing for

- Noninvasive Disease Detection in Hematologic Malignancies. *Blood* **2017**, *130*, 440–452, doi:10.1182/blood-2017-03-735639.
230. Chen, Q.; Zhang, Z.H.; Wang, S.; Lang, J.H. Circulating Cell-Free DNA or Circulating Tumor Dna in the Management of Ovarian and Endometrial Cancer. *Onco. Targets. Ther.* **2019**, *12*, 11517–11530, doi:10.2147/OTT.S227156.
231. Donaldson, J.; Park, B.H. Circulating Tumor DNA: Measurement and Clinical Utility. *Annu. Rev. Med.* **2018**, *69*, 223–234, doi:10.1146/annurev-med-041316-085721.
232. Newman, A.M.; Bratman, S. V.; To, J.; Wynne, J.F.; Eclov, N.C.W.; Modlin, L.A.; Liu, C.L.; Neal, J.W.; Wakelee, H.A.; Merritt, R.E.; et al. An Ultrasensitive Method for Quantitating Circulating Tumor DNA with Broad Patient Coverage. *Nat. Med.* **2014**, *20*, 548–554, doi:10.1038/nm.3519.
233. Newman, A.M.; Lovejoy, A.F.; Klass, D.M.; Kurtz, D.M.; Chabon, J.J.; Scherer, F.; Stehr, H.; Liu, C.L.; Bratman, S. V.; Say, C.; et al. Integrated Digital Error Suppression for Improved Detection of Circulating Tumor DNA. *Nat. Biotechnol.* **2016**, *34*, 547–555, doi:10.1038/nbt.3520.
234. Kurtz, D.M.; Scherer, F.; Jin, M.C.; Soo, J.; Craig, A.F.M.; Esfahani, M.S.; Chabon, J.J.; Stehr, H.; Liu, C.L.; Tibshirani, R.; et al. Circulating Tumor DNA Measurements as Early Outcome Predictors in Diffuse Large B-Cell Lymphoma. *J. Clin. Oncol.* **2018**, *36*, 2845–2853, doi:10.1200/JCO.2018.78.5246.
235. Alig, S.; Macaulay, C.W.; Kurtz, D.M.; Dührsen, U.; Hüttmann, A.; Schmitz, C.; Jin, M.C.; Sworder, B.J.; Garofalo, A.; Shahrokh Esfahani, M.; et al. Short Diagnosis-to-Treatment Interval Is Associated With Higher Circulating Tumor DNA Levels in Diffuse

- Large B-Cell Lymphoma. *J. Clin. Oncol. Off. J. Am. Soc. Clin. Oncol.* **2021**, *39*, 2605–2616, doi:10.1200/JCO.20.02573.
236. Roschewski, M.; Lindenberg, L.; Mena, E.; Lakhotia, R.; Melani, C.; Steinberg, S.M.; Schultz, A.; Hogan, G.; Chabon, J.J.; Close, S.; et al. End-of-Treatment Response Assessment after Frontline Therapy for Aggressive B-Cell Lymphoma: Landmark Comparison of a Singular PET/CT Scan Versus Ultrasensitive Circulating Tumor DNA. *Blood* **2023**, *142*, 192, doi:https://doi.org/10.1182/blood-2023-180007.
237. Herrera, A.F.; Tracy, S.; Sehn, L.H.; Jardin, F.; Lenz, G.; Trneny, M.; Salles, G.A.; Flowers, C.; Tilly, H.; Sharman, J.P.; et al. Circulating Tumor DNA (CtDNA) Status and Clinical Outcomes in Patients (Pts) with Previously Untreated Diffuse Large B-Cell Lymphoma (DLBCL) in the POLARIX Study. *J. Clin. Oncol.* **2023**, *41*, 7523, doi:10.1200/JCO.2023.41.16_suppl.7523.
238. Kurtz, D.M.; Soo, J.; Co Ting Keh, L.; Alig, S.; Chabon, J.J.; Sworder, B.J.; Schultz, A.; Jin, M.C.; Scherer, F.; Garofalo, A.; et al. Enhanced Detection of Minimal Residual Disease by Targeted Sequencing of Phased Variants in Circulating Tumor DNA. *Nat. Biotechnol.* **2021**, *39*, 1537–1547, doi:10.1038/s41587-021-00981-w.
239. Kilgour, E.; Rothwell, D.G.; Brady, G.; Dive, C. Liquid Biopsy-Based Biomarkers of Treatment Response and Resistance. *Cancer Cell* **2020**, *37*, 485–495, doi:10.1016/j.ccell.2020.03.012.
240. Rothwell, D.G.; Ayub, M.; Cook, N.; Thistlethwaite, F.; Carter, L.; Dean, E.; Smith, N.; Villa, S.; Dransfield, J.; Clipson, A.; et al. Utility of CtDNA to Support Patient Selection for Early Phase Clinical Trials: The TARGET Study. *Nat. Med.* **2019**, *25*, 738–743,

doi:10.1038/s41591-019-0380-z.

241. Kasi, P.M.; Fehringer, G.; Taniguchi, H.; Starling, N.; Nakamura, Y.; Kotani, D.; Powles, T.; Li, B.T.; Pusztai, L.; Aushev, V.N.; et al. Impact of Circulating Tumor DNA–Based Detection of Molecular Residual Disease on the Conduct and Design of Clinical Trials for Solid Tumors. *JCO Precis. Oncol.* **2022**, e2100181, doi:10.1200/PO.21.00181.
242. Cisneros-Villanueva, M.; Hidalgo-Pérez, L.; Rios-Romero, M.; Cedro-Tanda, A.; Ruiz-Villavicencio, C.A.; Page, K.; Hastings, R.; Fernandez-Garcia, D.; Allsopp, R.; Fonseca-Montaño, M.A.; et al. Cell-Free DNA Analysis in Current Cancer Clinical Trials: A Review. *Br. J. Cancer* **2022**, doi:10.1038/s41416-021-01696-0.
243. Cohen, S.A.; Liu, M.C.; Aleshin, A. Practical Recommendations for Using CtDNA in Clinical Decision Making. *Nature* **2023**, *619*, 259–268, doi:10.1038/s41586-023-06225-y.
244. Davis, A.A.; Iams, W.T.; Chan, D.; Oh, M.S.; Lentz, R.W.; Peterman, N.; Robertson, A.; Shah, A.; Srivas, R.; Wilson, T.J.; et al. Early Assessment of Molecular Progression and Response by Whole-Genome Circulating Tumor DNA in Advanced Solid Tumors. *Mol. Cancer Ther.* **2020**, *19*, 1486–1496, doi:10.1158/1535-7163.MCT-19-1060.
245. Herberts, C.; Annala, M.; Sipola, J.; Ng, S.W.S.; Chen, X.E.; Nurminen, A.; Korhonen, O. V.; Munzur, A.D.; Beja, K.; Schönlau, E.; et al. Deep Whole-Genome CtDNA Chronology of Treatment-Resistant Prostate Cancer. *Nature* **2022**, *608*, 199–208, doi:10.1038/s41586-022-04975-9.
246. Meriranta, L.; Alkods, A.; Pasanen, A.; Lepistö, M.; Mapar, P.; Blaker, Y.N.; Jørgensen, J.; Karjalainen-Lindsberg, M.-L.; Fiskvik, I.; Mikalsen, L.T.G.; et al. Molecular Features Encoded in the CtDNA Reveal Heterogeneity and Predict Outcome in High-Risk

- Aggressive B-Cell Lymphoma. *Blood* **2022**, *139*, 1863–1877,
doi:10.1182/blood.2021012852.
247. Esfahani, M.S.; Hamilton, E.G.; Mehrmohamadi, M.; Nabet, B.Y.; Alig, S.K.; King, D.A.; Steen, C.B.; Macaulay, C.W.; Schultz, A.; Nesselbush, M.C.; et al. Inferring Gene Expression from Cell-Free DNA Fragmentation Profiles. *Nat. Biotechnol.* **2022**, *40*, 585–597, doi:10.1038/s41587-022-01222-4.
248. Verma, S.; Moore, M.W.; Ringler, R.; Ghosal, A.; Horvath, K.; Naef, T.; Anvari, S.; Cotter, P.D.; Gunn, S. Analytical Performance Evaluation of a Commercial next Generation Sequencing Liquid Biopsy Platform Using Plasma CtDNA, Reference Standards, and Synthetic Serial Dilution Samples Derived from Normal Plasma. *BMC Cancer* **2020**, *20*, 1–15, doi:10.1186/s12885-020-07445-5.
249. Roberts, A.W.; Davids, M.S.; Pagel, J.M.; Kahl, B.S.; Puvvada, S.D.; Gerecitano, J.F.; Kipps, T.J.; Anderson, M.A.; Brown, J.R.; Gressick, L.; et al. Targeting BCL2 with Venetoclax in Relapsed Chronic Lymphocytic Leukemia. *N. Engl. J. Med.* **2016**, *374*, doi:10.1056/NEJMoa1513257.
250. Liu, T.; Lam, V.; Thieme, E.; Sun, D.; Wang, X.; Xu, F.; Wang, L.; Danilova, O. V; Xia, Z.; Tyner, J.W.; et al. Pharmacologic Targeting of Mcl-1 Induces Mitochondrial Dysfunction and Apoptosis in B-Cell Lymphoma Cells in a TP53- and BAX-Dependent Manner. *Clin. Cancer Res.* **2021**, *27*, 4910 LP – 4922, doi:10.1158/1078-0432.CCR-21-0464.
251. Rooswinkel, R.W.; Van De Kooij, B.; De Vries, E.; Paauwe, M.; Braster, R.; Verheij, M.; Borst, J. Antiapoptotic Potency of Bcl-2 Proteins Primarily Relies on Their Stability, Not

- Binding Selectivity. *Blood* **2014**, *123*, 2806–2815, doi:10.1182/blood-2013-08-519470.
252. Smith, V.M.; Dietz, A.; Henz, K.; Bruecher, D.; Jackson, R.; Kowald, L.; Wijk, S.J.L. Van; Jayne, S.; Macip, S.; Fulda, S.; et al. Specific Interactions of BCL-2 Family Proteins Mediate Sensitivity to BH3-Mimetics in Diffuse Large B-Cell Lymphoma. *Haematologica* **2019**, doi:10.3324/haematol.2019.220525.
253. Saleem, M.; Qadir, M.I.; Perveen, N.; Ahmad, B.; Saleem, U.; Irshad, T.; Ahmad, B. Inhibitors of Apoptotic Proteins: New Targets for Anticancer Therapy. *Chem. Biol. Drug Des.* **2013**, *82*, 243–251, doi:https://doi.org/10.1111/cbdd.12176.
254. Tamm, I.; Wang, Y.; Sausville, E.; Scudiero, D.A.; Vigna, N.; Oltersdorf, T.; Reed, J.C. IAP-Family Protein Survivin Inhibits Caspase Activity and Apoptosis Induced by Fas (CD95), Bax, Caspases, and Anticancer Drugs¹. *Cancer Res.* **1998**, *58*, 5315–5320.
255. Deveraux, Q.L.; Takahashi, R.; Salvesen, G.S.; Reed, J.C. X-Linked IAP Is a Direct Inhibitor of Cell-Death Proteases. *Nature* **1997**, *388*, 300–304, doi:10.1038/40901.
256. Deng, J.; Carlson, N.; Takeyama, K.; Dal Cin, P.; Shipp, M.; Letai, A. BH3 Profiling Identifies Three Distinct Classes of Apoptotic Blocks to Predict Response to ABT-737 and Conventional Chemotherapeutic Agents. *Cancer Cell* **2007**, *12*, 171–185, doi:10.1016/j.ccr.2007.07.001.
257. Wever, C.M.; Geoffrion, D.; Grande, B.M.; Yu, S.; Alcaide, M.; Lemaire, M.; Riazalhosseini, Y.; Hébert, J.; Gavino, C.; Vinh, D.C.; et al. The Genomic Landscape of Two Burkitt Lymphoma Cases and Derived Cell Lines: Comparison between Primary and Relapse Samples. *Leuk. Lymphoma* **2018**, 1–16, doi:10.1080/10428194.2017.1413186.

258. Tsujimoto, Y.; Shimizu, S. VDAC Regulation by the Bcl-2 Family of Proteins. *Cell Death Differ.* **2000**, *7*, 1174–1181, doi:10.1038/sj.cdd.4400780.
259. Chin, H.S.; Li, M.X.; Tan, I.K.L.; Ninnis, R.L.; Reljic, B.; Scicluna, K.; Dagley, L.F.; Sandow, J.J.; Kelly, G.L.; Samson, A.L.; et al. VDAC2 Enables BAX to Mediate Apoptosis and Limit Tumor Development. *Nat. Commun.* **2018**, *9*, doi:10.1038/s41467-018-07309-4.
260. Delage, L.; Lambert, M.; Bardel, É.; Kundlacz, C.; Chartoire, D.; Conchon, A.; Peugnet, A.-L.; Gorka, L.; Auberger, P.; Jacquet, A.; et al. BTG1 Inactivation Drives Lymphomagenesis and Promotes Lymphoma Dissemination through Activation of BCAR1. *Blood* **2023**, *141*, 1209–1220, doi:10.1182/blood.2022016943.
261. Mlynarczyk, C.; Teater, M.; Pae, J.; Chin, C.R.; Wang, L.; Arulraj, T.; Barisic, D.; Papin, A.; Hoehn, K.B.; Kots, E.; et al. BTG1 Mutation Yields Supercompetitive B Cells Primed for Malignant Transformation. *Science (80-.)*. **2024**, *379*, eabj7412, doi:10.1126/science.abj7412.
262. Wei, W.; Song, Z.; Chiba, M.; Wu, W.; Jeong, S.; Zhang, J.-P.; Kadin, M.E.; Nakagawa, M.; Yang, Y. Analysis and Therapeutic Targeting of the EP300 and CREBBP Acetyltransferases in Anaplastic Large Cell Lymphoma and Hodgkin Lymphoma. *Leukemia* **2023**, *37*, 396–407, doi:10.1038/s41375-022-01774-z.
263. Huang, Y.-H.; Cai, K.; Xu, P.-P.; Wang, L.; Huang, C.-X.; Fang, Y.; Cheng, S.; Sun, X.-J.; Liu, F.; Huang, J.-Y.; et al. CREBBP/EP300 Mutations Promoted Tumor Progression in Diffuse Large B-Cell Lymphoma through Altering Tumor-Associated Macrophage Polarization via FBXW7-NOTCH-CCL2/CSF1 Axis. *Signal Transduct. Target. Ther.*

2021, 6, 10, doi:10.1038/s41392-020-00437-8.

264. Liu, Y.; Wang, L.; Predina, J.; Han, R.; Beier, U.H.; Wang, L.-C.S.; Kapoor, V.; Bhatti, T.R.; Akimova, T.; Singhal, S. Inhibition of P300 Impairs Foxp3+ T Regulatory Cell Function and Promotes Antitumor Immunity. *Nat. Med.* **2013**, *19*, 1173–1177.
265. Jiang, Y.; Ortega-Molina, A.; Geng, H.; Ying, H.-Y.; Hatzi, K.; Parsa, S.; McNally, D.; Wang, L.; Doane, A.S.; Agirre, X. CREBBP Inactivation Promotes the Development of HDAC3-Dependent Lymphomas. *Cancer Discov.* **2017**, *7*, 38–53.
266. Hashwah, H.; Schmid, C.A.; Kasser, S.; Bertram, K.; Stelling, A.; Manz, M.G.; Müller, A. Inactivation of CREBBP Expands the Germinal Center B Cell Compartment, down-Regulates MHCII Expression and Promotes DLBCL Growth. *Proc. Natl. Acad. Sci.* **2017**, *114*, 9701–9706.
267. Meyer, S.N.; Scuoppo, C.; Vlasevska, S.; Bal, E.; Holmes, A.B.; Holloman, M.; Garcia-Ibanez, L.; Nataraj, S.; Duval, R.; Vantrimpont, T.; et al. Unique and Shared Epigenetic Programs of the CREBBP and EP300 Acetyltransferases in Germinal Center B Cells Reveal Targetable Dependencies in Lymphoma. *Immunity* **2019**, *51*, 535-547.e9, doi:10.1016/j.immuni.2019.08.006.
268. Qualls, D.; Noy, A.; Straus, D.; Matasar, M.; Moskowitz, C.; Seshan, V.; Dogan, A.; Salles, G.; Younes, A.; Zelenetz, A.D.; et al. Molecularly Targeted Epigenetic Therapy with Mocetinostat in Relapsed and Refractory Non-Hodgkin Lymphoma with CREBBP or EP300 Mutations: An Open Label Phase II Study. *Leuk. Lymphoma* **2023**, *64*, 738–741, doi:10.1080/10428194.2022.2164194.
269. Younes, A.; Berdeja, J.G.; Patel, M.R.; Flinn, I.; Gerecitano, J.F.; Neelapu, S.S.; Kelly,

- K.R.; Copeland, A.R.; Akins, A.; Clancy, M.S.; et al. Safety, Tolerability, and Preliminary Activity of CUDC-907, a First-in-Class, Oral, Dual Inhibitor of HDAC and PI3K, in Patients with Relapsed or Refractory Lymphoma or Multiple Myeloma: An Open-Label, Dose-Escalation, Phase 1 Trial. *Lancet Oncol.* **2016**, *17*, 622–631, doi:10.1016/S1470-2045(15)00584-7.
270. Crump, M.; Coiffier, B.; Jacobsen, E.D.; Sun, L.; Ricker, J.L.; Xie, H.; Frankel, S.R.; Randolph, S.S.; Cheson, B.D. Phase II Trial of Oral Vorinostat (Suberoylanilide Hydroxamic Acid) in Relapsed Diffuse Large-B-Cell Lymphoma. *Ann. Oncol.* **2008**, *19*, 964–969, doi:10.1093/annonc/mdn031.
271. Balmanno, K.; Cook, S.J. Tumour Cell Survival Signalling by the ERK1/2 Pathway. *Cell Death Differ.* **2009**, *16*, 368–377, doi:10.1038/cdd.2008.148.
272. Schmidt, J.; Ramis-Zaldivar, J.E.; Nadeu, F.; Gonzalez-Farre, B.; Navarro, A.; Egan, C.; Montes-Mojarro, I.A.; Marafioti, T.; Cabeçadas, J.; van der Walt, J.; et al. Mutations of MAP2K1 Are Frequent in Pediatric-Type Follicular Lymphoma and Result in ERK Pathway Activation. *Blood* **2017**, *130*, 323–327, doi:10.1182/blood-2017-03-776278.
273. Martinez, D.; Navarro, A.; Martinez-Trillos, A.; Molina-Urra, R.; Gonzalez-Farre, B.; Salaverria, I.; Nadeu, F.; Enjuanes, A.; Clot, G.; Costa, D. NOTCH1, TP53, and MAP2K1 Mutations in Splenic Diffuse Red Pulp Small B-Cell Lymphoma Are Associated with Progressive Disease. *Am. J. Surg. Pathol.* **2016**, *40*, 192–201.
274. Waterfall, J.J.; Arons, E.; Walker, R.L.; Pineda, M.; Roth, L.; Killian, J.K.; Abaan, O.D.; Davis, S.R.; Kreitman, R.J.; Meltzer, P.S. High Prevalence of MAP2K1 Mutations in Variant and IGHV4-34-Expressing Hairy-Cell Leukemias. *Nat. Genet.* **2014**, *46*, 8–10.

275. Mason, E.F.; Brown, R.D.; Szeto, D.P.; Gibson, C.J.; Jia, Y.; Garcia, E.P.; Jacobson, C.A.; Dal Cin, P.; Kuo, F.C.; Pinkus, G.S. Detection of Activating MAP2K1 Mutations in Atypical Hairy Cell Leukemia and Hairy Cell Leukemia Variant. *Leuk. Lymphoma* **2017**, *58*, 233–236.
276. Lacy, S.E.; Barrans, S.L.; Beer, P.; Painter, D.; Smith, A.; Roman, E.; Cooke, S.L.; Ruiz, C.; Glover, P.; van Hoppe, S.J.; et al. Targeted Sequencing in DLBCL, Molecular Subtypes, and Outcomes: A Haematological Malignancy Research Network Report. *Blood* **2020**, *135*, 1759–1771, doi:10.1182/blood.2019003535.
277. Grosche, L.; Knippertz, I.; König, C.; Royzman, D.; Wild, A.B.; Zinser, E.; Sticht, H.; Muller, Y.A.; Steinkasserer, A.; Lechmann, M. The CD83 Molecule - An Important Immune Checkpoint. *Front. Immunol.* **2020**, *11*, 721, doi:10.3389/fimmu.2020.00721.
278. Duns, G.; Viganò, E.; Ennishi, D.; Sarkozy, C.; Hung, S.S.; Chavez, E.; Takata, K.; Rushton, C.; Jiang, A.; Ben-Neriah, S.; et al. Characterization of DLBCL with a PMBL Gene Expression Signature. *Blood* **2021**, *138*, 136–148, doi:10.1182/blood.2020007683.
279. Ley, T.J.; Ding, L.; Walter, M.J.; McLellan, M.D.; Lamprecht, T.; Larson, D.E.; Kandoth, C.; Payton, J.E.; Baty, J.; Welch, J. DNMT3A Mutations in Acute Myeloid Leukemia. *N. Engl. J. Med.* **2010**, *363*, 2424–2433.
280. Yang, L.; Rau, R.; Goodell, M.A. DNMT3A in Haematological Malignancies. *Nat. Rev. Cancer* **2015**, *15*, 152–165, doi:10.1038/nrc3895.
281. Hilton, L.K.; Ngu, H.S.; Collinge, B.; Dreval, K.; Ben-Neriah, S.; Rushton, C.K.; Wong, J.C.H.; Cruz, M.; Roth, A.; Boyle, M.; et al. Relapse Timing Is Associated With Distinct Evolutionary Dynamics in Diffuse Large B-Cell Lymphoma. *J. Clin. Oncol. Off. J. Am.*

- Soc. Clin. Oncol.* **2023**, *41*, 4164–4177, doi:10.1200/JCO.23.00570.
282. Cytlak, U.; Resteu, A.; Pagan, S.; Green, K.; Milne, P.; Maisuria, S.; McDonald, D.; Hulme, G.; Filby, A.; Carpenter, B.; et al. Differential IRF8 Transcription Factor Requirement Defines Two Pathways of Dendritic Cell Development in Humans. *Immunity* **2020**, *53*, 353-370.e8, doi:10.1016/j.immuni.2020.07.003.
283. Yang, J.; Hu, X.; Zimmerman, M.; Torres, C.M.; Yang, D.; Smith, S.B.; Liu, K. Cutting Edge: IRF8 Regulates Bax Transcription in Vivo in Primary Myeloid Cells. *J. Immunol.* **2011**, *187*, 4426–4430, doi:10.4049/jimmunol.1101034.
284. Chipuk, J.E.; Kuwana, T.; Bouchier-Hayes, L.; Droin, N.M.; Newmeyer, D.D.; Schuler, M.; Green, D.R. Direct Activation of Bax by P53 Mediates Mitochondrial Membrane Permeabilization and Apoptosis. *Science* **2004**, *303*, 1010–1014, doi:10.1126/science.1092734.
285. Morin, R.D.; Arthur, S.E.; Hodson, D.J. Molecular Profiling in Diffuse Large B-cell Lymphoma: Why so Many Types of Subtypes? *Br. J. Haematol.* **2022**, *196*, 814–829.